

Aus dem Institut für Biochemie
der Deutschen Sporthochschule Köln
Geschäftsführender Leiter: Univ.-Prof. Dr. Mario Thevis

**Entwicklung neuer Nachweisverfahren von dopingrelevanten
peptidischen und pseudopeptidischen Substanzen aus
herkömmlichen sowie alternativen Matrices**

An der Deutschen Sporthochschule Köln
zur Erlangung des akademischen Grades

Doktor der Naturwissenschaften (Dr. rer. nat.)

angenommene Dissertation

vorgelegt von

Tobias Lange

aus

Karlsruhe

Köln 2021

Erster Gutachter: Univ.-Prof. Dr. Mario Thevis
Institut für Biochemie, Deutsche Sporthochschule Köln
Zentrum für Präventive Dopingforschung

Zweite Gutachterin: Priv.-Doz. Dr. Hilke Andresen-Streichert
Institut für Rechtsmedizin, Uniklinik Köln
Forensische Toxikologie/Alkohologie

Vorsitzender des

Promotionsausschusses: Univ.-Prof. Dr. Mario Thevis

Datum der Disputation: 08.12.2022

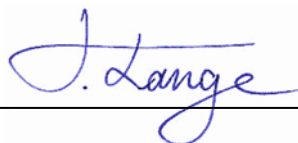
Eidesstattliche Versicherungen gem. § 7 Abs. 2 Nr. 9 der Promotionsordnung der Deutschen Sporthochschule Köln vom 30. März 2020:

Hierdurch versichere ich:

Ich habe die Arbeit selbstständig und nur unter Benutzung der angegebenen Quellen und technischen Hilfen angefertigt; sie hat noch keiner anderen Stelle zur Prüfung vorgelegen. Wörtlich übernommene Textstellen, auch Einzelsätze oder Teile davon sind als Zitate kenntlich gemacht worden.

Hierdurch erkläre ich, dass ich die „Leitlinien guter wissenschaftlicher Praxis“ der Deutschen Sporthochschule Köln eingehalten habe.

09.02.2021,



Datum, Unterschrift

Meinen Eltern

Danksagung

An erster Stelle möchte ich mich ganz herzlich bei meinem Doktorvater und Erstgutachter Herrn Univ.-Prof. Dr. Mario Thevis bedanken. Er gab mir die Möglichkeit und das Vertrauen, in einem exzellenten Forschungsumfeld mit modernsten analytischen Gerätschaften an herausfordernden und äußerst spannenden Projekten im Bereich der präventiven Dopingforschung zu arbeiten. Sein empathischer Führungsstil, zusammen mit seiner kontinuierlichen fachlichen und persönlichen Unterstützung, trug erheblich zum Gelingen der vorliegenden Arbeit bei.

Frau Priv.-Doz. Dr. Hilke Andresen-Streichert möchte ich für die Übernahme des zweiten Gutachtens danken.

Für den maßgeblichen Erfolg ist es an dieser Stelle unabdingbar, dem gesamten Team und allen Kolleginnen und Kollegen des Instituts für Biochemie, insbesondere denen vom Zentrum für Präventive Dopingforschung einen großen Dank auszusprechen. Im Einzelnen sind vor allem Frau Dr. Katja Walpurgis und Herr Priv.-Doz. Dr. Andreas Thomas hervorzuheben, welche mich mit größtmöglichem Engagement und Geduld in die Labor- und Analysetechniken einführten und weiter im gesamten Promotionsprozess kompetent begleiteten. Dazu gehörten unzählige produktive Diskussionen, ein fortlaufender wissenschaftlicher Austausch, die Überlassung von Projekten und jegliche Durchsichten meiner Manuskripte. Herrn Dr. Hans Geyer danke ich für die Mithilfe bei der Suche von Finanzierungen sowie seinen motivierenden Worten zu jeder Zeit.

Nicht unerwähnt sollen außerdem meine lieben Bürokollegen Herr Dr. André Knoop und Frau Alina Paßreiter bleiben, welche mir jederzeit mit gutem Rat, viel Humor und offenem Ohr zur Seite standen und den Laboralltag sehr angenehm bereiteten.

Weitere Akteure und Kooperationspartner, die durch ihre Zusammenarbeit für die erfolgreiche Realisierung unterschiedlichster Projekte beitrugen und welchen mein Dank gebührt, sind: Dr. Christian Görgens, Dr. Martin Bidlingmaier, Dr. Katharina Schilbach, Dr. Eric Fichant, Dr. Philippe Delahaut, Dr. Olivier Petricoul und Anna Dinter.

Schließlich gilt mein Dank allen Probanden und Studienteilnehmer für die Bereitstellung von Urin, Blut, und *Dried Blood Spots* Proben.

Aus meinem privaten Umfeld möchte ich meinen Freunden und meiner Familie, vor allem meinen Eltern und Großeltern, Onkel und Tante und meinem Bruder danken, welche für mich eine sehr wichtige Säule der Stabilität, sei es emotionaler oder finanzieller Art, durch die gesamte Zeit, waren.

Die Ergebnisse dieser kumulativen Dissertation wurden veröffentlicht in:

- T. Lange, K. Walpurgis, A. Thomas, H. Geyer & M. Thevis, Development of two complementary LC–HRMS methods for analyzing sotatercept in dried blood spots for doping controls, *Bioanalysis*, 2019, 11(10): 923-940.
- T. Lange, A. Thomas, K. Walpurgis & M. Thevis, Fully automated dried blood spot sample preparation enables the detection of lower molecular mass peptide and non-peptide doping agents by means of LC-HRMS, *Anal Bioanal Chem*, 2020, 412(15): 3765-3777.
- T. Lange, A. Thomas, C. Görgens, M. Bidlingmaier, K. Schilbach, E. Fichant, P. Delahaut & Mario Thevis, Comprehensive insights into the formation of metabolites of the ghrelin mimetics capromorelin, macimorelin and tabimorelin as potential markers for doping control purposes, *Biomed. Chromatogr.*, 2021, 35(6): e5075.

Teilergebnisse wurden vorab in folgenden Tagungsbeiträgen veröffentlicht:

Vorträge

- T. Lange, K. Walpurgis, A. Thomas, H. Geyer & M. Thevis, Development of two complementary LC-HRMS methods for analyzing Sotatercept in dried blood spots for doping controls, *Manfred Donike Workshop, 37th Cologne Workshop on Dope Analysis*, Köln, Deutschland, 17. - 22. Februar, 2019
- T. Lange, A. Thomas, K. Walpurgis & M. Thevis, Fully automated DBS sample preparation enables the detection of lower molecular mass peptide and non-peptide doping agents, *Manfred Donike Workshop, 38th Cologne Workshop on Dope Analysis*, Köln, Deutschland, 09. - 14. Februar, 2020
- T. Lange, A. Thomas, C. Görgens, M. Bidlingmaier, K. Schilbach, E. Fichant, P. Delahaut & M. Thevis, *In vivo/in vitro*-Metabolismusstudien von Ghrelin Mimetika als potenzielle Marker für Dopingkontrollen, *31. Doktorandenseminar des Arbeitskreis Separation Science der GDCh-Fachgruppe Analytische Chemie*, Hohenroda (online), Deutschland, 11. - 12. Januar 2021

Poster-Präsentationen

- T. Lange, K. Walpurgis, A. Thomas & M. Thevis, Determination of Sotatercept (ACE-011) in dried blood spots for doping control analysis by means of LC-HRMS, *European Mass Spectrometry Conference (EMSC) including the 51st annual meeting of the German Society for Mass Spectrometry (DGMS) and the 35th Journées Françaises de Spectrométrie de Masse (JFSM) of the French Mass Spectrometry Society*, Saarbrücken, Deutschland, 11. - 15. März, 2018
- T. Lange, K. Walpurgis, A. Thomas & M. Thevis, Determination of Sotatercept (ACE-011) in dried blood spots for doping control analysis by means of LC-HRMS, *Manfred Donike Workshop, 36th Cologne Workshop on Dope Analysis*, Köln, Deutschland, 22. - 27. April, 2018
- T. Lange, A. Thomas, K. Walpurgis & M. Thevis, Fully automated dried blood spot sample preparation enables the detection of lower molecular mass peptide and non-peptide doping agents by means of LC-HRMS, *53rd annual meeting of the German Society for Mass Spectrometry (DGMS) including 27th ICP-MS User's Meeting*, Münster, Deutschland, 1. - 4. April, 2020

INHALTSVERZEICHNIS

1	ZUSAMMENFASSENDE ÜBERBLICK UND DISKUSSION	1
1.1	EINLEITUNG UND ZIELSETZUNG	1
1.2	ÜBERSICHT ÜBER DEN ERSTEN ARTIKEL	10
1.3	ÜBERSICHT ÜBER DEN ZWEITEN ARTIKEL	13
1.4	ÜBERSICHT ÜBER DEN DRITTEN ARTIKEL	16
1.5	ZUSAMMENFASSENDE DISKUSSION	19
1.6	LITERATUR	26
2	DEVELOPMENT OF TWO COMPLEMENTARY LC-HRMS METHODS FOR ANALYZING SOTATERCEPT IN DRIED BLOOD SPOTS FOR DOPING CONTROLS	35
2.1	ABSTRACT	35
2.2	INTRODUCTION	36
2.3	MATERIAL AND METHODS	38
2.3.1	Chemicals and materials	38
2.3.2	Sample matrices	39
2.3.3	Solutions	39
2.3.4	Protein quantitation	39
2.3.5	DBS sampling	40
2.3.6	Sample preparation	40
2.3.7	LC-MS/MS	42
2.3.8	Method validation	43
2.4	RESULTS AND DISCUSSION	44
2.4.1	Method development	45
2.4.2	Method comparison	48
2.4.3	Method validation	49
2.4.4	ITP Proof-of-concept	52
2.4.5	DBS from clinical samples	54
2.5	CONCLUSION	55
2.6	FUTURE PERSPECTIVE	55
2.7	SUMMARY POINTS	56
2.8	SUPPLEMENTARY DATE	58

2.8.1	Method development and optimization	58
2.8.2	Material and methods	58
2.8.3	Results and discussion	58
2.9	ACKNOWLEDGEMENTS	68
2.10	REFERENCES	69
3	FULLY AUTOMATED DRIED BLOOD SPOT SAMPLE PREPARATION ENABLES THE DETECTION OF LOWER MOLECULAR MASS PEPTIDE AND NON-PEPTIDE DOPING AGENTS BY MEANS OF LC-HRMS.....	81
3.1	ABSTRACT.....	81
3.2	INTRODUCTION	82
3.3	MATERIALS AND METHODS.....	84
3.3.1	Chemicals and materials.....	84
3.3.2	Standard solutions	85
3.3.3	DBS sampling methods	85
3.3.4	Post-administration samples.....	86
3.3.5	Fully automated measurement of Hct and sample preparation.....	86
3.3.6	LC-HRMS/MS	86
3.3.7	Method validation of the initial testing procedure	87
3.4	RESULTS AND DISCUSSION	90
3.4.1	Method development and optimization	90
3.4.2	Method characterization and validation	91
3.4.3	Post-administration samples.....	96
3.4.4	Hct determination by NIR spectroscopy.....	97
3.4.5	DBS sampling methods	99
3.5	CONCLUSION.....	99
3.6	SUPPLEMENTARY DATE	101
3.6.1	DBS extraction.....	101
3.6.2	Programming the automated DBS sample preparation	101
3.7	ACKNOWLEDGEMENTS	107
3.8	REFERENCES	108
4	COMPREHENSIVE INSIGHTS INTO THE FORMATION OF METABOLITES OF THE GHRELIN MIMETICS CAPROMORELIN, MACIMORELIN AND	

TABIMORELIN AS POTENTIAL MARKERS FOR DOPING CONTROL PURPOSES**113**

4.1	ABSTRACT	113
4.2	INTRODUCTION.....	114
4.3	MATERIALS AND METHODS	116
4.3.1	Chemicals and materials.....	116
4.3.2	Standard solutions	116
4.3.3	<i>In vivo, in vitro, and in silico</i> experiments	117
4.3.4	LC-HRMS/MS	118
4.3.5	Method validation	120
4.4	RESULTS AND DISCUSSION.....	121
4.4.1	<i>In vivo, in vitro, and in silico</i> experiments	121
4.4.2	Method characterization and validation.....	134
	CONCLUSION	136
4.5	SUPPLEMENTARY DATA.....	138
4.5.1	Materials and methods.....	138
4.5.2	Results and discussion	139
4.5.3	Supplementary figures	143
4.5.4	Supplementary tables	157
4.6	ACKNOWLEDGEMENTS.....	160
4.7	REFERENCES.....	161
5	ZUSAMMENFASSUNG	167
6	ABSTRACT	169
7	ANHANG	173
7.1	ABBILDUNGSVERZEICHNIS.....	173
7.2	TABELLENVERZEICHNIS.....	181
7.3	VOLLSTÄNDIGE PUBLIKATIONSLISTE.....	183

ABKÜRZUNGSVERZEICHNIS

[M+2H] ²⁺	zweifach geladenes Vorläufer-Ion (engl. <i>doubly charged precursor ion</i>)
[M+H] ⁺	einfach geladenes Vorläufer-Ion (engl. <i>singly charged precursor ion</i>)
°C	Grad Celsius (engl. <i>degree celsius</i>)
µA	Mikroampere (engl. <i>microampere</i>)
µg	Mikrogramm (engl. <i>microgram</i>)
µL	Mikroliter (engl. <i>microliter</i>)
µm	Mikrometer (engl. <i>micrometer</i>)
AAF	ein von der Norm abweichendes (auffälliges) Analyseergebnis (engl. <i>adverse analytical finding</i>)
ABC	engl. <i>ammonium bicarbonate</i>
ADH	engl. <i>antidiuretic hormone</i>
AGC	automatische Verstärkungsregelung (engl. <i>automatic gain control</i>)
APCI	engl. <i>atmospheric pressure chemical ionization</i>
Arg	Arginin (engl. <i>arginine</i>)
CAM	engl. <i>S-carboxyamidomethylcysteine</i>
CFM-ID	engl. <i>competitive fragment modeling-ID</i>
CHAPS	engl. <i>3-[(3-cholamidopropyl)dimethylammonio]-1-propanesulfonate</i>
COVID-19	Coronavirus-Krankheit-2019 (engl. <i>coronavirus disease 2019</i>)
CP	Bestätigungsmethode (engl. <i>confirmation procedure</i>)
CV	Variationskoeffizient (engl. <i>coefficient of variation</i>)
CYP	Cytochrom P450 (engl. <i>cytochrome P450</i>)
D&I	engl. <i>dilute-and-inject</i>
Da	Dalton
DBS	Getrocknete Blutstropfen (engl. <i>dried blood spots</i>)
DBSA	Autosampler für getrocknete Blutstropfen (engl. <i>DBS-Autosampler</i>)
ddH ₂ O	doppelt destilliertes Wasser (engl. <i>double distilled water</i>)
dd-MS ²	engl. <i>data-dependend MS²</i>
DMSO	engl. <i>dimethyl sulfoxide</i>
DPS	Getrocknete Plasmatropfen (engl. <i>dried plasma spots</i>)
e.g.	zum Beispiel (lat. <i>exempli gratia</i>)
EC-C18	engl. <i>endcapped octadecyl phase</i>

EC-C8.....	engl. <i>endcapped octyl phase</i>
EDTA.....	engl. <i>ethylenediaminetetraacetic acid</i>
ELISA.....	engl. <i>enzyme-linked immunosorbent assay</i>
ESI.....	Elektrospray-Ionisation (engl. <i>electrospray ionization</i>)
eV.....	Elektronenvolt (engl. <i>electronvolt</i>)
Fc.....	Fc-Fragment (engl. <i>fragment crystallisable</i>) von Antikörpern
FDA.....	US-Behörde für Lebens- und Arzneimittel (engl. <i>U.S. Food and Drug Administration</i>)
FWHM.....	Halbwertsbreite (engl. <i>full width at half maximum</i>)
g.....	Gramm (engl. <i>gram</i>)
GH.....	engl. <i>growth hormone</i>
GHRF.....	engl. <i>growth hormone-releasing factor</i>
GHRP.....	engl. <i>growth hormone-releasing peptide</i>
GHS.....	engl. <i>growth hormone secretagogue</i>
Gly.....	Glycin (engl. <i>glycine</i>)
GMP.....	Gute Herstellungspraxis (engl. <i>good manufacturing practice</i>)
GnRH.....	engl. <i>gonadotropin-releasing hormone</i>
h.....	Stunde (engl. <i>hour</i>)
Hct.....	Hämatokrit (engl. <i>hematocrit</i>)
HEPES.....	engl. <i>2-[4-(2-hydroxyethyl)piperazin-1-yl]ethanesulfonic acid</i>
HESI.....	engl. <i>heated electrospray ionization</i>
hGh.....	engl. <i>human growth hormone</i>
HPD.....	engl. <i>high-pressure dispenser pump</i>
HRMS.....	...hochauflösende Massenspektrometrie (engl. <i>high resolution mass spectrometry</i>)
i. d. R.....	in der Regel
<i>i.e.</i>	das heißt (lat. <i>id est</i>)
i.v.....	intravenös (engl. <i>intravenous</i>)
IAA.....	engl. <i>iodoacetamide</i>
IGF-1.....	engl. <i>insulin-like growth factor-1</i>
IgG.....	engl. <i>immunoglobulin G</i>
IOC.....	Internationale Olympische Komitee (engl. <i>International Olympic Committee</i>)
IPC.....	..Internationale Paralympische Komitee (engl. <i>International Paralympic Committee</i>)

ISL	Internationale Standard für Laboratorien
ISTD	Interner Standard (engl. <i>internal standard</i>)
IT	Injektionszeit (engl. <i>injection time</i>)
ITP	Screeningverfahren (engl. <i>initial testing procedure</i>)
kDa	Kilodalton (engl. <i>kilodalton</i>)
kg	Kilogramm (engl. <i>kilogram</i>)
kV	Kilovolt (engl. <i>kilovolt</i>)
L	Liter (engl. <i>liter</i>)
LC	Flüssigkeitschromatographie (engl. <i>liquid chromatography</i>)
LHRH	engl. <i>luteinizing hormone-releasing hormone</i>
LOD	Nachweisgrenze (engl. <i>limit of detection</i>)
LOI	Identifikationsgrenze (engl. <i>limit of identification</i>)
Lys	Lysin (engl. <i>lysine</i>)
M	
	Metabolit (metabolite), molare Konzentration; mol/L (engl. <i>molar concentration; mol/L</i>)
m/z	Masse-zu Ladung-Verhältnis (engl. <i>mass-to-charge ratio</i>)
mbar	Millibar (engl. <i>millibar</i>)
MCX	engl. <i>mixed-mode cation exchange</i>
mg	Milligramm (engl. <i>milligram</i>)
min	Minute (engl. <i>minute</i>)
mL	Milliliter (engl. <i>milliliter</i>)
mm	Millimeter (engl. <i>millimeter</i>)
mM	millimolare Konzentration; mmol/L (engl. <i>millimolar concentration; mmol/L</i>)
MOPS	engl. <i>3-morpholinopropane-1-sulfonic acid</i>
MRM	engl. <i>multiple reaction monitoring</i>
MRPL	engl. <i>minimum required performance level</i>
MS	Massenspektrometrie (engl. <i>mass spectrometry</i>)
MS/MS (MS ²)	Tandem-Massenspektrometrie (engl. <i>tandem mass spectrometry</i>)
MS ³	Massenspektrometrie mit zweistufiger Fragmentierung
MSX	engl. <i>multiplexed scan event</i>
mVAP	engl. <i>multi-position evaporation station</i>
n	Anzahl (engl. <i>number</i>)
N	Newton

N/A nicht verfügbar / anwendbar (engl. <i>not available / applicable</i>)
NADA Nationale Anti-Doping Agentur Deutschland
NADOs Nationalen Anti-Doping-Organisationen
NAT2engl. <i>N-acetyltransferase</i>
NCEengl. <i>normalized collision energy</i>
ngNanogramm (engl. <i>nanogram</i>)
NHS engl. <i>N-Hydroxysuccinimide</i>
NIR Nahinfrarot (engl. <i>near-infrared</i>)
NL engl. <i>normalization level</i>
nmNanometer (engl. <i>nanometer</i>)
nmol Nanomol (engl. <i>nanomole</i>)
PAAF ein mutmaßlich von der Norm abweichendes (auffälliges) Analyseergebnis (engl. <i>presumptive adverse analytical finding</i>)
PB Phosphatpuffer (engl. <i>phosphate buffer</i>)
PBS engl. <i>phosphate-buffered saline</i>
pMS ³ engl. <i>pseudo MS³</i>
PP Proteinfällung (engl. <i>protein precipitation</i>)
ppm engl. <i>parts per million</i>
PS Partikelgröße (engl. <i>particle size</i>)
r Korrelationskoeffizient (engl. <i>correlation coefficient</i>)
RNS Ribonukleinsäure
rpmengl. <i>rounds per minute</i>
RT Raumtemperatur (engl. <i>room temperature</i>)
RT-qPCR quantitativer Echtzeit-Reverse-Transkriptase-Polymerase-Kettenreaktion (engl. <i>real-time quantitative reverse transcription polymerase chain reaction</i>)
rt _Rengl. <i>relative retention time</i>
sSekunde (engl. <i>second</i>)
s.c.subkutan (engl. <i>subcutaneous</i>)
S/NSignal-Rausch-Verhältnis (engl. <i>signal-to-noise ratio</i>)
SAR-PAGEengl. <i>sarcosyl-polyacrylamide gel electrophoresis</i>

SARS-CoV-2	„schweres akutes respiratorisches Syndrom“-Coronavirus-2 (engl. <i>severe acute respiratory syndrome coronavirus 2</i>)
SCX	engl. <i>strong cation exchange</i>
SDS	engl. <i>sodium dodecyl sulphate</i>
SID	engl. <i>source-induced dissociation</i>
SMAD	engl. <i>small body size + mothers against decapentaplegic</i>
SMILES	engl. <i>simplified molecular input line entry specification</i>
sog.	sogenannt
SPE	Festphasenextraktion (engl. <i>solid phase extraction</i>)
$t_{1/2}$	Halbwertszeit (engl. <i>half-life</i>)
TCEP	engl. <i>tris(2-carboxyethyl)phosphine</i>
TGF- β	transformierenden Wachstumsfaktor- β (engl. <i>transforming growth factor-β</i>)
t-MS ²	engl. <i>targeted MS²</i>
TPCK	engl. <i>tosyl phenylalanyl chloromethyl ketone</i>
t_R	Retentionszeit (engl. <i>retention time</i>)
TRIS	engl. <i>tris(hydroxymethyl)aminomethane</i>
t-SIM	engl. <i>targeted selected ion monitoring</i>
UDP	engl. <i>uridine diphosphate</i>
UGT	engl. <i>UDP-glucuronosyltransferase</i>
UPLC/UHPLC	Ultrahochleistungsflüssigkeitschromatographie (engl. <i>ultra high performance liquid chromatography</i>)
USADA US-amerikanische Anti-Doping Agentur (engl. <i>United States Anti-Doping Agency</i>)
V	Volt (engl. <i>volt</i>)
v. a.	vor allem
v/v	Volumenkonzentration (engl. <i>volume concentration</i>)
VAMS	volumetrisch absorptive Mikroprobennahme (engl. <i>volumetric absorptive microsampling</i>)
w/v	Gewichtprozent in Volumen (engl. <i>weight per volume</i>)
w/w	Massenprozent in Gesamtmasse (engl. <i>weight by weight</i>)
WADA	Welt Anti-Doping Agentur (engl. <i>World Anti-Doping Agency</i>)

WADC.....Welt Anti-Doping Code (engl. *World Anti-Doping Code*)

1 Zusammenfassender Überblick und Diskussion

1.1 Einleitung und Zielsetzung

Die internationale Anti-Doping Arbeit

An den Anstrengungen für einen dopingfreien, fairen und sauberen Sport sind weltweit verschiedene Akteure beteiligt. Die Welt Anti-Doping Agentur (WADA), gegründet 1999, fördert, organisiert und koordiniert die internationale Anti-Doping-Arbeit. Sie erarbeitete ein Regelwerk, den Welt Anti-Doping Code (WADC) [1], welcher 2003 in Kraft trat und heute von ca. 700 Sportorganisationen, darunter das Internationalen Olympische und Paralympische Komitee (IOC und IPC), die internationalen Sportfachverbände und die Nationalen Anti-Doping-Organisationen (NADOs), anerkannt wird. Ein wichtiger Bestandteil der internationalen Harmonisierung und Überprüfung der Anti-Doping-Regeln sind die 30 WADA-akkreditierten Laboratorien (Stand: 27.09.2020). Die Analyse von Dopingkontrollproben findet dort gemäß dem Internationalen Standard für Laboratorien (ISL) [2], Teil des WADC, statt. Die Urin- und/oder Blutproben, welche zu diesem Zwecke während und außerhalb des Wettkampfes von den Athleten angefordert werden, werden hinsichtlich verbotener Substanzen oder Methoden untersucht. Seit 2004 sind diese auf einer jährlich aktualisierten Verbotliste (*Prohibited List*) aufgeführt und in 11 unterschiedliche Substanzklassen sowie drei Arten von Methoden/Praktiken unterteilt [3]. Zuletzt wurden im Jahr 2019 weltweit knapp 280.000 Proben analysiert, davon ergaben 0,97% ein von der Norm abweichendes Analyseergebnis (engl. *adverse analytical finding*, AAF), einschließlich der medizinischer Ausnahmegenehmigungen [4].

Arbeit der Dopingkontroll-Labore

Die Aufgabe der Dopingkontroll-Laboratorien ist es, valide Testverfahren und Nachweismethoden durchzuführen und ihre Testergebnisse mit beweiskräftigen Daten zu berichten. Aufgrund des stetigen Zuwachses neuer dopingrelevanter Substanzen und der kontinuierlichen Neuentwicklung von Dopingpraktiken bei gleichzeitig rasantem Fortschritt der instrumentellen Analytik, welche für die Laboranalysen zur Verfügung steht, beschäftigt sich die präventive Dopingforschung vorrangig mit der Neu- und Weiterentwicklung verschiedener Nachweisverfahren im gesamten analytischen Spektrum. Daneben befassen sich die Laboratorien auch mit angrenzenden Themen,

wie der Kontamination von Lebensmittel, Medikamenten und Nahrungsergänzungsmitteln mit dopingrelevanten Substanzen [5, 6], um Athleten zu entlasten bzw. deren Risiko unbeabsichtigt zu Dopen zu minimieren. Zur Entwicklung von Nachweismethoden gehört auch die Unterscheidung zwischen endogenen Substanzen und strukturell identischen, jedoch exogen zugeführten Substanzen. Ein weiterer wichtiger Bestandteil ist die Identifizierung und Charakterisierung bislang unbekannter dopingrelevanter Substanzen und deren pharmakokinetischen Eigenschaften wie dem zugrundeliegenden Metabolismus oder dem renalen Ausscheidungsprofil. In einem jährlich erscheinenden Übersichtsartikel berichten Thevis *et al.* über die aktuellsten Entwicklungen von Methoden und Verfahren in der Dopinganalytik [7].

Metabolismusstudien

Neben dem Nachweis einer verbotenen Substanz an sich ist die Kenntnis über deren zugrunde liegenden Metabolismus von großer Wichtigkeit für die Dopinganalytik, da der Nachweis dieser Stoffwechselprodukte zu einer verbesserten Spezifität, Empfindlichkeit und Retrospektivität führen kann. Bedeutsame Beispiele für sogenannte Langzeitmetaboliten zur Detektion exogener anaboler androgener Steroide mit langen Nachweisfenstern wurden von Schänzer *et al.* zusammengefasst [8]. Neben Metaboliten niedermolekularer Substanzen wie den anabolen Wirkstoffen konnten auch Stoffwechselprodukte von dopingrelevanten Peptiden (< 2 kDa) mit erweiterten Nachweisfenstern identifiziert werden [9, 10]. Die Entdeckung von Metaboliten kann in kontrollierbarer, künstlicher Umgebung, z. B. im Reagenzglas (*in vitro*), im lebenden Organismus (*in vivo*) oder durch computergestützte Simulationen (*in silico*) erfolgen [11].

Herkömmliche und alternative Probenmatrices

Neben dem langjährigen routinemäßigen Einsatz der herkömmlichen Probenmatrices Blut und Urin nehmen die Forschungsprojekte für die Verwendung alternativer Matrices wie getrocknete Blutstropfen (engl. *dried blood spots*; DBS), Atemgas, Speichel/Oralflüssigkeit und Haaren einen immer größer werdenden Raum ein [12]. Von besonderer Bedeutung für diese Arbeit ist dabei die DBS-Analytik, welche ihren Einzug in die präventive Dopingforschung bereits in den 2010er-Jahren erfuhr. Die auf Cellulose-basierten Filterpapierkarten gesammelten DBS wurden ursprünglich für das Neugeborenen-Screening auf Stoffwechselerkrankungen verwendet [13] und sind heute in vielen Bereichen der klinischen Chemie zu finden [14]. DBS zeichnen sich vor

allem aufgrund der minimal-invasiven Probennahme ohne der Notwendigkeit von medizinischem Fachpersonal und den reduzierten Kosten bezüglich Lagerung und Transport aus. Für die Anti-Doping-Kontrollen erweisen sich die Proben im Scheckkartenformat daher als vielversprechende, zu konventionellen Blutproben komplementäre Probenmatrix. Die einfache Probennahme erfolgt nahezu schmerzfrei nach Punktierung der Fingerbeere mithilfe einer Lanzette, wonach ca. 20 Mikroliter (μL) Kapillarblut entnommen werden. Die Fortentwicklung der analytischen Instrumente und Techniken, wie dem Einsatz modernster Flüssigkeitschromatographie-Massenspektrometrie (LC-MS) und Immunoassays, ermöglicht den Laboratorien heute die Detektion dopingrelevanter Substanzen in pharmakologisch relevanten Blutkonzentrationen aus DBS.

Aktuelle Nachweisverfahren aus Dried Blood Spots

Seit etwa einem Jahrzehnt wurden in der präventiven Dopingforschung verschiedene massenspektrometrische Nachweisverfahren aus DBS für niedermolekulare, dopingrelevante Substanzen entwickelt. Beispiele hierfür sind anabole Steroide, β -Blocker, Stimulantien, β_2 -Adrenozeptor-Agonisten, Cannabinoide, Diuretika, Aromatasehemmer, Antiestrogene, selektive Androgenrezeptor-Modulatoren, Sirtuin-1-Aktivatoren, Immunsuppressiva, Tabakalkaloide, Opiode und Adiponektin-Rezeptor-Agonisten [15-31]. Darüber hinaus wurden Nachweise für Peptide, peptidähnliche Substanzen und Proteine aus DBS entwickelt, welche oft auf immunologischen Testverfahren basieren [32-45]. Zuletzt konnten Ribonukleinsäure (RNS)-basierte Biomarker zum Nachweis einer stimulierten Erythropoese (Blutdoping) aus DBS isoliert und mittels quantitativer Echtzeit-Reverse-Transkriptase-Polymerase-Kettenreaktion (engl. *real-time quantitative reverse transcription polymerase chain reaction*; RT-qPCR) vervielfältigt und nachgewiesen werden [46, 47].

Vorteile von Dried Blood Spots

Die auf der DBS-Karte getrockneten Analyten weisen selbst bei Raumtemperatur eine hohe Stabilität auf [29, 31, 45, 48] und ermöglichen aufgrund von Inaktivierung pathogener Viren einen sicheren, infektionsfreien Umgang der Proben [49, 50]. Die Nützlichkeit der DBS-Technik in der Anti-Doping-Arbeit ist darüber hinaus durch den kurzen Zeitaufwand der Vor-Ort-Kontrollen und die Möglichkeit einer erhöhten Testfrequenz gekennzeichnet. Außerdem ermöglicht es einen einfachen und großflächigen Einsatz im Breitensport und kann zur Aufklärungsarbeit beitragen. Ein direkter Nachweis der

unmetabolisierten Substanzen aus getrocknetem Kapillarblut kann ein ausgesprochener Mehrwert für dopingrelevante Substanzen sein, welche nach renaler Exkretion größtenteils als Metaboliten vorliegen und nur schwerlich als intakte Substanz im Urin nachweisbar sind. In diesem Fall erfordert das zum einen umfangreiche Metabolismustudien und zum anderen eine zeit- und materialaufwendige Probenvorbereitung des Urins. Dieser Umstand konnte z. B. mit einem alternativen Nachweis aus DBS umgangen werden, indem anabole Steroidester als intakte Substanzen nachgewiesen werden konnten [16]. Auch Substanzen, welche eine geringe Stabilität in den herkömmlichen Probenmatrices aufweisen, wie z. B. das Peptidhormon Synacthen®, lassen sich für längere Zeit aus DBS nachweisen [33]. Eine große Bedeutung in dieser Hinsicht kommen auch dopingrelevanten Proteinen zu, welche aufgrund ihrer Zersetzung durch proteolytische Enzyme und weiterer Metabolisierung oft nur noch begrenzt im Urin als intakte Substanzen wiederzufinden sind und deshalb Nachweismethoden aus Blut bzw. DBS präferiert werden. Zahlreiche Beispiele, darunter der insulinähnliche Wachstumsfaktor-1 (engl. *insulin-like growth factor-1*; IGF-1 aus DBS), Insulin (aus DBS) oder Sotatercept und Luspatercept (aus Blutserum), sind in der Literatur beschrieben [32, 43, 51]. Der Nachweis pharmakologisch relevanter Konzentrationen im Blut ist von großem Interesse für Substanzen, die nur im Wettkampf verboten sind, wie im Fall der meisten Stimulantien, und einem spezifischen Grenzwert unterliegen. Eine gesamtheitliche und individuelle Beurteilung eines auffälligen analytischen Dopingbefundes nach Überschreitung des Grenzwertes im Urin kann erst nach zusätzlicher Bestimmung der Blutkonzentration getroffen werden, wie mithilfe von DBS am Beispiel von Kokain/Benzoyllecgonin und Prednisolon/Prednison gezeigt wurde [30]. Ein zusätzlicher Vorteil der DBS-Technik ist der hohe Grad der potentiellen Automatisierbarkeit der Probenvorbereitung mit direkt anschließender (online) oder separater (offline) Analytik. Erste Anwendungen in der Anti-Doping-Forschung konnten bereits für niedermolekulare Substanzen wie verschiedene Stimulantien, Opioiden und adipoRon (ein synthetisch hergestellter Adiponektin-Rezeptor-Agonist) realisiert werden [20, 25-27] und deuten zukünftige Möglichkeiten höherer Probendurchsätze an. Aufgrund der Aktualität soll hier als Randnotiz nicht unerwähnt bleiben, dass auch die Anwendbarkeit von DBS für SARS-CoV-2-Antikörper Tests gezeigt werden konnte [52-54].

Herausforderungen von Dried Blood Spots

Die Herausforderungen für die Matrix DBS liegen im vergleichsweise geringen Probenvolumen (i. d. R. 20 µL je Spot), welches direkten Einfluss auf die Nachweisgrenze und das Nachweisfenster hat sowie den mehr oder weniger aufwendigen Extraktionsverfahren. Niedermolekulare, dopingrelevante Substanzen lassen sich vergleichsweise einfach und effektiv mit organischen Lösungsmittel aus der DBS-Karte extrahieren und mit ausreichenden Empfindlichkeiten im Bereich zwischen 0,05-0,5 ng/mL nachweisen [22]. Die Extraktion von peptid-/proteinbasierten Pharmazeutika erfordert dagegen meist einen hohen Anteil wässrigen Puffers [34, 41] und damit einhergehend die unerwünschte Ko-Extraktion von zellulären Bestandteilen und hochabundanten Blutproteinen. Für die Analytik mittels LC-MS sind vorher weitere Reinigungsschritte wie Immunoaffinitätsreinigung oder Festphasenextraktion erforderlich [35]. Weitere Faktoren, welche einen Einfluss auf die Stabilität, Extraktion oder Wiederfindung der Analyten in DBS haben können, sind die Luftfeuchtigkeit und die Temperatur bei Lagerung und Versand [55], das Verhältnis von Blutzellen zu Flüssigkeit (Hämatokrit) [56], die Viskosität des Blutes (chromatographischer „Vulkaneffekt“ auf dem Filterpapier [57]), die Herkunft des Blutes (venös vs. kapillar) [58] und der Einfluss von Antikoagulantien [35, 59], die z. B. über EDTA-beschichtete Kapillaren zur Probenahme ins Blut gelangen können. Viele der genannten Herausforderungen können mittlerweile durch bestimmte Techniken verringert oder kompensiert werden. Hempen *et al.* berichteten z. B. von einer Hämatokrit-unabhängigen Wiederfindung von Immunsuppressiva nach Durchflussdesorption bei erhöhter Temperatur von ca. 75 °C [24]. Der Effekt der ungleichmäßigen Analytenverteilung durch inhomogene Ausbreitung des Blutes auf dem Filterpapier kann durch die Analyse des gesamten Spots anstelle eines partiellen Ausschnitts minimiert werden [60]. Des Weiteren bestehen mittlerweile Möglichkeiten, den Hämatokrit von DBS mithilfe von Nahinfrarot (NIR)-Spektroskopie oder diffuser Reflexionsspektroskopie zerstörungs- und berührungsfrei vor der eigentlichen Extraktion zu messen [61, 62]. Dies ermöglicht die Einführung eines Korrekturfaktors für die Berechnung von Plasmakonzentrationen bei quantitativen Anwendungen, wie am Beispiel von Koffein demonstriert werden konnte [62]. Die beschriebenen Limitationen sind für einen qualitativen Nachweis von dopingrelevanten Substanzen aus DBS meist nur von geringer Bedeutung, umso wichtiger werden sie hingegen bei quantitativen Testmethoden.

Neue Testgeräte

Derweil existieren kommerzielle Testgeräte, sog. *TAP®-Devices* (Seventh Sense Biosystems, Boston, USA), mit denen sich die Anwender*innen nahezu schmerzfrei selbstständig, d. h. per Druckknopfvorrichtung an dem Einmaltester, bis zu 100 µL Blut durch Punktion des Oberarms abnehmen können [63]. Dabei gelangt das Blut, stabilisiert durch ein Antikoagulans, in ein Reservoir und kann später, z. B. nach Versand in ein Labor, zur Analyse oder zur Herstellung von DBS genutzt werden. Des Weiteren gibt es bereits erste kommerzielle Formate, in denen vier, 20 µL Blut fassende, Polymer-basierte VAMS (volumetrisch absorptive Mikroprobennahme) Probenzylinder integriert sind (*Tasso-M20-Device*; Tasso, Seattle, USA) [64]. Diese DBS-verwandte Technologie wurde bereits in der präventiven Dopingforschung für den Nachweis von IGF-1 eingesetzt [65]. Die VAMS-Technologie verspricht darüber hinaus die Überwindung des bereits thematisierten Hämatokrit-Bias bei Verwendung von DBS-Karten [66]. Inzwischen laufen bereits Pilotstudien der Nationalen Anti-Doping Agentur Deutschland (NADA) und der *United States Anti-Doping Agency* (USADA), welche die Anwendbarkeit der neuen *Tasso-M20-Devices* für die virtuelle Dopingkontrolle, d. h. kontaktlos, per Video-Sichtkontakt und ohne Ansteckungsgefahr während der COVID-19-Pandemie (seit 03/2020) untersuchen [67, 68].

WADA und Dried Blood Spots

Die WADA hat unlängst ein Lenkungskomitee eingesetzt, das die Entwicklung und Durchführung von DBS-Tests hinsichtlich des Ziels einer routinemäßigen Implementierung bis zu den Olympischen und Paralympischen Winterspielen 2022 in Peking, China, begleiten soll [69].

Ziel dieser Doktorarbeit

Ziel dieser kumulativen Doktorarbeit ist es, neue Nachweisverfahren für dopingrelevante Substanzen peptidischer und pseudopeptidischer Struktur, d. h. Peptide, peptidähnliche Verbindungen und Proteine aus herkömmlichen sowie alternativen Matrices zu entwickeln. Die im Rahmen dieser Arbeit behandelten Substanzen, welche der Substanzklasse S2 der WADA-Verbotsliste „Peptidhormone, Wachstumsfaktoren, verwandte Substanzen und Mimetika“ zugehörig sind, wurden erstmals 2015 bzw. 2017 namentlich erwähnt. Das allgemeine Verbot jeglicher Peptidhormone stand dahingegen bereits in der ersten Version (seit 2004) auf der WADA-Verbotsliste. Alle weiteren nicht explizit aufgeführten Substanzen dieser Studien sind als „Substanzen

mit ähnlicher chemischer Struktur oder ähnlicher/n biologischer/n Wirkung(en)“ inkludiert [3].

Wie in Abbildung 1.1 dargestellt, nimmt die Anzahl der durchgeführten Dopingkontrollen sowie der auffälligen analytischen Befunden für die größte Gruppe der Peptidhormone, den Wachstumshormon-freisetzende Faktoren aus Urin, jährlich zu [4]. So waren es nach erstmaliger Datenerhebung 2014 sechs auffällige analytische Befunde, 2016 bereits 15 und 2019 stieg die Zahl auf 26 weltweit berichtete Befunde. Der Bedarf nach neuen sowie alternativen oder verbesserten Nachweismethoden ist daher sehr hoch und die stetige Anpassung der analytischen Möglichkeiten dringend erforderlich.

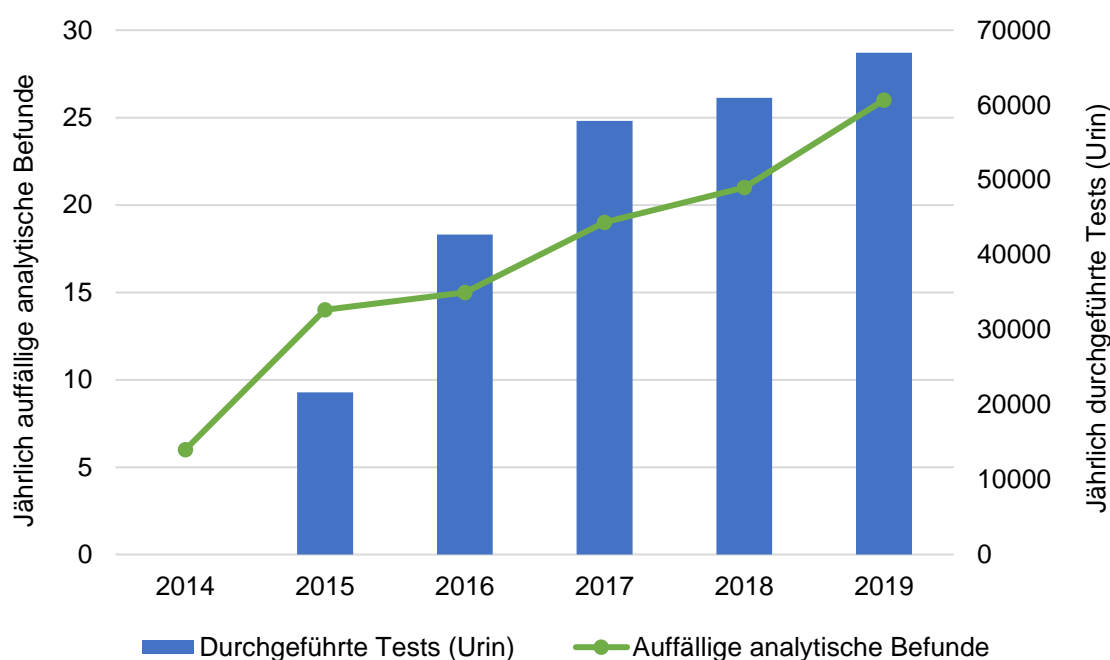


Abbildung 1.1: Anzahl der durchgeführten jährlichen Dopingtests (Urin) für Wachstumshormon-freisetzende Faktoren (blaue Balken) und die Anzahl der jährlich auffälligen analytischen Befunde (engl. *adverse analytical findings*, grüne Linie). Die Daten sind aus den *Anti-Doping Testing Figures 2019* der Welt-Anti-Doping-Agentur entnommen [70]. Für das Jahr 2014 sind keine Zahlen für die durchgeführten Tests angegeben.

Aufgrund der internationalen Bestrebungen, die DBS-Technik baldmöglichst als zusätzliche offizielle Matrix in die Dopingkontrollen aufzunehmen, besteht großes Interesse an Studien und Nachweisen von dopingrelevanten peptid-/proteinbasierter Substanzen auch aus DBS. Zum Zeitpunkt der Aufnahme dieses Promotionsvorhabens war die Datenlage diesbezüglich noch sehr limitiert.

Als Methode der Wahl sollte die hochauflösende Massenspektrometrie (engl. *high resolution mass spectrometry*; HRMS/MS) nach Auftrennung der Substanzen mittels Ultrahochleistungsflüssigkeitschromatographie (engl. *ultra high performance liquid chromatography*; UPLC/UHPLC) eingesetzt werden. Im Fokus standen dabei zum einen der Methodentransfer von aktuellen Nachweisverfahren aus Blut und Urin hin zu DBS und zum anderen die Erweiterung des analytischen Spektrums mit neuen peptidischen und pseudopeptidischen Analyten für verschiedene Matrices. Dazu gehörten auch die vollständige MS/MS-Charakterisierung neuer Substanzen inklusive ausführlicher Metabolismusstudien und die erstmalige Entwicklung von Nachweismethoden für diese Analyten auch aus den herkömmlichen Matrices Blut und Urin. Für alle Nachweisverfahren wurde eine vollständige Entwicklung und eingehende Optimierung der manuellen bzw. ggf. automatisierten Extraktions- und Reinigungsverfahren sowie LC-MS-Methoden angestrebt. Das beinhaltete neben der Methodvalidierung nach aktuellen WADA-Richtlinien [2] auch die Durchführung von Machbarkeitsstudien (engl. *proof of concept*) anhand authentischer humaner Proben nach Applikation.

Im ersten Projekt sollte erstmalig im Rahmen der präventiven Dopingforschung das therapeutische Fusionsprotein Sotatercept (> 100 kDa) mittels LC-HRMS aus DBS nachgewiesen werden. Zwar existierte bereits eine Nachweismethode aus Plasma [71], jedoch sollte mit dem Methodentransfer eine umfassende Optimierung bezüglich Probenvorbereitung und Analytik erfolgen, um eine ausreichende Nachweisgrenze in pharmakologisch wirksamen Bereichen zu erzielen. Als weitere Zielsetzung sollte eine zweite generische Probenvorbereitung für eine Multikomponenten-Screening-Methode erarbeitet werden, welche die Ko-Extraktion weiterer Fusionsproteine und therapeutischen Antikörper wie Luspatercept und Bimagrumab erlauben würde.

Das zweite Projekt hatte als Zielsetzung die Entwicklung einer vollautomatischen, Roboter-gestützten DBS-Probenvorbereitung mit anschließender Analytik mittels LC-HRMS. Nachdem erste Erfahrungen hinsichtlich einer automatisierten Probenvorbereitung für niedermolekulare, dopingrelevante Substanzen aus DBS gemacht wurden [25, 27], sollte eine Multikomponenten-Screening-Methode für hohe Probenaufkommen zum Nachweis (pseudo-)peptidischer Substanzen < 2 kDa entwickelt werden. Die Auswahl der Zielanalyten beruhte auf den aktuellen multianalytischen Nachweisverfahren dieser Substanzen aus Urin [72] und sollte von 35 auf 46 Analyten erweitert werden. Als weitere Neuerung sollte, der DBS-Extraktion vorgeschaltet, die

Einführung einer automatisierten und berührungsfreien Hämatokritmessung mittels NIR-Spektroskopie erfolgen. Des Weiteren sollte die selbstständige, nahezu schmerzfreie Blutabnahme mithilfe eines neuartigen Testgeräts (*TAP®-Device*) für den Oberarm evaluiert werden.

Für das dritte Projekt war die Charakterisierung und Entwicklung neuer LC-HRMS-basierter Nachweisverfahren für die drei Ghrelin Rezeptor-Agonisten/Ghrelin Mimetika Capromorelin (CP-424,391), Macimorelin (Macrilen, EP-01572) und Tabimorelin (NN703) geplant. Die Probenvorbereitungen (Blut und Urin) sollten anhand etablierter Protokolle erfolgen [72, 73] und die Zielanalyten sollten rasch in die bestehenden Routine-Nachweisverfahren implementiert werden. Darüber hinaus sollten umfassende Metabolismusstudien unter Anwendung einer Kombination von *in silico*, *in vitro*, und *in vivo* Experimenten durchgeführt werden. Die Kenntnis über die Metaboliten einer verbotenen Substanzen könnte im Falle eines auffälligen analytischen Befundes wichtige Hinweise zur zusätzlichen Identifizierung dieser Substanz liefern sowie zu verbesserten Nachweisgrenzen und/oder -fenster beitragen.

1.2 Übersicht über den ersten Artikel

T. Lange, K. Walpurgis, A. Thomas, H. Geyer & M. Thevis, Development of two complementary LC–HRMS methods for analyzing sotatercept in dried blood spots for doping controls, *Bioanalysis*, 2019, 11(10): 923-940.

Die Publikation beschreibt die Entwicklung und Optimierung zweier komplementärer LC-HRMS-Nachweisverfahren für das therapeutische Fusionsprotein Sotatercept (ACE-011, ActRIIA-Fc) aus DBS mit pharmakologisch relevanten Nachweisgrenzen (0,25-0,50 µg/mL) inklusive eines Machbarkeitsnachweises anhand authentischer DBS-Proben.

Die Klasse der therapeutischen Proteine hat eine vergleichsweise junge Geschichte. Zu den ersten dopingrelevanten Polypeptiden, welche ursprünglich als Substitutions-therapeutika entwickelt worden waren, gehörten Insulin (1922; erste erfolgreiche Anwendung) und Erythropoietin (1989; erstes rekombinantes Präparat). Erst seit der Entwicklung der Hybridom-Technologie (1975) und der Phage-Display-Technologie (1985) können auch monoklonale Antikörper sowie Rezeptoren und Fusionsproteine *in vivo/in vitro* hergestellt werden.

Sotatercept ist ein neues Fc-Fusionsprotein, welchem eine Erythropoese-stimulierende [74] und anti-osteoporotische Wirkung [75] zugeschrieben wird. Damit wäre die missbräuchliche Nutzung von z. B. Ausdauerathleten*innen denkbar, die sich davon eine verbesserte Sauerstoffversorgung der Muskulatur versprechen könnten. Seit 2017 ist das über 100 kDa große Protein, ein Dimer bestehend aus 344 Aminosäuren, als Inhibitor des transformierenden Wachstumsfaktor-β (engl. *transforming growth factor-β*, TGF-β), explizit auf der Verbotsliste der WADA aufgeführt [3]. Das Medikament des Pharmaunternehmens Acceleron Pharma befindet sich derzeit (2021) in Phase-2-Studien für die Behandlung der pulmonal-arteriellen Hypertonie, eine seltenen Blutgefäßerkrankung [76]. Ungeachtet der fehlenden Zulassung sind bereits diverse Sotatercept enthaltende Schwarzmarktprodukte erhältlich, was die Gefahr eines potentiellen Missbrauchs noch bekräftigt. Aus diesem Grund wurden bereits erste LC-MS-basierte Nachweismethoden mit Nachweisgrenzen zwischen 10-50 ng/mL aus Blutplasma oder -serum entwickelt [71, 77]. Durch die hohe Stabilität des Proteins aufgrund der strukturellen Eigenschaften und der damit einhergehenden langen Plasmahalbwertszeit sind lange Nachweisfenster von Wochen bis Monaten

nach Applikation zu erwarten [78]. Ein LC-MS-basierter Nachweis von Sotatercept oder einem vergleichbaren Fusionsprotein dieser Größe aus DBS war in der präventiven Dopingforschung bisher nicht verfügbar.

Für den Nachweis von Sotatercept aus DBS wurden zwei komplementäre Methoden entwickelt, zum einen ein Screeningverfahren (engl. *initial testing procedure*; ITP) und zum anderen eine Bestätigungsmethode (engl. *confirmation procedure*; CP). Beide manuellen Probenvorbereitungen umfassten die Extraktion eines ausgeschnittenen DBS in einer wässrigen Pufferlösung mittels Ultraschallbad, eine Immunoaffinitätsreinigung mit Liganden-gekoppelten magnetischen Partikeln und eine enzymatische Hydrolyse mittels Trypsin. Die daraus resultierenden Signaturpeptide, welche die eindeutige Herkunft des Analyten belegen, wurden nach Entwicklung einer geeigneten UHPLC Trennung mittels einer EC-C8 analytischen Säule mit einem Orbitrap-Analysator detektiert. Als interner Standard (ISTD) wurde ein rekombinantes Mausprotein (rmActRIIA-Fc) verwendet, welches sich nur an wenigen Positionen in der Aminosäuren-Sequenz unterscheidet. Die Unterscheidung beider Probenvorbereitungen beruhte im Wesentlichen in der Art der Immunoaffinitätsreinigung. Für die Bestätigungsmethode wurde ein Verfahren von Walpurgis *et al.* [71] adaptiert, welches die hochspezifische Wechselwirkung zwischen der Aktivin-Rezeptor-Domäne des Sotatercept und des vorher an Magnetpartikel gekoppeltes Aktivin A nutzt, um Sotatercept in hoher Reinheit anzureichern. Bei der Entwicklung des Screeningverfahrens wurde ein weniger spezifisches Verfahren vorgestellt, bei welchem die Immunglobulin G (IgG)-basierte Domäne von Sotatercept über kommerziell erhältliche Protein G-gekoppelten Magnetpartikeln isoliert wurde. Diese Prozedur erlaubte somit die Ko-Isolierung weiterer IgG-basierter Fusionsproteine und therapeutischer Antikörper, wie am Beispiel von Luspatercept und Bimagrumab, zweier weiterer dopingrelevanter rekombinanter Proteinanalyten, gezeigt werden konnte. Aufgrund des begrenzten Volumens von nur 20 µL getrockneten Bluts pro Spot mussten verschiedene Parameter wie das Verhältnis von Blut zu Magnetpartikel, das Verhältnis von Gesamtprotein zu Enzym (Trypsin), dem Volumen des Extraktions- und Bindepuffers sowie der Trypsin-Verdauzeit eingehend untersucht und optimiert werden, um die höchste Empfindlichkeit der Methode zu erreichen. Es erfolgten schließlich die WADA-konformen Validierungen mit Nachweisgrenzen zwischen 0,25-0,50 µg/mL und ein Machbarkeitsnachweis der Bestätigungsmethode für authentisch hergestellte DBS-

Proben, welche Bimagrumab nach intravenöser bzw. subkutaner Verabreichung im Rahmen einer klinischen Studie enthielten.

Der Fachartikel beschreibt die ersten Nachweisverfahren, welche für ein doping-relevantes Fusionsprotein aus DBS entwickelt und charakterisiert wurden. Bislang war außerdem keine Methode bekannt, weder aus Serum/Plasma noch aus DBS, welche die simultane Detektion IgG-basierter Fusionsproteine ermöglichte und mittels einer retrospektiven Datenanalyse auch die Detektion bisher unbekannter IgG-basierter Substanzen erlaubte.

1.3 Übersicht über den zweiten Artikel

T. Lange, A. Thomas, K. Walpurgis & M. Thevis, Fully automated dried blood spot sample preparation enables the detection of lower molecular mass peptide and non-peptide doping agents by means of LC-HRMS, *Anal Bioanal Chem*, 2020, 412(15): 3765-3777.

Die Publikation beschreibt die Entwicklung und Optimierung einer vollautomatischen DBS-Probenvorbereitung mit vorgeschalteter Hämatokritmessung, einschließlich Durchflussdesorption, Festphasenextraktion und Evaporation für 46 peptidische und nichtpeptidische (pseudopeptidische) Substanzen inklusive repräsentativer Metaboliten mit einem Molekulargewicht < 2 kDa sowie die Entwicklung eines LC-HRMS-Nachweisverfahrens dieser verbotenen Substanzen.

Die Wirkungen dieser potentiell exogen zugeführten Peptide und Pseudopeptide, welche erstmalig im Jahr 2015 auf der WADA-Verbotsliste namentlich erwähnt wurden, sind vielfältig. Die größte Gruppe umfasst die Ghrelin Rezeptor-Agonisten mit aktuell 22 Substanzen, darunter die GHRPs, deren Wirkort die Hirnanhangsdrüse (Hypophyse) ist. Dort erfolgt die Ausschüttung von Wachstumshormonen ins Blut, welches wiederum die Freisetzung von IGF-1 bewirkt und anabole Effekte auf den Knochen- und Muskelaufbau sowie den Fettabbau zur Folge hat. Die 12 Substanzen der zweitgrößten Gruppe der GnRH Rezeptor-Agonisten, wie z. B. Alarelin, Deslorelin oder Histrelin induzieren eine Hochregulierung der Wirkkaskade entlang der Hypothalamus-Hypophysen-Gonaden-Achse. Hierbei wird die Produktion von Testosteron in den Hoden angeregt und die anabolen Wirkungen im Sinne eines*einer missbräuchlich handelnden Athleten*in können zum Tragen kommen. Die Einnahme von antidiuretischem Hormon (ADH) Rezeptor Agonisten (auch: Vasopressin Analoga) wie Desmopressin und Felypressin, bringen harnreduzierende (antidiuretische) Effekte mit sich. Eine vermehrte Reabsorption von Wasser in den Nieren durch diese Derivate kann sich daher auf eine beabsichtigte Manipulation der Blutparameter auswirken.

Als Probenmatrix der Wahl hat sich für die Routine-Dopingkontrollanalytik dieser Substanzen Humanurin etabliert. [72, 79-81]. Die meisten der Wachstumshormon-freisetzenden Fragmente und Peptide zeigen im Urin ausreichende Stabilität mit Nachweisfenstern, welche länger (z. B. GHRP-2) oder ähnlich lang (z. B. GHRP-6) wie in

Serum ausfallen können [82]. Eine Limitation der Urinanalytik ist die komplexe Datenlage bzw. der erhöhte Informationsbedarf aufgrund der Vielzahl an vorliegenden Stoffwechselprodukten der Analyten [83]. So können manche der intakten Substanzen wie GHRP-1 und Alexamorelin, aufgrund ihrer raschen Zersetzung und Instabilität in Urin nur noch schwerlich nachgewiesen werden [72, 81].

Aufgrund der beschriebenen Vorzüge von DBS wurde in diesem Projekt eine voll automatisierte Probenextraktion und -reinigung für hohes Probenaufkommen entwickelt. Neben der herkömmlichen Methode der Herstellung von DBS über ein Punktieren der Fingerbeere wurde zur selbstständigen Gewinnung von Vollblut ein Einmaltester mit Druckknopfvorrichtung (*TAP®-Device*) für den Oberarm genutzt. Das roboter-gestützte Probenvorbereitungsverfahren startete mit einer kontaktlosen, zerstörungsfreien Hämatokrit-Messung der getrockneten DBS-Karte mittels NIR-Spektroskopie. Im nächsten Schritt erfolgte die Durchflusssorption mit ddH₂O bei 100 °C; gleichzeitig wurde über eine separate Probenschleife der ²H-stabil-isotopenmarkierte ISTD-Mix in den Fluss eingespeist. Die Analyten wurden unter Ausnutzung ionischer Wechselwirkungen mit einem Kationentauscher (Festphasenextraktion) konzentriert. Im Anschluss wurde das Eluat bei 50° C unter vermindertem Druck eingengt. Schließlich war die Probe für die Analyse an einem LC-HRMS-System vorbereitet. Die Datenanalyse der insgesamt 46 Substanzen erfolgte nach massenspektrometrischer Messung anhand der Identifikation der jeweiligen Vorläufer-Ionen. Erstmals befanden sich unter den Analyten neun Glycin (Gly)-Derivate der GHRPs - zuvor wurden Gly-GHRP-2, Gly-GHRP-6 und Gly-Ipamorelin in Schwarzmarktprodukten identifiziert [84, 85] - sowie Felypressin, ein neuartiges Vasopressin Analogon. Das LC-HRMS-Nachweisverfahren wurde vollständig charakterisiert und validiert. Die Nachweisgrenzen der Substanzen lagen zwischen 0,5 und 20 ng/mL, wovon mehr als 60% unter der von der WADA geforderten Mindestnachweisgrenze (engl. *minimum required performance level*; MRPL) von 2 ng/mL für Urin lagen. Schließlich wurde aus Serumproben, welche GHRP-2 sowie GHRP-6 enthielten, Vollblutmatrices mittels Zugabe frischer Blutzellen rekonstruiert, um damit authentische DBS nachzubilden. In einem Proof of Concept konnten die Analyten daraus eindeutig nachgewiesen werden.

Der Fachartikel präsentiert ein Verfahren zur effektiven und automatisierten Hochdurchsatzanalyse für DBS-Proben auf (pseudo-)peptidische Substanzen. Außerdem wurde erstmals die Möglichkeit einer zerstörungsfreien Hämatokritmessung im

Rahmen eines Anti-Doping-Nachweisverfahrens aus DBS vorgestellt, welche zukünftig für eine Hämatokrit-abhängige Korrektur bei quantitativen DBS-Analysen weitere Anwendung finden könnte.

1.4 Übersicht über den dritten Artikel

T. Lange, A. Thomas, C. Görgens, M. Bidlingmaier, K. Schilbach, E. Fichant, P. Delahaut & Mario Thevis, Comprehensive insights into the formation of metabolites of the ghrelin mimetics capromorelin, macimorelin and tabimorelin as potential markers for doping control purposes, *Biomed. Chromatogr.*, 2021, 35(6): e5075.

In dieser Publikation sind LC-HRMS-basierte Nachweisverfahren für die intakten Substanzen von drei neuen Ghrelin Mimetika Capromorelin (CP-424,391), Macimorelin (macrilen, EP-01572), und Tabimorelin (NN703) aus Urin und Blut beschrieben. Darüber hinaus sind außerdem die Resultate umfassender *in vitro/in vivo* Metabolismusstudien dargestellt.

Das sogenannte „Hungerhormon“ Ghrelin und zahlreiche Ghrelin Mimetika, wie z. B. Anamorelin und Ibutamoren, wurden erstmals 2015 namentlich auf der WADA Verbotliste aufgeführt. Diese synthetischen Ghrelin Mimetika wurden ursprünglich zur Behandlung von Patienten mit einem Wachstumshormonmangel entwickelt [86]. Sie sind Agonisten des Ghrelin Rezeptors im Hypothalamus und regen die Sekretion von Wachstumshormon aus der Hirnanhangsdrüse an. Die damit verbundene hohe Dopingrelevanz hinsichtlich der leistungssteigernden Effekte wie dem Knochen- und Muskelaufbau wurden bereits in Abschnitt 1.3 (S.13) erläutert.

Die Zielsubstanzen dieser Studien waren die drei oben genannten Ghrelin Mimetika. Während Tabimorelin niemals die Zulassung erhielt, wurde Capromorelin von der US-Behörde für Lebens- und Arzneimittel (engl. *U.S. Food and Drug Administration*; FDA) zur Appetitanregung bei Hunden zugelassen [87]. Macimorelin wird bei Erwachsenen als Stimulationstest zur Diagnose von Wachstumshormonmangel verwendet [88] und erhielt als einziges der drei Mimetika im Jahr 2017 die Zulassung durch die FDA.

Da bisher keine analytischen Verfahren zur Erfassung einer missbräuchlichen Verwendung dieser drei Substanzen zur Verfügung standen, wurden jeweils für die intakten Substanzen analytische Screeningverfahren und Bestätigungsmethoden aus den humanen Dopingkontrollmatrices Urin und Blutplasma entwickelt, optimiert und validiert. Dabei wurden abhängig von der Probenmatrix unterschiedliche Extraktionsmethoden wie Festphasenextraktion (Urin), Proteinfällung (Blutplasma) oder eine

Direktinjektion (Urin) durchgeführt. Die WADA-konformen LC-HRMS-basierten Nachweisverfahren mit Nachweisgrenzen zwischen 0,02-0,60 ng/mL (Screening) und 0,18-0,89 ng/mL (Bestätigung) konnten schließlich in bestehende Routine-Nachweisverfahren für Wachstumshormon-freisetzende Faktoren aus Humanurin implementiert werden.

Darüber hinaus wurden verschiedene Metabolismusstudien durchgeführt, um neue Stoffwechselprodukte der Ghrelin Mimetika zu identifizieren, die sich zusätzlich zu den intakten Substanzen zukünftig in analytische Nachweisverfahren integrieren lassen würden. Auf der Grundlage von *in silico* simulierten Daten zu den zuvor antizipierten Phase-I und -II Metaboliten wurden *in vivo* (Ratte) und *in vitro* (humane Lebermikrosomen und Inkubation in Humanserum) Experimente durchgeführt. Für den hier im Fokus stehenden Tierversuch wurden jeweils zwei Ratten eine Einzeldosis von 0,5-1,0 mg je Substanz oral verabreicht und zu verschiedenen Zeitpunkten bis zu 36 h nach Gabe, Blut- bzw. Urinproben gesammelt. Dabei wurden im Allgemeinen im Rattenurin höhere Konzentrationen der Vorläufersubstanzen und Metaboliten als im Blut vorgefunden. Alle Experimente zusammengenommen, konnten vorläufig 51 Metaboliten von Capromorelin, 12 Metaboliten von Macimorelin und 13 Metaboliten von Tabimorelin mittels LC-HRMS detektiert werden. Für sieben Hauptmetaboliten im Rattenurin mit einer Häufigkeit von mindestens 1% relativ zur unmetabolisierten Vorläufersubstanz, wurden ausführliche massenspektrometrische Untersuchungen und Charakterisierungen durchgeführt. Im Detail waren das für Capromorelin ein Hydroxylamin-Metabolit, ein hydrolysiertes Metabolit und ein *N*-dealkylierter Metabolit und für Tabimorelin ein *N*-glucuronidierter Metabolit. Für Macimorelin wurden ein Monohydroxy- oder Epoxid-Metabolit und zwei weitere Metaboliten, deren Entstehung sich durch einen C-N-Bindungsbruch im Molekül erklären lässt, mittels MS/MS Experimenten charakterisiert. Einer dieser beiden Metaboliten zeigte besonders hohe Konzentrationen (Rattenurin) mit bis zu zwei Größenordnungen über der des Macimorelin-Vorläufers und hätte voraussichtlich über einen deutlich längeren Zeitraum als für die Probensammlung dieser Studie vorgesehen, nachgewiesen werden können. Außer für die beiden Hauptmetaboliten von Macimorelin zeigten sich für die anderen Hauptmetaboliten von Capromorelin, Macimorelin, und Tabimorelin deutlich niedrigere relative Häufigkeiten (< 10%) über das gesamte Ausscheidungsprofil hinweg.

Der Fachartikel beschreibt die Erweiterung des analytischen Spektrums um drei dopingrelevante Substanzen aus der Klasse der Ghrelin Mimetika. Außerdem wurden nach eingehenden Metabolismusstudien Metaboliten detektiert und charakterisiert, wovon insbesondere die zwei Hauptmetaboliten von Macimorelin zukünftig einen wichtigen Beitrag zur Verbesserung von Empfindlichkeit, Spezifität und des Nachweisfensters für die Anti-Doping-Analytik aus Humanurin leisten könnten.

1.5 Zusammenfassende Diskussion

Alle in dieser Dissertation entwickelten und vorgestellten Nachweisverfahren, die zugehörige Studien und Daten sowie die Zusammenarbeit mit Kooperationspartnern dienen der internationalen Anti-Doping-Arbeit. Das übergeordnete Ziel ist die Aufrechterhaltung und Gewährleistung der „Fairness und Chancengleichheit im sportlichen Wettkampf für alle Athleten*innen“, der „Aufrechterhaltung der Werte des Sports“ und der „Schutz der Gesundheit des*der Einzelnen“ [89].

Zusammenfassend beschreibt die Dissertation unterschiedliche analytische Nachweisverfahren aus den WADA-konformen Dopingkontrollmatrices Urin und Blut sowie der alternativen Matrix DBS. Die hier im Fokus stehenden insgesamt 49 Substanzen gehören überwiegend zu den (pseudo-)peptidischen Agonisten des Ghrelin Rezeptors (auch: Ghrelin Mimetika), des GnRH Rezeptors und des ADH Rezeptors sowie zu den Fc-Fusionsproteinen bzw. therapeutischen Antikörpern. Im Rahmen der Methodenentwicklungen und Validierungen gemäß den aktuellen WADA-Richtlinien wurden sowohl multianalytische Screeningverfahren als auch Bestätigungsmethoden entwickelt. Ergänzend dazu wurden für drei neue Ghrelin Mimetika *in vitro/in vivo* Metabolismusstudien durchgeführt und erstmals Metaboliten detektiert und charakterisiert, welche zukünftig auch für Nachweisverfahren in Humanproben von besonderer Bedeutung sein könnten.

Ein besonderer Zugewinn der ersten beiden Studien liegt in der Erweiterung des analytischen Spektrums von (pseudo-)peptid- und proteinbasierte Substanzen aus DBS. Diese zu Urin und Blut komplementär einsetzbare, alternative Matrix ist bereits seit über einem Jahrzehnt Bestandteil der präventiven Dopingforschung. Ihr Einsatz kann vergleichsweise kostengünstig bewerkstelligt werden, die Probennahme ist minimal-invasiv und setzt im Gegensatz zur venösen Blutentnahme kein medizinisch geschultes Personal voraus. Für die Substanzen mit ihren speziellen physikochemischen Eigenschaften konnten sowohl manuelle (erster Artikel) als auch vollautomatische (zweiter Artikel) Probenvorbereitungen entwickelt werden. Abschließend konnten Machbarkeitsnachweise (*Proofs of Concept*), welche die Qualifizierung der neuen Methoden mit authentischen DBS-Proben belegen, präsentiert werden.

Die analytischen Herausforderungen aufgrund des geringen Probenvolumens von nur 20 µL Kapillarblut je Blutstropfen und der Komplexität der Matrix konnten mithilfe effizienter Probenvorbereitungen und modernsten analytischen Instrumenten bewältigt werden. Dadurch konnten Nachweisgrenzen im Bereich pharmakologisch relevanter Blutspiegel erreicht werden. Trotzdem war es und wird es eine der großen Herausforderungen bleiben, die Nachweisgrenzen der DBS-Analytik durch sorgfältige Probenvorbereitung und Weiterentwicklung instrumenteller Techniken stetig zu verbessern.

Die Bereitstellung komplementärer DBS-Screeningverfahren und Bestätigungsanalysen als Ergebnisse der vorliegenden Arbeit würde einerseits ein höheres Abschreckungspotential im Sinne der Dopingprävention bewirken und könnte andererseits aufgrund einer erhöhten Testfrequenz der Athleten*innen zu häufigeren Aufdeckungsraten führen.

Die gegenseitige Ergänzung von DBS und herkömmlichen Matrices (Urin/Blut) könnte dem Doping-Kontroll-System zukünftig einen großen Mehrwert verschaffen. Es besteht z. B. die Möglichkeit, dass nach einem DBS-Screeningverfahren ein auffälliger analytischer Befund festgestellt wird. Da zu diesem Zeitpunkt keine Bestätigungsanalyse für die entsprechende verbotene Substanz aus DBS verfügbar ist (siehe zweiter Artikel) oder die höhere Nachweisgrenze der Bestätigungsanalyse den eindeutigen Nachweis aus DBS erschwert (siehe erster Artikel), kann eine WADA-konforme Beurteilung noch nicht erfolgen. Nach solch einem Verdachtsfall könnte eine weitere Urin- oder Blut-Dopingkontrollprobe angefordert und analysiert werden. Aufgrund der niedrigeren Nachweisgrenzen und längeren Nachweisfenster könnten nun kleinste Wirkstoffdosen oder Dopingpraktiken, die bereits längere Zeit zurückliegen, noch nachgewiesen werden. Zum Beispiel lagen die Nachweisgrenzen von Sotatercept aus DBS in der hier vorgestellten Studie bei 0,25-0,50 µg/mL. Dahingegen konnte aus Blutserum ebenfalls mittels LC-HRMS-basierten Nachweisverfahren eine Konzentrationen von 10-50 ng/mL detektiert werden [71, 77] und mit Hilfe von Western Blots sogar Konzentrationen von subtherapeutischen Dosen im niedrigen ng/mL Bereich [90, 91]. Ähnlich verhält es sich mit den (pseudo-)peptidischen Substanzen. Während für das DBS-Screeningverfahren Nachweisgrenzen zwischen 0,5-20 ng/mL erreicht werden konnten, vermögen LC-MS-basierte Nachweisverfahren für humane Urinproben geringste Spuren von 0,02-1 ng/mL [72, 80, 81, 92] noch eindeutig nachzuweisen.

Einen weiteren perspektivischen Nutzen von DBS könnte das regelmäßige Sammeln und Lagern von DBS-Proben der Athleten*innen in Biobanken darstellen. So könnte im Bedarfsfall einer Folgeuntersuchung aufgrund eines atypischen oder auffälligen analytischen Befundes in einer routinemäßigen Dopingkontrollprobe (Blut/Urin), die aufbewahrten DBS-Proben analytenspezifisch analysiert werden [93]. Das würde eine verhältnismäßig kostengünstige Probenabdeckung über einen längeren Zeitraum gegenüber einer Momentaufnahme nach einer routinemäßigen Probennahme bedeuten und könnte ggf. die Entscheidungsprozesse unterstützen.

Die generische Anreicherung der Zielanalyten im Rahmen der Probenvorbereitung der hier vorgestellten Analyseverfahren in Kombination mit einer nicht-gerichteten (non-targeted) *Full-Scan*-Datenerfassung ermöglicht die retrospektive Datenanalyse neuer Zielanalyten, auch in älteren, eingelagerten Proben. Eine verbleibende Limitation bei der Verwendung der *Full-Scan*-Messmethode über einen definierten Masse-zu-Ladungsbereich war die niedrigere Empfindlichkeit gegenüber den gerichteten (*targeted*) Messmethoden. Aufgrund der Unverzichtbarkeit höchster Sensitivität und Selektivität in der DBS-Analytik war es von Vorteil, gerichtete Methoden wie t-SIM (engl. *targeted selected ion monitoring*) und t-MS² (engl. *targeted MS²*) Experimente für die bekannten Zielanalyten einzusetzen und die Messmodi analytenspezifisch zu optimieren. Die hier verwendeten Hybrid Quadrupol-Orbitrap Massenspektrometer vermögen es zwischen *un-/targeted* Messmodi im selben analytischen Lauf zu alternieren und die Vorteile beider Modi zu kombinieren. Das bedeutet, dass neue, bis dato den Dopingkontroll-Laboratorien noch unbekannte Substanzen auch noch nachträglich in der digitalen Matrix nachweisbar sind. Im Bedarfsfall können neue Analyten in die zielgerichteten Ansätze integriert werden und (langzeit)gelagerte DBS-Probe reanalysiert werden. Kürzlich wurde etwa von der Langzeitstabilität (> 2 Jahre) von GHRP-2 in DBS berichtet [45]. Ein*e heute missbräuchlich*e handelnde*r Athlet*in könnte also noch Jahre nach dem Vergehen sanktioniert werden.

Den Vorteilen der robotergestützten Automatisierung der DBS-Probenvorbereitungen (siehe zweiter Artikel) wie einem höheren und kosteneffizienteren Probendurchsatz stehen auch Herausforderungen gegenüber. So erforderte der hier eingesetzte DBS-Autosampler von Gerstel (Mülheim an der Ruhr, Deutschland) regelmäßige Wartungen zwischen den Anwendungen. Demzufolge wurden Wasch- und Reinigungsschritten durchgeführt, um das System von verbleibenden Matrixkomponenten zu befreien und

Verschleppungen der Analyten vorzubeugen. An anderer Stelle wurden auch Anwendungen vollautomatischer Probenextraktionen an einem weiteren DBS-Extraktionssystem von CAMAG (Muttens, Schweiz) vorgestellt [94], jedoch sind auch diese Systeme anfällig für eine Verstopfung des Extraktionskopfes und bedürfen häufigeren Wartungsintervallen nach v.a. wässrigen Extraktionen [95, 96]. Des Weiteren erfordert der Transfer manueller Methoden auf ein robotergestütztes System besondere Expertise in der Software-Programmierung und der Automatisierungstechnik. Bei sehr speziellen Probenvorbereitungen wie z. B. eine Immunoanreicherung eines Analyten über magnetische Partikel (siehe erster Artikel), kommen auch die automatisierten Lösungen an ihre Grenzen und es muss auf manuelle Strategien zurückgegriffen werden.

Im zweiten Artikel wurde außerdem vom Einsatz einer vorgeschalteten, automatisierten Hämatokritmessung mittels NIR-Spektroskopie, basierend auf einem Verfahren von Oostendorp *et al.* [61], berichtet. Die damit angestrebte Kompensation des einleitend thematisierten Hämatokriteffektes kann zukünftig für quantitative Nachweisverfahren von besonderer Bedeutung sein. Erste hier generierte Daten dazu zeigten, dass eine Trocknungszeit der DBS-Karten von 1-2 Tagen bei Raumtemperatur vor der Hämatokritmessung eingehalten werden sollte, da unter Umständen die Restfeuchtigkeit im DBS einen Einfluss auf das NIR-Spektrum haben könnte. Zusätzlich wurden für 10 Probanden*innen (5 männlich und 5 weiblich) der DBS-Hämatokrit gemessen; dieser lag sich zwischen 24 und 40%. Das sind relativ niedrige Werte im Vergleich zu Durchschnittswerten im Bereich zwischen 36 und 54% (i. d. R. von venösem Blut) [97]. Verschiedene Störfaktoren, welche auf die Art und Weise der alternativen Abnahme des kapillaren Fingerbluts oder den Unterschieden zu venösem Blut zurückzuführen sein könnten, wurden im Artikel bereits ausführlich diskutiert. In einem Folgeschritt wäre eine Vergleichsstudie mit einer größeren Anzahl an Probanden wünschenswert, in welcher Hämatokritmessungen für DBS mit verschiedenen Quellen (venös vs. kapillar) untersucht werden und/oder weitere zusätzliche Messmethoden zur Bestimmung des „wahren“ Hämatokrit-Wertes genutzt werden, wie dem Einsatz eines *Sysmex*-Analysators für venöse Vollblutproben. Daneben wurden erste Experimente zur Untersuchung der Anwendbarkeit eines neuartigen *TAP®-Devices* für den Oberarm, welcher die selbstständige DBS-Probennahme durch den*die Athleten*in weiter optimieren könnten, durchgeführt. Für das hier entwickelte Screeningverfahren

wurden DBS-Karten mit dem Kapillarblut von 10 Probanden*innen aus dem Lithium-Heparin-beschichteten Reservoir des Einmaltesters hergestellt und das Nachweisverfahren für die (pseudo-)peptidischen Substanzen für ausgewählte Parameter kreuzvalidiert. Ein ähnlicher, seit Kurzem kommerziell erhältlicher Einmaltester, das *Tasso-M20-Device*, wird bereits, wie einleitend beschrieben, in Pilotstudien durch verschiedene NADOs, getestet. Sollte sich diese Anwendung durchsetzen, sind dringend weitere Untersuchungen erforderlich, da relevante Forschungsdaten wie z. B. zu Wiederfindung, Matrixeffekten und Stabilität von dopingrelevanten Substanzen in dieser Probenmatrix noch fehlen. Allerdings wird aufgrund der Beschaffenheit und Form des *Tasso-M20-Device* eine automatisierte DBS-Probenvorbereitung, so wie in dieser Arbeit vorgestellt und für viele weiteren Anwendungen mittels den etablierten DBS-Karten bereits beschrieben [94], nicht möglich sein und es müsste auf manuelle Probenvorbereitungsprozeduren zurückgegriffen werden. Nicht unbeachtet sollten am Ende auch die höheren Materialkosten der *Devices* (20-25 \$/Stück) im Vergleich zu DBS-Karten (ca. 5 \$/Stück) bleiben.

Vor der Erarbeitung geeigneter analytischer Nachweisverfahren aus alternativen Matrices wie DBS werden i. d. R. Verfahren für die herkömmlichen offiziellen WADA-Matrices Blut und Urin entwickelt. Das Ziel ist es, schnellstmöglich ausreichend empfindliche und valide Analysemethoden zu entwickeln, um einen Missbrauch verbotener Substanzen nachweisen zu können. Der dritte Artikel beschreibt die Entwicklung und Validierung neuer analytischer Nachweisverfahren für die intakten Substanzen der drei neuen Ghrelin Mimetika Capromorelin, Macimorelin und Tabimorelin. Insgesamt wurden mehrere Tests (Screeningverfahren/Bestätigungsanalysen) für Humanurin und -blut entwickelt, welche fortan das analytische Spektrum der Routine-Nachweisverfahren für Wachstumshormon-freisetzende Faktoren in Urin ergänzen. Tabimorelin konnte bereits für das multianalytische DBS-Screeningverfahren (zweiter Artikel) berücksichtigt werden. Capromorelin und Macimorelin waren zu diesem Zeitpunkt noch nicht verfügbar, können jedoch ab sofort dort auch implementiert werden.

Für die Suche nach Metaboliten wurden im Rahmen dieser Studie verschiedene *in vivo*, *in vitro* und *in silico* Experimente durchgeführt. Da wegen ethischer Restriktionen keine humanen Ausscheidungsstudien realisierbar waren, beschränken sich die Ergebnisse auf die Auswertungen muriner Proben (Urin und Blutplasma). In präklinische Studien, die auf die Untersuchung der oralen Wirkstoffaufnahme beim

Menschen abzielen, hat sich die Ratte als Modellorganismus etabliert. So konnte bspw. für die orale Absorption von 64 Arzneimitteln mit unterschiedlichsten physikochemischen und pharmakologischen Eigenschaften eine lineare Korrelation zwischen Menschen und Ratten demonstriert werden [98]. Nichtsdestotrotz liegen einige physiologische Unterschiede beider Organismen vor, z. B. hat die Ratte einen kürzeren und schmaleren Dünndarm, einen etwas höheren pH-Wert im Magen-Darm-Trakt [99] und eine 18-mal höhere Gallenproduktion relativ zum Körpergewicht [100]. Daher stellt die Frage nach der Übertragbarkeit des Tiermodells auf den Menschen in den hier berichteten Ergebnissen der Metabolismusstudien eine Limitation dar. Durch die ergänzenden, vergleichsweise kostengünstigen *in vitro* Experimente mit humanen Lebermikrosomen konnten viele der in der Ratte detektierten Phase-I Metaboliten, insbesondere die Hydroxymetaboliten, bestätigt werden. Dennoch eignet sich dieses System nur für qualitative Aussagen bestimmter humaner Biotransformationen. Das liegt daran, dass in den isolierten Lebermikrosomen mit reduzierter Komplexität v. a. Cytochrom P450-Enzyme (CYP) und UDP-Glycosyltransferasen (diese machen den Großteil aller humanen Biotransformationen aus) in angereicherter Form vorliegen, andere Enzyme und Kofaktoren fehlen hingegen. Darüber hinaus existieren weitere *in vitro* Tools, wie z. B. die Verwendung von Hepatozyten, S9 Fraktionen, Cytosol, Supersomen und Bactosomen, deren Möglichkeiten an anderer Stelle zusammengefasst wurden [101]. Daneben ist der Einsatz von Datenbanken und computergestützten („*in silico*“) Simulationen, Vorhersagen und Berechnungen von Reaktionen, Strukturen, etc. heute allgegenwärtig. So wurden auch in dieser Studie zur Vorhersage potentieller Metaboliten unterstützende *in silico* Experimente durchgeführt. Dafür wurde einerseits das Software-Tool *XenoSite* genutzt, welches die Positionen im Molekül, an denen die intakte Substanz durch Biotransformationen modifiziert wird, vorhersagt [102] und andererseits das Software-Tool *BioTransformer*, das bereits die enzymkatalysierten biochemischen Reaktionen vorschlägt und die Strukturformeln der entstehenden Metaboliten angibt [103]. Dieses Vorgehen ersetzte nicht die wissenschaftliche Expertise und Erfahrung, gewährleistete jedoch einen möglichst vollständigen und breiten Zugang zu den antizipierten Metaboliten. Viele der einfachen, einstufigen enzymatischen Reaktionen, wie z. B. Oxidation, Reduktion oder Hydrolyse (Phase-I) bedurften keinem computergestützten Support zur gezielten Vorhersage der Metaboliten. Allerdings war aufgrund der Größe der zu untersuchenden Substanzen (~500 Da) und der damit verbundenen großen Anzahl an möglichen metabolischen

Modifizierungen an unterschiedlichen Stellen im Molekül, v. a. unter Berücksichtigung mehrstufiger Reaktionen, die Unterstützung durch *in silico* Simulationen hilfreich. So wurde bspw. durch *XenoSite* eine Position im Molekül von Macimorelin mit erhöhter Wahrscheinlichkeit für eine *N*-Dealkylierung vorausgesagt und tatsächlich, nach vermeintlichem C-N-Bindungsbruch und der Abspaltung eines Tryptophan-ähnlichen Restes, resultierten die beiden Hauptmetaboliten Macimorelin M2 und M3. An anderer Stelle wäre die Detektion des Phase-II Metaboliten M3-1 von Tabimorelin, welcher durch Reduktion und *N*-Glucuronidierung entstand, ohne Softwareunterstützung durch *BioTransformer* möglicherweise nicht zugänglich gewesen. Ein weiteres Web-Tool, *Competitive Fragment Modeling-ID (CFM-ID) 3.0*, wurde zur Unterstützung bei der Auswertung von Elektrospray-Ionisations-MS/MS (ESI-MS/MS) Daten verwendet [104]. Insgesamt trug die kombinierte Anwendung von computergestützten Techniken zu einer zeitsparenden, kosteneffizienten und umfassenden Bearbeitung der Daten bei. Dieses Vorgehen ermöglichte die Entdeckung und vorläufige Identifizierung von mehreren Phase-I und Phase-II Metaboliten der drei Ghrelin Mimetika. Die im Rattenurin identifizierten Hauptmetaboliten von Macimorelin könnten, unter der Annahme einer hinreichenden Übertragbarkeit vorliegender Stoffwechselprodukte in Humanproben, für ein erweitertes Nachweisfenster, eine verbesserte Nachweisgrenze und einen zusätzlichen, belastbaren Identifikationshinweis im Fall eines Dopingbefundes sorgen. Die Kenntnis von Metaboliten ist darüber hinaus auch hilfreich, um eine Kontamination in Dopingproben auszuschließen. Für eine vollumfängliche Charakterisierung der Hauptmetaboliten und eine erfolgreiche Dopingkontrollanalytik ist ein synthetischer Zugang zu den relevanten Metaboliten in Zukunft notwendig. Im Anschluss wäre dann eine Implementierung dieser Substanzen in ein analytisches Nachweisverfahren wünschenswert.

Diese Doktorarbeit liefert einen wichtigen Beitrag zur Realisierung von effizienten, sensitiven und eindeutigen analytischen Nachweisverfahren dopingrelevanter Peptide, peptidähnlicher Substanzen und Proteine aus DBS. Darüber hinaus wurden neue Metaboliten von drei Ghrelin Mimetika identifiziert und für diese pseudopeptidischen Substanzen analytische Nachweisverfahren aus den herkömmlichen, WADA-konformen Dopingkontrollmatrices Blut und Urin entwickelt und vollständig validiert.

1.6 Literatur

1. WADA. *The World Anti-Doping Code*. 2021 [11/18/2020]; Available from: https://www.wada-ama.org/sites/default/files/resources/files/2021_wada_code.pdf.
2. WADA. *The World Anti-Doping Code. International Standard for Laboratories January*. 2019 [25/03/2020]; Available from: https://www.wada-ama.org/sites/default/files/resources/files/isl_nov2019.pdf.
3. WADA. *The World Anti-Doping Code. International Standard. Prohibited List*. 2021 [10/12/2020]; Available from: https://www.leichtathletik.de/fileadmin/user_upload/2021_WADA_prohibited_list.pdf.
4. WADA. *Anti-Doping Testing Figures*. 2018 [09/06/2020]; Available from: <https://www.wada-ama.org/en/resources/laboratories/anti-doping-testing-figures-report>.
5. Martinez-Sanz, J.M., et al., *Intended or Unintended Doping? A Review of the Presence of Doping Substances in Dietary Supplements Used in Sports*. *Nutrients*, 2017. 9(10).
6. Walpurgis, K., et al., *Dietary Supplement and Food Contaminations and Their Implications for Doping Controls*. *Foods*, 2020. 9(8).
7. Thevis, M., T. Kuuranne, and H. Geyer, *Annual banned-substance review - Analytical approaches in human sports drug testing*. *Drug Test Anal*, 2020. 12(1): p. 7-26.
8. Schänzer, W., et al., *Long Term Metabolites - Historical Aspects and the Cologne Strategy*, in *6th Annual USADA Meeting*. 2017: Orlando, USA, .
9. Zvereva, I., et al., *Comparison of various in vitro model systems of the metabolism of synthetic doping peptides: Proteolytic enzymes, human blood serum, liver and kidney microsomes and liver S9 fraction*. *J Proteomics*, 2016. 149: p. 85-97.
10. Thomas, A., et al., *Metabolism of growth hormone releasing peptides*. *Anal Chem*, 2012. 84(23): p. 10252-9.
11. Ritam, R. and L. Sandeep, *Metabolic Screening in Drug Development: In-Vivo to In-Silico*. *J Anal Pharm Res*, 2017. 6(4).
12. Thevis, M., et al., *Sports drug testing using complementary matrices: Advantages and limitations*. *J Pharm Biomed Anal*, 2016. 130: p. 220-230.
13. Guthrie, R. and A. Susi, *A Simple Phenylalanine Method for Detecting Phenylketonuria in Large Populations of Newborn Infants*. *Pediatrics*, 1963. 32: p. 338-43.
14. Lehmann, S., et al., *Current and future use of "dried blood spot" analyses in clinical chemistry*. *Clin Chem Lab Med*, 2013. 51(10): p. 1897-909.

15. Ryona, I. and J. Henion, *A Book-Type Dried Plasma Spot Card for Automated Flow-Through Elution Coupled with Online SPE-LC-MS/MS Bioanalysis of Opioids and Stimulants in blood*. *Anal Chem*, 2016. 88(22): p. 11229-11237.
16. Tretzel, L., et al., *Use of dried blood spots in doping control analysis of anabolic steroid esters*. *J Pharm Biomed Anal*, 2014. 96: p. 21-30.
17. Peng, S.H., et al., *Oral testosterone administration detected by testosterone glucuronidation measured in blood spots dried on filter paper*. *Clin Chem*, 2000. 46(4): p. 515-22.
18. Ooms, J.A., L. Knecht, and E.H. Koster, *Exploration of a new concept for automated dried blood spot analysis using flow-through desorption and online SPE-MS/MS*. *Bioanalysis*, 2011. 3(20): p. 2311-20.
19. Tretzel, L., et al., *Dried blood spots (DBS) in doping controls: a complementary matrix for improved in- and out-of-competition sports drug testing strategies*. *Anal Methods*, 2015. 7: p. 7596.
20. Verplaetse, R. and J. Henion, *Hematocrit-Independent Quantitation of Stimulants in Dried Blood Spots: Pipet versus Microfluidic-Based Volumetric Sampling Coupled with Automated Flow-Through Desorption and Online Solid Phase Extraction-LC-MS/MS Bioanalysis*. *Anal Chem*, 2016. 88(13): p. 6789-96.
21. Thomas, A., et al., *Dried blood spots (DBS) for doping control analysis*. *Drug Testing and Analysis*, 2011. 3(11-12): p. 806-813.
22. Thomas, A., et al., *Sensitive determination of prohibited drugs in dried blood spots (DBS) for doping controls by means of a benchtop quadrupole/Orbitrap mass spectrometer*. *Anal Bioanal Chem*, 2012. 403(5): p. 1279-89.
23. Höppner, S., et al., *Mass spectrometric studies on the in vivo metabolism and excretion of SIRT1 activating drugs in rat urine, dried blood spots, and plasma samples for doping control purposes*. *J Pharm Biomed Anal*, 2014. 88: p. 649-59.
24. Hempen, C.M., E.H. Maarten Koster, and J.A. Ooms, *Hematocrit-independent recovery of immunosuppressants from DBS using heated flow-through desorption*. *Bioanalysis*, 2015. 7(16): p. 2019-29.
25. Tretzel, L., et al., *Fully automated determination of nicotine and its major metabolites in whole blood by means of a DBS online-SPE LC-HR-MS/MS approach for sports drug testing*. *J Pharm Biomed Anal*, 2016. 123: p. 132-40.
26. Verplaetse, R. and J. Henion, *Quantitative determination of opioids in whole blood using fully automated dried blood spot desorption coupled to on-line SPE-LC-MS/MS*. *Drug Test Anal*, 2016. 8(1): p. 30-8.
27. Dib, J., et al., *Screening for adiponectin receptor agonists and their metabolites in urine and dried blood spots*. *Clinical Mass Spectrometry*, 2017. 6(13-20).

28. Protti, M., et al., *Determination of oxycodone and its major metabolites in haematic and urinary matrices: Comparison of traditional and miniaturised sampling approaches*. J Pharm Biomed Anal, 2018. 152: p. 204-214.
29. Solheim, S.A., et al., *Single-dose administration of clenbuterol is detectable in dried blood spots*. Drug Test Anal, 2020.
30. Thevis, M., et al., *Do dried blood spots (DBS) have the potential to support result management processes in routine sports drug testing?* Drug Test Anal, 2020.
31. Luginbuhl, M., et al., *Automated high-throughput analysis of tramadol and O-desmethyltramadol in dried blood spots*. Drug Test Anal, 2020. 12(8): p. 1126-1134.
32. Cox, H.D., J. Rampton, and D. Eichner, *Quantification of insulin-like growth factor-1 in dried blood spots for detection of growth hormone abuse in sport*. Anal Bioanal Chem, 2013. 405(6): p. 1949-58.
33. Tretzel, L., et al., *Determination of Synacthen((R)) in dried blood spots for doping control analysis using liquid chromatography tandem mass spectrometry*. Anal Bioanal Chem, 2015. 407(16): p. 4709-20.
34. Ferro, P., et al., *Evaluation of fibronectin 1 in one dried blood spot and in urine after rhGH treatment*. Drug Test Anal, 2017. 9(7): p. 1011-1016.
35. Rosting, C., A. Gjelstad, and T.G. Halvorsen, *Water-Soluble Dried Blood Spot in Protein Analysis: A Proof-of-Concept Study*. Anal Chem, 2015. 87(15): p. 7918-24.
36. Cox, H.D., C.M. Hughes, and D. Eichner, *Sensitive quantification of IGF-1 and its synthetic analogs in dried blood spots*. Bioanalysis, 2014. 6(19): p. 2651-62.
37. Möller, I., et al., *Development and validation of a mass spectrometric detection method of peginesatide in dried blood spots for sports drug testing*. Anal Bioanal Chem, 2012. 403(9): p. 2715-24.
38. Reverter-Branchat, G., et al., *Determination of Recent Growth Hormone Abuse Using a Single Dried Blood Spot*. Clin Chem, 2016. 62(10): p. 1353-60.
39. Cox, H.D., et al., *Detection of Autologous Blood Transfusions using a Novel Dried Blood Spot Method*. Drug Test Anal, 2017.
40. Cox, H.D. and D. Eichner, *A mass spectrometry method to measure membrane proteins in dried blood spots for the detection of blood doping practices in sport*. Anal Chem, 2017. 89(18): p. 10029-10036.
41. Reverter-Branchat, G., et al., *Detection of Erythropoiesis Stimulating Agents in One Single Dried Blood Spot*. Drug Test Anal, 2018.
42. Rosting, C., et al., *Determination of the low-abundant protein biomarker hCG from dried matrix spots using immunocapture and nano liquid chromatography mass spectrometry*. J Chromatogr B Analyt Technol Biomed Life Sci, 2018. 1077-1078: p. 44-51.

43. Thomas, A. and M. Thevis, *Analysis of insulin and insulin analogues from dried blood spots by means of LC-HRMS*. Drug Test Anal, 2018.
44. Skjaervo, O., T.G. Halvorsen, and L. Reubsæet, *All-in-one paper-based sampling chip for targeted protein analysis*. Anal Chim Acta, 2019. 1089: p. 56-65.
45. Reverter-Branchat, G., J. Segura, and O.J. Pozo, *On the road of dried blood spot sampling for anti-doping tests. Detection of GHRP-2 abuse*. Drug Test Anal, 2020.
46. Salamin, O., et al., *Detection of Stimulated Erythropoiesis by the RNA-Based 5'-Aminolevulinat Synthase 2 Biomarker in Dried Blood Spot Samples*. Clin Chem, 2019. 65(12): p. 1563-1571.
47. Loria, F., et al., *Automation of RNA-based biomarker extraction from dried blood spots for the detection of blood doping*. Bioanalysis, 2020.
48. Moretti, M., et al., *A liquid chromatography-tandem mass spectrometry method for the determination of cocaine and metabolites in blood and in dried blood spots collected from postmortem samples and evaluation of the stability over a 3-month period*. Drug Test Anal, 2018. 10(9): p. 1430-1437.
49. Wannaratana, S., A. Thontiravong, and S. Pakpinyo, *Comparison of three filter paper-based devices for safety and stability of viral sample collection in poultry*. Avian Pathol, 2020: p. 1-22.
50. Jozwiak, M., et al., *Application of FTA® Cards for detection and storage of avian influenza virus*. J Vet Res, 2016. 60: p. 1-6.
51. Walpurgis, K., et al., *Combined detection of the ActRII-Fc fusion proteins Sotatercept (ActRIIA-Fc) and Luspatercept (modified ActRIIB-Fc) in serum by means of immunoaffinity purification, tryptic digestion, and LC-MS/MS*. Drug Test Anal, 2018. 10(11-12): p. 1714-1721.
52. Thevis, M., et al., *Can dried blood spots (DBS) contribute to conducting comprehensive SARS-CoV-2 antibody tests?* Drug Test Anal, 2020. 12(7): p. 994-997.
53. Karp, D.G., et al., *A serological assay to detect SARS-CoV-2 antibodies in at-home collected finger-prick dried blood spots*. medRxiv, 2020.
54. Gaugler, S., et al., *Fully automated dried blood spot sample handling and extraction for serological testing of SARS-CoV-2 antibodies*. Drug Test Anal, 2020.
55. Crimmins, E.M., et al., *Dried blood spots: Effects of less than optimal collection, shipping time, heat, and humidity*. Am J Hum Biol, 2020. 32(5): p. e23390.
56. Velghe, S., L. Delahaye, and C.P. Stove, *Is the hematocrit still an issue in quantitative dried blood spot analysis?* J Pharm Biomed Anal, 2019. 163: p. 188-196.
57. Denniff, P. and N. Spooner, *The effect of hematocrit on assay bias when using DBS samples for the quantitative bioanalysis of drugs*. Bioanalysis, 2010. 2(8): p. 1385-95.

58. Brauer, R., et al., *Preanalytical standardization of amino acid and acylcarnitine metabolite profiling in human blood using tandem mass spectrometry*. *Metabolomics*, 2011. 7: p. 344-352.
59. Zukunft, S., et al., *Targeted Metabolomics of Dried Blood Spot Extracts*. *Chromatographia*, 2013. 76: p. 1295-1305.
60. Zheng, N., et al., *"Center punch" and "whole spot" bioanalysis of apixaban in human dried blood spot samples by UHPLC-MS/MS*. *J Chromatogr B Analyt Technol Biomed Life Sci*, 2015. 988: p. 66-74.
61. Oostendorp, M., et al., *Measurement of Hematocrit in Dried Blood Spots Using Near-Infrared Spectroscopy: Robust, Fast, and Nondestructive*. *Clin Chem*, 2016. 62(11): p. 1534-1536.
62. Capiiau, S., et al., *Correction for the Hematocrit Bias in Dried Blood Spot Analysis Using a Nondestructive, Single-Wavelength Reflectance-Based Hematocrit Prediction Method*. *Anal Chem*, 2018. 90(3): p. 1795-1804.
63. Blicharz, T.M., et al., *Microneedle-based device for the one-step painless collection of capillary blood samples*. *Nat Biomed Eng*, 2018. 2(3): p. 151-157.
64. Roadcap, B., et al., *Clinical application of volumetric absorptive microsampling to the gefapixant development program*. *Bioanalysis*, 2020. 12(13): p. 893-904.
65. Marchand, A., et al., *Volumetric Absorptive Microsampling (VAMS) technology for IGF-1 quantification by automated chemiluminescent immunoassay in dried blood*. *Growth Horm IGF Res*, 2020. 50: p. 27-34.
66. Spooner, N., et al., *A device for dried blood microsampling in quantitative bioanalysis: overcoming the issues associated blood hematocrit*. *Bioanalysis*, 2015. 7(6): p. 653-9.
67. (NADA), N.A.-D.A. *CORONA-VIRUS (SARS-COV-2): UPDATE DER NADA*. 2020 18.05.2020 19.11.2020]; Available from: <https://www.nada.de/nada/aktuelles/news/newsdetail/news/detail/News/corona-virus-sars-cov-2-update-der-nada/>.
68. Fedoruk, M.N., *Virtual drug testing: redefining sample collection in a global pandemic*. *Bioanalysis*, 2020. 12(11): p. 715-718.
69. WADA. *WADA leads exciting collaboration on dried-blood-spot testing*. 2020; Available from: <https://www.wada-ama.org/en/media/news/2019-10/wada-leads-exciting-collaboration-on-dried-blood-spot-testing>.
70. WADA. *Anti-Doping Testing Figures*. 2019 12/30/2020]; Available from: <https://www.wada-ama.org/en/resources/laboratories/anti-doping-testing-figures-report>.

71. Walpurgis, K., et al., *Testing for the erythropoiesis-stimulating agent Sotatercept/ACE-011 (ActRIIA-Fc) in serum by means of Western blotting and LC-HRMS*. Drug Test Anal, 2016. 8(11-12): p. 1152-1161.
72. Goergens, C., et al., *Recent improvements in sports drug testing concerning the initial testing for peptidic drugs (< 2 kDa) - sample preparation, mass spectrometric detection, and data review*. Drug Test Anal, 2018.
73. Thomas, A., et al., *Metabolism of growth hormone releasing peptides*. Anal Chem, 2012. 84(23): p. 10252-9.
74. Carrancio, S., et al., *An activin receptor IIA ligand trap promotes erythropoiesis resulting in a rapid induction of red blood cells and haemoglobin*. Br J Haematol, 2014. 165(6): p. 870-82.
75. Ruckle, J., et al., *Single-dose, randomized, double-blind, placebo-controlled study of ACE-011 (ActRIIA-IgG1) in postmenopausal women*. J Bone Miner Res, 2009. 24(4): p. 744-52.
76. Acceleron Pharma, I. *A Study of Sotatercept for the Treatment of Pulmonary Arterial Hypertension (PAH) (PULSAR)*. 2020 14/12/2020].
77. Walpurgis, K., et al., *Combined detection of the ActRII-Fc fusion proteins Sotatercept (ActRIIA-Fc) and Luspatercept (modified ActRIIB-Fc) in serum by means of immunoaffinity purification, tryptic digestion, and LC-MS/MS*. Drug Test Anal, 2018.
78. Sherman, M.L., et al., *Multiple-dose, safety, pharmacokinetic, and pharmacodynamic study of sotatercept (ActRIIA-IgG1), a novel erythropoietic agent, in healthy postmenopausal women*. J Clin Pharmacol, 2013. 53(11): p. 1121-30.
79. Zvereva, I., G. Dudko, and M. Dikunets, *Determination of GnRH and its synthetic analogues' abuse in doping control: Small bioactive peptide UPLC-MS/MS method extension by addition of in vitro and in vivo metabolism data; evaluation of LH and steroid profile parameter fluctuations as suitable biomarkers*. Drug Test Anal, 2018. 10(4): p. 711-722.
80. Kim, Y., et al., *Development of a multi-functional concurrent assay using weak cation-exchange solid-phase extraction (WCX-SPE) and reconstitution with a diluted sample aliquot for anti-doping analysis*. Rapid Commun Mass Spectrom, 2018. 32(11): p. 897-905.
81. Thomas, A., et al., *Simplifying and expanding the screening for peptides <2 kDa by direct urine injection, liquid chromatography, and ion mobility mass spectrometry*. J Sep Sci, 2016. 39(2): p. 333-41.
82. Ferro, P., et al., *Detection of Growth Hormone Releasing Peptides in Serum by a Competitive Receptor Binding Assay*. J Chromatogr, 2017. 8(1).

83. Semenistaya, E., et al., *Determination of growth hormone releasing peptides metabolites in human urine after nasal administration of GHRP-1, GHRP-2, GHRP-6, Hexarelin, and Ipamorelin*. Drug Test Anal, 2015. 7(10): p. 919-25.
84. Poplawska, M. and A. Blazewicz, *Identification of a novel growth hormone releasing peptide (a glycine analogue of GHRP-2) in a seized injection vial*. Drug Test Anal, 2018.
85. Krug, O., et al., *Analysis of new growth promoting black market products*. Growth Horm IGF Res, 2018. 41: p. 1-6.
86. Cordido, F., et al., *Ghrelin and growth hormone secretagogues, physiological and pharmacological aspect*. Curr Drug Discov Technol, 2009. 6(1): p. 34-42.
87. Rhodes, L., et al., *Capromorelin: a ghrelin receptor agonist and novel therapy for stimulation of appetite in dogs*. Vet Med Sci, 2018. 4(1): p. 3-16.
88. Garcia, J.M., et al., *Macimorelin (AEZS-130)-stimulated growth hormone (GH) test: validation of a novel oral stimulation test for the diagnosis of adult GH deficiency*. J Clin Endocrinol Metab, 2013. 98(6): p. 2422-9.
89. NADA. *Nationaler Anti-Doping Code*. 2021 [12/15/2020]; Available from: https://www.nada.de/fileadmin/user_upload/2021_NADC21.pdf.
90. Reichel, C., et al., *Updated protocols for the detection of Sotatercept and Luspatercept in human serum*. Drug Test Anal, 2018.
91. Martin, L., et al., *A validated, sensitive electrophoretic method for the detection of activin receptor type II-Fc fusion proteins in human blood*. Drug Test Anal, 2018.
92. Judak, P., et al., *DMSO Assisted Electrospray Ionization for the Detection of Small Peptide Hormones in Urine by Dilute-and-Shoot-Liquid-Chromatography-High Resolution Mass Spectrometry*. J Am Soc Mass Spectrom, 2017. 28(8): p. 1657-1665.
93. Thevis, M., et al., *Do dried blood spots (DBS) have the potential to support result management processes in routine sports drug testing? - Part 2: Proactive sampling for follow-up investigations concerning atypical or adverse analytical findings*. Drug Test Anal, 2021.
94. Luginbühl, M. and S. Gaugler, *The Application of Fully Automated Dried Blood Spot Analysis for Liquid Chromatography-Tandem Mass Spectrometry using the CAMAG DBS-MS 500 Autosampler*. Clin Biochem, 2020.
95. Luginbühl, M., et al., *Automated High-Throughput Analysis of Tramadol and O-Desmethyltramadol in Dried Blood Spots*. Drug Test Anal, 2020.
96. Duthaler, U., et al., *Automated high throughput analysis of antiretroviral drugs in dried blood spots*. J Mass Spectrom, 2017. 52(8): p. 534-542.

97. Billett, H.H., *Hemoglobin and Hematocrit*, in *Clinical Methods: The History, Physical, and Laboratory Examinations*, rd, et al., Editors. 1990: Boston.
98. Chiou, W.L. and A. Barve, *Linear correlation of the fraction of oral dose absorbed of 64 drugs between humans and rats*. *Pharm Res*, 1998. 15(11): p. 1792-5.
99. Hurst, S., et al., *Impact of physiological, physicochemical and biopharmaceutical factors in absorption and metabolism mechanisms on the drug oral bioavailability of rats and humans*. *Expert Opin Drug Metab Toxicol*, 2007. 3(4): p. 469-89.
100. Mahmood, I. and C. Sahajwalla, *Interspecies scaling of biliary excreted drugs*. *J Pharm Sci*, 2002. 91(8): p. 1908-14.
101. Dudda, A. and G.U. Kuerzel, *Metabolism Studies In Vitro and In Vivo*, in *Drug Discovery and Evaluation: Safety and Pharmacokinetic Assays*, H.G. Vogel, Editor. 2013, Springer: Berlin Heidelberg.
102. Zaretski, J., M. Matlock, and S.J. Swamidass, *XenoSite: accurately predicting CYP-mediated sites of metabolism with neural networks*. *J Chem Inf Model*, 2013. 53(12): p. 3373-83.
103. Djoumbou-Feunang, Y., et al., *BioTransformer: a comprehensive computational tool for small molecule metabolism prediction and metabolite identification*. *J Cheminform*, 2019. 11(1): p. 2.
104. Djoumbou-Feunang, Y., et al., *CFM-ID 3.0: Significantly Improved ESI-MS/MS Prediction and Compound Identification*. *Metabolites*, 2019. 9(4).

2 Development of two complementary LC-HRMS methods for analyzing sotatercept in dried blood spots for doping controls

Tobias Lange¹, Katja Walpurgis¹, Andreas Thomas¹, Hans Geyer¹ & Mario Thevis^{1,2}

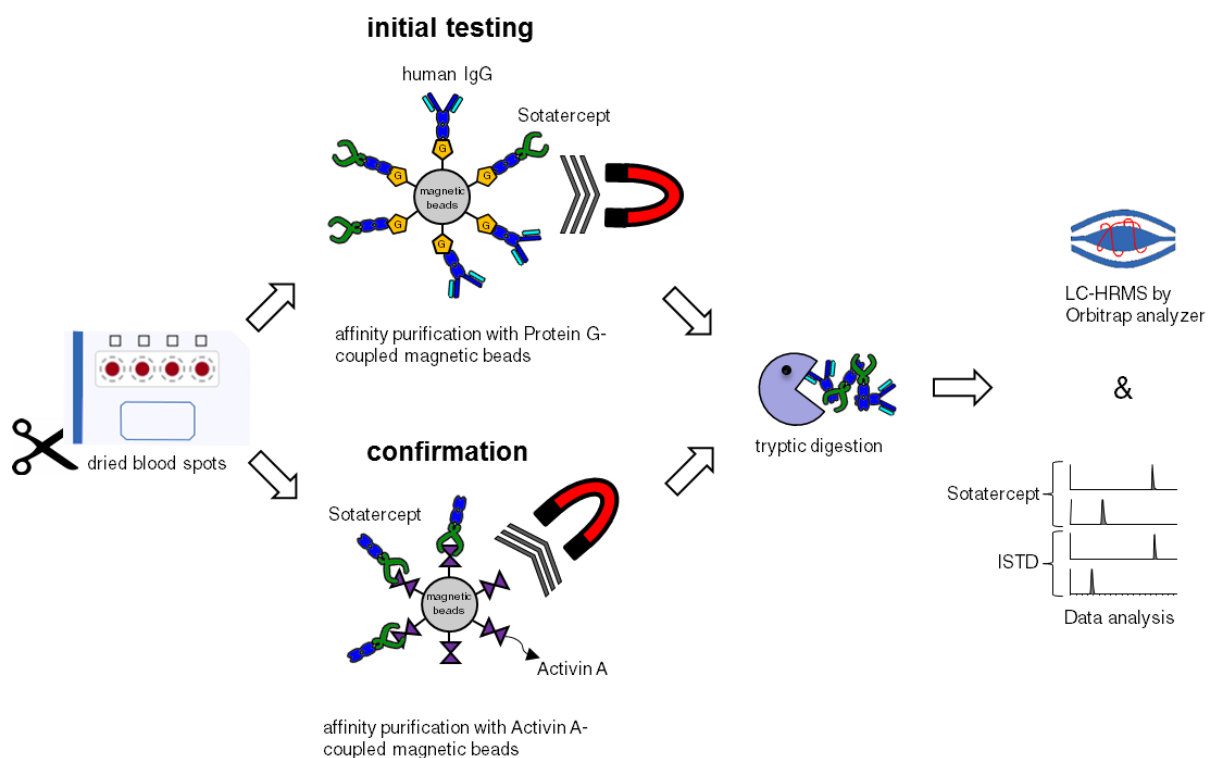
¹Center for Preventive Doping Research/Institute of Biochemistry, German Sport University Cologne, Cologne, Germany

²European Monitoring Center for Emerging Doping Agents (EuMoCEDA), Cologne/Bonn, Germany

Veröffentlicht in: *Bioanalysis* (2019), 11(10), 923-940

2.1 Abstract

Aim: Sotatercept is a therapeutic Fc-fusion protein with erythropoiesis-stimulating activity. Due to a potential abuse of the drug by athletes in professional sports, a sensitive detection method is required. In sports drug testing, alternative matrices such as dried blood spots (DBS) are gaining increasing attention as they can provide several advantages over conventional matrices. **Materials & methods:** Herein, two complementary LC–high-resolution mass spectrometry (HRMS) detection methods for sotatercept from DBS, an initial testing procedure (ITP) and a confirmation procedure (CP) were developed and validated for the first time. Both methods comprise an ultrasonication-assisted extraction, affinity enrichment, proteolytic digestion and HRMS detection. **Results & conclusion:** For the multianalyte ITP, artificial samples fortified with sotatercept, luspatercept and bimagrumab, and authentic specimens containing bimagrumab were successfully analyzed as proof-of-concept. The validated detection methods for sotatercept are fit for purpose and the ITP was shown to be suitable for the detection of novel IgG-based pharmaceuticals in doping control DBS samples.



2.2 Introduction

The current routine sampling of blood specimens in sports drug testing faces major challenges ranging from temperature-controlled shipment and storage, limited stability, and timely analysis [1] to the need of a phlebotomist for venous blood on-the-spot sampling. To overcome these limitations and increase the number of collected blood samples, the World Anti-Doping Agency (WADA) pays particular attention to the use of alternative matrices such as dried blood spots (DBS) [2]. This straightforward alternative matrix uses a minimal volume (10-20 μL) of capillary blood collected by a finger, heel or ear prick on a cellulose paper and allows high-throughput and automation of sample processing and analysis [3-5]. Its almost 100-year history and wide range of applications is summarized elsewhere [6]. DBS cards stabilize many analytes, hence are suitable for establishing biobanks, which ensure very long storage times of over 30-40 years [7]. As a simple, minimal-invasive and cost-effective microsample collection procedure robust against manipulation, it became interesting to doping analysis with the detection of testosterone in 2000 [8]. Subsequently, various DBS assays comprising small molecules [4, 5, 8-15], peptides [16-18], and proteins [19-25] have been established. Besides the improvements associated with DBS sampling, some challenges and limitations regarding sample workup, sensitivity, and reproducibility have

to be taken into account [26]. Nevertheless, it is ideal for drug monitoring, including therapeutic proteins [27].

The design and development of novel therapeutic protein drugs is becoming increasingly popular as they provide new therapeutic options for the treatment of various diseases. These recombinant protein pharmaceuticals include monoclonal antibodies, coagulation factors, enzymes, hormones, growth factors, plasma proteins, and fusion proteins (e.g. Fc-fusion [28] and albumin-fusion [29]) with post-translational modifications to enhance their biological functions. Despite elaborate production pathways of such drugs with molecular masses surpassing 100 kDa, they possess several therapeutic advantages such as a long biological half-lives, an increased functionality and specificity. Most recently, because of their wide range of clinical application areas including the treatment of anemia, muscle diseases, and metabolic disorders, novel fusion protein drugs got into the focus of cheating athletes and preventive doping research. For this reason, several detection methods for potential performance enhancing agents of the class of immunoglobulin (IgG)-based (fusion) proteins as for example sotatercept (ACE-011, ActRIIA-Fc), luspatercept (ACE-536, modified ActRIIB-Fc), ACE-031 (ActRIIB-Fc), stamulumab (MYO-029, anti-MSTN antibody), and bimagrumab (BYM338, anti-ActRII antibody) have been recently developed [30-37]. Different methods and technologies such as LC-HRMS [33], ELISA (enzyme-linked immunosorbent assay) [34], SAR-PAGE (sarcosyl-polyacrylamide gel electrophoresis) [31, 32, 34, 36], and Western blotting [31, 35, 36] enable the sensitive detection from small amounts of plasma/serum (50-300 μ L). However, detection methods for these substances from DBS are still missing so far, and principally LC-MS methods are particularly suited due to their superiority to protein immunoassays concerning specificity (see e.g. [38]) and a reduced variability of interassay results between doping-control laboratories [39]. Within this study, an initial testing procedure and a confirmation procedure (ITP and CP, respectively) for sotatercept (ActRIIA-Fc) from DBS were developed. Sotatercept (monomer: 344 amino acids) is a recombinant fusion homodimer consisting of an extracellular activin type IIA receptor (ActRIIA) domain linked to the Fc region of human IgG 1 [40, 41]. Its inhibitory mechanism of action is mediated by competitive binding to circulating activins and other members of the transforming growth factor beta (TGF- β) superfamily, thus blocking SMAD signaling [42]. Subsequently, this leads to

erythropoiesis-stimulation, similar to erythropoietin and its derivatives [43], albeit subject to a different mechanism of action, and anti-osteoporotic activity, as has been demonstrated in a series of preclinical [44-55] and clinical studies [56-79]. In professional sports, the application of sotatercept as well as all other aforementioned IgG-based (fusion) protein drugs is prohibited at-all-times by the WADA (Prohibited List January 2018; classes S0, S2 or S4) [80].

Two consecutively applied LC-HRMS detection methods for doping control purposes were desirable. One assay should allow for a general testing approach concerning decoy receptor-based substances with multianalyte detection capability as ITP and, in case of suspicious test results, the more specific second approach using a highly specific receptor-ligand interaction between activin A and sotatercept's ActRIIA domain for sample purification is used for confirmation purposes. Both LC-HRMS DBS methods for sotatercept were validated according to WADA's International Standard for Laboratories [81] with detection limits at physiologically relevant concentrations. Moreover, the ITP serves as a proof-of-concept for collecting retrospective data and to simultaneously detect different IgG-based protein drugs in a multiplexed approach, as shown exemplary for sotatercept, luspatercept and bimagrumab. In doping analysis, it is the first LC-MS-based detection method from DBS for a recombinant fusion protein exceeding 100 kDa.

2.3 Material and methods

2.3.1 Chemicals and materials

Ammonium sulfate, ammonium bicarbonate (ABC), iodoacetamide (IAA), phosphate-buffered saline (PBS; 0.01 M phosphate buffer, 0.0027 M potassium chloride, 0.137 M sodium chloride, pH 7.4), and TWEEN® 20 were purchased from Sigma-Aldrich (St. Louis, MO, USA) which is Merck (Darmstadt, Germany) since January 2017. LC grade acetonitrile and dimethyl sulfoxide (DMSO) were obtained from Merck. Tris(2-carboxyethyl)phosphine (TCEP) was supplied by Carl Roth (Karlsruhe, Germany). Honeywell Fluka™ formic acid (eluent additive for LC-MS) and pre-diluted protein assay standards of bovine serum albumin were obtained from Thermo Fisher Scientific (Bremen, Germany). Sequencing-grade modified trypsin was purchased from Promega (WI, USA). Recombinant human activin A was obtained from Peprotech (Hamburg,

Germany). Sotatercept (ActRIIA-Fc) was bought from Profacgen (NY, USA) and recombinant mouse ActRIIA-Fc Chimera, as internal standard (ISTD), was bought from R & D Systems (MN, USA). Luspatercept was purchased from Creative Biomart (NY, USA) [37], bimagrumab and stable isotope-labeled (^{13}C -Lys, ^{13}C -Arg) bimagrumab as ISTD were synthesized by Novartis (Basel, Switzerland) [33]. Sotatercept's signature peptides ALPVPIEK and SETQECLFFNANWEK, with free amine, free acid, and S-carboxyamidomethylcysteine (CAM) modification, were synthesized by Centic Biotech (Heidelberg, Germany). WhatmanTM FTA[®] DMPK-C sample collection cards (white), NHS Mag Sepharose, and Protein G Mag Sepharose Xtra were supplied by GE Healthcare (Uppsala, Sweden).

2.3.2 Sample matrices

Capillary whole blood was obtained by a finger prick from ten healthy volunteers, five male and five female. Venous whole blood was donated by healthy voluntaries in BD vacutainer[®] K2 EDTA tubes.

2.3.3 Solutions

Standard protein stock solutions of the fusion protein therapeutics and ISTDs (each 100 $\mu\text{g}/\text{mL}$) were prepared with Milli-Q water and stored at $-20\text{ }^{\circ}\text{C}$. Standard peptide stock solutions of the signature peptides (4 mg/mL) were prepared and stored under the same conditions. Working solutions of sotatercept (1 $\mu\text{g}/\text{mL}$ and 10 $\mu\text{g}/\text{mL}$), the ISTD (10 $\mu\text{g}/\text{mL}$ and 25 $\mu\text{g}/\text{mL}$), and the diagnostic peptides (ALPVPIEK: 0.86 $\mu\text{g}/\text{mL}$; SETQECLFFNANWEK: 1.95 $\mu\text{g}/\text{mL}$) were freshly prepared prior to usage.

2.3.4 Protein quantitation

During method development and optimization, the colorimetric quantitation of total protein and IgG was achieved by using the Pierce 660 nm protein assay, measured on a Victor³ 1420 Multilabel Counter (Perkin Elmer, MA, USA). The microplate procedure (10 μL sample volume) was carried out according to the manufacturer's instructions [82], and the obtained calibration curve was applied with an adaption factor of 0.57 for human IgG. For the final protocol, the IgG concentration was calculated based on measuring the absorbance at 280 nm with baseline correction at 340 nm of a 2 μL sample droplet via a NanoDrop One^C (Thermo Fisher Scientific; Bremen, Germany). The protein concentration of the IgG enriched sample was calculated using the

device's internal reference with a mass extinction coefficient of 13.7 at 280 nm for a 10 mg/mL IgG solution.

2.3.5 DBS sampling

Except where otherwise indicated, 20 μ L of whole blood fortified with the desired concentration of sotatercept (Iusatercept or bimagrumab) were spotted onto an untreated DBS card and allowed to dry for 2 h at room temperature (RT). The card was then stored overnight at 4°C in a sealed plastic bag with desiccant before sample extraction and preparation. All experiments were carried out with venous whole blood, besides samples of the method validation parameters 'specificity' and 'identification capability'. Here, capillary whole blood obtained by a finger prick was used.

2.3.6 Sample preparation

Initial testing procedure

One whole DBS was excised, quartered and transferred into a 1.5 mL Protein LoBind tube containing 300 μ L of PBS with 10 μ L of a 25 ppm ISTD. The sample was extracted from the DBS card by shaking on a ThermoMixer (15 min, RT, 1000 rpm) and ultrasonication (30 min, RT). After centrifugation at 11,000 \times *g* for 5 min, the supernatant was transferred to a new 1.5 mL Protein LoBind tube and 160 μ L of Protein-G-coupled magnetic beads were added. The sample was incubated by end-over-end mixing (1 h, RT) and magnetic beads were separated by utilization of a magnetic rack and washed three times with 500 μ L of PBS. The enriched IgGs and target compound(s) were eluted with 50 μ L of 3% acetic acid (15 min, RT, 1200 rpm) and collected in a fresh tube. Prior to tryptic digestion, the protein disulfide bonds were reduced with 500 nmol (5 μ L of a 100 mM solution) TCEP (15 min, 60°C, 900 rpm), brought to a pH of 7.5-8 with 25 μ L of 2 M ABC and alkylated with 1625 nmol (6.5 μ L of a 250 mM solution) IAA (30 min, RT, darkness). Total protein content was measured by using a NanoDrop One^C and proteins were digested with a tosyl phenylalanyl chloromethyl ketone (TPCK)-treated trypsin solution (200 μ g/mL in 50 mM ABC) with a protease:protein ratio of 1:50 (*w/w*; typically between 1 and 2 μ g) at 37°C and 500 rpm for 16 h. Trypsin activity was stopped with 2 μ L of acetic acid and undigested material was removed by centrifugation (10 min, RT, 11,000 \times *g*). If not otherwise indicated, the obtained sample was diluted 1:10 with 2% acetic acid, transferred to a 0.3 mL microtube, and 10 μ L were injected into the LC-MS system.

Confirmation procedure

For extraction, the whole spot was excised, quartered and transferred into a 2 mL Protein LoBind tube containing 800 μL of a freshly prepared 150 mM ABC solution fortified with 1 μL of a 100 ppm ISTD. The sample was extracted from the DBS card by ultrasonication (30 min, RT). Concentration of serum proteins was achieved by dropwise addition of an equal volume of saturated ammonium sulfate solution and incubation for 30 minutes at RT before centrifugation at 11,000 $\times g$ for 10 minutes. After protein precipitation, the pellet, containing the analyte was dissolved in a total of 150 μL of PBST (PBS with 0.02% TWEEN® 20, pH 7.4) and transferred to a 1.5 mL Protein LoBind tube with 200 μL of PBST containing 16.67 μL activin A conjugated 20% (v/v) magnetic beads solution. Magnetic beads consist of NHS Mag Sepharose and were prepared according to the manufacturer's instructions [83] with 0.1 μg activin A/ μL . The sample was incubated by end-over-end mixing (1 h, RT) and magnetic beads were separated by utilization of a magnetic rack and washed with 500 μL of PBST (once) and 500 μL of PBS (twice). The target compound was eluted with 50 μL of 3% acetic acid (15 min, RT, 1,200 rpm) and collected in a fresh tube. Magnetic beads were reconstituted by washing with 3% acetic acid (twice) and PBST (three times) and stored at 4°C for further usage. Prior to trypsin digestion, the protein disulfide bonds were reduced with 500 nmol (5 μL of a 100 mM solution) TCEP (15 min, 60°C, 900 rpm), neutralized with 25 μL of 2 M ABC and alkylated with 1625 nmol (6.5 μL of a 250 mM solution) IAA (30 min, RT, darkness). As acetonitrile improves digestion efficiency, 10% (v/v) acetonitrile were added to the vial and proteins were digested with 10 μL of a TPCK-treated trypsin solution (40 $\mu\text{g}/\text{mL}$ in 50 mM ABC) at 37°C and 500 rpm for 16 h. Trypsin activity was stopped with 2 μL of acetic acid, the sample was transferred to a 0.3 mL microtube and 5-15 μL were injected into the LC-MS system.

DBS from clinical samples

DBS were prepared on the basis of authentic clinical serum specimens collected post-administration of bimagrumab (kindly provided by Novartis, Basel, Switzerland). Serum was carefully mixed by several resuspensions with fresh blood cells obtained from a male volunteer to produce artificial DBS with a hematocrit of approximately 40%. Within the clinical study, healthy male volunteers with an average age of 73 years received either bimagrumab or placebo (intravenously or subcutaneously). Both pre- and post-

administration samples were obtained and the resulting DBS were subjected to the Protein G purification protocol (ITP) to demonstrate its fitness for purpose.

2.3.7 LC-MS/MS

The MS instruments were operated in positive ionization mode using nitrogen as source and collision gas (CMC, Eschborn, Germany). Due to enhanced sensitivity with regards to proteomic experiments using electrospray ionization [84], DMSO was added to the mobile phase B. Calibration was carried out according to the manufacturer's specification ensuring a mass error below 5 ppm. Thermo Xcalibur software, version 3.0.63, was used to evaluate the MS data.

Initial testing procedure

The UHPLC system was a Vanquish (split sampler FT with column compartment H) from Thermo Fisher Scientific (Dionex Softron, a part of Thermo Fisher Scientific, Germering, Germany) interfaced to a Q Exactive HF-X Hybrid Quadrupole-Orbitrap mass spectrometer from Thermo Fisher Scientific (Bremen, Germany). The LC was equipped with a Poroshell 120 EC-C8 analytical column, 3.0 x 50 mm, 2.7 μm particle size (PS) from Agilent Technologies (CA, USA), running a flow rate of 300 $\mu\text{L}/\text{min}$. The temperature of the split sampler FT was set to 10°C. The mobile phases consisted of A: 0.1% formic acid, and B: acetonitrile, 0.1% formic acid, and 1% DMSO. After equilibration with 1% B over 1 min, the chromatographic separation was achieved by a gradient from 1% to 40% B over 9.5 min, increasing to 100% B in 0.4 min, and re-equilibration at 1% B for 3.1 min. The overall runtime was 14 min. The MS was operated at an ionization voltage of 3.3 kV, a transfer capillary temperature of 320 °C and a column compartment temperature of 31 °C. Parameters of the full scan MS experiment, followed by a targeted-selected ion monitoring (SIM)/dd-MS² experiment were set as follows. Full MS: Resolution of 60,000 (FWHM at $m/z = 200$), AGC target of 3e6, maximum IT of 200 ms, and scan range from 330 to 2000 m/z ; targeted-SIM with an inclusion list of four peptides (sotatercept and ISTD; see Table 2.1): resolution of 60,000 (FWHM at $m/z = 200$), AGC target of 2e5, maximum IT of 100 ms, loop count of 2, MSX count of 2, isolation window of 4.0 m/z , and scan range from 150-2000 m/z ; dd-MS²: resolution of 30,000 (FWHM at $m/z = 200$), AGC target of 5e5, maximum IT of 100 ms, isolation window 2.0 m/z and a normalized collision energy of 35%.

Confirmation procedure

LC separation was carried out on a Thermo Dionex Ultimate 3000 UHPLC system interfaced with a Q Exactive HF Hybrid Quadrupole-Orbitrap mass spectrometer from Thermo Fisher Scientific with a flow rate of 300 $\mu\text{L}/\text{min}$. The system was equipped with an Accucore phenyl/hexyl trapping column, 3 mm x 10 mm, 2.6 μm PS from Thermo Fisher Scientific, preceded by a Poroshell 120 EC-C18 analytical column, 3.0 x 50 mm, 2.7 μm PS from Agilent Technologies. The temperature of the XRS Open Autosampler was set to 10°C. The mobile phases consisted of A: 0.2% formic acid and B: acetonitrile, 0.2% formic acid and 2% DMSO. Peptides were loaded on the trapping column with 1% B over 2 min, then separated on a gradient from 1% - 40% B over 10 min, increasing to 100% B for 0.4 min, and re-equilibration at 1% B for 3 min. The overall runtime was 15 min. The MS was operated at an ionization voltage of 3.5 kV and a transfer capillary temperature of 320 °C. Parameters of the full MS plus targeted-SIM/dd-MS² experiment were set as follows. Full MS: Resolution of 30,000 (FWHM at $m/z = 200$), AGC target of 3e6, maximum IT of 200 ms, and scan range from 330 to 2000 m/z ; targeted-SIM with an inclusion list of 4 peptides (sotatercept & ISTD; see Table 2.1): resolution of 30,000 (FWHM at $m/z = 200$), AGC target of 5e5, maximum IT of 100 ms, loop count of 2, MSX count of 2, isolation window of 4.0 m/z and scan range from 150 to 2000 m/z ; dd-MS²: resolution of 15,000 (FWHM at $m/z = 200$), AGC target of 5e5, maximum IT of 100 ms, isolation window 3.0 m/z , and a NCE of 35%. Chromeleon software, version 6.80 SR13 Build 3818, was used to monitor the progress of the chromatographic run.

2.3.8 Method validation

Both LC-HRMS methods for sotatercept, ITP and CP were validated according to WADA's International Standard for Laboratories [81] for non-threshold substances. The following validation parameters were determined: specificity, limit of detection (LOD), identification capability, linearity, intermediate precision, recovery, digestion efficiency, carryover, and matrix interference. For specificity, capillary whole blood samples collected by a finger prick from ten healthy volunteers (five male and five female) were used to test for the presence of interfering signals. The same ten DBS samples were fortified with 1 $\mu\text{g}/\text{mL}$ of sotatercept to demonstrate the method's identification capability. The LOD of the method was estimated with a signal-to-noise (S/N)

ratio > 3 and six sample replicates were analyzed at a low concentration (0.25 µg/mL and 0.50 µg/mL). A concentration series from venous whole blood with 0.00, 0.25, 0.50, 1.00, 2.50, 5.00, 7.50, and 10.00 µg/mL of sotatercept was prepared to study linearity. The intermediate precision of the method was estimated by the evaluation of the relative standard deviation of six sample replicates at four different concentrations (0.25, 0.50, 2.00, and 5.00 µg/mL). The recovery of the method was investigated in two ways. Firstly, recovery of the affinity purification was evaluated by comparing ISTD-normalized peak areas of six sample replicates (2.00 µg/mL) prepared with the aforementioned protocol with another set of six sample replicates fortified with the same concentration but after the elution step. Secondly, recovery after the proteolytic digestion was studied by a similar comparison of the first six sample replicates. This time, the second set of sample replicates was fortified with both peptide standards corresponding to concentration of 2.00 µg/mL of intact sotatercept. Finally, the digestion efficiency was calculated by comparing digested matrix samples fortified with the protein standard to samples fortified with the peptide standards. To determine the carryover of the method with regard to the LC-MS instrumentation, a prepared blank sample was measured directly after a high concentrated sample (e.g., 5.00 µg/mL). The comparison of three replicates fortified with an identical amount of a digested sotatercept standard (~1.65 ng), once in a blank matrix, and the other time in a neat solution, provided information about potential matrix effects [85].

2.4 Results and discussion

Firstly, the aim of this study was to develop and validate an ITP for sotatercept, which also enables a simultaneous detection of other IgG-based protein drugs. Secondly, a CP for sotatercept from DBS was required. While the ITP, as a multianalyte method, facilitates the detection of sotatercept plus other IgG-based proteins by collecting retrospective data, the confirmation procedure includes targeted analyte enrichment and has to be highly specific and selective. The unambiguous MS identification was ensured by the detection of unique signature peptides of sotatercept and the other tested protein drugs (luspatercept, bimagrumab) and their respective ISTDs after proteolytic digestion [30, 33, 37]. The location of the signature peptides, exact positions within the proteins, amino acid sequences, charge states, and *m/z* values are summarized in Table 2.1.

Table 2.1: Signature peptides of the target proteins for mass spectrometric detection.

Analyte	Domain	Position	Tryptic peptide	Amino acid sequence	Charge state	m/z
Sotatercept/ACE-011	ActRIIA	5-19	#2	SETQECLFFNANWEK	2	951.9200
	Fc	224-231	#24	ALPVP ^{I} EK	2	433.7709
Luspatercept/ACE-536	ActRIIB	4-16	#2	ECIYYNANWELER	2	880.3909
	ActRIIB	33-40	#6	LHCYASWR	2	546.7558
	ActRIIB	52-63	#9	GCWDDDFNCYDR	2	811.7854
rmActRIIA-Fc (ISTD sotatercept and luspatercept)	ActRIIA	25-39	#3	SETQECLFFNANWER	2	965.9231
	Fc	254-261	#26	DLPAPIER	2	455.7533
Bimagrumab/BYM338	Heavy chain	24-38	#4	ASGYTFTSSYINWVR	2	876.4230
	Heavy chain	99-119	#11	GGWFDYWGQGLTVTVSSASTK	2	1124.0395
¹³C-bimagrumab_† (ISTD)	Heavy chain	24-38	#4	ASGYTFTSSYINWVR [†]	2	879.4331
	Heavy chain	99-119	#11	GGWFDYWGQGLTVTVSSASTK [†]	2	1127.0495

[†]Stable isotope-labeled [¹³C-Lys, ¹³C-Arg].

The Valine (V; printed in bold) within the Fc-tag of sotatercept indicates the IgG domain modification compared to the endogenous protein.

ISTD: Internal standard.

2.4.1 Method development

Through ITP assay development, difficulties arising from the complexity of blood as sample matrix (according to the literature, the protein concentrations can differ in abundance by a factor of 10¹⁰ [86]) had to be managed. Various sample workup strategies as, for example different protein precipitation methods, the use of hexapeptide ligand libraries (ProteoMiner, HemoVoidTM and HemoglobindTM) and a plasma separation by using a homemade multilayered prototype dried plasma spot card were tested; a more detailed description can be found in the Supplementary Information (Method development & optimization section, Figures S2.1-6 & Table S2.1). Finally, the use of Protein G-coupled magnetic beads for selective trapping of IgGs [87, 88], as well as other IgG-derived protein drugs such as sotatercept, due to binding to the Fc and Fab region, was chosen. A schematic overview of the method is shown in Figure 2.1 A and C. After excision of the blood spot, PBS served as extraction buffer as well as binding buffer, which ensured interactions between sotatercept and the Protein G-coupled magnetic

beads in the next step. The elution was carried out with 3% acetic acid, followed by an overnight tryptic digestion (16 h). To effectively isolate sotatercept from DBS, four crucial parameters were optimized: extraction/binding buffer volume, Protein G beads volume, protein-to-enzyme ratio and digestion time (Figure 2.2). Optimal conditions were found with a buffer volume of 300 μ L, a 1:8 blood-to-beads ratio, a 1:50 trypsin-to-protein ratio, and a 16 h tryptic digestion.

Since immunoaffinity purification is the method of choice for a targeted analyte enrichment in highly complex matrices such as DBS [19, 25, 89-91] or serum/plasma [92-95], this strategy was chosen for the confirmation procedure. Moreover, it represents an additional identification point [96] through highly specific receptor ligand interaction. A procedure (Figure 2.1 A & B) using activin A-coupled magnetic beads for selective trapping of sotatercept could be successfully adapted from Walpurgis *et al.* [30]. The extraction of DBS was found to be most effective and reproducible with a 150 mM ABC solution followed by precipitation with a saturated ammonium sulfate solution. Then, the precipitate was solubilized in a minimal volume of 150 μ L of PBST (coupling buffer) and incubated with activin A-coupled magnetic beads as described in Materials & methods section. The elution, reduction, alkylation, and digestion of the proteins were performed as in the ITP. For a more detailed description of assay development and optimization please see the Supplementary Information (Method development & optimization section).

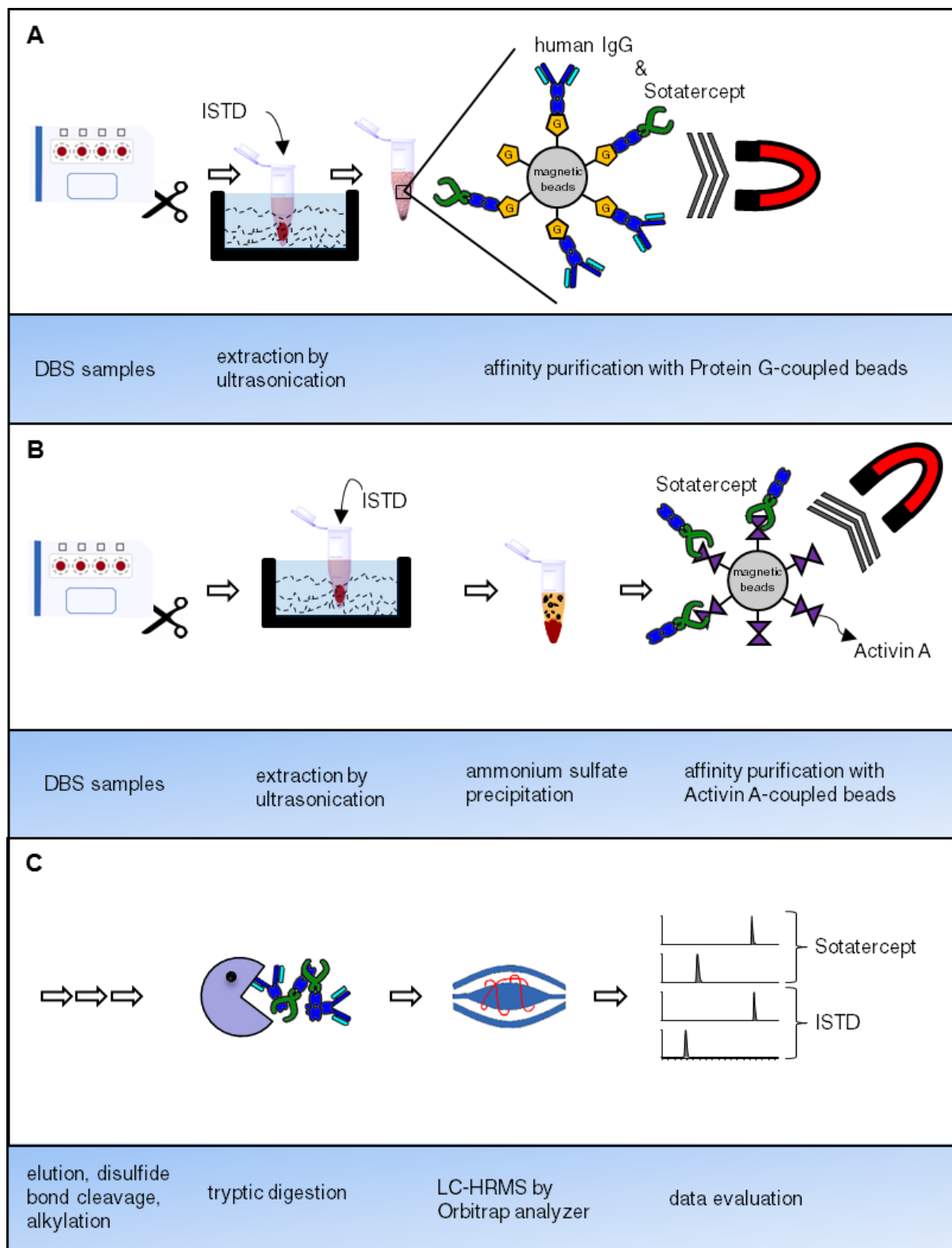


Figure 2.1: Method overview of the initial testing procedure (ITP) & confirmation procedure (CP). Detection of sotatercept from DBS with Protein G-based affinity purification (ITP) (A & C) and activin A-based affinity purification (CP) (B & C). DBS: Dried blood spot; ISTD: Internal standard

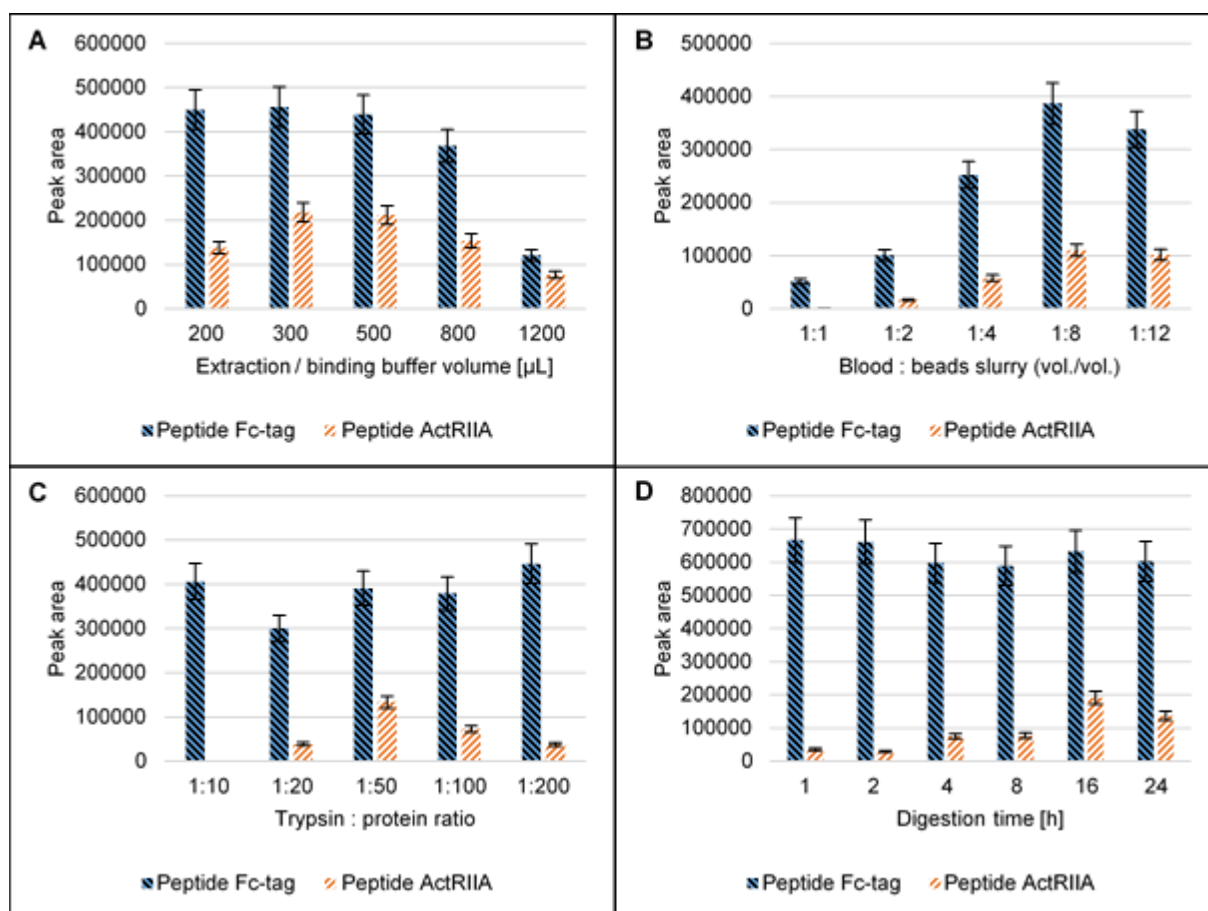


Figure 2.2: Assay development and optimization of the initial testing procedure. Four parameters that are crucial for the efficiency of the method were optimized. Extraction/binding buffer volume (A), blood-to-beads ratio (B), protein-to-enzyme ratio (C) and digestion time (D). In each experiment, one parameter was changed, while the others were kept close to the expected optimum. LC-MS results were evaluated with respect to the peak areas of the tryptic signature peptides. Optimal conditions were found with 300 μL of the buffer volume (A), with 160 μL of Protein G beads (blood : beads slurry volume of 1:8) (B), with a trypsin-to-protein ratio of 1:50 and an overnight digestion at 37 °C for 16 hours. Tosyl phenylalanyl chloromethyl ketone-treated trypsin T1426 (Sigma Aldrich) was used to cleave the proteins.

2.4.2 Method comparison

Immunocapture methods exhibit advantages and limitations [97]. On the one hand, Protein G beads (ITP) are commercially available and cost-effective. As the beads are not recycled after usage, sample carryover is excluded. The most obvious strength of this multianalyte method is the collection of full-scan MS data, which can be used for a retrospective detection of further IgG-based drugs with performance enhancing properties while identifying target compounds via targeted SIM experiments. On the other hand, Protein G beads co-isolate various endogenous IgGs of all classes. Hence, after tryptic digestion, these peptides lead to a significant number of analytical signals, which can negatively affect the target analytes' S/N ratio. For this reason, samples were

diluted 1:10 with 2% acetic acid just before injection into the LC-MS system and state-of-the-art mass spectrometric instrumentation (Q Exactive HF-X) was employed to allow for LODs similar to the CP approach (see Method validation section). The more laborious CP is an optimal complement to the ITP, as clean extracts are obtained due to highly specific receptor-ligand interactions (Figure 2.3).

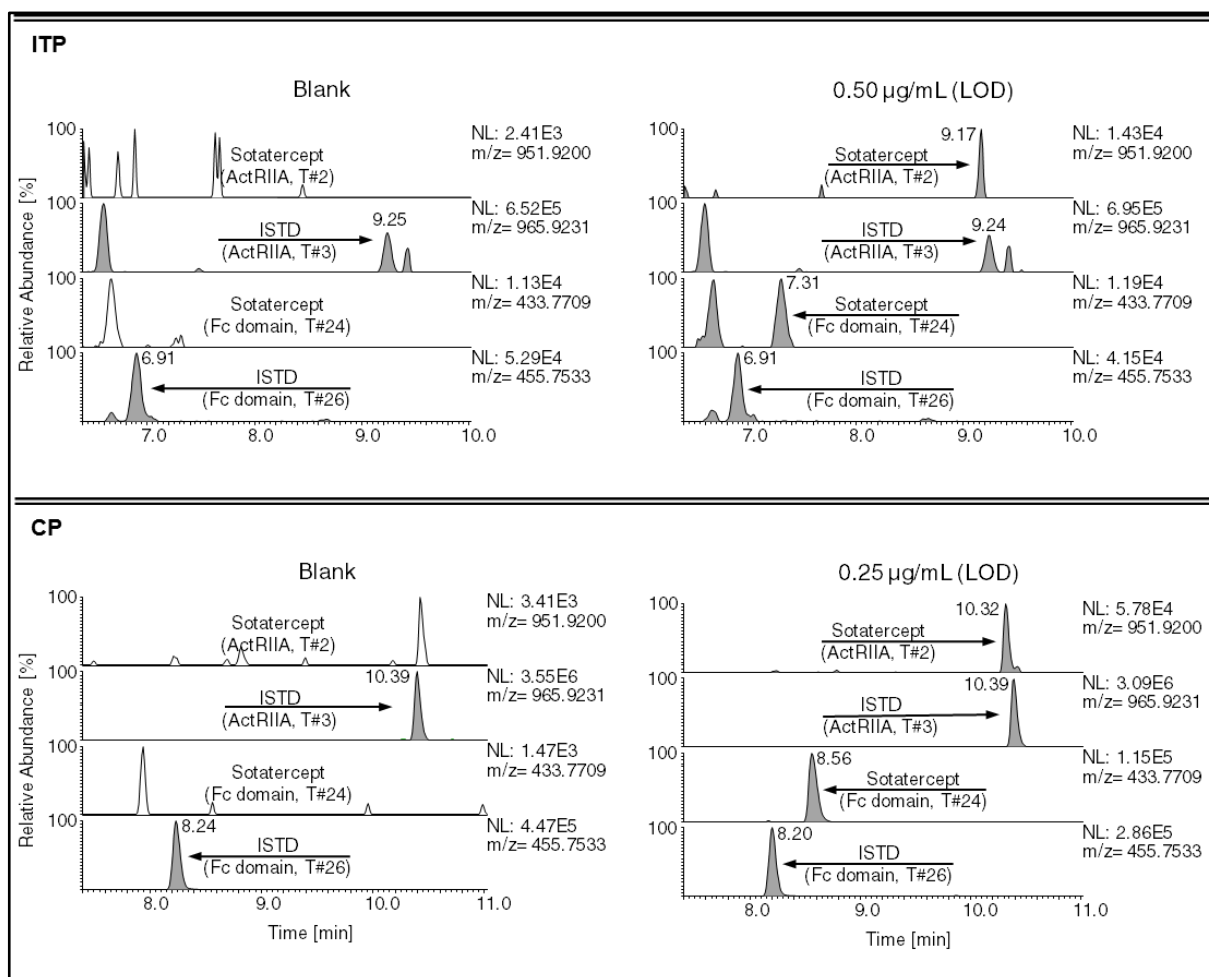


Figure 2.3: Extracted ion chromatograms (mass tolerance: ± 5 ppm) of a dried blood spot blank sample and a dried blood spot sample fortified with $0.25 \mu\text{g/mL}$ (=limit of detection) of sotatercept. Samples were either purified via Protein G strategy (initial testing procedure) or via activin A strategy (confirmation procedure), and LC-HRMS analysis was performed on a Q Exactive HF-X (initial testing procedure) and on a Q Exactive HF mass spectrometer (confirmation procedure), respectively.

ISTD: Internal standard; ITP: Initial testing procedure; LOD: Limit of detection

2.4.3 Method validation

Method validation results are summarized in Table 2.2. For each method, exemplary extracted ion chromatograms of a DBS blank and a DBS sample at the LOD of sotatercept are shown in Figure 2.3. The LOD was estimated at $0.25 \mu\text{g/mL}$ by applying a S/N ratio > 3 regarding the detection of both signature peptides (CP). For the ITP,

a LOD of 0.25 µg/mL (T_{24}) and 0.50 µg/mL (T_2), respectively, was estimated. Whenever one of the two signature peptides is identified by the ITP, the CP is applied to verify or falsify the ITP result. At a concentration of 1 µg/mL, both the specificity and identification capability were demonstrated for ten DBS from healthy volunteers (five male and five female). No interfering signals were observed in any of the blank samples (specificity), whereas after the analysis of the fortified samples all signals were clearly identified (identification capability). In the concentration range from 0.25 to 10 µg/mL, the assays were found to be linear with a coefficient of correlation of $r = 0.979$ (T_2 ; ITP) and $r = 0.996$ (T_2 ; CP) together with $r = 0.981$ (T_{24} ; ITP) and $r = 0.998$ (T_{24} ; CP). The precision was determined at the LOD and three higher concentrations and the coefficient of variation (CV) varied from 5.6 to 20.7%. The recovery of both methods was investigated after the affinity purification and showed satisfying results with recoveries from 55 to 69%. A carryover of 5.3% (ITP) and 1.4% (CP) of the signal of T_2 was determined after analyzing a sample containing sotatercept at high concentration (5 µg/mL) and has to be handled with special care. In both methods, no carryover was observed for T_{24} . The presence of matrix effects was investigated by comparing matrix samples to neat samples, each spiked with the identical amount of a digested protein standard. The addition of the standard was performed immediately before LC-MS injection and matrix effects were found to be 27% (ITP) and 68% (CP). Obviously, due to the increased sample complexity based on the sample workup, signal suppression was higher for the ITP than for the CP.

In addition, the overall recovery (after digestion) was estimated by using synthesized peptide standards as described before (ITP: $T_2 = \text{N/A}$ & $T_{24} = 63\%$; CP: $T_2 = 13\%$ & $T_{24} = 43\%$).

The peptide standard T_2 was found to be unstable when spiked into the blank samples (ITP), which were 1:10 diluted with 2% acetic acid before (not applicable; [N/A]). In contrast to eluates from authentic DBS samples, here, the pure peptide standard was most likely adsorbed on the vial surface due to its surface activity and only small remaining traces in the solution could be identified. This behavior probably caused by the lack of surrounding matrix was not observed for the CP as the fortified samples were not prediluted before LC-MS injection. The larger differences between T_2 and T_{24} (CP) led to the assumption of a different accessibility of sotatercept's cleavage sites for trypsin, which was reflected in the trypsin efficiency (ITP: $T_2 = \text{N/A}$ & $T_{24} = 91\%$; CP:

$T_2 = 15\%$ & $T_{24} = 75\%$). Trypsin efficiency was calculated by comparing digested matrix samples spiked with the protein standard to samples spiked with the peptide standards.

Table 2.2: LC-HRMS dried blood spots validation results of sotatercept for the initial testing procedure and the confirmation procedure.

Validation parameter	Concentration	Results	
		T_2 (951.92)	T_{24} (433.77)
Specificity ITP (n=10)	-	✓	✓
Specificity CP (n=10)	-	✓	✓
Identification Capability ITP (n=10)	1.00 µg/mL	✓	✓
Identification Capability CP (n=10)	1.00 µg/mL	✓	✓
Linearity ITP	0.25 µg/mL - 10 µg/mL	r = 0.979	r = 0.981
Linearity CP	0.25 µg/mL - 10 µg/mL	r = 0.996	r = 0.998
Limit of detection (LOD) ITP	0.25 µg/mL	S/N > 3 ✓	
Limit of detection (LOD) CP	0.25 µg/mL	S/N > 3 ✓	
Precision ITP (n=6)	0.25 µg/mL	-	CV = 10.2%
	0.50 µg/mL	CV = 20.5%	CV = 15.8%
	2.00 µg/mL	CV = 7.9%	CV = 6.9%
	5.00 µg/mL	CV = 20.2%	CV = 9.2%
Precision CP (n=6)	0.25 µg/mL	CV = 5.6%	CV = 15.8%
	0.50 µg/mL	CV = 19.4%	CV = 18.9%
	2.00 µg/mL	CV = 17.3%	CV = 20.7%
	5.00 µg/mL	CV = 10.7%	CV = 7.2%

Recovery: purification ITP (n=6)	2.00 µg/mL	62%	69%
Recovery: purification CP (n=6)	2.00 µg/mL	61%	55%
Carryover ITP	5.00 µg/mL	5.3%	-
Carryover CP	5.00 µg/mL	1.4%	-
Matrix interferences ITP	~1.65 ng	27%	27%
Matrix interferences CP	~1.65 ng	68%	68%

CP: Confirmation procedure; ITP: Initial testing procedure; LOD: Limit of detection; S/N: Signal-to-noise ratio.

2.4.4 ITP Proof-of-concept

The ITP was developed as a multianalyte approach. Its capability to simultaneously detect several IgG-based fusion drugs within the same sample with only one sample extraction and LC-MS measurement was demonstrated here. DBS were produced as described before with the fusion proteins sotatercept, luspatercept, and the therapeutic monoclonal antibody (mAb) bimagrumab. The experiment was carried out at analyte concentrations of 1, 2.5, and 5.0 µg/mL applying a 4 h and a 16 h tryptic digestion. All tested protein analyte concentrations were detected also after the shorter digestion time. Despite a yet incomplete digestion, this multianalyte approach was therefore found to be suited for a quick initial testing. An extracted ion chromatogram of a DBS blank and a DBS sample fortified with 5.0 µg/mL (16 h digestion) is illustrated in Figure 2.4. To unambiguously identify the protein drugs by MS, at least two unique signature peptides per analyte were detected. A recombinant mouse ActRIIA-Fc was used as ISTD for sotatercept and luspatercept, while for bimagrumab, a stable isotope-labeled [¹³C-Lys, ¹³C-Arg] variant served as ISTD. The ITP was shown to be fit for purpose for the analysis of real-doping control specimens (see next section) and demonstrated simplicity, cost efficiency, expandability to other analytes of IgG-based protein pharmaceuticals for collecting targeted MS data in the future, and retrospective data analysis. For luspatercept and bimagrumab, highly specific LC-MS methods employing serum as biological matrix have been reported [33, 37] and could be used for confirmation purposes. This strategy would be applicable due to the very long detection window of

several weeks of this analyte class. The implementation of DBS for the analysis of protein drugs would allow for an increased sample throughput.

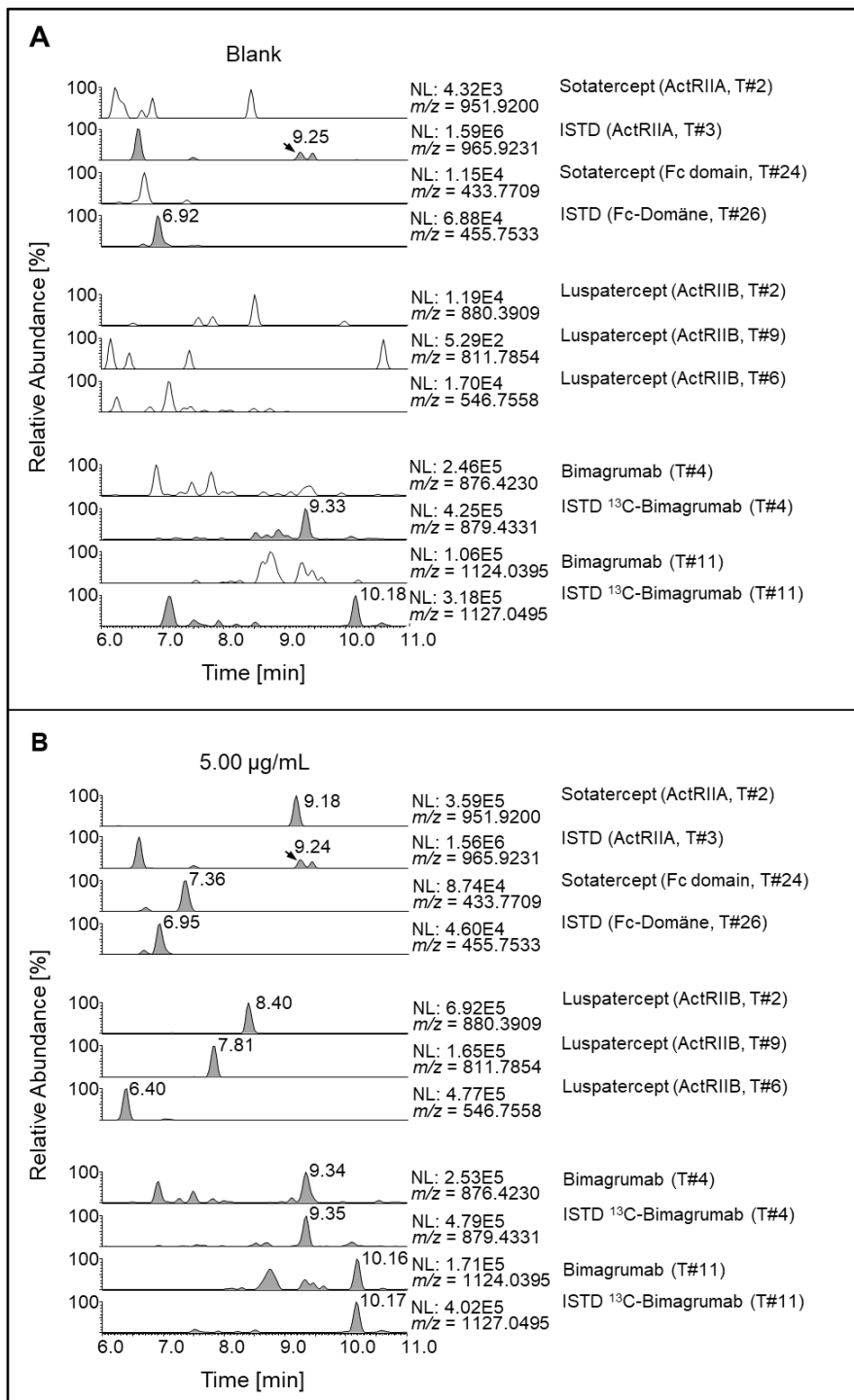


Figure 2.4: Extracted ion chromatograms (mass tolerance: ±10 ppm) of a dried blood spot blank sample (A) and a dried blood spot sample fortified with 5.0 µg/mL of sotatercept, luspatercept, and bimagrumab (B). The ¹³C-bimagrumab serves as a stable isotope-labeled (¹³C-Lys, ¹³C-Arg) ISTD. Samples were purified via Protein G strategy (ITP) and measured on a Q Exactive HF-X Hybrid Quadrupole-Orbitrap mass spectrometer.

ISTD: Internal standard; ITP: Initial testing procedure

2.4.5 DBS from clinical samples

In order to demonstrate the applicability of the presented ITP to post-administration samples, DBS were prepared on the basis of authentic clinical serum specimens containing bimagrumab. As illustrated in Figure 2.5, no signals indicating the presence of the performance-enhancing substance were observed in the pre-administration samples (blank intravenously and blank subcutaneously). At retention time 9.39 min, an interfering signal in the blank samples, appearing at a similar retention time as the signature peptide, was attributed to an unknown analyte exhibiting an m/z of 875.4320 ($z = 1$). By contrast, for both bimagrumab post-administration samples, the signature peptides from the heavy chain at $m/z = 876.4230$ and $m/z = 1124.0395$ were unambiguously identified. To prevent contamination of the LC-MS system, samples were diluted by a factor of 1:10-1:200 with 2% acetic acid prior to analysis. This qualitative analysis of bimagrumab using artificial DBS samples demonstrated the successful applicability of the ITP to authentic post-administration samples.

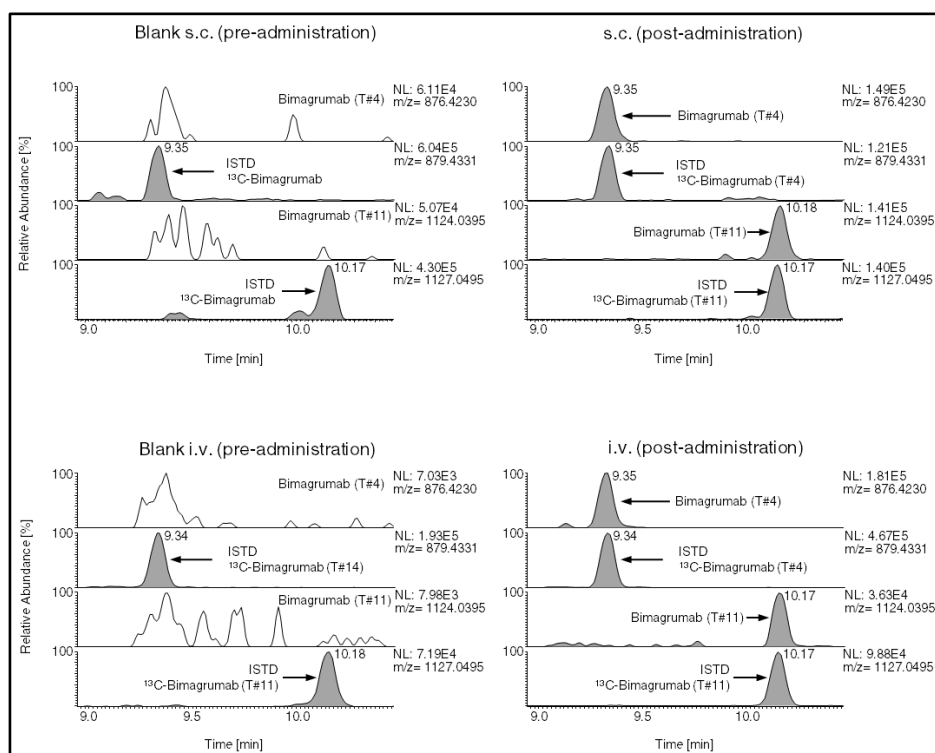


Figure 2.5: Extracted ion chromatograms (mass tolerance: ± 10 ppm) of pre-administration samples (blank subcutaneously and blank intravenously) and post-administration samples (subcutaneously and intravenously) of a bimagrumab clinical study by Novartis. The ^{13}C -bimagrumab serves as a stable isotope-labeled (^{13}C -Lys, ^{13}C -Arg) ISTD. Samples were purified via Protein G strategy (ITP) and measured on a Q Exactive HF-X Hybrid Quadrupole-Orbitrap mass spectrometer.

ISTD: Internal Standard; ITP: Initial testing procedure; i.v.: Intravenous; s.c.: Subcutaneous

2.5 Conclusion

Therapeutic Fc-fusion proteins such as sotatercept and luspatercept have different metabolic fates compared to lower molecular mass drugs. Similar to human IgGs, the Fc domain is recognized by endothelial cells followed by lysosomal degradation or it is recycled via endosomes [98]. Fc engineering is a method to increase biological half-lives to a week or more. Consequently, the medical benefit of increased efficacy also lends itself to a potential abuse by athletes, if there is any possible performance enhancing effect, and therefore, detection methods, especially in alternative matrices are warranted. Within this study, sensitive LC-HRMS ITP and CP methods for sotatercept in DBS were successfully developed and characterized. In preventive doping research, they are the first LC-MS-based detection methods for a fusion protein from DBS, which were validated according to WADA guidelines. So far, no method for this class of substances existed that enables a simultaneous detection of different IgG-based drug analytes relying on the collection of retrospective data due to a generic extraction neither from serum/plasma nor from DBS. Here, the multianalyte ITP's capability was successfully demonstrated for other IgG-based pharmaceuticals than sotatercept. In addition, the assay was found to be fit for purpose after analyzing DBS prepared from clinical study samples. DBS are a minimal invasive and cost-effective alternative matrix with a promising future in sports drug testing. In clinical studies, sotatercept was applied in concentrations from 0.1 to 3 mg/kg with a half-life period of more than 3 weeks [58, 68, 69, 74]. Both methods revealed sufficiently good detection sensitivity in the range of its clinical application and will allow to detect sotatercept for several weeks.

2.6 Future perspective

The use of DBS for sport drug testing is currently limited by the available sample volume constituting DBS and the most complex sample matrix in general. The resulting challenges, for example, reduced recovery due to limited extraction efficiency for analytes from the DBS card, are largely compensated by the development of LC-MS instruments exhibiting continuously increasing sensitivities. As a result, method workflows have become more straightforward and cost-effective compared to commonly used targeted (immuno)affinity enrichment strategies for proteins. Notwithstanding, developments in sample preparation steps from proteins to (signature) peptides,

including denaturation, reduction, alkylation, and proteolytic digestion, will have to be further improved. Consequently, in terms of initial testing procedures, targeted enrichment and analysis for doping control purposes could be gradually complemented by multianalyte methodologies or the simultaneous analysis of the entire proteome as for example performed by Chambers *et. al.* [99]. As a complementary matrix, the comparably inexpensive DBS enables more frequent out-of-competition sampling. Finally, current research for automated robotic high-throughput processes and analysis will be further expanded and such approaches will be applicable for more multianalyte methods in the future.

2.7 Summary points

Background

- Within anti-doping test methods, dried blood spots (DBS) represent an alternative matrix with several advantages over conventional serum samples, despite their small-sample volume and the need for dedicated extraction protocols.
- Sotatercept is an Fc-fusion protein with erythropoiesis-stimulating activity, and therefore potentially abused by athletes.
- An LC-MS detection method from DBS can complement existing serum/plasma-based analytical methods.

Experimental

- Two complementary methods, an initial testing procedure (ITP) and a confirmation procedure (CP) for sotatercept in DBS, were developed, thoroughly optimized and characterized.
- The ITP comprises an extraction step from the DBS card with phosphate-buffered saline, an analyte enrichment by Protein G-coupled magnetic beads, and an overnight tryptic digestion before LC-HRMS analysis. Due to the IgG-specific protein enrichment, other antibody-derived pharmaceuticals such as luspatercept and bimagrumab can readily be implemented.
- The CP uses protein extraction with an ammonium bicarbonate solution, analyte enrichment by protein precipitation with ammonium sulfate followed by analyte

trapping via activin A-coupled magnetic beads and an overnight digestion. The proteolytic digest was analyzed by LC-HRMS.

- Artificial DBS containing bimagrumab, a monoclonal antibody classified as myostatin inhibitor with a stimulating effect on muscle differentiation, prepared from clinical serum samples, were subjected to the protocol and analyzed as proof-of-concept.

Results and Discussion

- Specificity and identification capability were demonstrated according to the World Anti-Doping Agency guidelines (ITP and CP).
- Both methods were sufficiently precise and linear in a concentration range from 0.25 to 10 µg/mL with a limit of detection of 0.25 µg/mL (CP: T₂ and T₂₄, ITP: T₂₄) and 0.50 µg/mL (ITP: T₂).
- To demonstrate the ITP's suitability as multianalyte approach, several potential performance enhancing IgG-based pharmaceuticals (sotatercept, luspatercept and bimagrumab) were implemented into the assay and could be unambiguously identified.
- DBS containing bimagrumab derived from clinical samples could be successfully analyzed by applying the ITP.

Conclusion

- Two complementary sensitive LC-HRMS methods for detecting sotatercept in DBS were successfully developed and validated.
- For this purpose, DBS represent a suitable alternative matrix with several advantages to conventional serum samples usually analyzed in doping laboratories. As shown here, DBS analytics was very suitable for both an ITP and a CP.
- In the near future, DBS multianalytical LC-MS methods for prohibited substances of peptidic nature, as presented here in form of an ITP, will have a considerable positive impact on doping control analysis as they allow high-throughput analysis.

- Remarkably, a more frequent out-of-competition sampling via DBS would extend and improve the quality of the method portfolio of preventive doping research.

2.8 Supplementary data

2.8.1 Method development and optimization

In order to develop two complementary strategies for the isolation of sotatercept from DBS extracts for an ITP and a CP, different sample purification strategies have been tested. Eventually, affinity purification by Protein G-coupled magnetic beads (ITP) and activin A-coupled magnetic beads (CP), respectively, were found to be suitable for adequate test sensitivity. The method optimization included the approaches and parameters presented below.

2.8.2 Material and methods

Methanol, TRIS, ammonium acetate, urea, guanidine hydrochloride, sodium deoxycholate, Triton-X100, CHAPS, HEPES, and MOPS were purchased from Merck (Darmstadt, Germany). SDS was bought from GE Healthcare (Uppsala, Sweden). ProteoMiner protein enrichment small-capacity kit was purchased from Bio-Rad Laboratories (CA, USA). Multi-layered prototype dried plasma spot cards were prepared in-house. HemoVoid and Hemoglobind test kits were provided by Biotech Support Group (NJ, USA). All other chemicals and materials were obtained as described in the main article.

2.8.3 Results and discussion

Initial testing procedure

General approaches

One single DBS (20 μ L) contains between 3.6-5.2 mg protein, taken into account human total plasma protein (60-80 g/L [100]), and hemoglobin (120-180 g/L [101]) from red blood cells, which complicated sample workup during ITP assay development. To overcome these difficulties, different (antibody-free) purification strategies were tested until an acceptable compromise regarding recovery, purification, limit of detection, time and costs was found. The simplest approach comprised DBS extraction, organic solvent or ammonium sulfate protein precipitation with subsequent proteolytic pellet

digestion and detection of unique surrogate peptides, which have been already successfully applied in protein assays from plasma/serum [102-109]. Even LC-MS detection of therapeutic proteins from DBS with direct tryptic digestion was reported [110-113]. Unfortunately, while testing these straightforward workflows, none of them resulted in a satisfying performance. Insufficient protein digestion or signal suppression due to interfering matrix (from high abundant proteins, for example hemoglobin and albumin) was the main issue in sample workup and LC-MS analysis, respectively. To overcome these difficulties, enriching low abundance proteins, for example with hexapeptide ligand libraries, could be a promising approach [114, 115], and attempts with ProteoMiner and HemoVoid (hemoglobin depletion reagent; schematic overview in Figure 2.S1 B) were carried out. Despite partial good sensitivity and overall results, sample preparation was time-consuming and costly, hence not suited for a multianalyte ITP. In another experiment, an attempt was made to separate the blood cells from the plasma by using a multilayered prototype dried plasma spot card. Unfortunately, not only the erythrocytes, but also the analyte was retained, which resulted in a significant loss of sensitivity (Figure 2.S2).

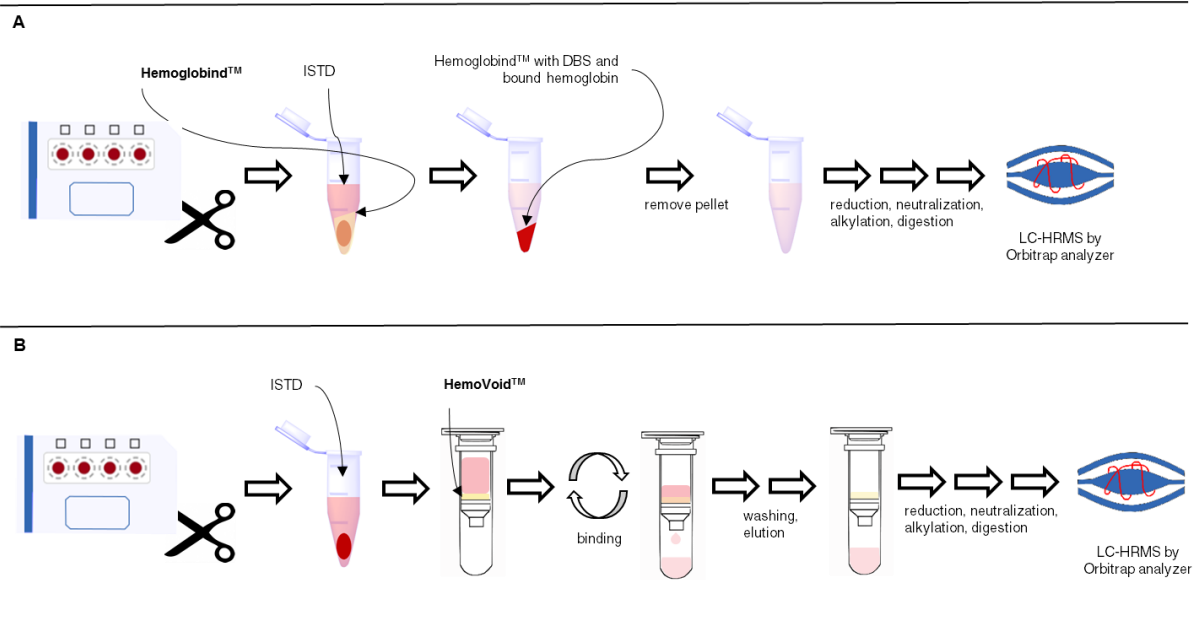


Figure 2.S1: Schematic overview. Purification of a DBS extract using Hemoglobind (A) or HemoVoid (B). The Hemoglobind reagent was given to the dried blood spot extract, thus binding hemoglobin. After removing the obtained pellet, a hemoglobin-free sample extract was resulted. This sample could be further purified by for example Protein G and/or reduced, alkylated and digested before LC-HRMS analysis (A). The HemoVoid was placed in a filter tube and a dried blood spot extract was added. After binding, the extract, free of red cell lysates, was eluted and the obtained sample was further processed and analyzed (B).

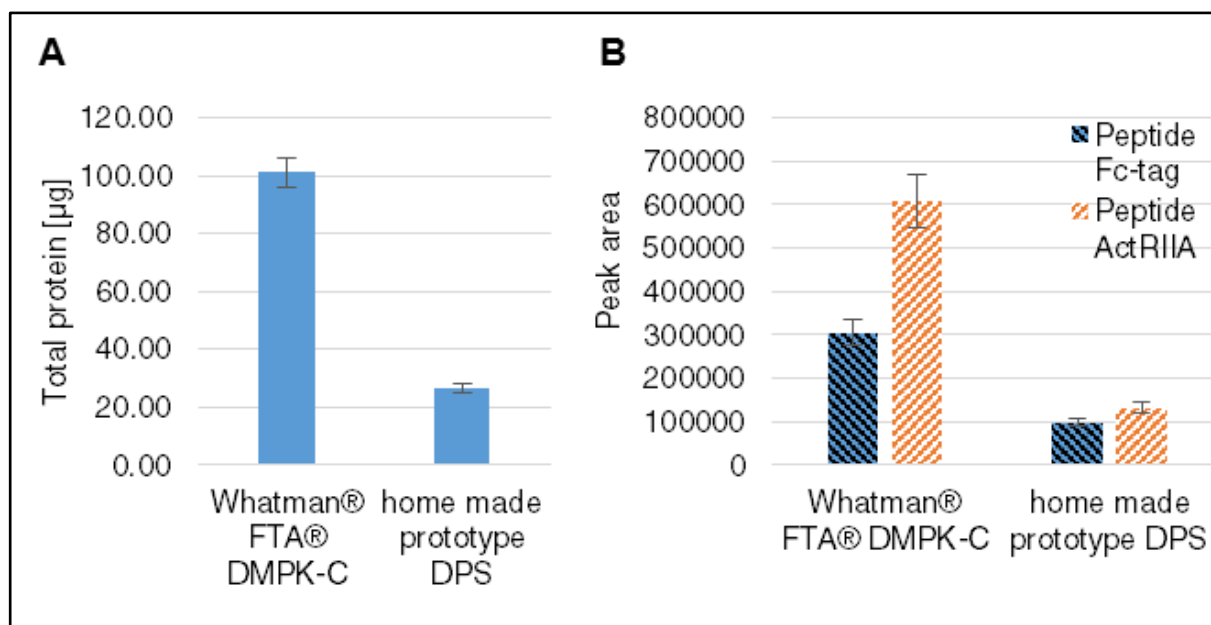


Figure 2.S2: Comparison of two different dried blood spot cards, the Whatman FTA DMPK-C and the Q2 Solution DPS prototype. Colorimetric determination of IgG content was carried out using the Pierce 660 nm Protein assay (A). The LC-HRMS analyses was visualized as peak areas of the tryptic signature peptides of sotatercept originating from the Fc-tag and the AcRIIA domain, respectively (B).

Protein G-coupled magnetic beads purification

Lastly, Protein G-coupled magnetic beads were used to isolate sotatercept from the matrix and four parameters (extraction/binding buffer volume, blood-to-beads ratio, protein-to-enzyme ratio, and digestion time) were optimized one after another. In practice, one parameter was changed, while the others were kept close to expected optimum. Increasing the PBS buffer volume was recommended for an effective blood spot extraction, however was diluting the magnetic beads in the same way, resulting in less interactions with the analyte. The optimal buffer volume of 300 μ L was determined by evaluating signal peak areas of the signature peptides after LC-MS experiments; the outcome is shown in Figure 2.2 A. As a supplement to the LC-MS data, protein/IgG quantitation via Pierce 660 nm protein assay was carried out (Figure 2.S3). Thus, the amount of IgGs purified by Protein G-coupled magnetic beads could be quantified as a function of the amount of beads added. A second, additional elution step resulted in an 11% increase of human IgG yield, however was not implemented to the final protocol due to an adverse time-cost factor (Figure 2.S3 A). Changing the extraction/binding buffer from PBS to 150 mM ABC, as it was used in the CP (see below), did not result in higher IgG yields (Figure 2.S3 B).

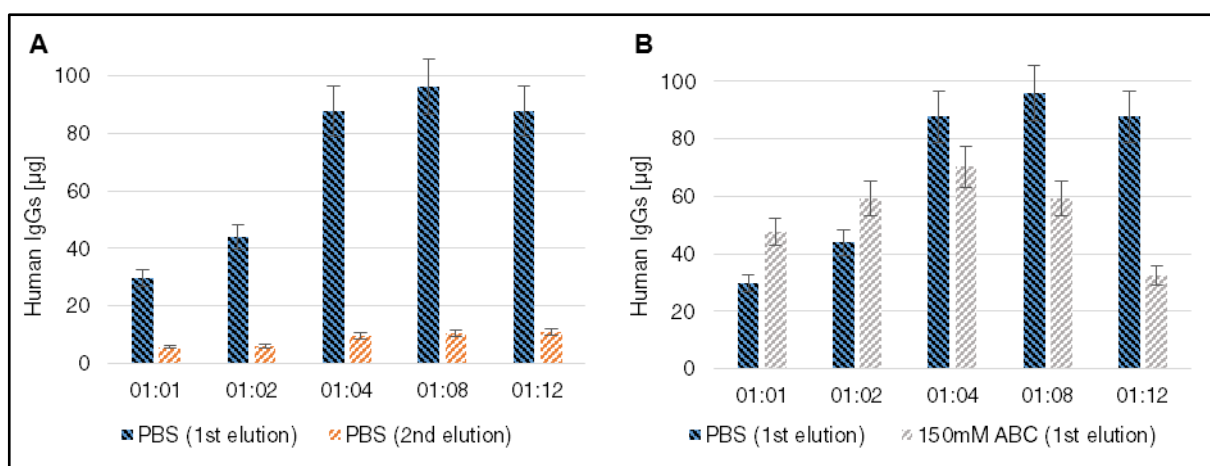


Figure 2.S3: Assay development and optimization; visualization of colorimetric quantitation experiments of human IgG using the Pierce 660 nm protein assay. Within the method, human IgG yields after the first and an additional, second acidic elution from the Protein G-coupled magnetic beads were investigated (A). Further, the extraction/binding buffers PBS and ABC were compared and human IgG yields were quantified (B).

Testing different amounts of beads was carried out to obtain the optimal Protein G beads volume of 160 μ L, corresponding to a 1:8 blood-to-beads volume ratio (Figure 2.S3 & Figure 2.2 B). An IgG capture carried out in this way provided a total protein depletion of 97% (quantified with the aforementioned protein assay), thus reduce sample complexity without losing IgG-based drug candidates (Figure 2.S4).

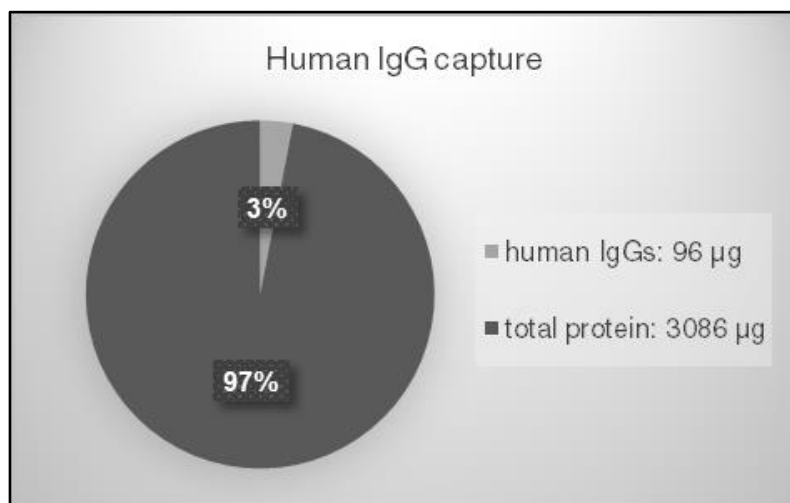


Figure 2.S4: An IgG capture experiment by using a blood-to-beads slurry (v/v) ratio of 1:8 provided a total protein depletion of 97%, thus reduce sample complexity without losing IgG-based drug candidates. Colorimetric quantitation was carried out using the Pierce 660 nm protein assay. The amount of protein was estimated by using a BSA standard calibration for total protein, and an adaption factor of 0.57 for human IgG.

An efficient digestion was dependent on a certain amount of trypsin as the enzyme can be self-digested, and so the right amount had to be chosen with caution. Different trypsin-to-protein ratios (1:10, 1:20, 1:50, 1:100, 1:200) were tested and finally, a ratio of 1:50 (Figure 2.2 C) revealed the best cleavage performance. Here, all experiments were conducted with trypsin from Sigma Aldrich (T1426), however another trypsin preparation from Promega (V511A) was later found to cleave more efficiently, as it increased the signal peak area of the ActRIIA's signature peptide more than twice.

Moreover, an overnight proteolytic digestion of 16 hours arose as optimal digestion time, however even after four hours already 80-90% of the Fc-tag peptide, but only 40-50% of ActRIIA domain peptide were cleaved (Figure 2.2 D). It is of utmost importance to determine the IgG concentration and to calculate the required trypsin amount for each experiment, as the IgG content in blood can vary between 407-2170 mg/dL

depending on age, sex, common habits and metabolic abnormalities (e.g. recent illnesses) [116].

The results through assay development showed differences in LC-MS responses of the signature peptides. In general, LC-MS response derived from the Fc-tag peptide was less influenced from the optimization parameters than the ActRIIA peptide.

Pre-purification approaches

Further improvements regarding a cleaner sample extract could be achieved by several additional steps before Protein G purification. Thus, the use of HemoVoid (Figure 2.S1 B) resulted in the cleanest samples, closely followed by Hemoglobind (hemoglobin removal and capture reagent; schematic overview in Figure 2.S1 A), while protein precipitation by saturated ammonium sulfate yielded only small improvements regarding interfering (data not shown). At the same time, the reduction of interfering molecules also caused a loss of the analyte itself and so reduced signal intensities in all strategies was observed (Figure 2.S5). Eventually, these steps were not implemented due to an insufficient cost-benefit ratio. In Table 2.S1 an overview that summarizes the most promising sample preparation strategies is shown. Here, the parameters recovery, effectiveness of purification, time, costs, and sensitivity were roughly estimated or evaluated from LC-MS data.

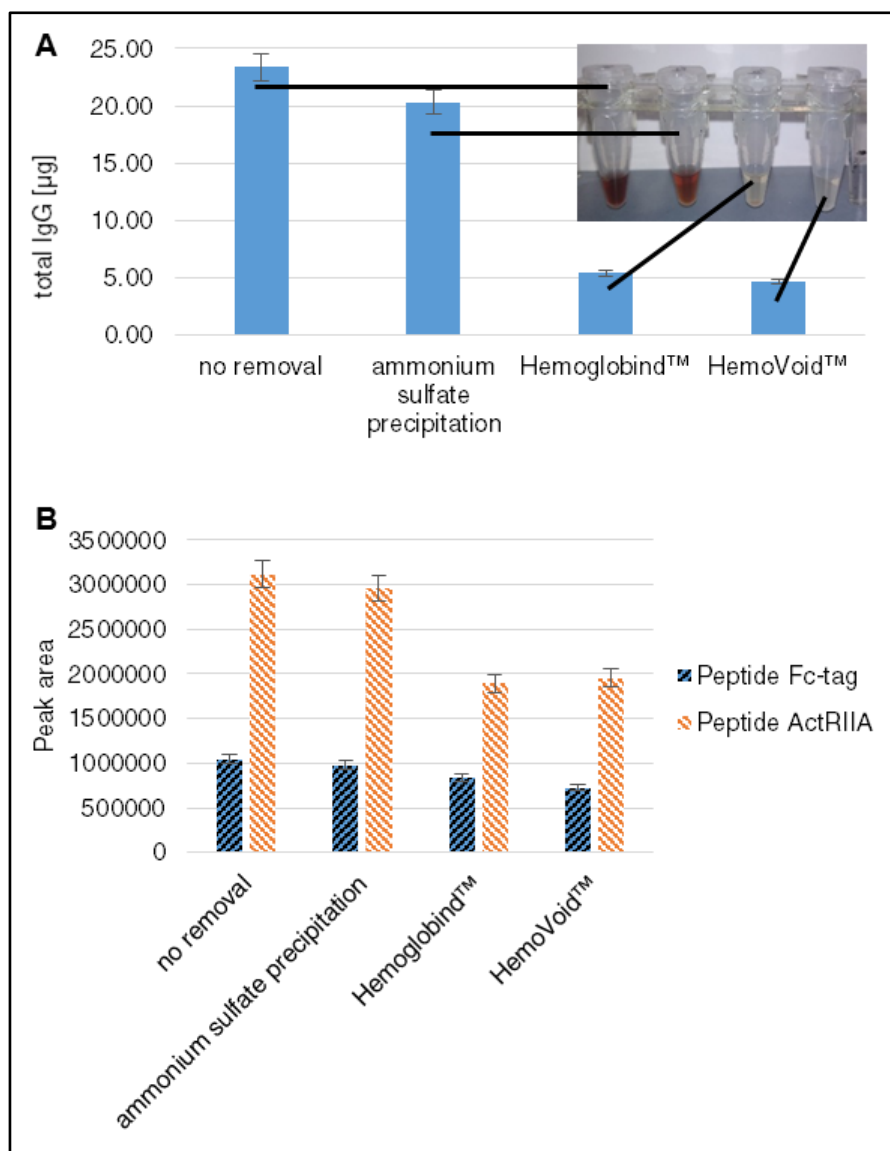


Figure 2.S5: Pre-purification using different strategies (no removal, ammonium sulfate precipitation, Hemoglobind, HemoVoid) within the sample work-up of the initial testing procedure for detecting sotatercept. Colorimetric determination of IgG concentration of the eluate was carried out using the Pierce 660 nm Protein assay (**A**). The LC-HRMS analyses revealed different responses visualized as peak areas of the tryptic signature peptides of sotatercept originating from the Fc-tag and the ActRIIA domain, respectively (**B**).

Table 2.S1: Overview of the most promising sample preparation strategies (ITP) under consideration of recovery, effectiveness of purification, time, costs and sensitivity. The parameters were roughly estimated or evaluated from LC-MS data. Light grey means a good value/property, grey a medium and dark grey a rather poor one.

Method	Recovery	Effectiveness	Time	Costs	Sensitivity
Protein G	Light grey	Dark grey	Light grey	Light grey	Light grey
Precipitation + Protein G	Light grey	Dark grey	Dark grey	Light grey	Light grey
Hemoglobind + Protein G	Dark grey	Light grey	Dark grey	Dark grey	Light grey
HemoVoid + Protein G	Dark grey	Light grey	Dark grey	Dark grey	Light grey
Hemoglobind	Dark grey	Dark grey	Light grey	Dark grey	Dark grey
HemoVoid	Dark grey	Dark grey	Light grey	Dark grey	Dark grey
HemoVoid on-bead digestion	Dark grey	Dark grey	Light grey	Light grey	Dark grey
Proteominer	Dark grey	Dark grey	Dark grey	Dark grey	Dark grey

LC-MS & DMSO

Enhancing sensitivity in electrospray ionization experiments could be achieved by adding DMSO to the mobile phase [84]. Adding 1% DMSO to the organic eluent, acetonitrile, fortunately resulted in a 1.9-fold increase of signal peak area of the ActRIIA domain peptide, and a minor decrease by a factor of 0.8 of the signal peak area of the Fc-tag peptide (Figure 2.S6), giving an overall benefit of this application.

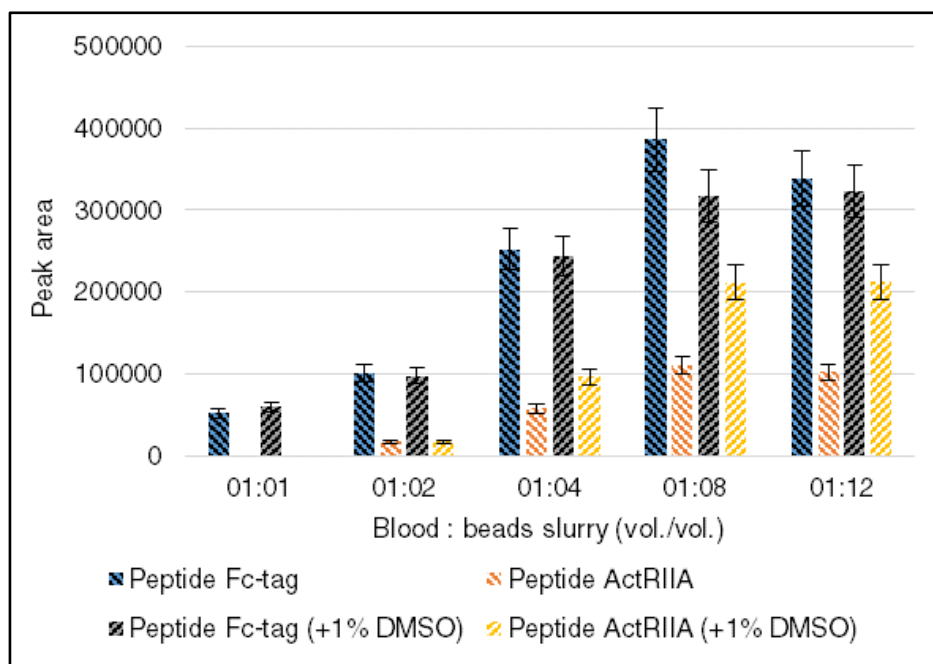


Figure 2.S6: Addition of DMSO to the eluent. Adding 1% DMSO to the organic eluent, acetonitrile, resulted in a 1.9-fold increase of signal peak area of the Fc-tag peptide of sotatercept, and a minor decrease of 0.8 of the signal peak area of the ActRIIA domain peptide using a 1:8 blood-to-beads slurry (v/v) ratio. Tosyl phenylalanyl chloromethyl ketone-treated trypsin T1426 (Sigma Aldrich) was used to cleave the proteins.

Confirmation procedure

Choice of activin A

Activin A from two different manufacturers, Peprtech (Hamburg, Germany) and Thermo Fisher Scientific (Bremen, Germany), was tested for affinity purification. No significant performance difference could be observed (Figure 2.S7).

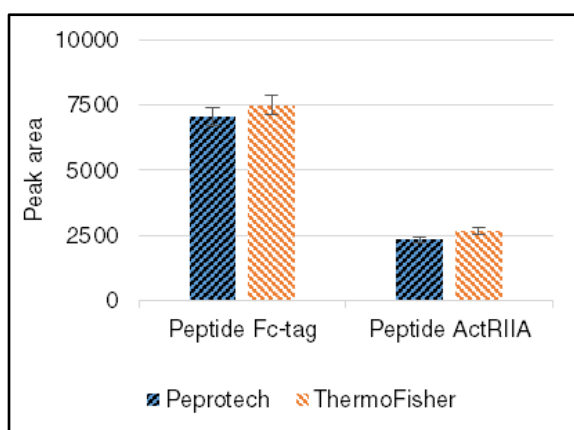


Figure 2.S7: NHS magnetic beads were coupled to activin A from two different suppliers, Peprtech and ThermoFisher. The average peak areas from 12 (Peprtech) respective 10 (ThermoFisher) LC-HRMS experiments are shown here. As no significant difference in performance was observed, Peprtech's activin A was chosen due to cost issues.

Choice of the DBS extractant

As DBS extractant, a series of organic solvents (e.g. acetonitrile, methanol) and aqueous buffers (e.g. 50 mM TRIS, PBS, ammonium bicarbonate, ammonium acetate), mixtures of both, partially acidified with 0.1% formic acid, with or without additives such as denaturing agents (8 M urea, 6 M guanidine hydrochloride, 1-5% (w/v) sodium deoxycholate) or detergents (0.059 mM Tween, 0.3 mM Triton-X100, 6.5 mM CHAPS, 8.2 mM SDS, 25 mM HEPES, 20 mM MOPS), were tested. Finally, a 150 mM ABC solution without additives yielded the best extraction efficiency and reproducibility.

Choice of extraction volume

In order to extract the DBS effectively, the maximum possible volume of 800 μ L for a 2 mL Protein LoBind tube was chosen. In the following step, protein precipitation with the same volume of a saturated ammonium sulfate solution resulted in a total volume of 1.6 mL which could be still centrifuged without any problems. To reduce the dilution of the precipitating agent, smaller extraction volumes (200 μ L, 400 μ L, and 600 μ L) were also tested. However, this did not lead to any improvement.

Choice of precipitant

Organic protein precipitation with methanol or acetonitrile did not improve IgG enrichment compared to salting-out with saturated ammonium sulfate.

Precipitate solution volume

The precipitate was dissolved in a minimal volume of 150 μ L PBST (coupling buffer) by carefully resuspending the pellet several times.

Amount of beads

Since no sensitivity loss was observed, the amount of the expensive activin A-coupled beads could be decreased by one third compared to the original protocol [30]. Accordingly, 200 μ L of magnetic beads or 1:10 blood-to-beads (v/v) were used to capture sotatercept from the extract.

Further parameters

Incubation time, amount and type of trypsin, and digestion time were adopted as developed before [30].

LC-MS & DMSO

Similar to the ITP LC-MS method, adding 2% DMSO to the organic mobile phase, improved the signal peak areas of the peptides by a factor of 1.6 (Fc-tag) and 2.3 (ActRIIA domain).

2.9 Acknowledgements

The study was funded by the Federal Ministry of the Interior, Building and Community of the Federal Republic of Germany (Berlin, Germany), the Manfred-Donike Institute for Doping Analysis (Cologne, Germany), Anti-Doping Switzerland (Berne, Switzerland), the National Anti-Doping Agency (Bonn, Germany), and the World Anti-Doping Agency (Montreal, Canada, grant #ISF17A12MT).

The authors thank Olivier Petricoul (Novartis, Switzerland) for providing the post-administration serum samples for proof-of-concept analyses.

2.10 References

1. Robinson, N., et al., *Validation of a Blood Stability Score as an easy-to-use blood sample quality index*. International Journal of Laboratory Hematology, 2016. 38(6): p. 685-693.
2. Thevis, M., et al., *Sports drug testing using complementary matrices: Advantages and limitations*. J Pharm Biomed Anal, 2016. 130: p. 220-230.
3. Abu-Rabie, P., et al., *DBS direct elution: optimizing performance in high-throughput quantitative LC-MS/MS analysis*. Bioanalysis, 2015. 7(16): p. 2003-17.
4. Dib, J., et al., *Screening for adiponectin receptor agonists and their metabolites in urine and dried blood spots*. Clinical Mass Spectrometry, 2017. 6(13-20).
5. Tretzel, L., et al., *Fully automated determination of nicotine and its major metabolites in whole blood by means of a DBS online-SPE LC-HR-MS/MS approach for sports drug testing*. J Pharm Biomed Anal, 2016. 123: p. 132-40.
6. W. Harry Hannon and B.L.T. Jr, *Dried Blood Spots: Applications and Techniques*. Overview of the History and Applications of Dried Blood Samples. Vol. Chapter 1 - History, Applications, and healthcare. 2014: John Wiley & Sons, Inc.
7. Bjorkesten, J., et al., *Stability of Proteins in Dried Blood Spot Biobanks*. Mol Cell Proteomics, 2017. 16(7): p. 1286-1296.
8. Peng, S.H., et al., *Oral testosterone administration detected by testosterone glucuronidation measured in blood spots dried on filter paper*. Clin Chem, 2000. 46(4): p. 515-22.
9. Tretzel, L., et al., *Use of dried blood spots in doping control analysis of anabolic steroid esters*. J Pharm Biomed Anal, 2014. 96: p. 21-30.
10. Thomas, A., et al., *Dried blood spots (DBS) for doping control analysis*. Drug Testing and Analysis, 2011. 3(11-12): p. 806-813.
11. Tretzel, L., et al., *Analyses of Meldonium (Mildronate) from Blood, Dried Blood Spots (DBS), and Urine Suggest Drug Incorporation into Erythrocytes*. Int J Sports Med, 2016. 37(6): p. 500-2.
12. Höppner, S., et al., *Mass spectrometric studies on the in vivo metabolism and excretion of SIRT1 activating drugs in rat urine, dried blood spots, and plasma samples for doping control purposes*. J Pharm Biomed Anal, 2014. 88: p. 649-59.
13. Tretzel, L., et al., *Dried blood spots (DBS) in doping controls: a complementary matrix for improved in- and out-of-competition sports drug testing strategies*. Anal Methods, 2015. 7: p. 7596.
14. Protti, M., et al., *Determination of oxycodone and its major metabolites in haematic and urinary matrices: Comparison of traditional and miniaturised sampling approaches*. J Pharm Biomed Anal, 2018. 152: p. 204-214.

15. Thomas, A., et al., *Sensitive determination of prohibited drugs in dried blood spots (DBS) for doping controls by means of a benchtop quadrupole/Orbitrap mass spectrometer*. *Anal Bioanal Chem*, 2012. 403(5): p. 1279-89.
16. Möller, I., et al., *Development and validation of a mass spectrometric detection method of peginesatide in dried blood spots for sports drug testing*. *Anal Bioanal Chem*, 2012. 403(9): p. 2715-24.
17. Tretzel, L., et al., *Determination of Synacthen((R)) in dried blood spots for doping control analysis using liquid chromatography tandem mass spectrometry*. *Anal Bioanal Chem*, 2015. 407(16): p. 4709-20.
18. Thomas, A. and M. Thevis, *Analysis of insulin and insulin analogues from dried blood spots by means of LC-HRMS*. *Drug Test Anal*, 2018.
19. Reverter-Branchat, G., et al., *Determination of Recent Growth Hormone Abuse Using a Single Dried Blood Spot*. *Clin Chem*, 2016. 62(10): p. 1353-60.
20. Cox, H.D., C.M. Hughes, and D. Eichner, *Sensitive quantification of IGF-1 and its synthetic analogs in dried blood spots*. *Bioanalysis*, 2014. 6(19): p. 2651-62.
21. Cox, H.D., J. Rampton, and D. Eichner, *Quantification of insulin-like growth factor-1 in dried blood spots for detection of growth hormone abuse in sport*. *Anal Bioanal Chem*, 2013. 405(6): p. 1949-58.
22. Ferro, P., et al., *Evaluation of fibronectin 1 in one dried blood spot and in urine after rhGH treatment*. *Drug Test Anal*, 2017. 9(7): p. 1011-1016.
23. Cox, H.D., et al., *Detection of Autologous Blood Transfusions using a Novel Dried Blood Spot Method*. *Drug Test Anal*, 2017.
24. Cox, H.D. and D. Eichner, *A mass spectrometry method to measure membrane proteins in dried blood spots for the detection of blood doping practices in sport*. *Anal Chem*, 2017. 89(18): p. 10029-10036.
25. Reverter-Branchat, G., et al., *Detection of Erythropoiesis Stimulating Agents in One Single Dried Blood Spot*. *Drug Test Anal*, 2018.
26. Zakaria, R., et al., *Advantages and Challenges of Dried Blood Spot Analysis by Mass Spectrometry Across the Total Testing Process*. *EJIFCC*, 2016. 27(4): p. 288-317.
27. Kneepkens, E.L., et al., *Dried blood spots from finger prick facilitate therapeutic drug monitoring of adalimumab and anti-adalimumab in patients with inflammatory diseases*. *Br J Clin Pharmacol*, 2017. 83(11): p. 2474-2484.
28. Jafari, R., et al., *Fc-fusion Proteins in Therapy: An Updated View*. *Curr Med Chem*, 2017. 24(12): p. 1228-1237.
29. Rogers, B., et al., *Recombinant human serum albumin fusion proteins and novel applications in drug delivery and therapy*. *Curr Pharm Des*, 2015. 21(14): p. 1899-907.

30. Walpurgis, K., et al., *Testing for the erythropoiesis-stimulating agent Sotatercept/ACE-011 (ActRIIA-Fc) in serum by means of Western blotting and LC-HRMS*. Drug Test Anal, 2016. 8(11-12): p. 1152-1161.
31. Reichel, C., et al., *Detection of Sotatercept (ACE-011) in human serum by SAR-PAGE and western single blotting*. Drug Test Anal, 2017.
32. Martin, L., et al., *A validated, sensitive electrophoretic method for the detection of activin receptor type II-Fc fusion proteins in human blood*. Drug Test Anal, 2018.
33. Walpurgis, K., et al., *Detection of the Human Anti-ActRII Antibody Bimagrumab in Serum by Means of Affinity Purification, Tryptic Digestion, and LC-HRMS*. Proteomics Clin Appl, 2018. 12(3): p. e1700120.
34. Reichel, C., G. Gmeiner, and M. Thevis, *Antibody-based strategies for the detection of Luspatercept (ACE-536) in human serum*. Drug Test Anal, 2017. 9(11-12): p. 1721-1730.
35. Walpurgis, K., et al., *Myostatin inhibitors in sports drug testing: Detection of myostatin-neutralizing antibodies in plasma/serum by affinity purification and Western blotting*. Proteomics Clin Appl, 2016. 10(2): p. 195-205.
36. Reichel, C., et al., *Updated protocols for the detection of Sotatercept and Luspatercept in human serum*. Drug Test Anal, 2018.
37. Walpurgis, K., et al., *Combined detection of the ActRII-Fc fusion proteins Sotatercept (ActRIIA-Fc) and Luspatercept (modified ActRIIB-Fc) in serum by means of immunoaffinity purification, tryptic digestion, and LC-MS/MS*. Drug Test Anal, 2018.
38. Xie, C., et al., *LC-MS/MS quantification of sulfotransferases is better than conventional immunogenic methods in determining human liver SULT activities: implication in precision medicine*. Scientific Reports, 2017. 7.
39. Barroso, O., et al., *Analytical challenges in the detection of peptide hormones for anti-doping purposes*. Bioanalysis, 2012. 4(13): p. 1577-90.
40. Iancu-Rubin, C., et al., *Stromal cell-mediated inhibition of erythropoiesis can be attenuated by Sotatercept (ACE-011), an activin receptor type II ligand trap*. Exp Hematol, 2013. 41(2): p. 155-166 e17.
41. Raje, N. and S. Vallet, *Sotatercept, a soluble activin receptor type 2A IgG-Fc fusion protein for the treatment of anemia and bone loss*. Curr Opin Mol Ther, 2010. 12(5): p. 586-97.
42. Santini, V., *Of blood and bone: the sotatercept adventure*. Lancet Haematology, 2018. 5(2): p. E54-E55.
43. Mies, A. and U. Platzbecker, *Increasing the effectiveness of hematopoiesis in myelodysplastic syndromes: erythropoiesis-stimulating agents and transforming growth factor-beta superfamily inhibitors*. Semin Hematol, 2017. 54(3): p. 141-146.

44. De Rosa, G., et al., *Unraveling the Molecular Pathogenesis of Ineffective Erythropoiesis in Congenital Dyserythropoietic Anemia Type Ii: In Vitro Evaluation of Rap-011 Treatment*. Haematologica, 2017. 102: p. 333-334.
45. Morse, A., et al., *RAP-011 augments callus formation in closed fractures in rats*. J Orthop Res, 2016. 34(2): p. 320-30.
46. Langdon, J.M., et al., *RAP-011, an activin receptor ligand trap, increases hemoglobin concentration in hepcidin transgenic mice*. Am J Hematol, 2015. 90(1): p. 8-14.
47. Ear, J., et al., *RAP-011 improves erythropoiesis in zebrafish model of Diamond-Blackfan anemia through antagonizing lefty1*. Blood, 2015. 126(7): p. 880-90.
48. Ear, J., et al., *RAP-011 Efficiently Rescues Erythropoiesis In Zebrafish Models Of Diamond Blackfan Anemia*. Blood, 2013. 122(21).
49. Dussiot, M., et al., *Modulation of Activin Signaling by RAP-011 (ActRIIA-IgG1) Improve Anemia, Increases Hemoglobin Levels and Corrects Ineffective Erythropoiesis in beta-Thalassemia*. Blood, 2012. 120(21).
50. Lotinun, S., et al., *A soluble activin receptor Type IIA fusion protein (ACE-011) increases bone mass via a dual anabolic-antiresorptive effect in Cynomolgus monkeys*. Bone, 2010. 46(4): p. 1082-8.
51. Fajardo, R.J., et al., *Treatment with a soluble receptor for activin improves bone mass and structure in the axial and appendicular skeleton of female cynomolgus macaques (Macaca fascicularis)*. Bone, 2010. 46(1): p. 64-71.
52. Mulivor, A.W., et al., *RAP-011, a Soluble Activin Receptor Type Ila Murine IgG-Fc Fusion Protein, Prevents Chemotherapy Induced Anemia*. Blood, 2009. 114(22): p. 72-72.
53. Pearsall, R.S., et al., *A soluble activin type IIA receptor induces bone formation and improves skeletal integrity*. Proc Natl Acad Sci U S A, 2008. 105(19): p. 7082-7.
54. Lotinun, S., et al., *Soluble Activin Receptor Type IIA Fusion Protein, ACE-011, Increases Bone Mass by Stimulating Bone Formation and Inhibiting Bone Resorption in Cynomolgus Monkeys*. Journal of Bone and Mineral Research, 2008. 23: p. S337-S337.
55. Fajardo, R.J., et al., *ACE-011, a soluble activin receptor type IIA fusion protein, increases BMD and improves microarchitecture in cynomolgus monkeys*. Journal of Bone and Mineral Research, 2007. 22: p. S65-S65.
56. Komrokji, R., et al., *Sotatercept with long-term extension for the treatment of anaemia in patients with lower-risk myelodysplastic syndromes: a phase 2, dose-ranging trial*. Lancet Haematology, 2018. 5(2): p. E63-E72.

57. Bose, P., et al., *Sotatercept (ACE-011) Alone and in Combination with Ruxolitinib in Patients (pts) with Myeloproliferative Neoplasm (MPN)-Associated Myelofibrosis (MF) and Anemia*. *Blood*, 2017. 130.
58. Raftopoulos, H., et al., *Sotatercept (ACE-011) for the treatment of chemotherapy-induced anemia in patients with metastatic breast cancer or advanced or metastatic solid tumors treated with platinum-based chemotherapeutic regimens: results from two phase 2 studies*. *Support Care Cancer*, 2016. 24(4): p. 1517-25.
59. Bose, P., et al., *Phase-2 Study of Sotatercept (ACE-011) in Myeloproliferative Neoplasm-Associated Myelofibrosis and Anemia*. *Blood*, 2016. 128(22).
60. Yee, A.J., et al., *Phase 1 Dose-Escalation Study of Sotatercept (ACE-011) in Combination with Lenalidomide and Dexamethasone in Patients with Relapsed and/or Refractory Multiple Myeloma*. *Blood*, 2015. 126(23).
61. Smith, W.T., et al., *Long-Term Effects of 3 Dose Levels of Sotatercept Compared with Placebo for Correction of Anemia in Hemodialysis Subjects: Interim Analysis of Ace-011-Ren-001*. *Nephrology Dialysis Transplantation*, 2015. 30.
62. Smith, W., H. Malluche, and K. Hruska, *Quantitative Computed Tomography Results for Bone Mass and Abdominal Aortic Vascular Calcification in Hemodialysis Subjects Treated with Escalating Dose Levels of Sotatercept: Interim Analysis of Ace-011-Ren-001*. *Nephrology Dialysis Transplantation*, 2015. 30.
63. Komrokji, R., et al., *A Phase 2, Dose-Finding Study of Sotatercept (Ace-011) in Patients (Pts) with Lower-Risk Myelodysplastic Syndromes (Mds) and Anemia Requiring Transfusion*. *Haematologica*, 2015. 100: p. 192-192.
64. Cappellini, M.D., et al., *Interim Results from a Phase 2a, Open-Label, Dose-Finding Study of Sotatercept (Ace-011) in Adult Patients (Pts) with Beta-Thalassemia*. *Haematologica*, 2015. 100: p. 17-18.
65. Komrokji, R.S., et al., *An Open-Label, Phase 2, Dose-Finding Study of Sotatercept (ACE-011) in Patients with Low or Intermediate-1 (Int-1)-Risk Myelodysplastic Syndromes (MDS) or Non-Proliferative Chronic Myelomonocytic Leukemia (CMML) and Anemia Requiring Transfusion*. *Blood*, 2014. 124(21).
66. El-Shahawy, M., et al., *Long-Term Effects of Sotatercept Compared with Placebo for Correction of Anemia in Hemodialysis Subjects: Interim Analysis of Ace-011-Ren-001 Phase 2a Study*. *Nephrology Dialysis Transplantation*, 2014. 29: p. 152-153.
67. El-Shahawy, M., et al., *Interim Analysis of Ace-011-Ren-001: The First 28-Day Dose Cycle of Low and Medium Starting Doses of Sotatercept Compared to Placebo for Correction of Anemia in Hemodialysis Subjects*. *American Journal of Kidney Diseases*, 2014. 63(5): p. A104-A104.

68. Abdulkadyrov, K.M., et al., *Sotatercept in patients with osteolytic lesions of multiple myeloma*. Br J Haematol, 2014. 165(6): p. 814-23.
69. Sherman, M.L., et al., *Multiple-dose, safety, pharmacokinetic, and pharmacodynamic study of sotatercept (ActRIIA-IgG1), a novel erythropoietic agent, in healthy postmenopausal women*. J Clin Pharmacol, 2013. 53(11): p. 1121-30.
70. Cappellini, M.D., et al., *A Phase 2a, Open-Label, Dose-Finding Study To Determine The Safety and Tolerability Of Sotatercept (ACE-011) In Adults With Beta (beta)-Thalassemia: Interim Results*. Blood, 2013. 122(21).
71. Chen, N.H., et al., *Exposures and Erythropoietic Responses to Sotatercept (ACE-011) in Healthy Volunteers and Cancer Patients: Implications for Mechanism of Action*. Blood, 2012. 120(21).
72. Raftopoulos, H., et al., *A phase II/III study of sotatercept (ACE-011), an activin antagonist, for chemotherapy-induced anemia in patients with metastatic non-small cell lung cancer treated with first-line platinum-based chemotherapy*. Journal of Clinical Oncology, 2011. 29(15).
73. Borgstein, N.G., et al., *ACE-011, a Soluble Activin Type IIA Receptor IgG-Fc Fusion Protein, Significantly Increases Bone Mineral Density in Healthy Postmenopausal Women with Normal or Low Bone Mass*. Bone, 2010. 47: p. S281-S282.
74. Ruckle, J., et al., *Single-dose, randomized, double-blind, placebo-controlled study of ACE-011 (ActRIIA-IgG1) in postmenopausal women*. J Bone Miner Res, 2009. 24(4): p. 744-52.
75. Borgstein, N.G., et al., *ACE-011, a soluble activin receptor type IIA IgG-Fc fusion protein, increases BMD within 4 months in postmenopausal healthy women*. Osteoporosis International, 2009. 20(1): p. 186-186.
76. Borgstein, N.G., et al., *ACE-011, a soluble activin receptor type IIA IgG-Fc fusion protein, decreases follicle stimulating hormone and increases bone-specific alkaline phosphatase, a marker of bone formation, in postmenopausal healthy women*. Cancer Research, 2009. 69(2): p. 154s-154s.
77. Abdulkadyrov, K.M., et al., *ACE-011, a Soluble Activin Receptor Type IIA IgG-Fc Fusion Protein, Increases Hemoglobin (Hb) and Improves Bone Lesions in Multiple Myeloma Patients Receiving Myelosuppressive Chemotherapy: Preliminary Analysis*. Blood, 2009. 114(22): p. 312-312.
78. Kim, K.T., et al., *ACE-011, a Soluble Activin Receptor Type IIA IgG-Fc Fusion Protein, Increases Hemoglobin and Hematocrit Levels in Postmenopausal Healthy Women*. Blood, 2008. 112(11): p. 1316-1316.

79. Ruckle, J., et al., *A single dose of ACE-011 is associated with increases in bone formation and decreases in bone resorption markers in healthy, postmenopausal women*. *Journal of Bone and Mineral Research*, 2007. 22: p. S38-S38.
80. (WADA), W.A.D.A. *The World Anti-Doping Code. International Standard. Prohibited List January 2018*. 2018 accessed: 12/07/2018]; Available from: https://www.wada-ama.org/sites/default/files/prohibited_list_2018_en.pdf.
81. (WADA), W.A.-D.A. *The World Anti-Doping Code. International Standard for Laboratories January 2015*. 2015 accessed: 12/07/2018]; Available from: <https://www.wada-ama.org/sites/default/files/resources/files/WADA-ISL-2015-Final-v8.0-EN.pdf>.
82. Scientific, T. *Instruction manual Pierce 660nm Protein Assay*. accessed: 09/27/2018]; Available from: https://assets.thermofisher.com/TFS-Assets/LSG/manuals/MAN0011636_Pierce_660nm_Protein_Asy_UG.pdf.
83. Healthcare, G. *Instruction manual NHS Mag Sepharose™ 28-9537-64 AB*. accessed: 09/27/2018]; Available from: <https://www.sigmaaldrich.com/technical-documents/protocols/biology/affinity-chromatography-biomolecules/preactivated-magnetic-beads.html>.
84. Hahne, H., et al., *DMSO enhances electrospray response, boosting sensitivity of proteomic experiments*. *Nat Methods*, 2013. 10(10): p. 989-91.
85. Matuszewski, B.K., M.L. Constanzer, and C.M. Chavez-Eng, *Strategies for the assessment of matrix effect in quantitative bioanalytical methods based on HPLC-MS/MS*. *Anal Chem*, 2003. 75(13): p. 3019-30.
86. Anderson, N.L. and N.G. Anderson, *The human plasma proteome: history, character, and diagnostic prospects*. *Mol Cell Proteomics*, 2002. 1(11): p. 845-67.
87. Legeron, R., et al., *A new reliable, transposable and cost-effective assay for absolute quantification of total plasmatic bevacizumab by LC-MS/MS in human plasma comparing two internal standard calibration approaches*. *J Chromatogr B Analyt Technol Biomed Life Sci*, 2017. 1070: p. 43-53.
88. Chiu, H.H., et al., *Development of an LC-MS/MS method with protein G purification strategy for quantifying bevacizumab in human plasma*. *Anal Bioanal Chem*, 2017.
89. Razavi, M., et al., *Multiplexed longitudinal measurement of protein biomarkers in DBS using an automated SISCAPA workflow*. *Bioanalysis*, 2016. 8(15): p. 1597-1609.
90. Rosting, C., A. Gjelstad, and T.G. Halvorsen, *Water-Soluble Dried Blood Spot in Protein Analysis: A Proof-of-Concept Study*. *Anal Chem*, 2015. 87(15): p. 7918-24.
91. Rosting, C., et al., *Determination of the low-abundant protein biomarker hCG from dried matrix spots using immunocapture and nano liquid chromatography mass*

- spectrometry*. *J Chromatogr B Analyt Technol Biomed Life Sci*, 2018. 1077-1078: p. 44-51.
92. Schneck, N.A., et al., *Quantification of cardiac troponin I in human plasma by immunoaffinity enrichment and targeted mass spectrometry*. *Anal Bioanal Chem*, 2018.
93. Mesonzhnik, N.V., et al., *Characterization and detection of EPO-Fc fusion proteins using LC-MS*. *J Proteome Res*, 2017.
94. Smits, N.G., et al., *Monolith immuno-affinity enrichment liquid chromatography tandem mass spectrometry for quantitative protein analysis of recombinant bovine somatotropin in serum*. *Anal Bioanal Chem*, 2015. 407(20): p. 6041-50.
95. Hess, C., et al., *Simultaneous determination and validated quantification of human insulin and its synthetic analogues in human blood serum by immunoaffinity purification and liquid chromatography-mass spectrometry*. *Anal Bioanal Chem*, 2012. 404(6-7): p. 1813-22.
96. Thevis, M., *Mass Spectrometry and the List of Prohibited Substances and Methods of Doping*, in *Mass Spectrometry in Sports Drug Testing*, D.M. Desiderio and N.M. Nibbering, Editors. 2010, John Wiley & Sons, Inc.: Wiley-Interscience Series on Mass Spectrometry
97. Fung, E.N., P. Bryan, and A. Kozhich, *Techniques for quantitative LC-MS/MS analysis of protein therapeutics: advances in enzyme digestion and immunocapture*. *Bioanalysis*, 2016. 8(8): p. 847-56.
98. Ordas, I., et al., *Anti-TNF monoclonal antibodies in inflammatory bowel disease: pharmacokinetics-based dosing paradigms*. *Clin Pharmacol Ther*, 2012. 91(4): p. 635-46.
99. Chambers, A.G., et al., *Multiple Reaction Monitoring Enables Precise Quantification of 97 Proteins in Dried Blood Spots*. *Mol Cell Proteomics*, 2015. 14(11): p. 3094-104.
100. Busher, J.T., *Serum Albumin and Globulin*, in *Clinical Methods: The History, Physical, and Laboratory Examinations*, rd, et al., Editors. 1990: Boston.
101. Billett, H.H., *Hemoglobin and Hematocrit*, in *Clinical Methods: The History, Physical, and Laboratory Examinations*, rd, et al., Editors. 1990: Boston.
102. Zhu, Y., et al., *LC-MS/MS multiplexed assay for the quantitation of a therapeutic protein BMS-986089 and the target protein Myostatin*. *Bioanalysis*, 2016. 8(3): p. 193-204.
103. Bults, P., et al., *LC-MS/MS-Based Monitoring of In Vivo Protein Biotransformation: Quantitative Determination of Trastuzumab and Its Deamidation Products in Human Plasma*. *Anal Chem*, 2016. 88(3): p. 1871-7.

104. Such-Sanmartin, G., et al., *Targeted mass spectrometry analysis of the proteins IGF1, IGF2, IBP2, IBP3 and A2GL by blood protein precipitation*. J Proteomics, 2015. 113: p. 29-37.
105. Such-Sanmartin, G., et al., *Detection and differentiation of 22 kDa and 20 kDa Growth Hormone proteoforms in human plasma by LC-MS/MS*. Biochim Biophys Acta, 2015. 1854(4): p. 284-90.
106. Shen, Y., et al., *Online 2D-LC-MS/MS assay to quantify therapeutic protein in human serum in the presence of pre-existing antidrug antibodies*. Anal Chem, 2015. 87(16): p. 8555-63.
107. Kushnir, M.M., et al., *Measurement of thyroglobulin by liquid chromatography-tandem mass spectrometry in serum and plasma in the presence of antithyroglobulin autoantibodies*. Clin Chem, 2013. 59(6): p. 982-90.
108. Ouyang, Z., et al., *Pellet digestion: a simple and efficient sample preparation technique for LC-MS/MS quantification of large therapeutic proteins in plasma*. Bioanalysis, 2012. 4(1): p. 17-28.
109. Furlong, M.T., et al., *A universal surrogate peptide to enable LC-MS/MS bioanalysis of a diversity of human monoclonal antibody and human Fc-fusion protein drug candidates in pre-clinical animal studies*. Biomed Chromatogr, 2012. 26(8): p. 1024-32.
110. Slecza, B.G., et al., *Quantitation of therapeutic proteins following direct trypsin digestion of dried blood spot samples and detection by LC-MS-based bioanalytical methods in drug discovery*. Bioanalysis, 2012. 4(1): p. 29-40.
111. Kehler, J., et al., *Application of DBS for the quantitative assessment of a protein biologic using on-card digestion LC-MS/MS or immunoassay*. Bioanalysis, 2011. 3(20): p. 2283-90.
112. Rosting, C., A. Gjelstad, and T.G. Halvorsen, *Expanding the knowledge on dried blood spots and LC-MS-based protein analysis: two different sampling materials and six protein targets*. Anal Bioanal Chem, 2017. 409(13): p. 3383-3392.
113. Henderson, C.M., et al., *Quantification by nano liquid chromatography parallel reaction monitoring mass spectrometry of human apolipoprotein A-I, apolipoprotein B, and hemoglobin A1c in dried blood spots*. Proteomics Clin Appl, 2017.
114. Altomare, A., et al., *An in depth proteomic analysis based on ProteoMiner, affinity chromatography and nano-HPLC-MS/MS to explain the potential health benefits of bovine colostrum*. J Pharm Biomed Anal, 2016. 121: p. 297-306.
115. Million, R., et al., *High abundance proteins depletion vs low abundance proteins enrichment: comparison of methods to reduce the plasma proteome complexity*. PLoS One, 2011. 6(5): p. e19603.

116. Gonzalez-Quintela, A., et al., *Serum levels of immunoglobulins (IgG, IgA, IgM) in a general adult population and their relationship with alcohol consumption, smoking and common metabolic abnormalities*. Clin Exp Immunol, 2008. 151(1): p. 42-50.

3 Fully automated dried blood spot sample preparation enables the detection of lower molecular mass peptide and non-peptide doping agents by means of LC-HRMS

Tobias Lange¹, Andreas Thomas¹, Katja Walpurgis¹, & Mario Thevis^{1,2}

¹Center for Preventive Doping Research/Institute of Biochemistry, German Sport University Cologne, Cologne, Germany

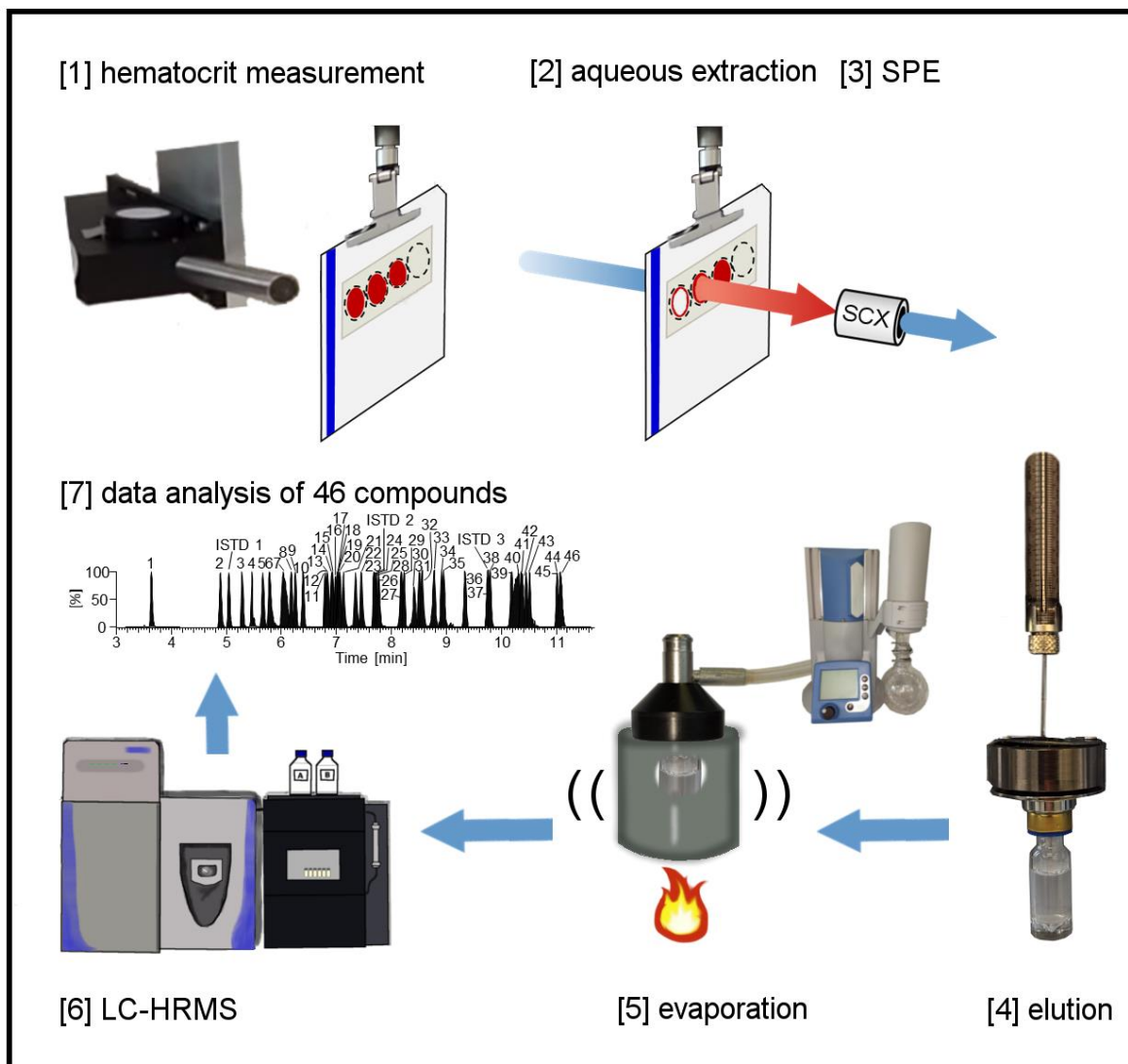
²European Monitoring Center for Emerging Doping Agents (EuMoCEDA), Cologne/Bonn, Germany

Veröffentlicht in: *Analytical and Bioanalytical Chemistry* (2020), 412:3765-3777.

3.1 Abstract

The added value of dried blood spot (DBS) samples complementing the information obtained from commonly routine doping control matrices is continuously increasing in sports drug testing. In this project, a robotic-assisted non-destructive hematocrit measurement from dried blood spots by near-infrared spectroscopy followed by a fully automated sample preparation including strong cation exchange solid phase extraction and evaporation enabled the detection of 46 lower molecular mass (< 2 kDa) peptide and non-peptide drugs and drug candidates by means of LC-HRMS. The target analytes included, amongst others, agonists of the gonadotropin-releasing hormone receptor, the ghrelin receptor, the human growth hormone receptor, and the antidiuretic hormone receptor. Furthermore, several glycine derivatives of growth hormone-releasing peptides (GHRPs), arguably designed to undermine current anti-doping testing approaches, were implemented to the presented detection method. The initial testing assay was validated according to the World Anti-Doping Agency guidelines with estimated LODs between 0.5 and 20 ng/mL. As a proof-of-concept, authentic post-administration specimens containing GHRP-2 and GHRP-6 were successfully analyzed. Furthermore, DBS obtained from a sampling device operating with microneedles

for blood collection from the upper arm were analyzed and the matrix was cross-validated for selected parameters. The introduction of the hematocrit measurement method can be of great value for doping analysis as it allows for quantitative DBS applications by managing the well-recognized “hematocrit effect”.



3.2 Introduction

The use of prohibited peptidic drugs and non-peptide mimetics of lower molecular mass (< 2 kDa) to illegally increase performance in professional sports has been in the focus of preventive doping research for almost a decade. In 2010, the first LC-MS detection method for growth hormone-releasing peptide-2 (GHRP-2) in human urine was described [1] following the identification of the peptide in a nutritional supplement [2]. Subsequently, detection methods were developed and the analytical spectrum was continuously expanded. While initially mainly SPE extracts from urine samples were

used for the detection of lower molecular mass peptides by anti-doping laboratories [1, 3-9], more recent approaches include a total of 21-36 target peptides or their metabolites which can be directly detected from urine by LC-HRMS (“dilute-and-inject”) [10-12]. The growing list of analytes comprises agonists of the ghrelin receptor (e.g. the GHRPs), the gonadotropin-releasing hormone (GnRH) receptor, the human growth hormone (hGh) receptor, and the antidiuretic hormone (ADH) receptor. As they act on different biological axes, their variety of performance-enhancing effects range from fat loss, bone formation, muscle and blood vessel growth to the masking of prohibited substances [4, 13]. Since the World Anti-Doping Agency (WADA) listed the GHRFs (growth hormone-releasing factors) including growth hormone secretagogues (GHS) and GHRPs in 2013 under section S2 “peptide hormones, growth factors, related substances, and mimetics”, several adverse analytical findings (AAF) were reported, mostly from strength sports, which can be attributed to the anabolic effects of these drugs. From 2016 to 2017, the number of GHRF testing was increased by 17% [14]. Recently, glycine-modified analogues of GHRP-2, GHRP-6, and ipamorelin were identified in seized material [15-17]. All of these compounds are classified as non-threshold substances and are prohibited by WADA at all times [18] (in- and out-of-competition).

Urine has been the preferred matrix for the detection of these lower molecular mass peptides in routine doping controls as most analytes demonstrated sufficient stability in urine. Pharmacokinetic studies have demonstrated rapid elimination rates for GHRP-2 [19] and GHRP-6 [20] from blood with a biological half-life of 2.5 ± 1.1 h for GHRP-6. After intravenous (i.v.) administration of GHRP-2, detection times appeared shorter in serum than in urine samples, but for GHRP-6, detection windows were found to be comparable in both matrices [21, 22]. Nevertheless, for urine analysis, knowledge about the metabolic fate of peptide drugs is desirable as the presence of metabolites alongside the intact and unmodified drug (candidate) was shown in the past [3, 9, 23]. For example, GHRP-1 and alexamorelin are rapidly degraded and are traceable in urine only with significantly inferior sensitivity when compared to their metabolites [11].

Dried blood spots (DBS) represent an alternative matrix, which was found to be minimally invasive, cost-efficient, and analyte-stabilizing. Furthermore, sample preparation and analysis were automatable [24, 25] with the prospect of effective high-throughput testing. However, the limited sample volume of 10-20 μ L blood, obtained e.g., from the fingertip, and the highly complex matrix including hemolyzed blood cells and a high

content of soluble and insoluble proteins pose a challenging task for sports drug testing laboratories. This suggests the use of modern chromatographic-mass spectrometric instrumentation, preferably in combination with an automated DBS sample preparation workflow, to enable testing for physiologically relevant concentration levels for these compounds without extensive manual sample preparation such as affinity enrichment. Another aspect to consider in DBS analysis is the “hematocrit (Hct) effect” [26, 27]. The influence of blood dispersal on the DBS filter paper was described to result in a Hct-dependent bias in quantitative assays, and the determination of Hct in DBS may contribute to overcome this limitation.

The aim of this study was to develop and optimize a fully automated DBS sample preparation as a multi-analyte initial testing approach for 46 lower molecular mass peptide and non-peptide agonists. The subsequent LC-HRMS detection method was validated according to WADA guidelines and reconstructed post-administration DBS samples containing GHRP-2 and GHRP-6 were successfully analyzed for proof-of-concept. Moreover, an upstream near-infrared (NIR) spectroscopic measurement was envisaged to support the non-destructive Hct determination before starting with the sample extraction as described by Oostendorp *et al.* [28]. In the context of anti-doping research, fully automated determination of small molecules from DBS was already achieved as, for example, for nicotine and adipoRon (a synthetic adiponectin receptor agonist) with LODs of 5 ng/mL [24, 25].

3.3 Materials and methods

3.3.1 Chemicals and materials

Ammonium hydroxide, acetonitrile, acetic acid, methanol, and MiniPax® absorbent packets were obtained from Merck (Darmstadt, Germany). Albumin solution 20% (v/v) was purchased from Carl Roth (Karlsruhe, Germany). Formic acid was bought from Thermo Fisher Scientific (Bremen, Germany), dimethyl sulfoxide (DMSO) was supplied by Alfa Aesar (Haverhill, MA, USA), and Whatman™ FTA® DMPK-C sample collection cards were obtained from GE Healthcare (Uppsala, Sweden). For blood collection from the upper arm, “TAP” microneedle-based devices were purchased from Seventh Sense Biosystems (Cambridge, MA, USA), and for blood collection from the finger, a Microlet 2 lancing device with lancets from Bayer AG (Leverkusen, Germany) was used. The GHRP-2 metabolite and d₃-Ala-GHRP-2 metabolite (ISTD 2) were in-house

synthesized as described elsewhere [3]. A total of 47 peptide and non-peptide compounds, including 45 analytes and 2 internal standards (ISTDs), were purchased from different suppliers: Auspep (Melbourne, Australia), Bachem (Bubendorf, Switzerland), BMFZ (Düsseldorf, Germany), Centic Biotec (Heidelberg, Germany), Genscript (Piscataway, NJ, USA), MedChem Express (Princeton, NJ, USA), Pepscan (Lelystad, Netherlands), Prospec (Rehovot, Israel), Sigma Aldrich (St. Louis, MO, USA), Sanofi (Paris, France) and Toronto Research Chemicals (North York, ON, Canada). The reference material had a specified purity between 90 and 99% and a specified peptide content between 60 and 94% (Table 3.S1).

3.3.2 Standard solutions

Standard and ISTD stock solutions of the peptides were prepared in Milli-Q water with 10% acetonitrile, 2% acetic acid and 0.5% albumin (v/v) in LoBind tubes. For peptides that were hardly soluble, more acetic acid was added (GHRP-1 met.: 6%, Gly-GHRP-4: 3%, Gly-GHRP-5: 6%). The stock solutions had concentrations between 0.5 and 1 mg/mL and were stored at -20°C. A standard stock mix of all compounds was prepared by diluting the stock solutions to 10 µg/mL (-20°C). Working solutions of the analytes (25-1000 ng/mL) and ISTD (100 ng/mL) were freshly prepared with the solvent mixture used to prepare the aforementioned stock solutions.

3.3.3 DBS sampling methods

EDTA-stabilized blood samples from healthy volunteers were used as a matrix for the preparation of DBS during method development, optimization, and validation. The blood was fortified with the desired concentration of the peptide standard and mixed briefly before spotting 20 µL onto a DBS card. To demonstrate specificity and identification capability, capillary whole blood from the fingertip (by micro lancet) or upper arm (by “TAP” blood collection device) was obtained from five female and five male volunteers. After pricking the fingertip, the first drop of blood was wiped off and then 20 µL were taken with a pipette and placed onto a DBS card. The microneedle-based “TAP” blood collection device combines capillary action and vacuum extraction to collect capillary blood from the upper arm into a Li-heparin coated chamber (100 µL) [29]. After several minutes, the completion of the blood collection is displayed by a blood indicator window. A pipette was used to transfer 20 µL from the device onto the filter

paper. Unless otherwise stated, DBS cards were dried for 2 h at room temperature (RT) and then stored overnight at 4°C in plastic bags with desiccant.

3.3.4 Post-administration samples

From a previous application study, EDTA plasma samples were available from a male subject (59 years, 78 kg) [30]. Here, a single injection containing 666 µg of GHRP-2 and 200 µg of GHRP-6 (Hallandale Pharmacy, FL, USA) was administered subcutaneously. Serum samples were collected after 30, 90, and 270 min and stored at -20°C. For the preparation of artificial DBS specimens, the serum was mixed carefully with fresh blood cells (obtained from EDTA-stabilized venous blood) up to a Hct of 40%.

3.3.5 Fully automated measurement of Hct and sample preparation

The determination of the Hct was realized using a NIRFlex N-500 spectrometer equipped with a fiber optics solids cell from Büchi Labortechnik AG (Essen, Germany) connected to an automated DBS sample preparation system from Gerstel (Mülheim an der Ruhr, Germany). Before initiating sequenced measurements, an internal reference spectrum was recorded by an internal calibration based on a NIR model designed by Oostendorp *et al.* [28] using 261 patient DBS samples (EDTA full blood) with different Hct, age, and sex. After every 10 measurements, a white reference cap was placed manually in front of the fiber optic probe in order to perform a white balance (external calibration). The calibrations were performed according to the manufacturer's advice. DBS cards were automatically moved in front of the optic probe tip in order to non-destructively measure the Hct within 2-3 s. Robotic-assisted sample preparation was then accomplished by a dual-head multi-purpose sampler (MPS) interfaced with a DBS autosampler (DBSA), a solid-phase extraction (SPE) module loaded with strong cation exchange (SCX) polymer cartridges, a multi-position evaporation station (mVAP), and a high-pressure dispenser pump (HPD). The devices were controlled by the Gerstel Maestro 1 software (version 1.4.49.8) and NIRWare (version 1.5.3000).

3.3.6 LC-HRMS/MS

LC-HRMS/MS analysis was accomplished using a Vanquish UHPLC system coupled to a Q Exactive HF-X Hybrid Quadrupole-Orbitrap mass spectrometer, both from Thermo Fisher Scientific (Bremen, Germany) with nitrogen as source/collision gas (CMC, Eschborn, Germany). A Poroshell 120 EC-C8 analytical column, 3.0 x 50 mm, 2.7 µm particle size (PS) from Agilent Technologies (Santa Clara, CA, USA) separated

the analytes chromatographically with 0.1% formic acid as solvent A and acetonitrile, 0.1% formic acid, and 1% DMSO as solvent B, with a flow rate of 350 $\mu\text{L}/\text{min}$. After the injection of 10-20 μL of the sample into the instrument, the chromatographic run with an overall runtime of 15 min was as follows: 1-40% B over 10 min, 40-90% B in 0.5 min, 90% B over 1.5 min, and 1% B for 3 min. The temperature of the sampler was set to 10°C, the column compartment to 30°C and the transfer capillary to 320°C. The ion source was operated in positive mode with an ionization voltage of 3.3 kV. The MS analysis comprised alternating full scan MS experiments with a scan range from m/z 300 to 1500 and targeted-SIM (t-SIM)/dd-MS² experiments with an inclusion list of 53 ions. The resolution (FWHM at $m/z = 200$) was set to 60,000 (full MS), 45,000 (t-SIM), and 15,000 (dd-MS²), automatic gain control target value to 3e6 (full MS), 2e5 (t-SIM), and 5e5 (dd-MS²), and maximum ion injection time to 200 ms (full MS), 25 ms (t-SIM), and 50 ms (dd-MS²), respectively. The t-SIM experiments were acquired with a retention time window of ± 0.5 min around the expected elution time of each analyte, with an isolation window of 3.0 m/z , and an offset of 1.0 m/z . A total of five scan events with a maximum number of five multiplexed ions were acquired before the next full MS started. The normalized collision energy was 35%. The instrument was operated by Thermo Scientific Xcalibur, version 4.1.31.9.

The t-SIM experiments were used to identify the substances by their precursor ions. Full scan MS experiments were acquired alternately with t-SIM/dd-MS² experiments; thus enabling a retrospective data analysis for the detection of formerly unknown substances and metabolites by their precursor ions. The dd-MS² data provided additional information to confirm the selected ion signals of the inclusion list. However, unknown substances cannot be additionally identified via MS/MS within this method.

3.3.7 Method validation of the initial testing procedure

The robotic-assisted DBS sample preparation with subsequent LC-HRMS detection for 46 analytes (Table 3.1) was validated according to WADA guidelines for the validation of initial testing procedures (ITPs) for non-threshold substances [31]. Each analyte was identified by t-SIM experiment at its retention time using two signals, referred to as target ion and confirming ion. The signals are isotopes of the respective precursor ions of the dominant charge state. Gly-GHRP-2 was an exception, as isotope signals of different charge states 1+ and 2+ were used for identification. Five male and five

female volunteers were chosen to demonstrate specificity and identification capability. For the “identification capability”, the blood spots prepared from capillary finger or capillary upper arm blood were allowed to dry on the filter paper for 30 min before 4 μ L of a 100 ng/mL standard mix was added onto the middle of the spot to obtain a concentration of 20 ng/mL. Varying Hct values (24-44%) from different individuals of these DBS samples were used to prove the assay’s robustness towards extractability-related issues. Since different limits of detection (LODs) were expected for the individual analytes, six sample replicates at different concentrations (0.5, 1, 2, 5, 10 and 20 ng/mL) were prepared. The precision was estimated using six sample replicates each at 20 ng/mL, 50 ng/mL, and 100 ng/mL and the coefficient of variation (CV) of the ISTD-normalized peak areas was calculated. In order to study linearity a series of standards within the working range with 2, 5, 10, 20, 50 and 100 ng/mL was prepared and the ISTD-normalized peak areas were analyzed assuming a linear (1st order) regression. The analyte concentrations of the DBS for the validation parameters “LOD”, “linearity”, “precision”, and “carryover” were prepared by carefully mixing venous EDTA-blood with an appropriate amount of the standard mix (volume \leq 5% of the total volume) before spotting onto the DBS card. The recovery was estimated by comparing six samples containing 20 ng/mL of the standard mix (pre-extraction) and six blank samples that were fortified with 20 ng/mL of all target analytes after the evaporation (post-extraction). The pre-extraction DBS samples were prepared by adding 4 μ L of a 100 ng/mL standard mix onto an already dried 20 μ L EDTA-blood spot (in the same way as for “identification capability”). Analytes were thus located in the center of the spot, which allowed their complete extraction by means of the 6 mm clamp. Prior to LC-MS analysis, pre-extraction samples were fortified with 4 μ L ddH₂O and post-extraction samples were fortified with 4 μ L of a 100 ng/mL standard mix and mixed briefly. Three blank samples and three neat samples each fortified with 20 ng/mL immediately before the LC-MS analysis were analyzed to determine absolute matrix effects. The stability of the analytes on the DBS cards as well as the stability of the Hct values was investigated with respect to different storage times (1, 2, 3, 7, 14, 21 days) and temperatures (-20°C, 4°C, 20°C). Two DBS sample replicates were prepared for each storage condition. LC-MS carryover was determined by analyzing a negative control sample (same matrix) immediately after a sample containing a high analyte concentration of 100 ng/mL. To further study the DBSA-SPE carryover, a blank sample was extracted after this sample. For the specificity and identification capability, a cross-

validation for DBS obtained from the upper arm (“TAP” device) from the same ten volunteers was realized.

Table 3.1: LC-HRMS related characteristics and categories of the target compounds.

Compound	Pre-dominant charge state	Target ion [m/z]	Confirming ion [m/z]	RT [min]	Category
Alarelin	2+	584.3065	584.8080	7.01	GnRH receptor agonist
Alexamorelin	2+	479.7560	480.2574	7.42	Ghrelin receptor agonist
Alexamorelin (3-6) met.	1+	623.2957	624.3030	10.35	Ghrelin receptor agonist
Anamorelin	1+	547.3391	548.3421	11.08	Ghrelin receptor agonist
AOD9604	2+	907.9375	908.4388	6.98	hGH receptor agonist
AOD9604 (7-16) met.	2+	521.7077	522.2092	5.27	hGH receptor agonist
Buserelin	2+	620.3353	620.8367	8.50	GnRH receptor agonist
(d ₃)-Ala-GHRP-2 met. (ISTD)	1+	361.1948	362.1979	7.68	Ghrelin receptor agonist
(d ₄)-Ala-GHRP-4 (ISTD)	1+	612.3231	613.3262	9.54	Ghrelin receptor agonist
Deslorelin	2+	641.8276	642.3291	8.54	GnRH receptor agonist
Desmopressin	1+	1069.4342	1070.4370	7.04	ADH receptor agonist
Felypressin	2+	520.7257	521.2271	6.16	ADH receptor agonist
Fertirelin	2+	577.2987	577.8001	6.81	GnRH receptor agonist
GHRP-1	2+	478.2505	478.7520	7.65	Ghrelin receptor agonist
GHRP-1 (3-6) met.	1+	620.2883	621.2913	11.02	Ghrelin receptor agonist
GHRP-2	2+	409.7210	410.7240	8.88	Ghrelin receptor agonist
GHRP-2 (1-3) met.	1+	358.1761	359.1792	7.69	Ghrelin receptor agonist
GHRP-3	1+	655.4038	656.4067	6.03	Ghrelin receptor agonist
GHRP-4	1+	608.2980	609.3010	9.74	Ghrelin receptor agonist
GHRP-5	1+	771.3613	772.3643	10.27	Ghrelin receptor agonist
GHRP-6	2+	437.2296	437.7312	6.81	Ghrelin receptor agonist
GHRP-6 (2-5) met.	1+	609.2820	610.2850	10.19	Ghrelin receptor agonist
Gly-Alexamorelin	2+	508.2667	508.7681	7.08	Ghrelin receptor agonist
Gly-GHRP-1	2+	506.7612	507.2627	7.71	Ghrelin receptor agonist
Gly-GHRP-2	2+	438.7330	876.4592	8.93	Ghrelin receptor agonist
Gly-GHRP-3	1+	712.4253	713.4281	6.24	Ghrelin receptor agonist
Gly-GHRP-4	1+	665.3194	666.3224	9.77	Ghrelin receptor agonist
Gly-GHRP-5	1+	828.3828	829.3858	10.52	Ghrelin receptor agonist
Gly-GHRP-6	2+	465.7403	466.2417	6.91	Ghrelin receptor agonist
Gly-Hexarelin	2+	472.7481	473.2496	6.98	Ghrelin receptor agonist
Gly-Ipamorelin	2+	385.2108	385.7123	6.79	Ghrelin receptor agonist
Goserelin	2+	635.3280	635.8294	8.17	GnRH receptor agonist
Hexarelin	2+	444.2374	444.7388	6.94	Ghrelin receptor agonist
Hexarelin (1-3) met.	1+	427.2088	428.2117	4.87	Ghrelin receptor agonist
Histirelin	2+	662.3409	662.8423	6.92	GnRH receptor agonist
Ibutamoren	1+	529.2479	530.2505	10.38	Ghrelin receptor agonist
Ipamorelin	2+	356.7001	357.2016	5.77	Ghrelin receptor agonist
Ipamorelin (1-4) met.	1+	585.2820	586.2850	7.65	Ghrelin receptor agonist
Lecirelin (Dalmarelin)	2+	605.3300	605.8314	8.40	GnRH receptor agonist

Leuprolide	2+	605.3300	605.8314	8.16	GnRH receptor agonist
Leuprolide (1-3) met.	1+	453.1881	454.1910	5.27	GnRH receptor agonist
LHRH	2+	591.7938	592.2953	6.39	GnRH receptor agonist
[Lys8]-Vasopressin (ISTD)	2+	528.7231	529.2248	5.02	ADH receptor agonist
Nafarelin	2+	661.8251	662.8279	9.36	GnRH receptor agonist
Nafarelin (5-10) met.	2+	401.2242	401.7257	8.75	GnRH receptor agonist
Peforelin	2+	630.2889	630.7903	5.47	GnRH receptor agonist
Tabimorelin	1+	529.3173	530.3205	10.31	Ghrelin receptor agonist
TB500	2+	445.2531	445.7546	3.61	Synthetic version of an active region of thymosin β_4
Triptorelin	2+	656.3227	656.8241	8.21	GnRH receptor agonist

3.4 Results and discussion

3.4.1 Method development and optimization

The fully automated sample preparation was optimized with regard to the extraction agent, the employed extraction volume, the SPE purification, and the duration, temperature and vacuum of the evaporation step. Due to the good water solubility of the analytes, an aqueous solution was used for the extraction from the DBS card. Different stationary phases (CN, C12, C8, C18, SCX, strong hydrophobic, general purpose, and mixed mode cation/anion exchange) were tested for solid-phase extraction and ion exchange cartridges, especially SCX, yielded the best results.

Briefly, a DBS was extracted with 1.5 mL ddH₂O (4 mL/min, 100°C) through a clamp with a diameter of 6 mm. Sixty microliters of the deuterated ISTD mix (100 ng/mL) were automatically added through a separate loop and the sample extract was loaded onto a pre-conditioned SCX SPE. The SCX cartridge was washed with 2% formic acid and analytes were eluted with 1.4 mL of 5% ammonium hydroxide in methanol into a glass vial. Then, the sample eluate was evaporated in the mVAP for 37 min at 50°C and 250 rpm with ramping pressure from 200 to 60 mbar. Finally, the sample containing 100 μ L could be transferred manually to the LC-HRMS system.

With a cold system start, the total time for a batch of 6 samples (maximum number of positions in the mVAP) was approximately 2 h. By programming a nesting of individual sample preparation steps, the total time of various batches could be significantly reduced. More details about the individual steps and information about volumes, flow velocities, pressure, temperature, and agitation can be found in the Supplementary data section.

3.4.2 Method characterization and validation

As shown in Table 3.1, a total of 46 target analytes were included within this study, comprising “classical” peptide drugs such as ipamorelin (pentapeptide) or goserelin (decapeptide), non-peptide drugs (mimetics) such as anamorelin as well as several potentially performance enhancing Gly-derivatives of the GHRPs. Moreover, GHRP-1, which was stable in urine only as its metabolite [10], was successfully analyzed in DBS. Felypressin, a new vasoconstrictor related to vasopressin, was determined for the first time.

The lower molecular mass peptides < 2 kDa were observed to predominantly form doubly-charged molecules under the chosen conditions. However, as already described by others, DMSO as an additive in the LC solvent does not only improve the ionization efficiency [32] but also influences the charge state distribution of the peptides, shifting the equilibrium to the direction of lower charge states [33]. Therefore, a relatively large number of 17 singly charged molecules compared to 29 doubly charged species was utilized for an unambiguous identification (target ion) within this assay (t-SIM experiments).

The assay was characterized by a homogeneous chromatographic distribution of the analytes with most substances eluting between 5 and 11 min.

The ITP was validated according to WADA’s international standard for laboratories 10.0 [31] (Table 3.2). As the analytes are non-threshold substances, the minimum criteria for LC-MS confirmation of the identity of analytes are applied to demonstrate the presence of a prohibited substance. The selectivity for the 46 substances was demonstrated by analyzing 10 blank samples collected from different individuals (male and female). As exemplarily shown in Figure 3.1 (dashed line) and Figure 3.S1, no interfering signals were detected in the blank samples (specificity). Subsequently, 10 samples from the same volunteers were fortified with 20 ng/mL of the standard mix and analyzed again (Figure 3.1, solid line). Hereafter, all substances of interest could be unambiguously identified (identification capability). The LC conditions were very suitable for the efficient separation of the analytes with the only exception of tabimorelin (poor peak shape). In case of a suspicious finding, adapted LC conditions can be used for a “confirmation procedure” for tabimorelin. In the ion chromatogram at RT = 7.3 min, a second peak of hexarelin with an identical mass was observed that originated from alexamorelin metabolite (2-7)-NH₂. Due to an intensive degradation of alexamorelin in

blood as was shown by others [23, 34], several metabolites can be formed. This metabolite was not included for initial testing purposes; however, it may assist the confirmation of an alexamorelin finding. Following this, the alternative “TAP” sampling method for the upper arm was tested and cross-validated for these parameters. In the same way as for the blood collected from the fingertip, the assay’s selectivity was shown for all target analytes. Furthermore, the LOD was estimated by applying a signal-to-noise ratio > 3 for the individual target and confirming ions with the following results: 7 analytes at 0.5 ng/mL, 7 analytes at 1 ng/mL, 12 analytes at 2 ng/mL, 10 analytes at 5 ng/mL, 9 analytes at 10 ng/mL, and 1 analyte at 20 ng/mL.

For a more comprehensive assay characterization, additional parameters were determined, as, for example, required for confirmation procedures. The individually variable Hct values of the DBS samples from a finger prick determined by the NIR spectrometer ranged between 24 and 40%. No impact on the LC-HRMS/MS identification of the analytes was observed, and the method’s robustness was demonstrated. Some articles reported on a Hct-dependent bias concerning quantitative bioanalysis using DBS, especially when a small punch of the DBS was excised [27]. Such phenomena were not observed in the present study, attributed to the fact that almost the entire spot was extracted using the 6 mm clamp, and the issue of nonhomogeneous analyte distribution described before was therefore negligible. However, within this assay, the robustness for post-fortified DBS samples (from blank samples with different Hct) was studied, since the smallest volume of non-coagulated capillary blood that could be obtained from the fingertip was not suitable for mixing with the standard before spotting onto the DBS card. Due to this way of DBS sample preparation, in which the analytes were pipetted onto the DBS card, the analytes were rather localized in the center of the spot. Thus, the impact of e.g. differential spreading of blood with different Hct was not evaluated here. The carryover after extracting a sample with a high concentration of 100 ng/mL was determined for both the DBSA and the LC-HRMS/MS system and was from 0 to 18.9% (data not shown) and from 0 to 9.9%, respectively. Despite the low probability of such highly concentrated doping control samples, it is recommended to rinse the DBSA system thoroughly on a regular basis to remove any potential residues of blood cell components and proteins. The total recovery of the method for the different analytes varied between 3.7% and 69.6%, and the matrix effects ranged from 33% to 156%. Values $< 100\%$ indicate ionization suppression effects and values

> 100% indicate ionization enhancement effects caused by the sample matrix [35]. The linearity was determined from the LOD to 100 ng/mL or not lower than 2 ng/mL for analytes with LOD < 2 ng/mL and yielded coefficients of correlation r between 0.9862 and 0.9999. For the linear regression, slope and intercept were additionally specified (Table 3.S2). The precision was estimated for 6 replicates per analyte at 20 ng/mL, 50 ng/mL, and 100 ng/mL and was found to be below 25% for most substances. All analytes remained stable on the DBS card at all storage conditions over 3 weeks and were repeatedly identified at a concentration of 20 ng/mL for 2 replicates each. The variations of the observed ISTD-normalized peak areas were found to be within the range of variation of this method. A time-dependent degradation of the compounds could not be observed.

Table 3.2: Main results of validation.

Compound	LOD [ng/mL] (n = 6)	Linearity (R) LOD-100 ng/mL (n = 1)	Precision at 20 ng/mL [%] (n = 6)	Precision at 50 ng/mL [%] (n = 6)	Precision at 100 ng/mL [%] (n = 6)	Recovery at 20 ng/mL [%] (n = 6)	Carryover after 100 ng/mL [%] (n = 1)	Matrix effects [%] (n = 3)
Alarelin	5	0.9991	14.9	17.3	15.4	24.6	0.1	67
Alexamorelin	1	0.9967	16.8	17.5	7.8	9.9	8.5	113
Alexamorelin (3-6) met.	10	0.9979	31.2	35.3	21.9	13.0	0.1	49
Anamorelin	0.5	0.9998	15.2	16.4	5.2	33.7	0.7	48
AOD9604	10	0.9907	32.4	11.9	17.8	3.7	1.8	64
AOD9604 (7-16) met.	5	0.9888	37.7	22.4	11.9	10.5	0.6	54
Buserelin	5	0.9970	11.6	4.5	14.5	20.9	0	55
Deslorelin	5	0.9952	11.8	4.0	7.1	12.1	0.1	55
Desmopressin	10	0.9935	13.6	23.3	21.6	7.3	0	67
Felypressin	0.5	0.9990	14.7	6.3	3.6	25.5	0.7	86
Fertirelin	1	0.9993	14.5	14.5	18.5	22.1	0.1	69
GHRP-1	10	0.9919	21.8	17.4	12.7	11.2	3.6	142
GHRP-1 (3-6) met.	5	0.9991	18.4	53.4	8.9	14.9	0.1	48
GHRP-2	2	0.9991	13.3	5.2	6.8	11.2	0.1	55
GHRP-2 (1-3) met.	2	0.9998	17.5	7.8	5.3	25.1	0.1	76
GHRP-3	5	0.9973	19.5	2.7	27.8	27.4	0.1	79
GHRP-4	2	0.9996	15.7	14.7	2.6	28.2	0	53
GHRP-5	2	0.9964	16.8	14.6	4.8	22.4	0	33
GHRP-6	2	0.9975	7.9	15.2	25.6	41.6	9.1	96
GHRP-6 (2-5) met.	2	0.9982	24.7	31.6	10.6	19.8	0.1	52
Gly-Alexamorelin	5	0.9990	16.9	11.5	18.7	13.8	8.7	117
Gly-GHRP-1	2	0.9949	12.3	18.8	5.8	19.4	4.2	156
Gly-GHRP-2	10	0.9988	7.8	11.9	16.0	17.4	5.3	55
Gly-GHRP-3	5	0.9965	18.9	4.7	21.0	24.6	0.1	77
Gly-GHRP-4	1	0.9993	14.5	17.4	4.0	26.1	0	52
Gly-GHRP-5	5	0.9972	12.2	19.9	6.8	12.8	0.1	45
Gly-GHRP-6	2	0.9987	18.1	15.7	7.8	17.8	7.8	135
Gly-Hexarelin	2	0.9986	15.4	13.4	13.9	13.0	6.4	123

FULLY AUTOMATED DRIED BLOOD SPOT SAMPLE PREPARATION ENABLES THE DETECTION OF LOWER MOLECULAR MASS PEPTIDE AND NON-PEPTIDE DOPING AGENTS BY MEANS OF LC-HRMS

Gly-Ipamorelin	1	0.9984	10.0	12.6	9.9	69.6	7.8	125
Goserelin	2	0.9965	8.7	10.8	10.9	17.3	0.1	57
Hexarelin	10	0.9999	19.7	15.1	12.3	14.6	5.7	84
Hexarelin (1-3) met.	0.5	0.9958	25.7	14.9	5.6	24.4	6.9	51
Histrelin	5	0.9980	18.3	15.5	14.7	20.8	1.5	62
Ibutamoren	1	0.9999	24.9	15.5	13.2	46.3	0.4	46
Ipamorelin	0.5	0.9989	13.5	17.9	7.1	50.9	9.9	76
Ipamorelin (1-4) met.	0.5	0.9966	19.6	20.1	7.8	33.8	3.4	68
Lecirelin (Dalmarelin)	0.5	0.9992	11.1	3.4	13.9	24.2	0	54
Leuprolide	0.5	0.9985	10.3	5.3	10.5	27.5	0	56
Leuprolide (1-3) met.	1	0.9981	23.1	16.7	11.5	23.6	0.1	75
LHRH	2	0.9992	14.4	4.7	24.0	21.4	0.2	70
Nafarelin	10	0.9862	13.8	4.0	8.3	8.0	0.2	49
Nafarelin (5-10) met.	2	0.9948	19.8	15.9	9.5	11.5	0.1	57
Peforelin	20	0.9985	26.6	12.8	14.0	34.9	0.5	61
Tabimorelin	10	0.9991	23.3	10.6	8.1	46.4	0	51
TB500	1	0.9996	22.2	12.8	6.7	19.5	1.6	54
Triptorelin	10	0.9961	15.5	3.5	7.3	14.0	0	56

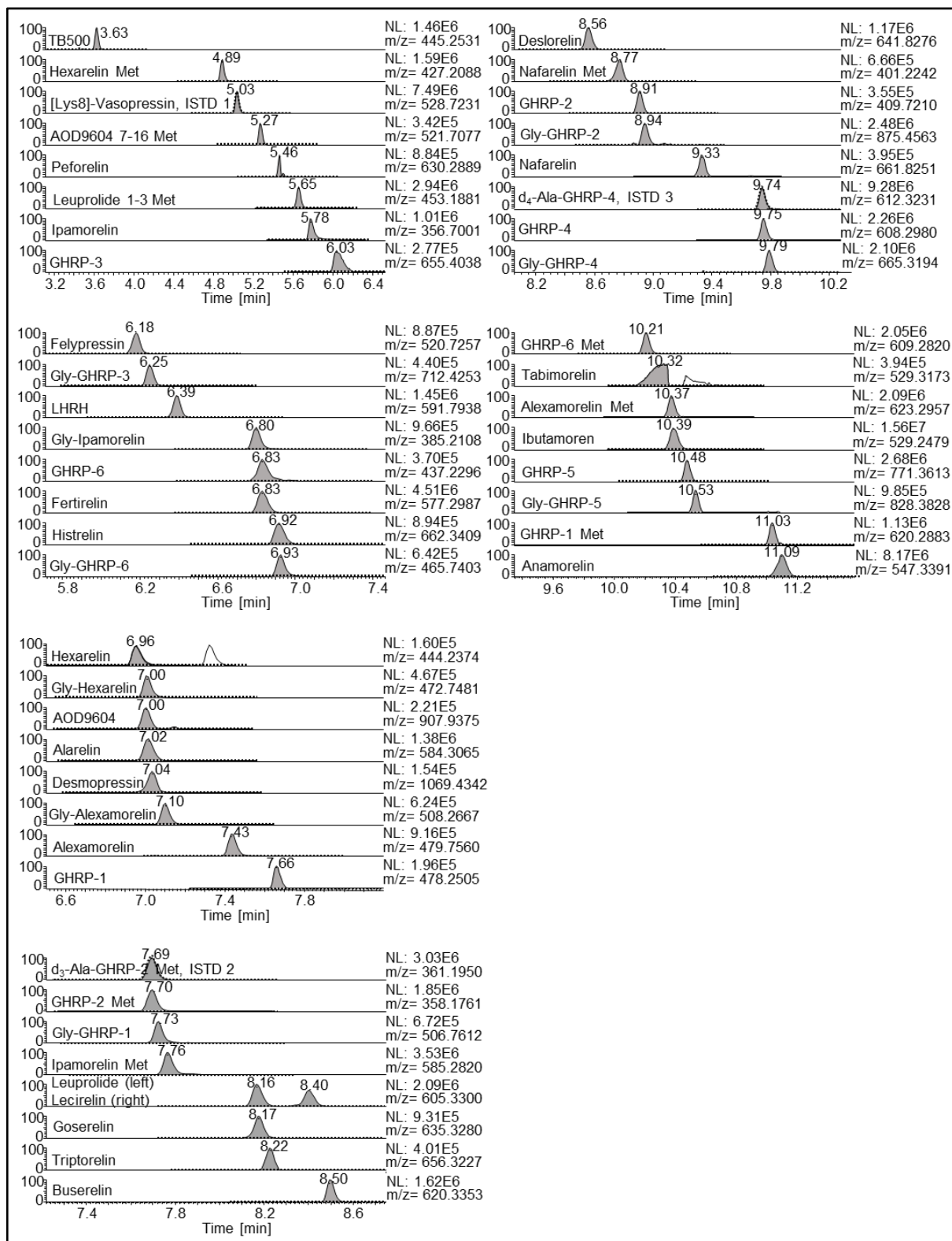
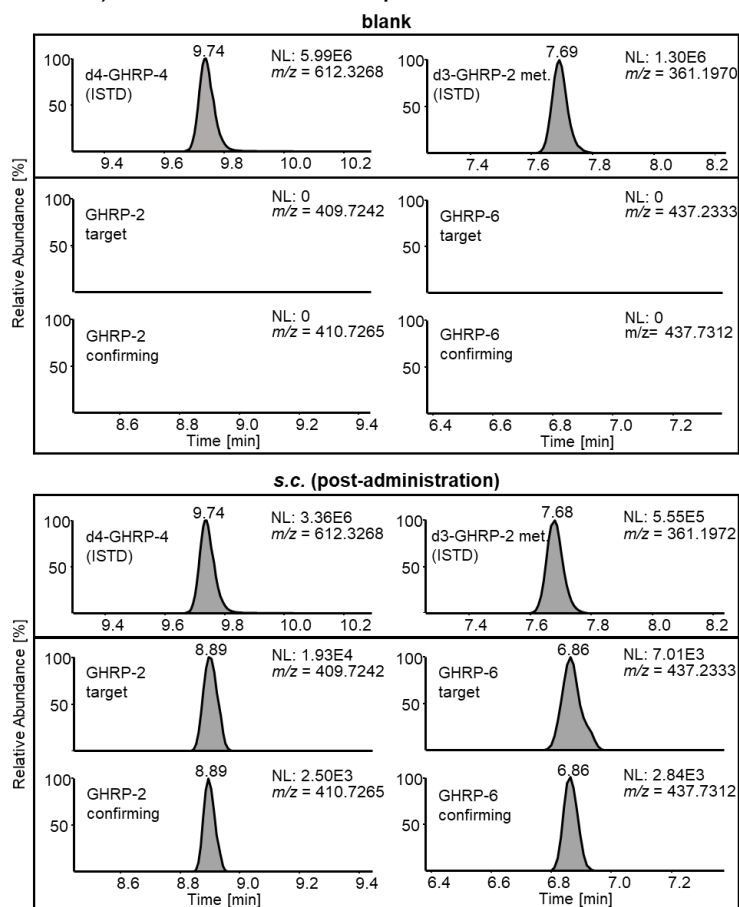


Figure 3.1: Extracted ion chromatograms (mass tolerance \pm 5 ppm) of a sample from a female volunteer obtained by a finger prick. The sample was either analyzed as blank (dashed line) or with 20 ng/mL of a peptide mix containing all 46 target compounds. The rows of the 3 ISTDs are also shown at their respective retention time.

3.4.3 Post-administration samples

It is desirable to show that the substances cannot only be detected in fortified samples but also in authentic specimens, for example, collected in the course of administration studies. Since serum samples from a previous elimination study with GHRP-2 and GHRP-6 were available, DBS with a Hct = 40% were reconstructed. As shown in Figure 3.2, both GHRP-2 and GHRP-6 could be unambiguously identified by their characteristic target and confirming ions in DBS generated from blood samples reconstructed with serum that was collected up to 90 min after application.

In DBS generated from blood reconstituted with serum that was collected 4.5 post-administration, specific signals were still detectable but could not be confirmed by a second isotopic peak (confirming signal). A blank sample showed no interfering signals at the respective retention times. A standard calibration curve for GHRP-2 and GHRP-6 between 5 and 50 ng/mL was applied to estimate the concentration from the DBS samples, yielding levels between 2 and 10 ng/mL within the detection window (30-90 min). The results correspond with the concentrations of GHRP-2 and GHRP-6 after



a single i.v. injection from other studies [19, 20]. It should be noted here that serum blood levels are expected to be slightly different from full blood levels because the analytes will most likely not be found at identical concentrations in red blood cells and serum. Nevertheless, the applicability of the testing procedure to post-administration samples could be successfully demonstrated.

Figure 3.2: Extracted ion chromatograms (mass tolerance \pm 10 ppm) of a blank sample and a s.c. post-administration sample showing signals of GHRP-2 and GHRP-6.

3.4.4 Hct determination by NIR spectroscopy

The NIR spectroscope was used for non-destructive Hct measurements of DBS to obtain preliminary data in a pilot project only. A previously developed NIR model [28] was adopted to determine the Hct, and the influence of storage time and temperature on the Hct measurements was studied. For this purpose, EDTA-stabilized venous blood from one volunteer was utilized, and regular measurements in triplicate (spot 1-3) were performed over a period of 3 weeks while storing DBS cards in the dark at RT, 4°C, and -20°C. DBS cards were dried for 6 h at RT and then stored under the conditions described above. A reference value of 38% measured by a Sysmex XN-1000 analyzer was determined on the first day after blood drawing. Regardless of the storage time, slight differences in a temperature-dependent manner in the range of 32.0-38.7% were observed. The DBS cards stored for at least 1 day at RT showed Hct values close to the reference value while cards stored at 4°C and -20°C resulted in lower values as visualized in Figure 3.3. In spite of sealing the cards in plastic bags with a desiccant, the differences in temperature or humidity might influence the molecular vibrations of the DBS matrix that are crucial for the NIR spectrum calculation. A time-dependent change in total hemoglobin was not assumed as others have already shown its stability in DBS [36]. A considerably slower drying or freezing of remaining moisture of the DBS matrix at reduced temperatures would be in accordance with this observation, suggesting a prolonged drying phase (1-2 days at RT followed by storage at RT with desiccant) for a reliable Hct measurement using the presented approach with DBS cards.

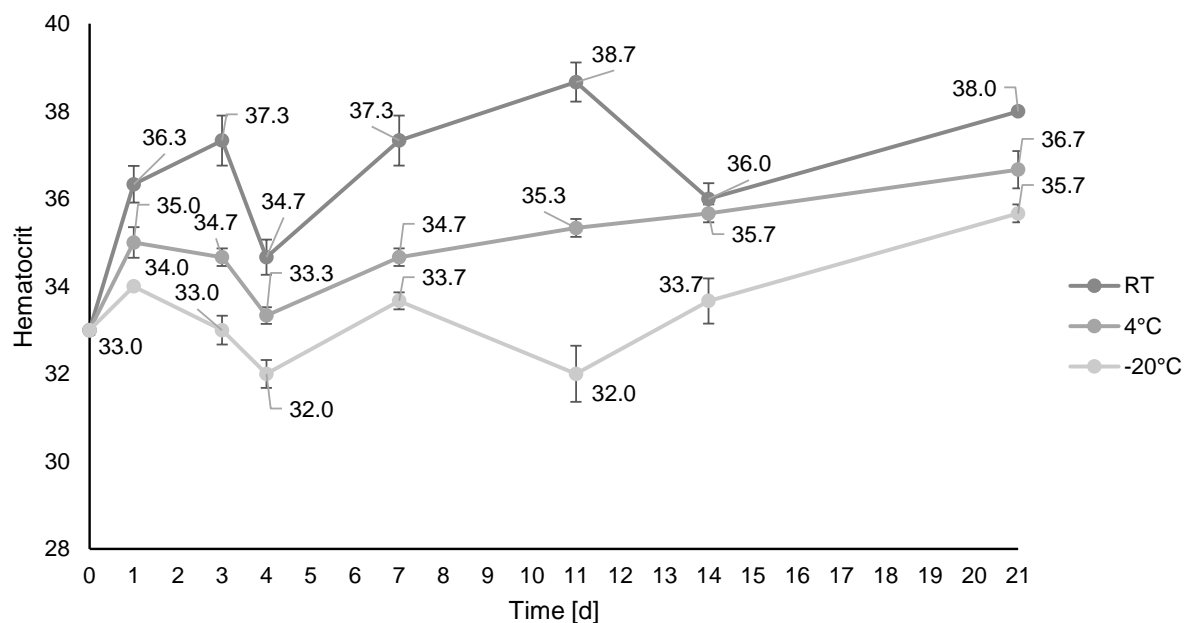


Figure 3.3: The influence of storage time and temperature on the capillary DBS Hct measurements by NIR spectroscopy was studied. Several DBS cards were stored over a period of 3 weeks at RT, 4°C and -20°C and samples were measured in triplicate (spot 1-3). The error bars result from the standard deviations of the respective experiments.

Since all measurements on the NIR spectroscope by Oostendorp *et al.* were based on DBS prepared from venous EDTA-stabilized blood [28], the applicability of the Hct calculation to capillary DBS collected by finger prick was investigated. Therefore, the Hct of different authentic DBS samples collected from ten volunteers was determined. DBS were sealed and dried for 2 days at RT. The measured Hct were found to be considerably lower than expected with a range from 24 to 40% (and an average of 31%), potentially resulting from different confounding factors. In some cases, finger blood collection was complicated by a slow blood flow, and even a slight squeezing of the finger can provoke exudate leaking into the collected blood causing a dilution of the sample. In addition, Hct values reportedly differ between body regions [37] and variation in capillary density, cutaneous blood content and red blood cell velocity must be taken into account [38]. The influence of anticoagulant (K2EDTA) on the NIR spectra might necessitate further investigations as well, suggesting more comprehensive studies in order to enable a holistic classification of Hct values obtained from NIR spectroscopy. As shown before, the different Hct values had no effect on the detection of the substances in this qualitative assay. However, the Hct is relevant in case of quantitative analyses regarding threshold substances determined from DBS, since the conversion from full blood into plasma concentrations seems to be decisive for the

determination of concentration thresholds. A Hct-dependent correction factor could overcome this previous limitation when using DBS.

3.4.5 DBS sampling methods

Both DBS sampling methods either from the arm or from the finger were successfully validated regarding selectivity. Compared with DBS collection from the finger prick, most volunteers described the arm device to be virtually painless and more comfortable to use. It is noteworthy that sample collection failure was reduced compared to the procedure with the finger lancet. The “TAP” devices could be leveraged to refine the method of blood collection.

3.5 Conclusion

In sports drug testing, the demand for a higher sample throughput is continuously increasing. DBS sample collection may contribute to this development. The complementary matrix is mainly characterized by its cost efficiency (in terms of storage and shipping) and minimal invasiveness. In order to deter doping, a fully automated robotic DBS sample preparation with LC-HRMS detection was developed. The multi-analyte initial testing approach comprises 46 lower molecular mass peptide or non-peptide (mimetic) target analytes <2 kDa of different receptor agonist categories such as agonists that bind to ghrelin receptors, GnRH receptors, hGh receptors, and ADH receptors. Due to the discovery of glycine-modified analogues, the list of analytes was extended preventively with a series of nine glycine-modified peptides, mainly GHRPs. In addition, GHRP-1 that could not be detected in urine before [10], and felypressin, an ADH receptor agonist, were implemented for the first time in an anti-doping detection procedure. The vast majority of the drug candidates are still under development, in clinical trials or were discontinued. To the best of our knowledge, leuprolide, felypressin, LHRH, histrelin, desmopressin, GHRP-2, goserelin, triptorelin, buserelin, and nafarelin have obtained clinical approval. For veterinary use only, the application for marketing authorization was concerned for peforelin, alarelin, lecirelin, and deslorelin. Independent from the state of development, all these pharmaceuticals are available on the black market and pose a potential risk in relation to doping practices.

Despite the small DBS volume of 20 μ L, sensitivities enabling the detection of an illicit use were achieved. Remarkably, more than 60% of the analytes could be detected

below the WADA's minimum required performance limit (MRPL) of 2 ng/mL for urine [39]. Until now, no MRPL specification is available for serum/plasma or DBS.

Furthermore, an upstream NIR spectroscope for non-destructive Hct measurement was implemented and the assay's robustness in terms of extractability was demonstrated for different Hct values. This approach could contribute to a Hct-dependent correction and would support quantitative DBS applications in the future.

As a proof-of-concept, artificial DBS samples obtained from post-administration specimens containing GHRP-2 and GHRP-6 were successfully analyzed.

The automated DBS preparation of 6 samples lasted approximately 2 h, as long as the subsequent LC-HRMS analysis and was therefore ideally suited for a just-in-time workflow. The automation and the possibility of a programmable nesting of the preparation steps within the sequence would allow for an increased sample throughput compared to sophisticated manual sample preparation. Finally, if desired, the entire assay could be easily extended with new compounds.

3.6 Supplementary data

3.6.1 DBS extraction

To ensure an efficient DBS extraction of the analytes, different organic-aqueous compositions were tested: 100%, 80%, 60%, 40%, 20%, and 0% acetonitrile. The addition of acetonitrile was found to reduce the co-elution of interfering proteins such as hemoglobin. At the same time, however, the amount of extracted analytes also decreased with increasing amounts of acetonitrile. Finally, an aqueous extraction (no organic component) was applied. Further purification of the DBS extract was achieved by a subsequent strong cation exchange (SCX) solid phase extraction (SPE).

3.6.2 Programming the automated DBS sample preparation

The protocol for the automated sample preparation was programmed as follows: First, a SCX SPE cartridge is loaded into position, conditioned with 1 mL methanol (3 mL/min) and washed with 1 mL water (3 mL/min). Second, the right arm of the MPS takes the first DBS card from the sample rack (maximum capacity: 40 cards) and inserts it into the DBSA. There, the position of the spot is determined by a camera recognition system and the card is moved in front of a 6 mm clamp, which now closes with 2900 N around the spot. Third, 60 μ L of the deuterated ISTD mix (100 ng/mL) are automatically added through a separate loop before 1.5 mL aqueous flow extraction starts with 4 mL/min at 100°C. To avoid carry-over, the first 300 μ L of the extract are discarded. For the same reason, the clamp now moves to an empty position on the DBS card and is rinsed with 1 mL water, 1 mL 80% acetonitrile, and 2 mL water. Meanwhile, the sample extract is loaded onto the SCX cartridge and is washed with 1 mL of 2% formic acid (3 mL/min). Fourth, the analytes are eluted with 1.4 mL of 5% ammonium hydroxide in methanol (2 mL/min) and transferred via the syringe of the left arm into a glass vial (10 mm vial penetration). Again, the first 50 μ L of the eluate are discarded. The syringe is rinsed twice with 20% acetonitrile and water (fill/eject speed is 50 μ L/s), before fifth, it is transported to the mVAP and there the eluate is evaporated by agitation (250 rpm) for 37 minutes at 50°C and ramping pressure from 200-60 mbar. The mVAP offers the simultaneous handling of a maximum of 6 samples and is therefore the limiting factor of the sample preparation workflow. Finally, the syringe is again rinsed twice and the sample containing 100 μ L is now ready for LC-MS analysis.

The software allows a nesting of the preparation steps within the sequence. This means, for example, that 6 blood spots can be extracted while the robot is still evaporating the previous 6 samples. That results in a considerable reduction of total sample preparation time.

FULLY AUTOMATED DRIED BLOOD SPOT SAMPLE PREPARATION ENABLES THE DETECTION OF LOWER MOLECULAR MASS PEPTIDE AND NON-PEPTIDE DOPING AGENTS BY MEANS OF LC-HRMS

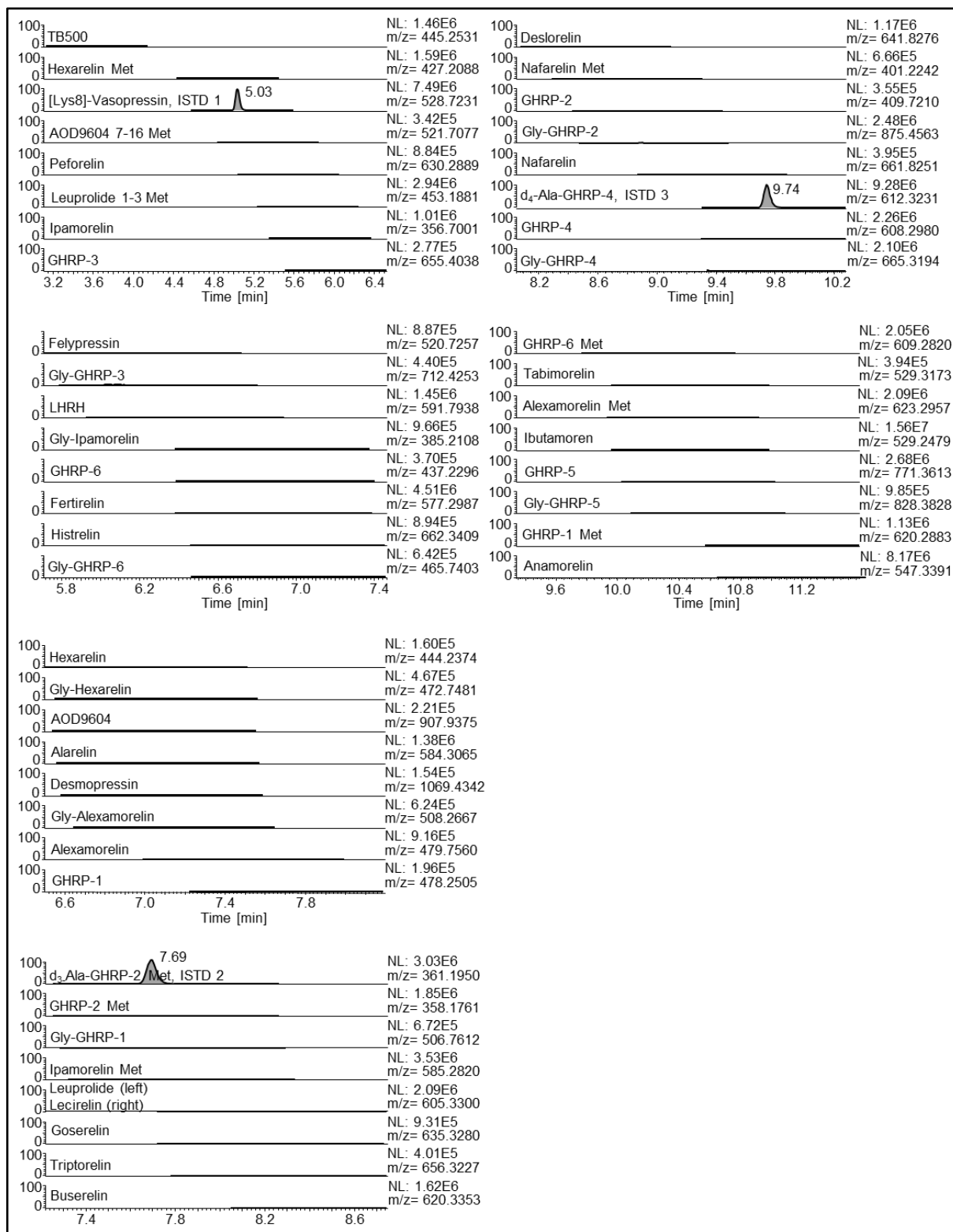


Figure 3.S1: Extracted ion chromatograms (mass tolerance ± 5 ppm) of a blank sample from a female volunteer obtained by a finger prick. The rows of the 3 ISTDs are also shown at their respective retention time. Normalization levels (NL) are adapted from Figure 3.1.

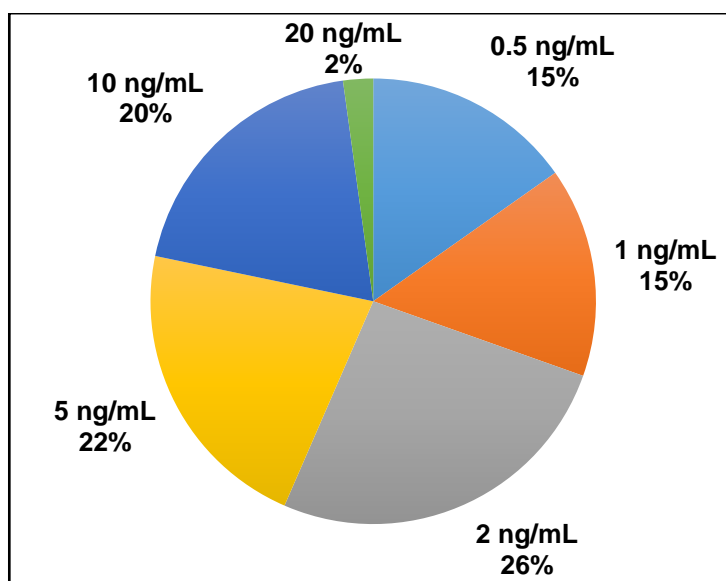


Figure 3.S2: The distribution of LODs. Different LODs of the analytes in the range between 0.5-20 ng/mL were obtained after analysis of a DBS sample.

Table 3.S1: Supplier, location, specified peptide purity and peptide content of the standard substances.

Compound	Supplier	Location	Peptide purity [%]	Peptide content [%]
Alarelin	Auspep	Tullamarine, Australia	98	77
Alexamorelin	BMFZ	Düsseldorf, Germany	> 90*	n.a.
Alexamorelin (3-6) met.	Centic Biotec	Heidelberg, Germany	> 90	n.a.
Anamorelin	Auspep	Tullamarine, Australia	> 95	n.a.
AOD9604	Auspep	Tullamarine, Australia	98	94
AOD9604 (7-16) met.	Auspep	Tullamarine, Australia	95	73
Buserelin	Bachem	Bubendorf, Switzerland	> 95	n.a.
Deslorelin	Prospec	Rehovot, Israel	> 99	n.a.
Desmopressin	Sigma Aldrich	St. Louis, MO, USA	98	87
Felypressin	Sigma Aldrich	St. Louis, MO, USA	99.4	n.a.
Fertirelin	Bachem	Bubendorf, Switzerland	99.3	87.3
GHRP-1	BMFZ	Düsseldorf, Germany	> 90*	n.a.
GHRP-1 (3-6) met.	Centic Biotec	Heidelberg, Germany	> 90	n.a.
GHRP-2	Bachem	Bubendorf, Switzerland	97.1	75.7
GHRP-2 (1-3) met.	In-house synthesis	Cologne, Germany	99	n.a.
(d ₃)-GHRP-2 (1-3) met. (ISTD 1)	In-house synthesis	Cologne, Germany	72	n.a.
GHRP-3	Pepscan	Lelystad, Netherlands	96.9	n.a.
GHRP-4	Auspep	Tullamarine, Australia	99	76
(d ₄)-GHRP-4 (ISTD 2)	BMFZ	Düsseldorf, Germany	> 90*	n.a.
GHRP-5	Auspep	Tullamarine, Australia	99	74
GHRP-6	Auspep	Tullamarine, Australia	99	71.5
GHRP-6 (2-5) met.	Auspep	Tullamarine, Australia	99	76.2

FULLY AUTOMATED DRIED BLOOD SPOT SAMPLE PREPARATION ENABLES THE DETECTION OF LOWER MOLECULAR MASS PEPTIDE AND NON-PEPTIDE DOPING AGENTS BY MEANS OF LC-HRMS

Gly-Alexamorelin	Genscript	Leiden, Netherlands	98	n.a.
Gly-GHRP-1	Genscript	Leiden, Netherlands	99.4	n.a.
Gly-GHRP-2	Genscript	Leiden, Netherlands	98.4	n.a.
Gly-GHRP-3	Genscript	Leiden, Netherlands	96.2	n.a.
Gly-GHRP-4	Genscript	Leiden, Netherlands	99.3	n.a.
Gly-GHRP-5	Genscript	Leiden, Netherlands	97.7	n.a.
Gly-GHRP-6	Genscript	Leiden, Netherlands	99.1	n.a.
Gly-Hexarelin	Genscript	Leiden, Netherlands	98.1	n.a.
Gly-Ipamorelin	Genscript	Leiden, Netherlands	97.2	n.a.
Goserelin	Prospec	Rehovot, Israel	> 98	n.a.
Hexarelin	Auspep	Tullamarine, Australia	99	69.8
Hexarelin (1-3) met.	Auspep	Tullamarine, Australia	97	62
Histrelin	Sigma Aldrich	St. Louis, MO, USA	97	74
Ibutamoren	MedChem Express	Princeton, NJ, USA	> 98	n.a.
Ipamorelin	Auspep	Tullamarine, Australia	99	60
Ipamorelin (1-4) met.	Auspep	Tullamarine, Australia	99	67
Lecirelin (Dalmarelin)	Auspep	Tullamarine, Australia	97	76
Leuprolide	Sigma Aldrich	St. Louis, MO, USA	> 98	n.a.
Leuprolide (1-3) met.	Auspep	Tullamarine, Australia	95	n.a.
LHRH	Sanofi	Paris, France	GMP grade**	n.a.
[Lys8]-Vasopressin (ISTD 3)	Sigma Aldrich	St. Louis, MO, USA	98	87
Nafarelin	Sigma Aldrich	St. Louis, MO, USA	97	n.a.
Nafarelin (5-10) met.	Auspep	Tullamarine, Australia	96	71
Peforelin	Bachem	Bubendorf, Switzerland	98.2	75.3
Tabimorelin	TRC	North York, ON, Canada	98	n.a.
TB500	Centic Biotech	Heidelberg, Germany	96.1	n.a.
Triptorelin	Sigma Aldrich	St. Louis, MO, USA	> 98.8	86.2

* Peptides were obtained by custom synthesis. 'High' purity was estimated to be at least 90%.

** LHRH was purchased under the trade name Kryptocur® (Sanofi). 'Highest' purity due to GMP/clinical grade is guaranteed.

Table 3.S2: In order to estimate the linearity of the analytes between LOD–100 ng/mL, a linear (1st order) regression was assumed. LOD, coefficient of correlation (r), intercept, and slope are indicated.

Compound	LOD [ng/mL]	Coefficient of correlation (r)	Intercept	Slope
Alarelin	5	0.9991	-0.0484062	0.0189082
Alexamorelin	1	0.9967	-0.015622	0.0046915
Alexamorelin (3-6) met.	10	0.9979	-0.0224924	0.00297027
Anamorelin	0.5	0.9998	0.00360475	0.0207482
AOD9604	10	0.9907	-0.013225	0.00170851
AOD9604 (7-16) met.	5	0.9888	-0.000170072	0.0000336746
Buserelin	5	0.9970	-0.0200733	0.00494489
Deslorelin	5	0.9952	-0.0199836	0.00326135
Desmopressin	10	0.9935	-0.0130102	0.00200175
Felypressin	0.5	0.9990	-0.00437096	0.00276108
Fertirelin	1	0.9993	-0.136574	0.0603397

FULLY AUTOMATED DRIED BLOOD SPOT SAMPLE PREPARATION ENABLES THE DETECTION OF LOWER MOLECULAR MASS PEPTIDE AND NON-PEPTIDE DOPING AGENTS BY MEANS OF LC-HRMS

GHRP-1	10	0.9919	-0.00481472	0.00121262
GHRP-1 (3-6) met.	5	0.9991	-0.00231903	0.00135471
GHRP-2	2	0.9991	-0.00763612	0.00250229
GHRP-2 (1-3) met.	2	0.9998	-0.00965567	0.00824783
GHRP-3	5	0.9973	-0.00330112	0.000470546
GHRP-4	2	0.9996	-0.0220946	0.00877921
GHRP-5	2	0.9964	-0.0447691	0.00962491
GHRP-6	2	0.9975	-0.00454555	0.000100606
GHRP-6 (2-5) met.	2	0.9982	-0.00870166	0.00292029
Gly-Alexamorelin	5	0.9990	-0.0130556	0.00222534
Gly-GHRP-1	2	0.9949	-0.00357233	0.000713673
Gly-GHRP-2	10	0.9988	-0.00776704	0.00213614
Gly-GHRP-3	5	0.9965	0.000477426	0.000186978
Gly-GHRP-4	1	0.9993	-0.0231385	0.00929519
Gly-GHRP-5	5	0.9972	-0.0352012	0.00483793
Gly-GHRP-6	2	0.9987	-0.00650108	0.00323691
Gly-Hexarelin	2	0.9986	-0.00738083	0.00263126
Gly-Ipamorelin	1	0.9984	-0.0020315	0.00106991
Goserelin	2	0.9965	-0.00252871	0.00333681
Hexarelin	10	0.9999	-0.0104049	0.00181617
Hexarelin (1-3) met.	0.5	0.9958	0.0012266	0.000346481
Histrelin	5	0.9980	-0.00350599	0.00274993
Ibutamoren	1	0.9999	0.0176974	0.0223254
Ipamorelin	0.5	0.9989	0.0016851	0.00127155
Ipamorelin (1-4) met.	0.5	0.9966	-0.00678853	0.00952589
Lecirelin (Dalmarelin)	0.5	0.9992	-0.0190056	0.00647131
Leuprolide	0.5	0.9985	-0.0173169	0.00707388
Leuprolide (1-3) met.	1	0.9981	-0.000376364	0.000287541
LHRH	2	0.9992	-0.0067248	0.00254222
Nafarelin	10	0.9862	0.00260311	0.000837598
Nafarelin (5-10) met.	2	0.9948	-0.0095818	0.00245437
Peforelin	20	0.9985	-0.0117727	0.00110986
Tabimorelin	10	0.9991	-0.00251807	0.00200117
TB500	1	0.9996	-0.000370692	0.00237711
Triptorelin	10	0.9961	-0.0113033	0.000969089

3.7 Acknowledgements

The study was funded by the Federal Ministry of the Interior, Building and Community of the Federal Republic of Germany (Berlin, Germany), the Manfred-Donike Institute for Doping Analysis (Cologne, Germany), Anti-Doping Switzerland (Berne, Switzerland), the National Anti-Doping Agency (Bonn, Germany), and the World Anti-Doping Agency (Montreal, Canada, grant #ISF17A12MT).

3.8 References

1. Okano, M., et al., *Determination of growth hormone secretagogue pralmorelin (GHRP-2) and its metabolite in human urine by liquid chromatography/electrospray ionization tandem mass spectrometry*. Rapid Commun Mass Spectrom, 2010. 24(14): p. 2046-56.
2. Thomas, A., et al., *Identification of the growth-hormone-releasing peptide-2 (GHRP-2) in a nutritional supplement*. Drug Test Anal, 2010. 2(3): p. 144-8.
3. Thomas, A., et al., *Determination of growth hormone releasing peptides (GHRP) and their major metabolites in human urine for doping controls by means of liquid chromatography mass spectrometry*. Anal Bioanal Chem, 2011. 401(2): p. 507-16.
4. Thomas, A., et al., *Determination of Vasopressin and Desmopressin in urine by means of liquid chromatography coupled to quadrupole time-of-flight mass spectrometry for doping control purposes*. Anal Chim Acta, 2011. 707(1-2): p. 107-13.
5. Pinyot, A., et al., *Growth hormone secretagogues: out of competition*. Anal Bioanal Chem, 2012. 402(3): p. 1101-8.
6. Thomas, A., et al., *Determination of prohibited, small peptides in urine for sports drug testing by means of nano-liquid chromatography/benchtop quadrupole orbitrap tandem-mass spectrometry*. J Chromatogr A, 2012. 1259: p. 251-7.
7. Timms, M., et al., *A high-throughput LC-MS/MS screen for GHRP in equine and human urine, featuring peptide derivatization for improved chromatography*. Drug Test Anal, 2014. 6(10): p. 985-95.
8. Cox, H.D., C.M. Hughes, and D. Eichner, *Detection of GHRP-2 and GHRP-6 in urine samples from athletes*. Drug Test Anal, 2015. 7(5): p. 439-44.
9. Semenistaya, E., et al., *Determination of growth hormone releasing peptides metabolites in human urine after nasal administration of GHRP-1, GHRP-2, GHRP-6, Hexarelin, and Ipamorelin*. Drug Test Anal, 2015. 7(10): p. 919-25.
10. Goergens, C., et al., *Recent improvements in sports drug testing concerning the initial testing for peptidic drugs (< 2 kDa) - sample preparation, mass spectrometric detection, and data review*. Drug Test Anal, 2018.
11. Thomas, A., et al., *Simplifying and expanding the screening for peptides <2 kDa by direct urine injection, liquid chromatography, and ion mobility mass spectrometry*. J Sep Sci, 2016. 39(2): p. 333-41.
12. Judak, P., et al., *DMSO Assisted Electrospray Ionization for the Detection of Small Peptide Hormones in Urine by Dilute-and-Shoot-Liquid-Chromatography-High Resolution Mass Spectrometry*. J Am Soc Mass Spectrom, 2017. 28(8): p. 1657-1665.

13. Handelsman, D.J., *Performance Enhancing Hormone Doping in Sport*, in *Endotext*, K.R. Feingold, et al., Editors. 2015, MDText.com, Inc.: South Dartmouth (MA)
14. WADA. *Anti-Doping Testing Figures*. 2017 [12/07/2018]; Available from: <https://www.wada-ama.org/en/resources/laboratories/anti-doping-testing-figures-report>.
15. Poplawska, M. and A. Blazewicz, *Identification of a novel growth hormone releasing peptide (a glycine analogue of GHRP-2) in a seized injection vial*. *Drug Test Anal*, 2018.
16. Krug, O., et al., *Analysis of new growth promoting black market products*. *Growth Horm IGF Res*, 2018. 41: p. 1-6.
17. Gajda, P.M., et al., *Glycine-modified growth hormone secretagogues identified in seized doping material*. *Drug Test Anal*, 2018.
18. WADA. *The World Anti-Doping Code. International Standard. Prohibited List January 2020* [07/02/2020]; Available from: https://www.wada-ama.org/sites/default/files/wada_2020_english_prohibited_list_0.pdf.
19. Pihoker, C., et al., *Pharmacokinetics and pharmacodynamics of growth hormone-releasing peptide-2: A phase I study in children*. *Journal of Clinical Endocrinology & Metabolism*, 1998. 83(4): p. 1168-1172.
20. Cabrales, A., et al., *Pharmacokinetic study of Growth Hormone-Releasing Peptide 6 (GHRP-6) in nine male healthy volunteers*. *Eur J Pharm Sci*, 2013. 48(1-2): p. 40-6.
21. Ferro, P., et al., *Detection of Growth Hormone Releasing Peptides in Serum by a Competitive Receptor Binding Assay*. *J Chromatogr*, 2017. 8(1).
22. Ferro, P., et al., *Structure-activity relationship for peptidic growth hormone secretagogues*. *Drug Test Anal*, 2017. 9(1): p. 87-95.
23. Thomas, A., et al., *Metabolism of growth hormone releasing peptides*. *Anal Chem*, 2012. 84(23): p. 10252-9.
24. Dib, J., et al., *Screening for adiponectin receptor agonists and their metabolites in urine and dried blood spots*. *Clinical Mass Spectrometry*, 2017. 6(13-20).
25. Tretzel, L., et al., *Fully automated determination of nicotine and its major metabolites in whole blood by means of a DBS online-SPE LC-HR-MS/MS approach for sports drug testing*. *J Pharm Biomed Anal*, 2016. 123: p. 132-40.
26. Lehmann, S., et al., *Current and future use of "dried blood spot" analyses in clinical chemistry*. *Clin Chem Lab Med*, 2013. 51(10): p. 1897-909.
27. O'Mara, M., et al., *The effect of hematocrit and punch location on assay bias during quantitative bioanalysis of dried blood spot samples*. *Bioanalysis*, 2011. 3(20): p. 2335-47.

28. Oostendorp, M., et al., *Measurement of Hematocrit in Dried Blood Spots Using Near-Infrared Spectroscopy: Robust, Fast, and Nondestructive*. Clin Chem, 2016. 62(11): p. 1534-1536.
29. Blicharz, T.M., et al., *Microneedle-based device for the one-step painless collection of capillary blood samples*. Nat Biomed Eng, 2018. 2(3): p. 151-157.
30. Knoop, A., et al., *Qualitative identification of growth hormone-releasing hormones in human plasma by means of immunoaffinity purification and LC-HRMS/MS*. Anal Bioanal Chem, 2016. 408(12): p. 3145-53.
31. WADA. *The World Anti-Doping Code. International Standard for Laboratories January*. 2019 25/03/2020]; Available from: https://www.wada-ama.org/sites/default/files/resources/files/isl_nov2019.pdf.
32. Hahne, H., et al., *DMSO enhances electrospray response, boosting sensitivity of proteomic experiments*. Nat Methods, 2013. 10(10): p. 989-91.
33. Meyer, J.G. and A.K. E, *Charge state coalescence during electrospray ionization improves peptide identification by tandem mass spectrometry*. J Am Soc Mass Spectrom, 2012. 23(8): p. 1390-9.
34. Zvereva, I., et al., *Comparison of various in vitro model systems of the metabolism of synthetic doping peptides: Proteolytic enzymes, human blood serum, liver and kidney microsomes and liver S9 fraction*. J Proteomics, 2016. 149: p. 85-97.
35. Matuszewski, B.K., M.L. Constanzer, and C.M. Chavez-Eng, *Strategies for the assessment of matrix effect in quantitative bioanalytical methods based on HPLC-MS/MS*. Anal Chem, 2003. 75(13): p. 3019-30.
36. Capiiau, S., et al., *A Novel, Nondestructive, Dried Blood Spot-Based Hematocrit Prediction Method Using Noncontact Diffuse Reflectance Spectroscopy*. Anal Chem, 2016. 88(12): p. 6538-46.
37. McHedlishvili, G., et al., *Regional hematocrit changes related to blood flow conditions in the arterial bed*. Clin Hemorheol Microcirc, 2003. 29(2): p. 71-9.
38. Simonen, P., et al., *Normal variation in cutaneous blood content and red blood cell velocity in humans*. Physiol Meas, 1997. 18(3): p. 155-70.
39. WADA. *WADA Technical Document - Minimum Required Performance Levels of Non-Threshold Substances*. 2019 25/03/2020]; Available from: https://www.wada-ama.org/sites/default/files/resources/files/td2019mrpl_eng.pdf.

4 Comprehensive insights into the formation of metabolites of the ghrelin mimetics capromorelin, macimorelin and tabimorelin as potential markers for doping control purposes

Tobias Lange¹, Andreas Thomas¹, Christian Görgens¹, Martin Bidlingmaier², Katharina Schilbach², Eric Fichant³, Philippe Delahaut³ & Mario Thevis^{1,4}

¹Center for Preventive Doping Research/Institute of Biochemistry, German Sport University Cologne, Cologne, Germany

²Endocrine Laboratory, Medizinische Klinik und Poliklinik IV, Klinikum der Universität München, Munich, 80336 Germany

³Département Santé, CER Groupe, Rue du Point du Jour, 8, Marloie, Belgium

⁴European Monitoring Center for Emerging Doping Agents (EuMoCEDA), Cologne/Bonn, Germany

Veröffentlicht in: *Biomedical Chromatography* (2021), 35(6): e5075.

4.1 Abstract

Analytical methods to determine the potential misuse of the ghrelin mimetics capromorelin (CP-424,391), macimorelin (macrilen, EP-01572), and tabimorelin (NN703) in sports were developed. Therefore, different extraction strategies, *i.e.* solid-phase extraction, protein precipitation, as well as a “dilute-and-inject” approach, from urine and EDTA-plasma were assessed and comprehensive *in vitro/in vivo* experiments were conducted, enabling the identification of reliable target analytes by means of high resolution mass spectrometry. The drugs’ biotransformation led to the preliminary identification of 51 metabolites of capromorelin, 12 metabolites of macimorelin, and 13 metabolites of tabimorelin. Seven major metabolites detected in rat urine samples collected post-administration of 0.5-1.0 mg of a single oral dose underwent in-depth

characterization, facilitating their implementation into future confirmatory test methods. In particular, two macimorelin metabolites exhibiting considerable abundances in post-administration rat urine samples were detected, which might contribute to an improved sensitivity, specificity, and detection window in case of human sports drug testing programs. Further, the intact drugs were implemented into World Anti-Doping Agency (WADA)-compliant initial testing (LOD: 0.02-0.60 ng/mL) and confirmation procedures (LOI: 0.18-0.89 ng/mL) for human urine and blood matrices. The obtained results allow extending the test spectrum of doping agents in multi-target screening assays for growth hormone-releasing factors from human urine.

4.2 Introduction

The ghrelin receptor agonists or ghrelin mimetics capromorelin (CP-424,391), macimorelin (macrilen, EP-01572), and tabimorelin (NN703) are included in the World Anti-Doping Agency's (WADA's) Prohibited List [1], categorized as growth hormone secretagogues (GHS). Like the growth hormone releasing peptides (GHRPs), which also act as agonists of the ghrelin receptor, the GHS are classified as non-threshold substances under section S2 "peptide hormones, growth factors, related substances, and mimetics"; prohibited at all times, *i.e.* in- and out-of-competition. These synthetic selective ligands of the ghrelin receptor, which is located in the hypothalamus and commonly referred to as GHS receptor, were originally developed for the treatment of growth hormone (GH) deficiency [2, 3]. Due to the stimulation of GH and insulin-like growth factor I (IGF-I), these peptidomimetic drugs possess considerable potential for misuse in sports, as supported by 26 adverse analytical findings (AAF) reported in 2019 for GHRPs and GHS [4] and, consequently, it is critical to continuously update and improve detection methods for these substances.

All three compounds considered in this study are orally-active GHS receptor agonists. Since the tripeptidyl derivative tabimorelin was found to have only modest clinical effects in adults with GH deficiency [5] and functioned as an inhibitor of CYP3A4 with associated undesirable interactions [6], US Food and Drug Administration (FDA) approval was not achieved. The modified dipeptide capromorelin slightly increased total lean body mass and physical performance in elderly men [7], but the effects were not considered sufficient to conduct follow-up studies. Instead, the drug was approved

by the FDA for appetite stimulation in dogs [8]. In 2017, tripeptidyl derivative macimorelin received FDA approval for the purpose of GH deficiency diagnosis (stimulation test).

The therapeutic dosing combined with short half-lives for tabimorelin (4.1 ± 0.4 h in swine) [9], capromorelin (2.5 ± 0.4 h at 50 mg dosage) [10], and macimorelin (1.9 ± 0.3 h at 0.25 mg/kg dosage) [11] might pose a challenge for the sensitive detection of illicit applications. Today, anti-doping laboratories apply different sample preparation methods to target GHRPs/GHS in routine doping control samples, *i.e.* urine, plasma/serum, and dried blood spots, for initial testing procedures (ITP). In most cases, the “dilute-and-inject” (D&I) approach [12-15] or the purification and concentration using solid-phase extraction [16-19] were preferred for LC-MS/MS-based analytical approaches.

In the past, *in vitro* experiments using serum/plasma, human liver microsomes, S9 fractions and *in vivo* experiments with human and rat model were successfully applied to identify various biotransformation products of administered (pseudo-)peptides as demonstrated for the GHRPs [20-23]. In order to optimize detection assays with regards to specificity, sensitivity, and retrospectivity, such metabolites are commonly included into the list of target analytes. For instance, the metabolites of GHRP-1, GHRP-2, alexamorelin, hexarelin, and ipamorelin offered superior detection windows compared to the intact drugs/drug candidates [23-28]. In contrast to the GHRPs and their metabolites, tabimorelin, capromorelin, and macimorelin are compounds of lower molecular mass (< 600 Da) and feature rather nonpeptidic characteristics. Therefore, main metabolic transformation reactions are expected to occur in liver and kidney tissues, catalyzed by enzymes with relatively low substrate specificity such as cytochromes P450 (CYPs).

Recently, Sobolevsky *et al.* reported a multiclass ITP including the detection of capromorelin, macimorelin and tabimorelin in human urine [29]. However, detection methods from both matrices, *i.e.* blood plasma and urine, as well as confirmation procedures (CP) and information about the formed metabolites of these drugs are still missing. Therefore, the focus of this work was the identification of metabolites using different *in vitro/in vivo/in silico* approaches. In addition, using efficient extraction procedures for both matrices, adequate analytical detection methods for the analysis of the intact drugs by LC-HRMS/MS should be established. Samples and data on the

compounds' metabolism were obtained by *in vivo* (rat) and *in vitro* (human liver microsomes & human serum incubation) experiments. The identification of metabolites was assisted by software prediction and *in silico*-generated data [30, 31], and MS/MS-based metabolite structural elucidations were supported by utilizing competitive fragmentation modeling ("CFM-ID 3.0") via a freely available web server [32].

4.3 Materials and methods

4.3.1 Chemicals and materials

The analytes of this study, capromorelin (L)-tartrate (2-Amino-*N*-[(1*R*)-2-[(3*aR*)-2,3,3*a*,4,6,7-hexahydro-2-methyl-3-oxo-3*a*-(phenylmethyl)-5*H*-pyrazolo[4,3-*c*]pyridin-5-yl]-2-oxo-1-propanamide (2*R*,3*R*)-2,3-dihydroxybutanedioate) with a specified purity of 98.0% and tabimorelin (*N*-[(2*E*)-5-Amino-5-methyl-1-oxo-2-hexenyl]-*N*-methyl-3-(2-naphthalenyl)-*D*-alanyl-*N,N* α -dimethyl-*D*-phenylalaninamide) with a specified purity of 98.7%, were purchased from Toronto Research Chemicals (North York, ON, Canada) Macimorelin acetate (2-amino-*N*-((*R*)-1-(((*R*)-1-formamido-2-(1*H*-indol-3-yl)ethyl)amino)-3-(1*H*-indol-3-yl)-1-oxopropan-2-yl)-2-methylpropanamide acetate) with a specified purity of 99.9% was obtained from NucleoSyn (Olivet, France). The internal standard (ISTD) (d_3)-GHRP-2 (1-3) metabolite (purity 72%) was in-house synthesized [24] and (d_4)-GHRP-4 (purity >90%) was obtained from BMFZ (Düsseldorf, Germany). Chemicals for *in vitro* studies were pooled human liver microsomes from Sekisui XenoTech (Kansas City, KS, USA), β -Nicotinamide adenine dinucleotide 2'-phosphate (NADPH) from Roche (Basel, Switzerland), and Na_2HPO_4 and NaH_2PO_4 from Merck (Darmstadt, Germany). Other chemicals that were used for sample preparation or as LC solvents were acetonitrile, methanol, acetic acid, and 25% (*v/v*) ammonia solution bought from Merck, formic acid obtained from Thermo Fisher Scientific (Waltham, MA, USA), and dimethyl sulfoxide (DMSO) supplied from Alfa Aesar (Haverhill, MA, USA). The Oasis mixed-mode cation exchange (MCX) 1 cm^3 cartridges with 10 mg sorbent per unit were received from Waters (Milford, MA, USA).

4.3.2 Standard solutions

The 1 mg/mL stock solutions of capromorelin, macimorelin, tabimorelin, (d_3)-GHRP-2 (1-3) metabolite, and (d_4)-GHRP-4 were prepared with Milli-Q[®] water in LoBind tubes

(Eppendorf, Hamburg, Germany) and stored at -20°C. Tabimorelin required an additional 20% of DMSO and 2% of acetic acid for complete solubilization. Immediately before each experiment, stock solutions were diluted with Milli-Q® water to obtain working solutions of the desired concentrations. Urine and plasma samples were fortified to the desired analyte concentration with 5% (v/v) of the working solution.

4.3.3 *In vivo*, *in vitro*, and *in silico* experiments

In order to study the metabolic profile of the drugs, different strategies were employed. *In vitro* incubation experiments with human serum or human liver microsomes and *in silico* predictions should confirm and complement the findings of the rat experiments as well as accelerate and facilitate the data analysis.

In vivo experiments

Animal studies were conducted with approval of the local ethical committee and following the directive 2010/63/EU of the European parliament and the Council of 22 September, 2010 on the protection of animals used for scientific purposes. Six female brown rats (*Rattus norvegicus*, Wistar) with 200-300 g bodyweight received a single oral dose of 0.5 mg of capromorelin, tabimorelin, or 1 mg of macimorelin (two rats per drug). In addition, one rat not receiving any medication provided negative control test samples. The animals had free access to food and water. Urine samples of 1-13 mL were collected by means of a metabolic cage after 0, 6, 12, 24, and 36 h. Sample collections of blood with a volume of 2 mL each were performed after 0, 3, 12, and 36 h, yielding EDTA-plasma for the intended studies.

For urine sample preparation, 1 mL of rat urine with 2 ng of the ISTD mix was subjected to a generic SPE method (mixed-mode cation exchange cartridge) following the manufacturer's instructions for mixed-mode sorbents. For plasma sample preparation, a previous protocol for serum samples was adapted [26] and 100 µL of rat EDTA-plasma with 2 ng of the ISTD mix were subjected to protein precipitation with acetonitrile. The details of both protocols can be obtained from the Supplementary Information.

In vitro experiments

The *in vitro* metabolism of capromorelin, macimorelin, and tabimorelin was studied by incubation of the substrates with human serum and human liver microsomal preparations. As described in a previous study [22], 100 µL of human serum were fortified with

1 µg of each compound. For the production and identification of phase I metabolites using liver microsomes, a protocol from Knights *et al.* [33] was adapted. A substrate blank (control) sample and an enzyme blank (control) sample were additionally prepared for both experiments. The details for the protocols can be found in the Supplementary Information.

In silico experiments

The generation of various possible metabolites by software prediction provided a general insight into possible metabolic products of the drugs. The open-access software tool BioTransformer [31] was operated with the task 'metabolism prediction' and 'human [tissues] and human gut microbial transformation'. Three consecutive reaction steps were conducted. As input type a SMILES string was included. In addition, a similar approach was followed by the XenoSite web predictor tool [30]. A total of six different prediction systems (P450 metabolism, epoxidation, quinone formation, reactivity, and UGT metabolism) were chosen, and molecules were uploaded as MDL-molfiles. In contrast to BioTransformer, which provided proposed structures of the metabolites, this freely available tool predicted the atomic sites that could undergo metabolic modification. After applying both approaches, the putative metabolites generated were added to a target list (not shown) for further studies by LC-HRMS/MS of the *in vivo/in vitro* prepared samples.

4.3.4 LC-HRMS/MS

The metabolites generated from *in vivo/in vitro* experiments were separated on a Vanquish UHPLC system (Thermo Fisher Scientific, Bremen, Germany) equipped with a Poroshell 120 EC-C₁₈ analytical column, 3.0 x 50 mm, 2.7 µm particle size (Agilent Technologies, Santa Clara, CA, USA) and analyzed on an Orbitrap Exploris 480 MS (Thermo Fisher Scientific, Bremen, Germany). The supply of nitrogen (source and collision gas) was ensured by a nitrogen membrane generator (cmc Instruments, Eschborn, Germany). The 15 min LC run with flow rate of 350 µL/min and linear gradients was carried out with solvent A (ddH₂O and 0.1% formic acid) and solvent B (acetonitrile and 0.1% formic acid). In order to achieve ultimate sensitivities with regards to the limit of identification (LOI) and limit of detection (LOD) within the method validation, 1% DMSO was added to solvent B. The chromatographic gradient of the method started at 1% B and reached 40% B after 10 min. Subsequently, the organic phase (B) was increased to 90% in 0.5 min and held for 1.5 min before the analytical

column was re-equilibrated at 1% B for 3 min. The samples in the autosampler were kept at 10°C, while the analytical column was tempered to 30°C. The global MS settings using a heated electrospray ion (HESI) source were as follows: spray voltage (positive ion) at 3 kV, ion transfer tube temperature at 320°C, sheath gas at 30 arbitrary units, auxiliary gas at 10 arbitrary units, maximum spray current at 10 μ A, and vaporizer temperature at 300°C. For an in-depth characterization of the anticipated *N*-hydroxylation of a capromorelin metabolite, an atmospheric pressure chemical ionization (APCI) source was installed with the following experimental setup: spray voltage at 3 kV, ion transfer tube temperature at 275°C, sheath gas at 35 arbitrary units, auxiliary gas at 5 arbitrary units, maximum spray current at 4 μ A, and vaporizer temperature at 350°C. Full-scan HRMS experiments were acquired at an orbitrap resolution (r) of 120,000 (FWHM at $m/z = 200$) with a scan range (m/z) from 120 to 1,200, a maximum injection time of 100 ms, and an AGC target of 1×10^6 . For structural elucidation and confirmation purposes, targeted MS² (tMS²) experiments with an inclusion list of 1-4 entries and a quadrupole isolation window (m/z) of 1, and a retention time window of 1 min were applied. The MS² scans were acquired with $r = 60,000$, a maximum injection time of 100 ms, an AGC target of 1×10^5 and stepped HCD collision with normalized collision energies (NCE) at 10, 20, and 40%. Optional pseudo MS³ (pMS³) experiments were conducted using the same settings but with an activated source-induced fragmentation (SID) voltage of 35 V and an inclusion list adapted accordingly. For initial testing purposes, a targeted SIM (tSIM) scan with inclusion list was performed at $r = 60,000$, a quadrupole isolation window (m/z) of 4, maximum injection time of 100 ms, and AGC target of 1×10^5 . The small number of analytes allowed alternating experiments of full HRMS, tMS², and tSIM scans between 7 and 12 min within the same method, controlled by Xcalibur version 4.3.

For the implementation of the three new compounds into the multi-target screening assay for GH-releasing factors from urine, the routinely applied LC-HRMS/MS-based testing procedure [12] employing a Q Exactive™ Plus Hybrid Quadrupole-Orbitrap™ MS (Thermo Fisher Scientific, Bremen, Germany) was re-validated. Further, a Xevo TQ-XS mass spectrometer from Waters (Melford, MA, USA) was used for in-depth characterization of a metabolite of capromorelin. Details about the LC-TQMS/MS method can be found in the Supplementary Information in “Supplementary material and methods”.

4.3.5 Method validation

Sample preparation

LC-HRMS/MS detection methods for the intact compounds were established and validated. Here, different method validation protocols were chosen, depending on whether urine or EDTA-plasma was used as test matrix. For urine, a D&I approach [12] was used for the ITP and CP. Therefore, 90 μ L of native urine were fortified with 10 μ L of a 20 ng/mL ISTD working solution, mixed thoroughly, and 40 μ L were injected into LC-HRMS. In addition, a second CP approach by solid-phase extraction allowing utmost sensitivity and selectivity was adopted from the *in vivo* experiments as described above. The sample preparation for ITP and CP of plasma samples by protein precipitation (PP) with acetonitrile was conducted likewise as described before in the protocol of the *in vivo* experiments.

Validation for non-threshold substances

The minimum required performance level (MRPL) for capromorelin, macimorelin, and tabimorelin in urine is 2 ng/mL as specified by WADA. Although no regulatory specifications exist, the same MRPL was assumed for plasma samples. A total of five LC-HRMS/MS detection methods, *i.e.* an ITP and a CP for each matrix, plus an additional CP using SPE for urine, were validated according to WADA's international standard for laboratories (ISL) 10.0 [34]. For fast and reliable initial testing purposes, tSIM experiments scanned for two diagnostic precursor ions originating from the intact compounds' protonated molecules' isotopes at the respective retention times. A presumptive adverse analytical finding triggers the CP. For confirmation purposes, three diagnostic precursor-product ion transitions were monitored by means of tMS² scans, all of which need to fulfill the criteria of signal-to-noise ratio > 3 and relative retention time (rt_R) < 1% (to the ISTD signal). The precursor ion of each compound was identical to the tSIM ion 1 (see Table 4.2). For MS² identification, the transitions were additionally subjected to a maximum tolerance window for the relative abundance in a sample, relative to the base peak in a reference spectrum as specified in TD2015IDCR [35].

According to these criteria and following WADA guidelines, the validation of the qualitative ITPs and CPs were carried out for the parameters selectivity, repeatability, robustness, carryover, LOD and LOI.

Validation parameters

For the assessment of selectivity of the ITP, ten different urine blank and EDTA-plasma blank samples (female $n = 5$ and male $n = 5$) were analyzed with the particular MS method. Repeatability of detection at MRPL (ITP) was evaluated by analyzing the same set of samples, fortified with an analyte concentration of 2 ng/mL. For the estimation of the LOD (ITP), six different urine and plasma samples were fortified at 1% MRPL (0.02 ng/mL), 10% MRPL (0.2 ng/mL), 25% MRPL (0.5 ng/mL), 50% MRPL (1 ng/mL), and 100% MRPL (2 ng/mL). The LOD is defined as the lowest concentration of a compound with a 95% detection rate, calculated using a detection response curve according to the WADA's ISL 10.0. [34] The carryover of the ITP was evaluated by analyzing a blank sample directly after a sample containing a high concentration of 400% MRPL (8 ng/mL). A re-analysis of the "repeatability samples" at the MRPL was used to test whether the sample extracts were stable in the autosampler over a longer period of time (24 h). With regard to the diagnostic ion transitions, similar validation parameters were predetermined for the CPs. Selectivity and carryover were subjected to the same requirements as for the ITP. The LOI, again at 95% identification rate, was calculated with the same series of the MRPL levels as for the LOD estimation before, yet must meet the identification criteria of a CP. LC-HRMS method robustness was verified during the series of measurements for LOI estimation and a batch of six samples of 100% MRPL ("D&I" from urine and "PP" from plasma) and 50% MRPL ("SPE" from urine) were prepared and analyzed again on a different day.

4.4 Results and discussion

4.4.1 *In vivo*, *in vitro*, and *in silico* experiments

Prior to the metabolite screening, the intact, unmodified compounds were monitored, identified and characterized by LC-HRMS/MS. In the upper panel of Figure 4.1 A-C, the extracted ion chromatograms of a rat urine sample at 0 h and 6 h post-administration of the respective drug – capromorelin (A), macimorelin (B), and tabimorelin (C) – are shown with the obtained isotopic patterns of the detected protonated molecules. A corresponding MS² spectrum of the [M+H]⁺ ion at NCE of 20% was provided in the middle panel. As indicated, several fragments and neutral losses were tentatively assigned by fragmentation modeling via CFM-ID 3.0 taking a set of three input MS² spectra at NCE of 10%, 20%, and 40%. As demonstrated in the lower panel,

all substances reached their maximum concentration 6 h or 3 h post-administration in urine or EDTA-plasma (data not shown), respectively. In rat urine, the drugs were still detected at the end of sample collection at 36 h. Although of considerably lower concentration in EDTA-plasma samples, capromorelin and tabimorelin were also still be detectable at the end of the sample collection period. In contrast, signals corresponding to macimorelin were only detectable in plasma samples collected 3 h post-administration. The excretion half-lives for the tested drugs in rats as estimated from the available urine samples were ~7.5 h for capromorelin, ~3 h for macimorelin, and ~5 h for tabimorelin. The estimated plasma half-lives, albeit only based on four data points, were 3.5 h for capromorelin and 5.5 h for tabimorelin and are in agreement with other studies in human or swine as mentioned above [9, 10]. Among these substances, the shortest (human) plasma half-life was reported for macimorelin ($t_{1/2} = 1.9$ h) [11], which may have also complicated the detection in rat EDTA-plasma in the present study. Whether certain metabolites of these drugs would eventually allow for a longer detection window compared to the intact compound and could increase the assay's sensitivity or specificity was subsequently investigated.

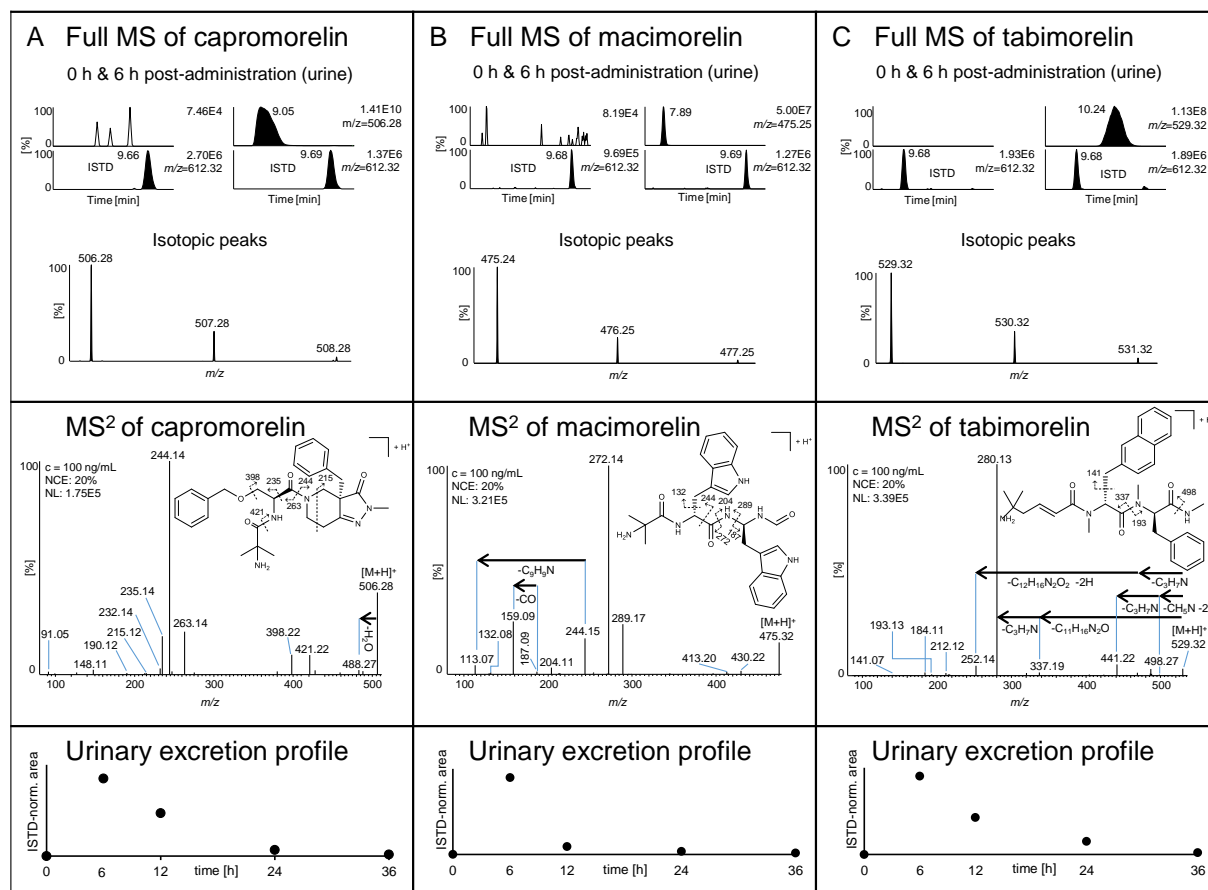


Figure 4.1: In the upper panel, the extracted ion chromatogram (mass tolerance ± 5 ppm) of a full HRMS experiment of capromorelin (A), macimorelin (B), and tabimorelin (C) at 0 h and 6 h post-administration is shown. The corresponding isotope signals are shown in the mass spectrum below. The middle panel contains a MS² spectrum of the reference compound ($c = 100$ ng/mL). The lower panel shows the drug's urinary excretion profile in rat.

The strategy for identifying metabolites consisted of the targeted scanning for isotopic masses (5 ppm accuracy) in full HRMS scans. The list of putative metabolites was generated beforehand by a combination of different *in silico* experiments and metabolite anticipations. The metabolic fate of the drugs resulted in a whole range of different phase I and phase II metabolites. Considering all *in vivo/in vitro* experiments, a total of 51 capromorelin metabolites, 12 macimorelin metabolites, and 13 tabimorelin metabolites were detected. They were found predominantly in rat urine, rat EDTA-plasma, and human microsomal preparations, and partially also using human serum incubation experiments. A set diagram showing the number of metabolites of capromorelin (A), macimorelin (B), and tabimorelin (C), detected by full HRMS experiments, is depicted in Figure 4.2. The overlapping sets represent the shared metabolites from two or all four different matrices and/or *in vitro/in vivo* approaches. By far the most urinary phase I and phase II metabolites were found for capromorelin (45), followed by

macimorelin (10) and tabimorelin (5). In rat EDTA-plasma, significantly fewer metabolites were observed for capromorelin (11) and none for macimorelin and tabimorelin. The *in vitro* (human microsomes) experiments revealed several phase I metabolites for capromorelin (19), macimorelin (7), and tabimorelin (10). Also the *in vitro* incubation with human serum yielded metabolic products for capromorelin (7), macimorelin (7), and tabimorelin (1). In accordance with the fact that mainly CYPs and UDP-glucuronosyltransferases (UGTs) are enriched in the liver microsomes, a high diversity and abundance of hydroxy metabolites were observed. Phase II conjugates were not identified in microsomes because of the lack of an additional cofactor (UDP-glucuronic acid). Other metabolites, however, were less concentrated and diverse than in the *in vivo* studies (urine). Of note, the evaluation of the enzyme blank control samples of both *in vitro* assays demonstrated that 47% (liver microsomes) and 67% (human serum) of the obtained metabolites was also produced, albeit with partially reduced signal intensities, suggesting, e.g., spontaneous oxidations or environmental microbial transformation during sample preparation and/or incubation.

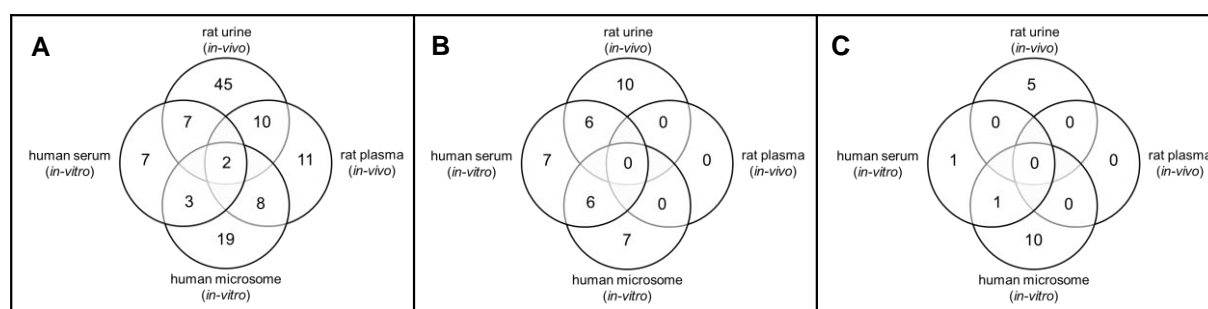


Figure 4.2: A set diagram showing the number of metabolites of capromorelin (A), macimorelin (B), and tabimorelin (C), detected by full HRMS experiments. The overlapping sets represent the shared metabolites from two or all four different matrices and/or different *in vitro/vivo* approaches.

Within doping research projects for GHRP metabolite identification, it has already been demonstrated that urinary metabolites detected for a rat model [21] could also be determined in human urine after nasal administration [27]. Here, assuming a similar transferability from the animal model to human, the main focus was on the rat *in vivo* experiments. An overview of the urinary metabolites observed in full HRMS data obtained from rat 6 h post-administration of capromorelin (A), macimorelin (B), and tabimorelin (C) is shown in Figure 4.3.

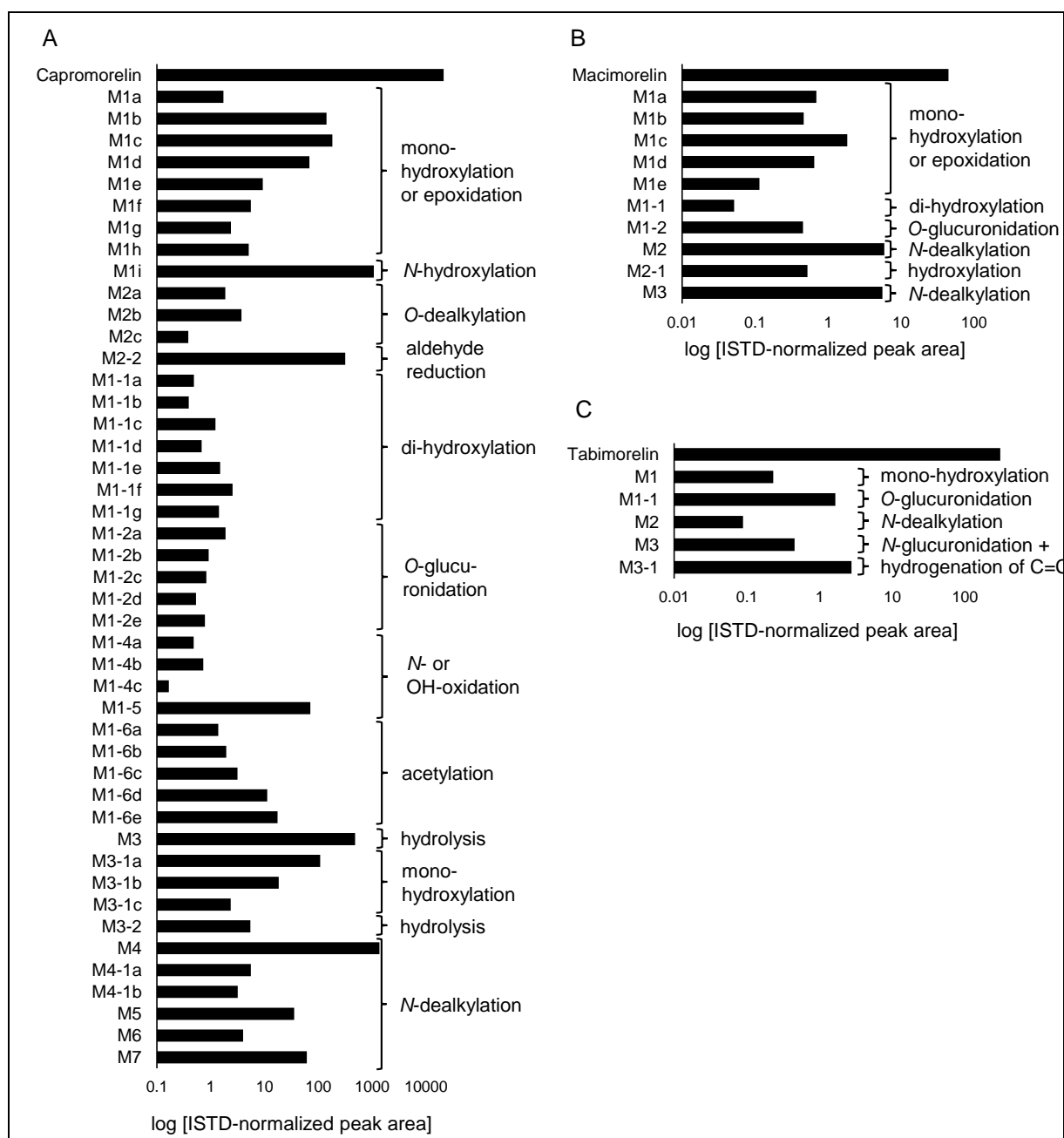


Figure 4.3: Overview of all metabolites (M) found in the drug-administered rat urine 6 h post-administration of A) capromorelin, B) macimorelin, and C) tabimorelin. The assumed chemical or enzymatic reactions that formed a metabolite are indicated on the right.

As demonstrated here, the metabolite profiles of the analytes were different in number and abundance of metabolites and yet some similarities existed. At least for the rat urine collected 6 h post-administration, the metabolite concentrations were below those of their precursor compounds. Capromorelin, macimorelin, and tabimorelin were all prone to CYP-mediated mono(/di)-hydroxylation/epoxidation and *N*-dealkylation, resulting in several phase I metabolites. Furthermore, phase II metabolites such as *O/N*-glucuronidated metabolites were detected for the three drugs.

The thorough characterization of the most abundant urinary metabolites was completed with subsequent complementary experiments by tMS², pMS³, neutral loss scan, precursor ion scan, or the temporary use of an APCI source instead of a HESI source. Finally, a list of the major metabolites of each compound was established with the prerequisite of reaching a relative (to the unmodified compound) abundance of at least > 1% at any given sample collection time or matrix. Table 4.1 contains the main analytical characteristics of each metabolite, e.g. molecular formula, t_R [min], predominant charge state, and isotope signals [*m/z*].

As the individual drugs showed unique metabolite profiles *in vivo/in vitro*, these were presented in separate sections. Here, the focus was on the major rat urinary metabolites; however, various minor metabolites were additionally characterized and described (Supplementary Information with Figure 4.S1 - Figure 4.S21, and Table 4.S1 - Table 4.S3).

Table 4.1: Overview of the most abundant metabolites of capromorelin, macimorelin, and tabimorelin detected after *in vivo* or *in vitro* experiments.

Compound	Mol. formula	t _R [min]	Charge state	Isotope 1 Isotope 2 Isotope 3 [m/z]	Reaction type	Metabolite detected in: 1) rat EDTA-plasma (in vivo) 2) rat urine (in vivo) 3) human microsomes (in vitro) 4) human serum (in vitro)
Capromorelin	C ₂₈ H ₃₅ N ₅ O ₄	9.05	1+	506.2762 507.2795 508.2829	-	1) 3-36 h post-administration 2) 6-36 h post-administration 3) S, E+S 4) S, E+S
Capromorelin M1i	C ₂₈ H ₃₅ N ₅ O ₅	10.03	1+	522.2711 523.2745 524.2778	N-hydroxylation	1) 3-12 h post-administration 2) 6-36 h post-administration 3) E+S 4) no signal
Capromorelin M3	C ₂₄ H ₂₉ N ₄ O ₃	8.77	1+	421.2234 422.2265 423.2293	Hydrolysis of amide	1) 3-36 h post-administration 2) 6-36 h post-administration 3) S, E+S 4) S, E+S
Capromorelin M4	C ₂₇ H ₃₃ N ₅ O ₄	8.37	1+	492.2605 493.2639 494.2672	N-dealkylation	1) 3-12 h post-administration 2) 6-36 h post-administration 3) S, E+S 4) S, E+S
Macimorelin	C ₂₆ H ₃₀ N ₆ O ₃	7.89	1+	475.2452 476.2486 477.2519	-	1) 3 h post-administration (weak signal) 2) 6-36 h post-administration 3) S, E+S 4) S, E+S
Macimorelin M1c	C ₂₆ H ₃₀ N ₆ O ₆	6.83	1+	491.2401 492.2435 493.2468	Hydroxylation	1) no signal 2) 6-12 h post-administration 3) S, E+S 4) S, E+S
Macimorelin M2	C ₁₅ H ₂₀ N ₄ O ₂	4.62	1+	289.1659 290.1693 291.1726	N-dealkylation	1) no signal 2) 6-36 h post-administration 3) S, E+S 4) S, E+S
Macimorelin M3	C ₁₁ H ₁₀ N ₂ O	4.16	1+	187.0866 188.0899 189.0933	N-dealkylation	1) no signal 2) 6-36 h post-administration 3) E+S (weak signal) 4) no signal
Tabimorelin	C ₃₂ H ₄₀ N ₄ O ₃	10.24	1+	529.3173 530.3207 531.3240	-	1) 3-12 h post-administration 2) 6-36 h post-administration 3) S, E+S 4) S, E+S
Tabimorelin M3-1	C ₃₈ H ₅₀ N ₄ O ₉	8.65	1+	707.3579 708.3612 709.3647	N-glucuronidation, hydrogenation of C=C	1) no signal 2) 6-24 h post-administration 3) E+S (weak signal) 4) no signal

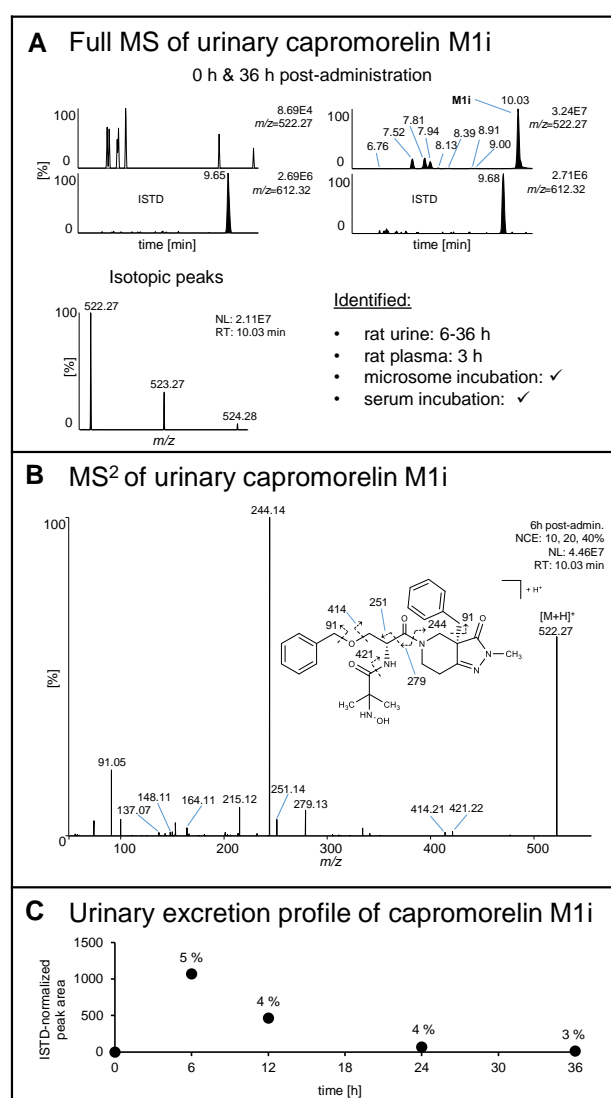
t_R, Retention time; S, substrate incubated; E, enzyme incubated.

Capromorelin

The interpretation of the full HRMS scan revealed 45 metabolites detected in rat urine (Figure 4.2 A), 11 metabolites detected in rat EDTA-plasma, 19 metabolites detected in microsome incubated drug samples, and seven metabolites detected after human serum incubation. Subsequent MS characterization and monitoring of the urinary excretion profile was accomplished for the most abundant metabolites observed in rat urine. In comparison to the intact drug, the amount of traceable capromorelin metabolites was relatively low, independent of the *in vitro* or *in vivo* experiments conducted. The three most abundant metabolites (M) detected in rat urine and, therefore, the most

interesting ones with regards to sports drug testing were the hydroxylamine M1i (Figure 4.4), the hydrolyzed M3 (Figure 4.5), and the *N*-dealkylated M4 (Figure 4.S2).

In rat urine, between t_R 6.67 and 10.03 min, at least nine different metabolites (M1a-i), presumably originating from CYP-mediated mono-hydroxylation or epoxidation, were observed by full HRMS (Figure 4.4 A, upper panel) and characterized by tMS² experiments. The majority of them, eluting between t_R 6.67 and 8.39 min, contain the introduced hydroxy group (or epoxide) within the left or right benzyl moiety, ascertained by respective diagnostic product ions (data not shown). The main hydroxylated metabolite, found in rat urine 6-36 h post-administration, in rat EDTA-plasma 3 h post-administration, and in human microsomal preparations (*in vitro*), was the putative hydroxylamine M1i, eluting at 10.03 min. In contrast to the most C-hydroxylated metabolites, the biotransformation from amines to hydroxylamine or *N*-oxide metabolites frequently result in an increased retention time on reversed phase LC under acidic conditions [36-38]. A number of further indications substantiated the proposed structure of this metabolite.



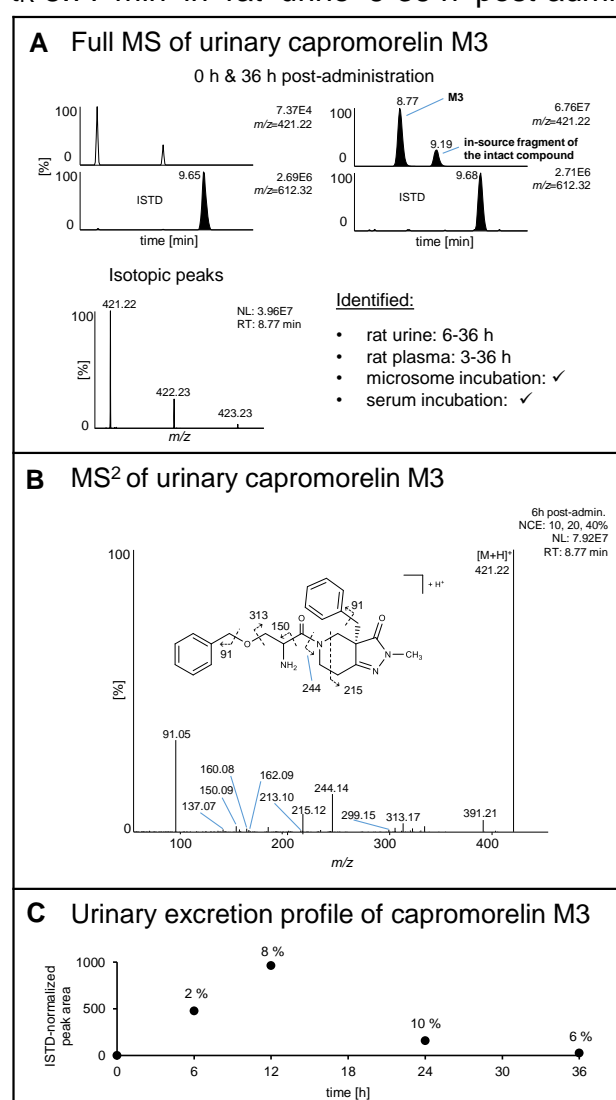
First, as observed in the MS² spectrum of the [M+H]⁺ ion at $m/z = 522.2711$, the additional accurate mass of an oxygen atom (15.9944 u) was neither located at the benzyl moieties nor the hexahydropyrazolopyridine residue of the molecule (Figure 4.4 B). Second, the abundance of the ion at $m/z = 522.2711$ was not affected by employing APCI instead of

Figure 4.4: A) The extracted ion chromatogram (mass tolerance ± 5 ppm) of the full HRMS of the urinary capromorelin hydroxylamine M1i with the [M+H]⁺ ion of $m/z = 522.2711$ at 0 h and 36 h post-administration and, below, the isotope signals of the mass spectrum at retention time, t_R , 10.03 min (36 h post-administration). B) The MS² spectrum of the [M+H]⁺ ion of a sample collected 6 h post-administration. C) The urinary excretion profile with the indicated percentages referring to the relative abundance of the ISTD-normalized peak area.

ESI, which would be expected in case of *N*-oxides owing to the reported thermal instability during APCI [39]. Third, the pMS³ mass spectrum of m/z 522.2711 \rightarrow 421.2233 (Figure 4.S3), representing the precursor capromorelin minus the *N*-terminal α -methylalanine residue, confirmed the absence of a hydroxyl group in this structural part of the metabolite. Furthermore, m/z = 421.2233 also represents the hydrolyzed capromorelin M3, identified at t_R 8.77 min (Figure 4.5, A) and its MS² mass spectrum (Figure 4.5, B) was in good agreement with the pMS³ mass spectrum of m/z 522.2711 \rightarrow 421.2233. In contrast, the pMS³ mass spectrum of m/z 522.2711 \rightarrow 279.1337, representing (*Z*)-2-amino-*N*-(1-(benzyloxy)-3-oxoprop-1-en-2-yl)-2-methylpropanamide (Figure 4.S4), showed the neutral losses of CO (27.9949 u) and C₃H₇NO (73.0528 u), with the latter indicating *N*-(prop-1-en-2-yl)hydroxylamine or 2-aminoprop-2-en-1-ol. The product ion mass spectrum of an additional pMS³ experiment at m/z 522.2711 \rightarrow 251.1390, representing (*Z*)-2-amino-*N*-(2-(benzyloxy)vinyl)-2-methylpropanamide (Figure 4.S5), was in good agreement with the pMS³ mass spectrum of m/z 522.2711 \rightarrow 279.1337 and thus, the loss of CO was assigned to the aldehyde moiety. Eventually, this evaluation supported the presumption of a hydroxyl group at the primary amine. Fourth, the CYP-mediated *N*-oxidation of primary amines is a common phenomenon, reported e.g., for phentermine, an aliphatic amine, or sulfamethoxazole, an aniline derivate, to respective hydroxylamine metabolites [40, 41]. It was further shown that hydroxylamine derivatives can autoxidize to nitroso (intermediate) and nitro derivatives [42]. Consequently, it is conceivable that similar reaction sequences of the *N*-oxidation pathway for capromorelin occur as visualized in Figure 4.S6. Indeed, the urinary capromorelin nitro M1-5 with the [M+H]⁺ ion found at m/z = 536.2504 was observed at t_R 11.89 min and characterized by tMS² (Figure 4.S7). In addition, the neutral loss of NO₂ could be tracked in the product ion scan mass spectra and by a neutral loss scan and precursor ion scan performed on a triple quadrupole MS (Figure 4.S8). Sixth, within a period of almost 50 days and three freeze-thaw cycles, the capromorelin post-administration samples of both rats (6 h) were analyzed. Interestingly, both of them clearly demonstrated a time-dependent relative decrease in the abundance of the hydroxylamine M1i, accompanied by an increase in intensity of the corresponding nitro M1-5 (Figure 4.S9), most likely due to autoxidation. Moreover, a corresponding [M+H]⁺ ion at m/z = 520.2554, which could be assigned to the putative nitroso M1-4 (t_R = 11.92 min), was identified at low abundance (MS² data not available). This observation was consistent with Naisbitt *et al.* who described the instability of a sulfamethoxazole nitroso

metabolite due to spontaneous reaction in solution [43], further supporting the suggested formation of the capromorelin hydroxylamine M1i. However, the continuous chemical transformation of a metabolite is undesirable in sports drug testing and has to be taken into account for the (long-term) storage of a doping control sample. Nevertheless, it is one of the three major metabolites of capromorelin found in rat urine with the highest urinary concentration at 6 h post-administration and with a relative abundance of 3-5% over the total period of time compared to the unmodified compound (Figure 4.4 C).

The second major metabolite was the capromorelin hydrolyzed M3, detected at t_R 8.77 min in rat urine 6-36 h post-administration, rat EDTA-plasma 3-36 h post-



administration, human microsomes (*in vitro*), and human serum (*in vitro*) (Figure 4.5 A). The presence of this metabolite could be confirmed by tMS^2 experiment. The product ion spectrum of a 6 h post-administration rat sample of the $[M+H]^+$ ion at $m/z = 421.2234$ is shown in Figure 4.5 B. The formation of this metabolite is not exclusive due to the activity of amidases, since it was also observed in the enzyme blank control samples of both *in vitro* experiments with similar concentrations. The highest metabolite concentration excreted by rats was found at 12 h post-administration and the relative abundance over the total time compared to the unmodified compound was between 2-10 % (Figure 4.5 C).

Figure 4.5: A) The extracted ion chromatogram (mass tolerance ± 5 ppm) of the full HRMS of the urinary capromorelin hydrolyzed M3 with the $[M+H]^+$ ion of $m/z = 421.2234$ at 0 h and 36 h post-administration and, below, the isotope signals of the mass spectrum at t_R 8.77 min (36 h post-administration). B) The MS^2 spectrum of the $[M+H]^+$ ion of a sample collected 6 h post-administration. C) The urinary excretion profile with the indicated percentages referring to the relative abundance of the ISTD-normalized peak area.

The third major metabolite was suggested to represent the *N*-dealkylated capromorelin M4, detected at t_R 8.37 min in rat urine 6-36 h post-administration, rat EDTA-plasma 3-12 h post-administration, human microsomes (*in vitro*), and human serum (*in vitro*) (Figure 4.S2 A). Again, this metabolite was additionally observed in the *in vitro* enzyme blank control samples. *N*-dealkylation of tertiary amines is catalyzed by cytochrome P450 enzymes [44], and thus, high concentrations of M4 were found in rat urine. The metabolite was characterized by the product ion spectrum of the $[M+H]^+$ ion at $m/z = 492.2605$ of the 6 h post-administration rat urine sample as demonstrated in Figure 4.S2 B. Its maximum urinary concentration was found at 6 h post-administration and the relative abundance over the total time compared to the unmodified compound was between 4 and 6% (Figure 4.S2 C).

Briefly, the three predominant metabolites of capromorelin were predominantly found in rat urine and could all be detected from the start to the end of the sample collection period with relative abundances of 2-10%. The intact drug and the metabolite concentrations of the rat EDTA-plasma samples were significantly lower with approximately 2-3 orders of magnitude below the urinary concentration levels.

Macimorelin

The interpretation of the full HRMS scan revealed 10 metabolites detected in rat urine (Figure 4.2 B), zero metabolites in rat EDTA-plasma, seven metabolites detected in microsome-incubated drug samples, and seven metabolites were found after human serum incubation. Subsequent MS characterization and monitoring of the urinary excretion profile was accomplished for the most abundant metabolites observed in rat urine, which were proposed to represent monohydroxylated or epoxide M1c (Figure 4.S13), *N*-dealkylated M2 (Figure 4.6), and M3 (Figure 4.7).

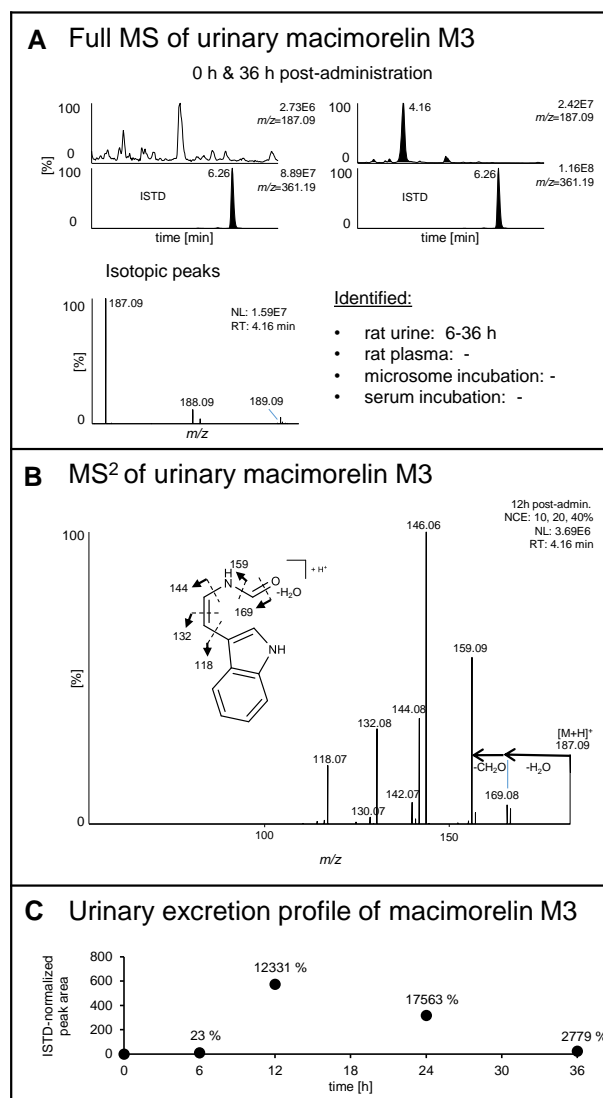
The CYP-mediated mono-hydroxylation or epoxidation revealed at least five metabolites eluting between t_R 6.30 and 7.33 min, detected in rat urine samples 6-24 h post-administration (Figure 4.S13 A). In order to determine the hydroxy or epoxide position in each compound, the four most abundant metabolites ($t_R = 6.30 - 7.02$ min) were subsequently characterized by tMS^2 experiments and the respective product ion mass spectrum of the $[M+H]^+$ ion at $m/z = 491.2401$ and the indication of the most likely site of modification are depicted in Figure 4.S14. Finally, M1c at t_R 6.83 min presented highest relative abundances and was thus considered as a potential marker for sports

drug testing approaches. The simultaneous presence in the enzyme blank control sample, although with an abundance four times less than observed in microsomes-incubated samples, illustrates that microbial transformation or spontaneous and/or enzymatic oxidation could be involved in the formation of this metabolite. The results of the tMS² characterization minimized the possibilities of the available sites of metabolic reactions to the methyleneindole residue proximal to the 2-amino-2-methylpropanamide moiety as indicated in Figure 4.S13 B. This metabolite was primarily excreted after 6 h and the relative abundance was between 1 and 8% (Figure 4.S13 C).

The elimination of a tryptophan-like residue via C-N bond cleavage of macimorelin was proposed to yield two additional major metabolites, *N*-dealkylated macimorelin M2 (Figure 4.6) and macimorelin M3 (Figure 4.7). In the extracted ion chromatograms of the full HRMS scans of a rat urine sample collected 36 h post-administration, they were still clearly detected at *t_R* 4.62 min (M2) and *t_R* 4.16 min (M3). At *t_R* 7.89 min, two in-source-generated fragments of macimorelin were observed with identical [M+H]⁺ ions as for the two metabolites (not shown). Both metabolites were present in rat urine 6-36 h post-administration, but were not found in rat EDTA-plasma. In addition, M2 was found *in vitro*, although M3 was absent. Figure 4.6 B shows the MS² spectrum of the [M+H]⁺ ion at *m/z* = 289.1659 (M2) and Figure 4.7 B shows the MS² spectrum of the [M+H]⁺ ion at *m/z* = 187.0866 (M3); both spectra were acquired from a rat urine sample collected 12 h post-administration. M2 reached its maximum concentration at 12 h post-administration and the ISTD-normalized peak area at this time was more than three times higher than that of the intact compound (Figure 4.6 C). Remarkably, this observation appeared to be even more significant for M3. While the shape of the excretion profile of M3 (Figure 4.7 C) was similar to M2, the relative abundances at 12 h and 24 h post-administration were two orders of magnitude higher than the intact compound's peak area.

Figure 4.6: A) The extracted ion chromatogram (mass tolerance ±5 ppm) of the full HRMS of the urinary macimorelin *N*-dealkylated M2 with the [M+H]⁺ ion of *m/z* = 289.1659 at 0 h and 36 h post-administration and, below, the isotope signals of the mass spectrum at *t_R* 4.62 min (36 h post-administration). B) The MS² spectrum of the [M+H]⁺ ion of a sample collected 12 h post-administration. C) The urinary excretion profile with the indicated percentages referring to the relative abundance of the ISTD-normalized peak area.

Briefly summarized, the three predominant metabolites of macimorelin were exclusively discovered in rat urine. High amounts of capromorelin M2 and M3 were observed over a presumably extended period of time exceeding the time of sample collection of this study. Moreover, the urinary concentration of macimorelin was sufficiently high to unambiguously detect it at any time up to 36 h post-administration. Although no metabolites were detected in rat EDTA-plasma, traces of the intact drug were found 3 h after the administration.



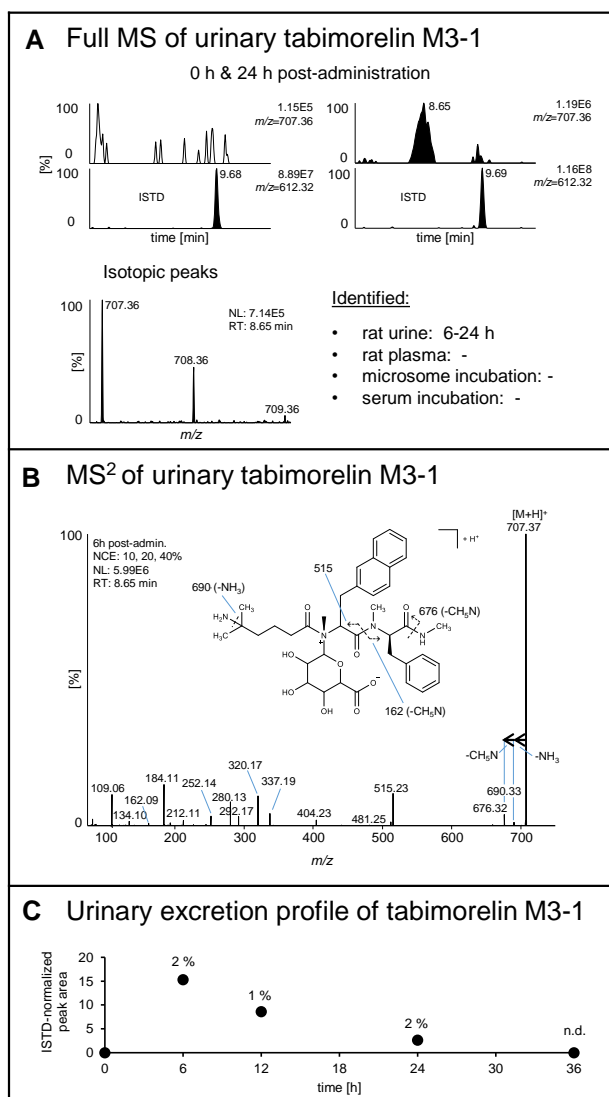
Tabimorelin

The interpretation of the full HRMS scan revealed five metabolites detected in rat urine (Figure 4.2 C), zero metabolites in rat EDTA-plasma, 10 metabolites detected in microsome-incubated drug samples and one metabolite detected after human serum incubation. Subsequent MS² characterization and monitoring the urinary excretion profile was accomplished for the predominant metabolite in rat, which was suggested

Figure 4.7: A) The extracted ion chromatogram (mass tolerance ± 5 ppm) of the full HRMS of the urinary macimorelin M3 with the $[M+H]^+$ ion of $m/z = 187.0866$ at 0 h and 36 h post-administration and, below, the isotope signals of the mass spectrum at t_R 4.16 min (36 h post-administration). B) The MS² spectrum of the $[M+H]^+$ ion of a sample collected 12 h post-administration. C) The urinary excretion profile with the indicated percentages referring to the relative abundance of the ISTD-normalized peak area.

to represent the *N*-glucuronidated M3-1 (Figure 4.8).

The tabimorelin phase II M3-1 was exclusively detected in rat urine from 6-24 h post-administration and could not be confirmed by any other *in vitro/in vivo* experiment. The



compound eluted at t_R 8.65 min and the extracted ion chromatogram of the $[M+H]^+$ ion at $m/z = 707.3651$ is shown in Figure 4.8 A. The metabolite was characterized by a tMS² experiment and its product ion mass spectrum of a rat urine sample 6 h post-administration is provided in Figure 4.8 B. M3-1 was primarily excreted at 6 h post-administration and the relative abundance was found to be between 0 and 2% (Figure 4.8 C). Other studies suggested a significantly decreased *N*-glucuronidation of drugs in rat compared to human [45, 46]. This metabolite seems promising for human doping control purposes. No other metabolite achieved the minimum required 1% of relative abundance that would entail further characterizations at this point. In contrast to the few urinary metabolites

observed for tabimorelin, the intact drug was traceable in both rat urine and rat EDTA-plasma by the end of sample collection. However, the concentration levels of the intact compound of rat EDTA-plasma samples were significantly lower with approximately three orders of magnitude below the urinary concentration levels.

4.4.2 Method characterization and validation

In order to deter doping using the three new compounds, namely capromorelin, macimorelin, and tabimorelin, it was desirable to establish a WADA-validated anti-

Figure 4.8: A) The extracted ion chromatograms (mass tolerance ± 5 ppm) of the full HRMS of the urinary tabimorelin *N*-glucuronidated M3-1 with the $[M+H]^+$ ion of $m/z = 707.3579$ at 0 h and 24 h post-administration, and below, the isotope signals of the mass spectrum at t_R 8.65 min from a sample collected 24 h post-administration. B) The MS² spectrum of the $[M+H]^+$ ion of a sample collected 6 h post-administration. C) The urinary excretion profile with the indicated percentages referring to the relative abundance of the ISTD-normalized peak area.

doping test. Owing to their physicochemical properties, the substances were implemented into an existing routine initial test method, which also covers other GHRPs/GHS analytes, such as alexamorelin, GHRP-2, or anamorelin. This screening was devised for the detection of GH-releasing factors, which are peptides and peptide-related compounds (< 2 kDa), in human urine [12]. A second detection method for human EDTA-plasma was validated in the same manner. The results of the method validation are summarized in Table 4.2. For initial testing purposes, the selectivity was demonstrated by analyzing 10 different blank samples (female $n = 5$ and male $n = 5$).

Table 4.2: Results of the qualitative initial testing procedure (ITP) and confirmation procedure (CP) validation for human urine and human EDTA-plasma matrix

No interfering signals were identified in either urine or plasma. The repeatability of six different urine samples or plasma samples, expressed in r_{TR} [%], was between 0.05 and 0.37% and thus below the required < 1%. For urinary matrix, the assessment of carryover after analyzing a blank sample after a sample containing a high concentration of the analyte (400% MRPL) revealed no carryover for tabimorelin and macimorelin, and a minor carryover of 0.1% for capromorelin. For EDTA-plasma matrix, no carryover was observed for any of the analytes. The LOD of the analytes was estimated between 0.17 and 0.45 ng/mL (urine) and 0.02 and 0.60 ng/mL (EDTA-plasma).

The occurrence of a presumptive adverse analytical finding can be confirmed in three different CP methods depending on the matrix and the choice of sample preparation as described in 'Material and Methods'. Regardless of the procedure or sample matrix, all CP assays showed excellent selectivity after analyzing 10 different blank samples. Robustness was evaluated by analyzing six different urine samples with a concentration of 50% MRPL (SPE sample preparation) or 100% MRPL (D&I and PP), prepared on another day. The r_{TR} [%] of all test batches was between 0.07 and 0.57% and thus considered to be robust. No carryover was observed and LOI was estimated between 0.46 and 0.89 ng/mL for urine direct injection (D&I), between 0.18 and 0.41 ng/mL for urine after SPE sample preparation, and between 0.19 and 0.89 ng/mL for plasma matrix via PP.

In clinical studies, maximum plasma concentration(s) of 29 ng/mL (tabimorelin) [6], 30-250 ng/mL (capromorelin) [10], and 0.9-7.6 ng/mL (macimorelin) [11] were reached

after single or multiple oral doses of the drugs. Thus, sensitive analytical testing in the range of pharmacologically relevant drug concentrations can be performed with the EDTA-plasma assays presented here.

ITP for urine (D&I) and plasma (PP) samples						
Compound	tSIM ion 1	tSIM ion 2	Selectivity (n = 10)	Repeatability rtR (RSD, %) (n = 6)	Carryover [%] (n = 1)	LOD [ng/mL] (n = 6)
Tabimorelin	529.3173	530.3201	OK (D&I) OK (PP)	0.19 (D&I) 0.10 (PP)	0.0 (D&I) 0.0 (PP)	0.30 (D&I) 0.60 (PP)
Macimorelin	475.2442	476.2477	OK (D&I) OK (PP)	0.21 (D&I) 0.05 (PP)	0.0 (D&I) 0.0 (PP)	0.45 (D&I) 0.18 (PP)
Capromorelin	506.2762	507.2795	OK (D&I) OK (PP)	0.37 (D&I) 0.08 (PP)	0.1 (D&I) 0.0 (PP)	0.17 (D&I) 0.02 (PP)

CP for urine (D&I), urine (SPE) and plasma (PP) samples							
Compound	tMS ² ion 1	tMS ² ion 2	tMS ² ion 3	Selectivity (n = 10)	Robustness rtR (RSD, %) (n = 6)	Carryover [%] (n = 1)	LOI [ng/mL] (n = 6)
Tabimorelin	184.1120 280.1331	252.1382 184.1120	212.1073 252.1382	OK (D&I) OK (SPE) OK (PP)	0.12 (D&I) 0.12 (SPE) 0.12 (PP)	0.0 (D&I) 0.0 (SPE) 0.0 (PP)	0.64 (D&I) 0.18 (SPE) 0.89 (PP)
Macimorelin	113.0714 272.1394	159.0916 289.1659	244.1446 159.0916	OK (D&I) OK (SPE) OK (PP)	0.12 (D&I) 0.57 (SPE) 0.07 (PP)	0.0 (D&I) 0.0 (SPE) 0.0 (PP)	0.89 (D&I) 0.41 (SPE) 0.19 (PP)
Capromorelin	244.1448 244.1448	245.1484 263.1390	215.1179 215.1179	OK (D&I) OK (SPE) OK (PP)	0.46 (D&I) 0.11 (SPE) 0.08 (PP)	0.0 (D&I) 0.0 (SPE) 0.0 (PP)	0.46 (D&I) 0.19 (SPE) 0.19 (PP)

tMS² ions upper row (urine assays) and tMS² ions lower row (plasma assay).

D&I, "Dilute-and-inject"; t-SIM, targeted SIM; LOD, limit of detection; LOI, limit of identification.

Conclusion

In sports drug testing, the primary analysis matrices are urine and blood. As soon as new substances emerge and an illegal use in sports cannot be excluded, these compounds require a detailed characterization and appropriate analytical detection methods must be provided immediately. The missing information about the metabolic conversion and excretion pathway of the short-lived ghrelin mimetics capromorelin, macimorelin and tabimorelin are of particular interest as they could improve sensitivity, specificity, and detection window of a detection assay. Indeed, combining distinct pre-analytical and computational techniques (*in vitro/in vivo/in silico*), several metabolites of capromorelin, macimorelin and tabimorelin were observed and thoroughly characterized by LC-HRMS/MS. Notwithstanding, the rather nonpeptidic precursor compounds were not subjected to proteolytic degradation unlike other peptide ghrelin

receptor agonists, such as GHRPs, and while various proteolytic metabolites exhibited comparable or increased relative abundances [27], this observation was the exception here. Thus, most of the metabolites were found less concentrated than their precursor compounds with relative abundances < 10%, both in urine and blood. Nonetheless, in case of an adverse analytical finding, they might be of important value to complement the confirmation of identity of the ghrelin mimetic. Furthermore, macimorelin M2 and macimorelin M3 were detected with substantially elevated urinary excretion levels compared to the intact compound. Based on the assumption that metabolic conversions are transferable from rat model to human, these metabolites are highly valuable as they are likely to increase sensitivity, specificity, and detection windows. In addition, macimorelin M3 could prove to be a useful longer-term metabolite, as it still remained with significantly higher relative concentration by the end of urine sample collection. Finally, in accordance with the WADA guidelines, the commercially available intact substances (in contrast to their metabolites) were incorporated into initial testing procedures (LOD: 0.02-0.60 ng/mL) and confirmation procedures (LOI: 0.18-0.89 ng/mL) for human urine and blood matrix.

4.5 Supplementary data

4.5.1 Materials and methods

In vivo experiments

Urine sample preparation: One mL of rat urine was fortified with 10 μ L of a 200 ng/mL ISTD working solution and acidified with acetic acid to pH 4-6. The sample was loaded directly to a MCX cartridge (10 mg sorbent), washed with 1 mL of 2% formic acid and 1 mL of methanol, and then eluted with 1 mL of 5% NH_4OH in methanol with a flow rate of 1 mL/min into a new LoBind tube. The eluate was centrifuged (2 min/10 000 g) and the supernatant was evaporated (45°C/reduced pressure) and afterwards reconstituted in 100 μ L ddH₂O. The final sample was centrifuged again (2 min/10 000 g) and 2-10 μ L were subjected to LC-HRMS.

Plasma sample preparation: One hundred μ L of rat EDTA-plasma were fortified with 10 μ L of a 200 ng/mL ISTD working solution. The sample was diluted with an equal volume of ddH₂O followed by a protein precipitation (PP) due to the addition of 400 μ L of acetonitrile and brief vortexing. After centrifugation (10 min/17 000 g) and evaporation (45°C/reduced pressure) of the supernatant, the sample was reconstituted in 100 μ L ddH₂O. The final sample was centrifuged again (2 min/17 000 g) and 10 μ L were subjected to LC-HRMS analysis.

In vitro experiments

Serum preparation: One hundred μ L of human serum were fortified with 10 μ L of a 100 μ g/mL (= 1 μ g) working solution of each compound in a LoBind tube. A substrate blank sample was prepared by substituting the analyte with ddH₂O, and a serum blank sample was prepared by substituting the serum matrix with PBS. All samples were diluted with 100 μ L of ddH₂O and incubated for 22 h at 37°C and 500 rpm. The reaction was stopped and proteins were precipitated with 400 μ L of ice-cold acetonitrile. Samples were centrifuged (10 min/17 000 g), the obtained supernatants were evaporated (45°C/reduced pressure) to dryness, reconstituted with 100 μ L of ddH₂O, and 10 μ L were injected into LC-HRMS.

Microsomal incubation: Briefly, in a 1.5 mL LoBind tube, 427 μ L of a 0.1 M potassium phosphate buffer (PB), pH 7.4 and pre-warmed to 37°C, were mixed with 50 μ L of 10 mM NADPH and fortified with 10 μ L of a 100 μ g/mL working solution of each drug.

After an incubation of 5 min at 37°C, 13 µL of a 20 mg/mL microsome solution in PB were added to result in a final concentration of 0.5 mg/mL. For a substrate blank (control) sample, the working solution of the drug was substituted with 10 µL of PB. In the same manner, an enzyme blank (control) sample was prepared by adding 13 µL of PB instead of the microsomes. All test tubes contained a final volume of 500 µL and were briefly mixed and then incubated for 2 h at 37°C. The reaction was stopped by adding 250 µL ice-cold acetonitrile. Samples were vortexed shortly and centrifuged (5 min/10 000 g/4°C). Finally, 10 µL of the supernatant were analyzed by LC-HRMS.

LC-TQMS/MS

To further characterize the putative capromorelin hydroxylamine M1i, a neutral loss scan, precursor ion scan, and multiple reaction monitoring (MRM) scans were performed on a Xevo TQ-XS from Waters (Melford, MA, USA) with a UniSpray ion source, used in positive ionization mode. The Waters Acquity UPLC system was equipped with a Poroshell 120 EC-C₈ analytical column, 3.0 x 50 mm, 2.7 µm pore size from Agilent Technologies (Santa Clara, CA, USA). The autosampler's temperature was 4°C and the analytical column was heated to 35°C. The same chromatographic gradient as for the LC-HRMS/MS experiments was applied. The soft transmission mode was activated and global MS settings were: impactor voltage at 3.1 kV, cone voltage at 30 V, collision energy at 20 eV with argon as collision gas, desolvation temperature at 500°C, desolvation gas flow at 750 L/h, cone gas flow at 150 L/h and nebulizer at 7 bar. The system was controlled by MassLynx V4.2.

4.5.2 Results and discussion

A number of metabolites of capromorelin, macimorelin, and tabimorelin were detected *in vivo* and *in vitro* and the major metabolites from drug administered rat urine were described in detail. In particular, the rat experiments were essential to obtain a comprehensive insight into the metabolic profile of the drugs, because studies with humans were limited due to ethical reasons. However, the transferability of *in vivo* systems, such as allometric scaling from rat to human, remains a difficult task [47]. Thus, it was necessary to also characterize some of the rather weak concentrated metabolites, in case they are present in human specimens with increased amounts and could therefore be of great interest for anti-doping purposes. Here, some of the minor metabolites, analyzed by means of full HRMS scans, were further characterized by tMS² experiments. As in the main manuscript, several fragments were tentatively assigned with

the support of a fragmentation modeling software tool ("CFM-ID 3.0"). This includes, but is not limited to the characterization of capromorelin nitro M1-5 (Figure 4.S7), capromorelin *N*-acetylated M1-6 (Figure 4.S10), capromorelin M2-2 (Figure 4.S11), macimorelin mono-hydroxy M1a, M1b, M1c, and M1d (Figure 4.S14), macimorelin dihydroxy M1-1b (Figure 4.S15), macimorelin *O*-glucuronide M1-2 (Figure 4.S16), tabimorelin mono-hydroxy M1 (Figure 4.S18), tabimorelin mono-*O*-glucuronide M1-1 (Figure 4.S19), tabimorelin *N*-dealkylated M2 (Figure 4.S20), and tabimorelin *N*-glucuronide M3 (Figure 4.S21).

The *N*-acetylated capromorelin M1-6 may have been preferentially metabolized by an *N*-acetyltransferase (NAT2) and was detected at t_R 10.70 min in the full HRMS scan of the *in vivo* samples (rat urine; 6-24 h post-administration) and *in vitro* samples (human microsome). The product ion spectra of the $[M+H]^+$ ion at $m/z = 548.2867$ of a rat urine sample collected 6 h post-administration is shown in Figure 4.S10. In addition, at least four other potential *N*-acetylated metabolites with the same $[M+H]^+$ ion were observed in rat urine at t_R 8.78 min, 9.58 min, 10.04 min, and 10.25 min. As they were found to be less concentrated, no further MS characterization was performed.

The capromorelin M2-2 with the $[M+H]^+$ ion of $m/z = 416.2292$ was detected in all matrices at t_R 7.63 min with the exception of the *in vitro* samples (human serum). In rat EDTA-plasma it was detected from 3-12 h post-administration and in rat urine it was detected to the end of sample collection (36 h post-administration). The metabolite was most likely formed by a 2-step reaction process: firstly, the *O*-dealkylation of the dialkylether and secondly, the reduction of the obtained aldehyde. In addition, it was observed as an in-source fragment of M1b (t_R 7.51 min), which is an aromatic mono-hydroxylated metabolite and its formation was obviously initiated after the cleavage of methylphenol or benzyl alcohol (C_7H_8O). In Figure 4.S11 the product ion spectra of the $[M+H]^+$ ion of M2-2 of a rat urine sample collected 6 h post-administration can be observed.

The presence of four macimorelin mono-hydroxy M1a, M1b, M1c, and M1d was already mentioned in the main manuscript. Here, the product ion spectra of the $[M+H]^+$ ion at $m/z = 491.2401$ at t_R 6.30 min, 6.56 min, 6.83 min, and 7.02 min from a rat sample collected 6 h post-administration is demonstrated (Figure 4.S14). In general, they could be detected in rat urine from 6-12 h post-administration, in the case of M1b up to 24 h post-administration. The small inlet in each MS^2 spectrum on the upper left

shows the extracted ion chromatogram and the black arrow indicates the respective t_R [min] of each metabolite. The dotted lines within the structural formula indicate the most likely sites of modification due to the MS^2 assignments. Except for the earliest eluting metabolite at t_R 6.30 min, all other metabolites could also be detected in the *in vitro* samples. Their additional presence in the enzyme blank samples indicates spontaneous oxidation reactions. Finally, at t_R 7.93 min an in-source fragment of the macimorelin precursor compound was observed (not shown).

Figure 4.S15 shows the MS^2 spectrum of the $[M+H]^+$ ion of macimorelin di-hydroxy M1-1b ($m/z = 507.2350$) at t_R 6.96 min from a rat urine sample. Within the *in vivo* experiments it could only be found in the rat urine samples collected 6 h post-administration. The dotted lines within the structural formula indicate the most likely site of modification due to the MS^2 assignment, however hydroxylation on the second tryptophan residue of this compound would also be possible. In the enzyme blank control samples as well as in the enzyme samples of both *in vitro* experiments, this metabolite could also be observed, which again indicates spontaneous oxidations. Two other signals with the identical $[M+H]^+$ ion could be observed in the full HRMS scans at t_R 7.26 min (human microsome) and t_R 6.29 min (human serum), however they were not further characterized.

The urinary macimorelin O-glucuronide M1-2 could be detected as a phase II metabolite at t_R 6.12 min. The corresponding product ion spectra of the $[M+H]^+$ ion ($m/z = 667.2722$) from a rat urine sample collected 6 h post-administration is shown in Figure 4.S16. For the samples collected later than 6 h post-administration the signal already disappeared. The neutral loss of a dehydrated glucuronide moiety (176.03 Da) is indicated in the MS^2 spectrum and the dotted line within the structural formula indicate the most likely site of modification.

In vitro experiments (human microsomes) revealed the identification of three tabimorelin mono-hydroxy metabolites (M1a, M1b, and M1c) at t_R 9.04 min, 9.59 min, and 10.68 min. The first one at t_R 9.04 min could also be detected *in vivo* (rat urine) 6-12 h post-administration and its product ion spectrum of the $[M+H]^+$ ion at $m/z = 545.3122$ of a rat sample collected 6 h post-administration is visualized in Figure 4.S18. The grey area within the structural formula indicates the most likely site of modification.

From 6-36 h post-administration, the phase II tabimorelin mono-*O*-glucuronide M1-1 was detected solely in rat urine (*in vivo*). The MS² spectrum of the [M+H]⁺ ion with $m/z = 721.3443$ is shown in (Figure 4.S19). The grey area within the structural formula indicates the most likely site of modification.

The *N*-dealkylation of tertiary carboxamide yielded tabimorelin *N*-dealkylated M2 ($m/z = 545.3122$) which was detected at t_R 9.77 min *in vivo* for 6-12 h post-administration and *in vitro* (human microsomes). The product ion spectrum of a rat urine sample collected 6 h post-administration is shown in Figure 4.S20. A signal of an identical mass was additionally detected in the *in vitro* enzyme blank samples at t_R 10.47 min which could have been formed after *N*-dealkylation of the second tertiary carboxamide within the unmodified compound.

In Figure 4.S21, the MS² spectrum of the phase II tabimorelin *N*-glucuronide M3 detected solely in rat urine 6-24 h post-administration is depicted. In the full HRMS scan, both the [M+H]⁺ ion at $m/z = 705.3428$ and the [M+2H]²⁺ ion at $m/z = 353.1783$ could be detected. The product ion spectra of the [M+H]⁺ ion at t_R 7.11 min was from a rat urine sample collected 6 h post-administration. This unsaturated metabolite differed from tabimorelin's main metabolite (M3-1), which is described in the manuscript, only in an additional C-C double bond.

In summary, three minor metabolites of capromorelin, six minor metabolites of macimorelin, and four minor metabolites of tabimorelin were characterized here. Furthermore, an overview of all putative metabolites detected after *in vitro* or *in vivo* experiments by full HRMS experiments is accessible for capromorelin (Table 4.S1), macimorelin (Table 4.S2), and tabimorelin (Table 4.S3). The compound list provides the molecular formula, the predominant charge state, the three isotopic masses [m/z], the reaction type, the SMILES, and the matrices in which the correspondent metabolite was detected.

4.5.3 Supplementary figures

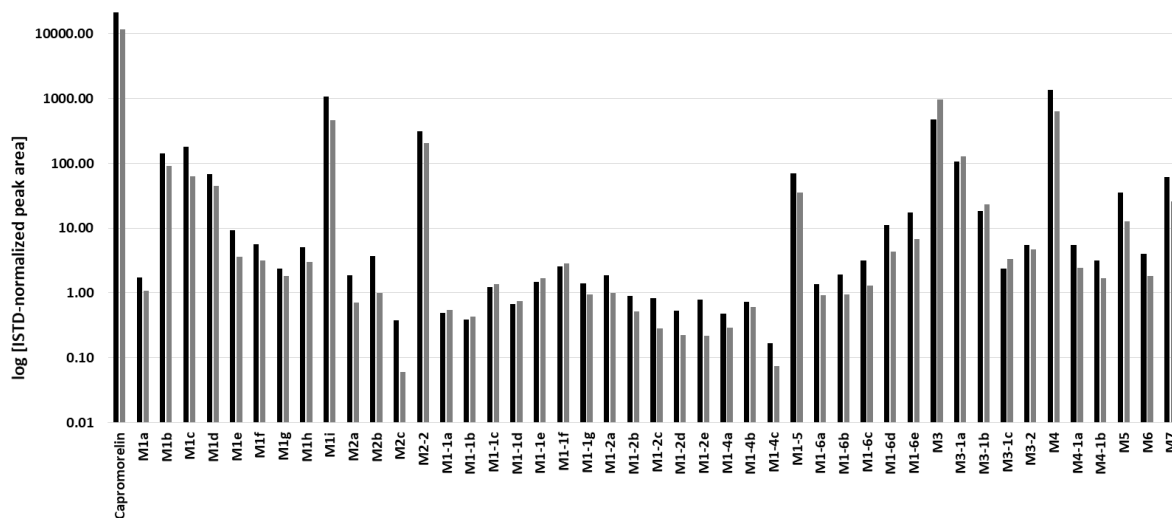


Figure 4.S1: Comparison of the absolute abundance of all metabolites of capromorelin detected in rat urine 6 h (black) and 12 h (grey) post-administration. The samples were analyzed on a Q Exactive HF-X mass spectrometer in full HRMS mode.

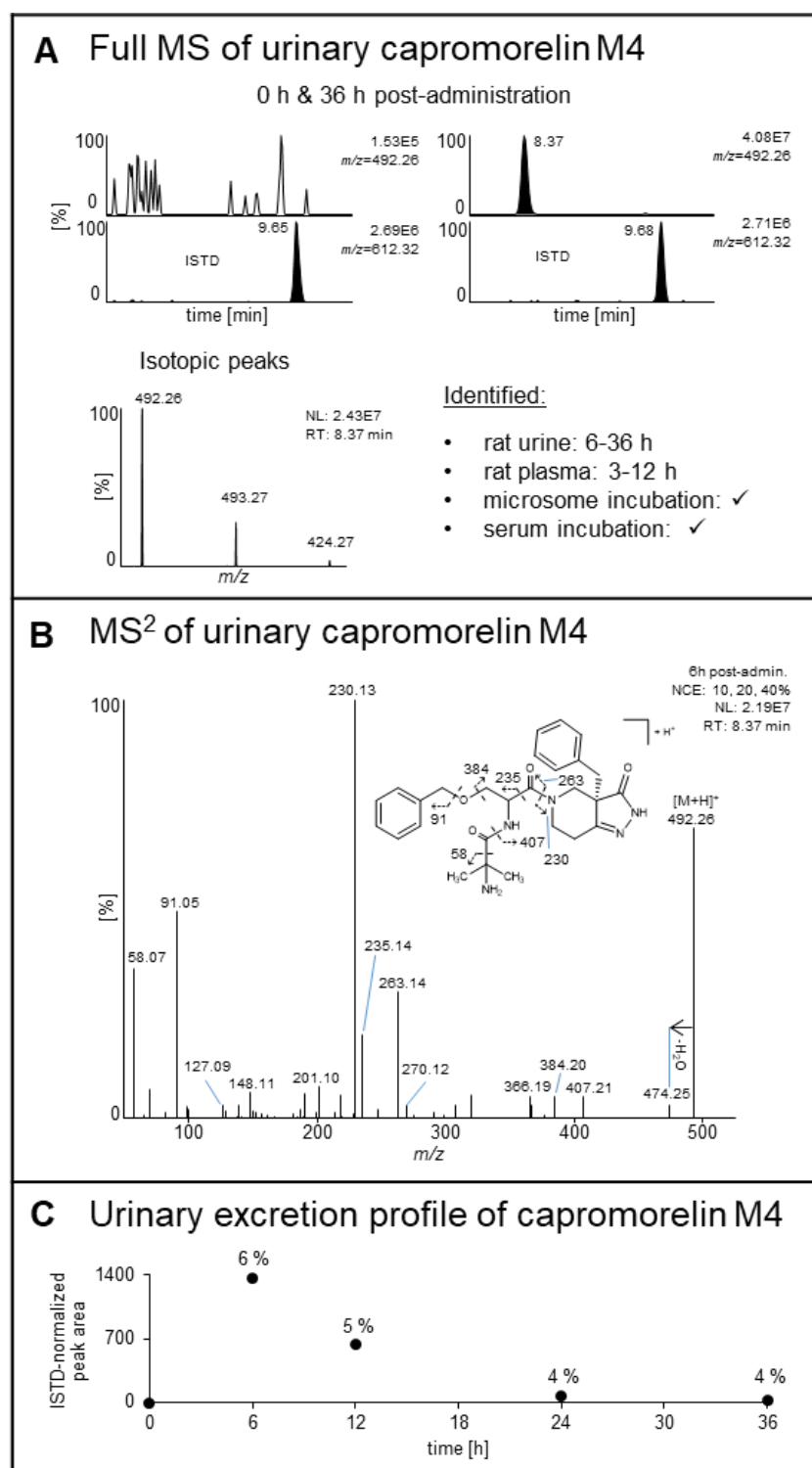


Figure 4.S2 A) The extracted ion chromatogram (mass tolerance ± 5 ppm) of the full HRMS of the urinary capromorelin *N*-dealkylated M4 with the $[M+H]^+$ ion of $m/z = 492.2605$ at 0 h and 36 h post-administration. Below, there are the isotope signals of the mass spectrum at t_R 8.37 min from a sample collected 36 h post-administration, and the different matrices and *in vitro/in vivo* experiments in which this metabolite was detected with the corresponding detection windows for rat urine and rat EDTA-plasma. B) The MS² spectrum of the $[M+H]^+$ ion of the urinary capromorelin *N*-dealkylated M4 of a sample collected 6 h post-administration. C) The urinary excretion profile of capromorelin *N*-dealkylated M4 with the indicated percentages referring to the relative abundance of the ISTD-normalized peak area.

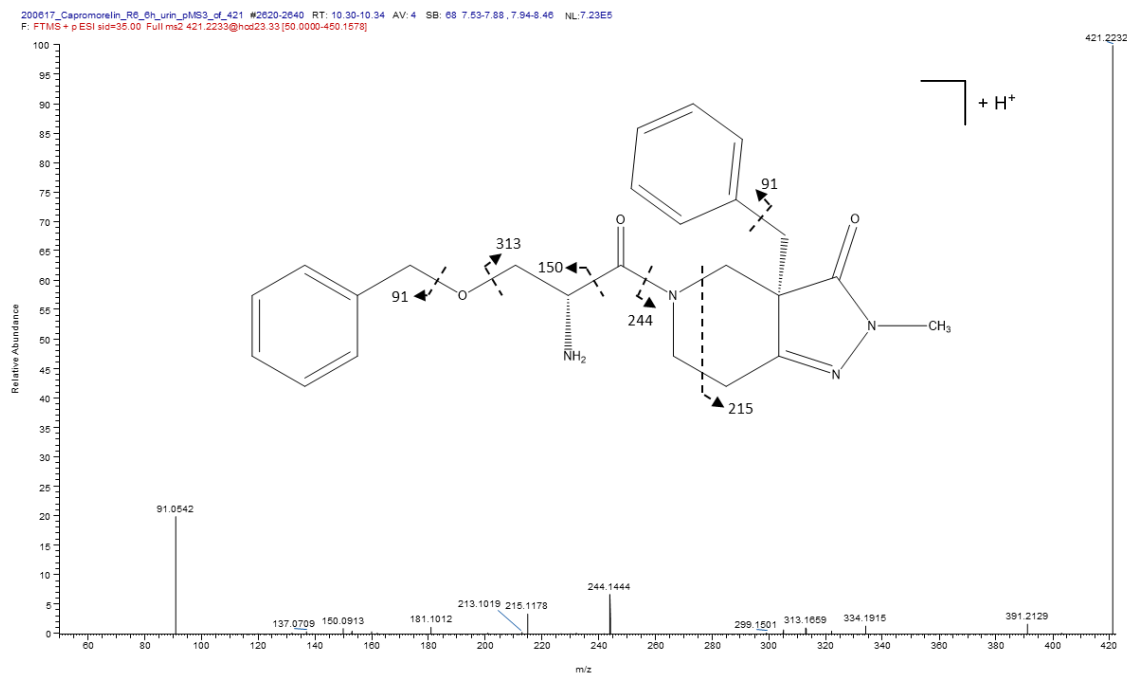


Figure 4.S3: Pseudo-MS³ spectrum (SID + MS²) of the [M+H]⁺ ion of $m/z = 421.2233$ which is a MS² fragment of capmorelin hydroxylamine M1i. The sample (rat urine, 6 h post-administration) was analyzed on an Orbitrap Exploris 480 mass spectrometer.

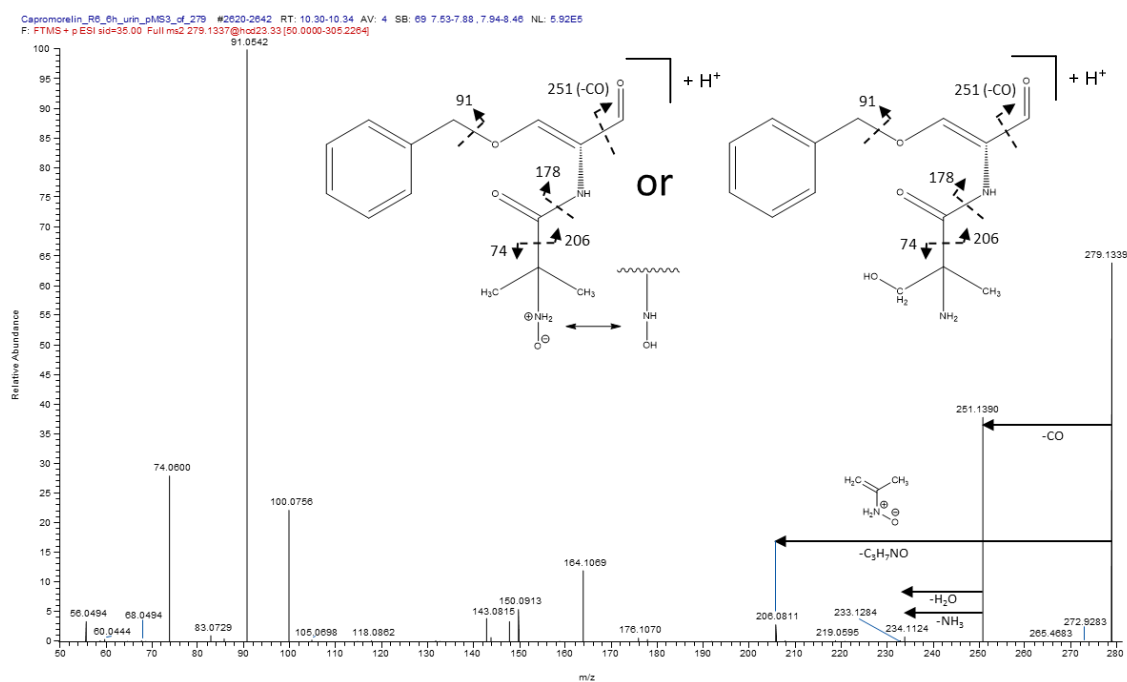


Figure 4.S4: Pseudo-MS³ spectrum (SID + MS²) of the [M+H]⁺ ion of $m/z = 279.1339$ which is a MS² fragment of capmorelin hydroxylamine M1i. In theory, both structures shown here would be plausible. The sample (rat urine, 6 h post-administration) was analyzed on an Orbitrap Exploris 480 mass spectrometer.

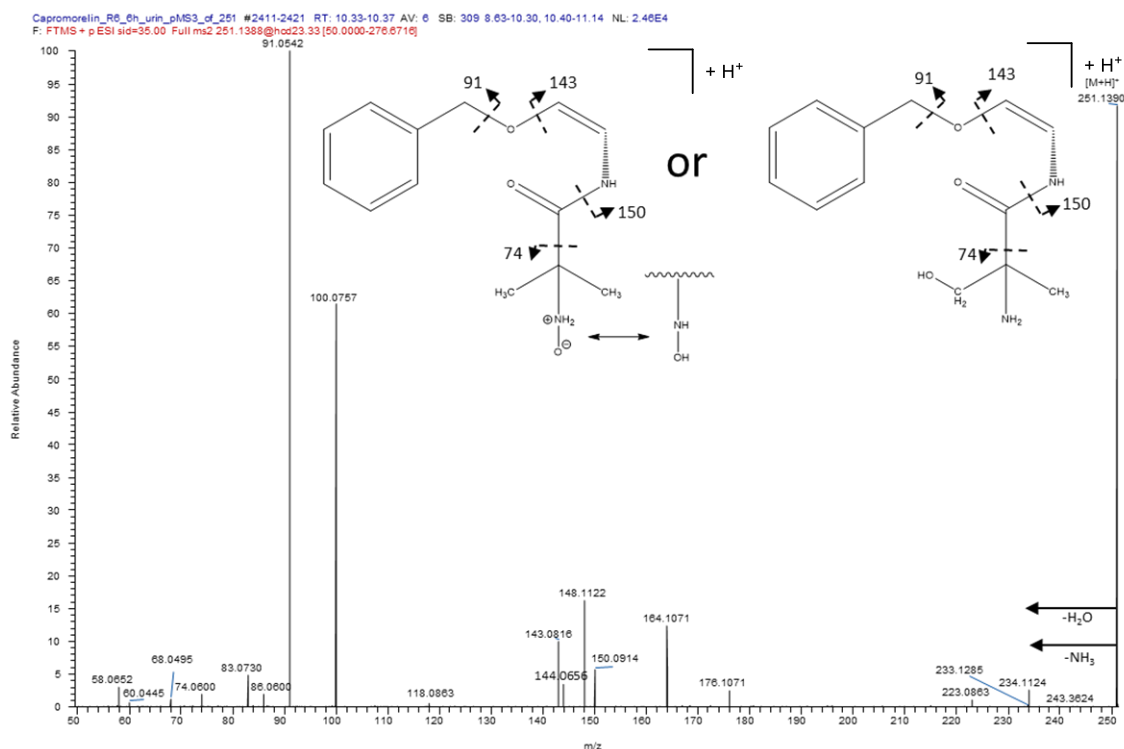


Figure 4.S5: Pseudo-MS³ spectrum (SID + MS²) of the [M+H]⁺ ion of *m/z* = 251.1390 which is a MS² fragment of capromorelin hydroxylamine M1i. In theory, both structures shown here would be plausible. The sample (rat urine, 6 h post-administration) was analyzed on an Orbitrap Exploris 480 mass spectrometer.

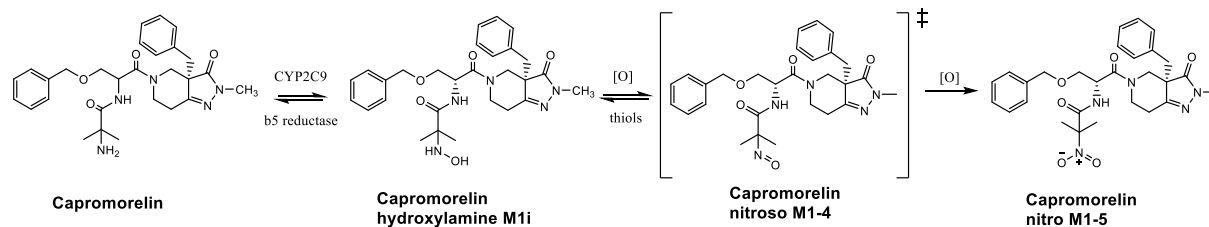


Figure 4.S6: A possible mechanism of capromorelin oxidation: First, capromorelin hydroxylamine M1i was generated by CYP2C9. Second, this compound was autoxidized to the nitroso M1-4 intermediate. Third, further oxidation resulted the capromorelin nitro M1-5.

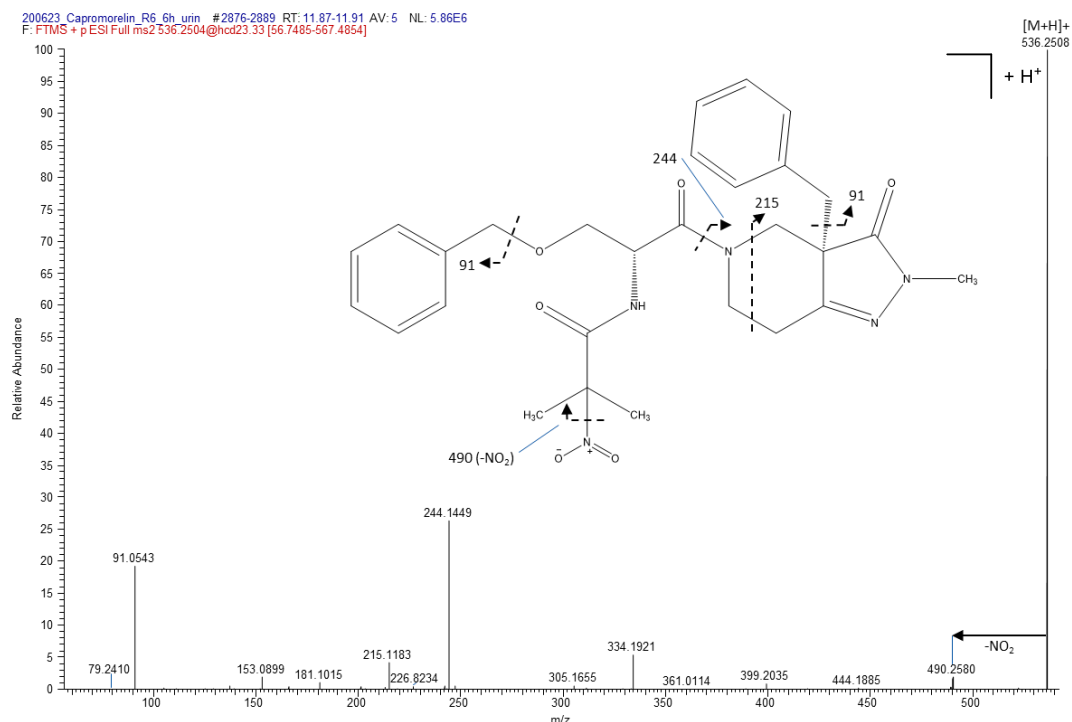


Figure 4.S7: MS² spectrum of the [M+H]⁺ ion of capromorelin nitro M1-5 ($m/z = 536.2504$) from a rat urine sample collected 6 h post-administration of capromorelin, analyzed on an Orbitrap Exploris 480 mass spectrometer.

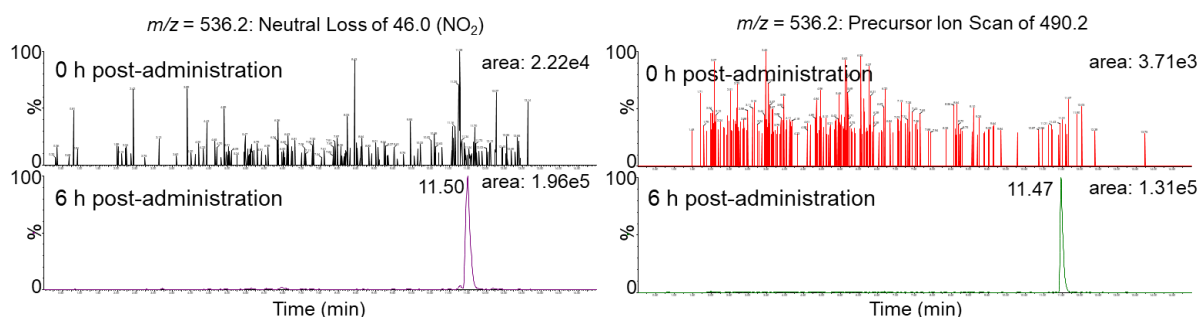


Figure 4.S8: To verify the identity of capromorelin nitro M1-5 ($m/z = 536.2$ (1+)), both a neutral loss experiment (left) and a precursor ion scan experiment (right) were conducted. The upper panel shows the extracted ion chromatogram of the [M+H]⁺ ion of a blank rat urine sample collected at 0 h and the lower panel shows the a sample collected 6 h post-administration. The samples were analyzed on a Xevo TQ-XS mass spectrometer.

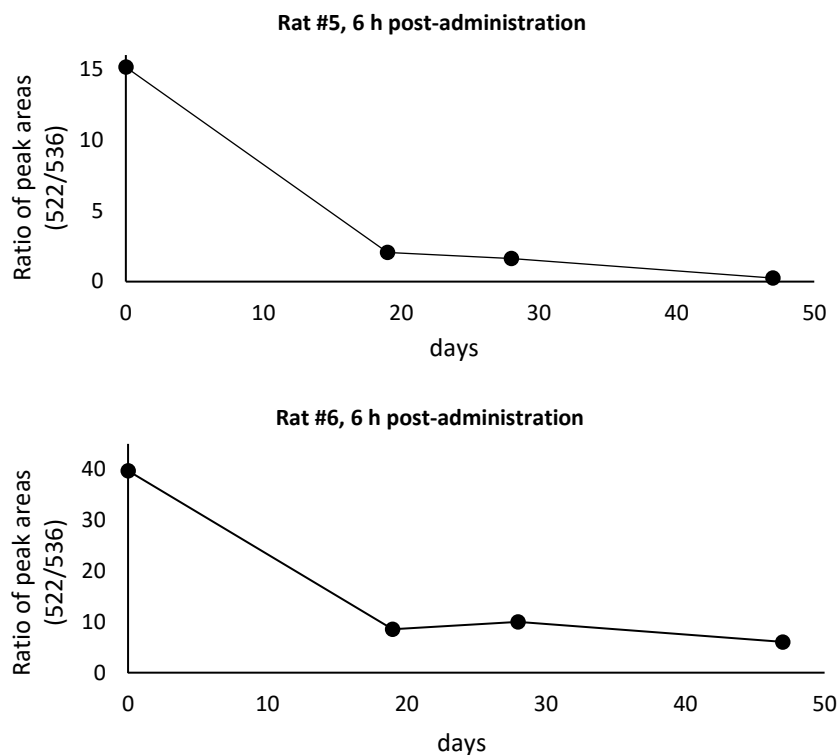


Figure 4.S9: Two rat urine samples (rat #5 and rat #6) containing capromorelin and its metabolites after 6 h post-administration were analyzed on four different days (full HRMS scan) within a period of almost 50 days and three freeze-thaw cycles of the samples. The ratios of the peak areas of capromorelin hydroxylamine M1i ($m/z = 522.27$ (1+)) and capromorelin nitro M1-5 ($m/z = 536.25$ (1+)) are shown. The samples were analyzed on a Q Exactive HF-X mass spectrometer.

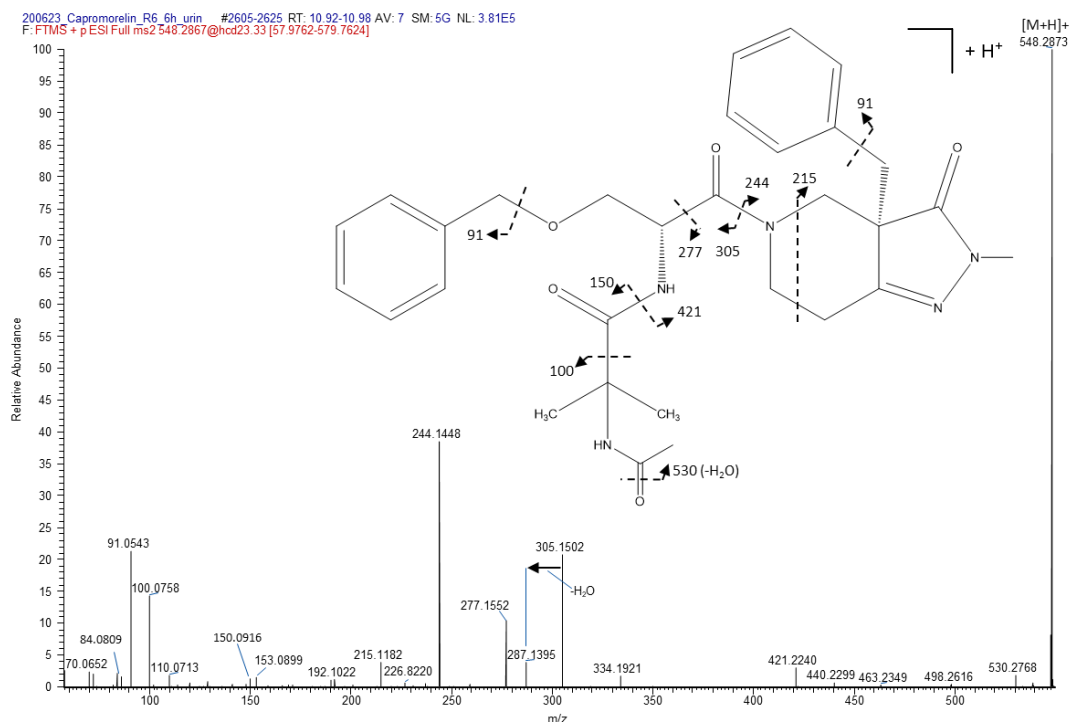


Figure 4.S10: MS² spectrum of the [M+H]⁺ ion of capromorelin *N*-acetylated M1-6 ($m/z = 548.2867$) from a rat urine sample collected 6 h post-administration, analyzed on an Orbitrap Exploris 480 mass spectrometer.

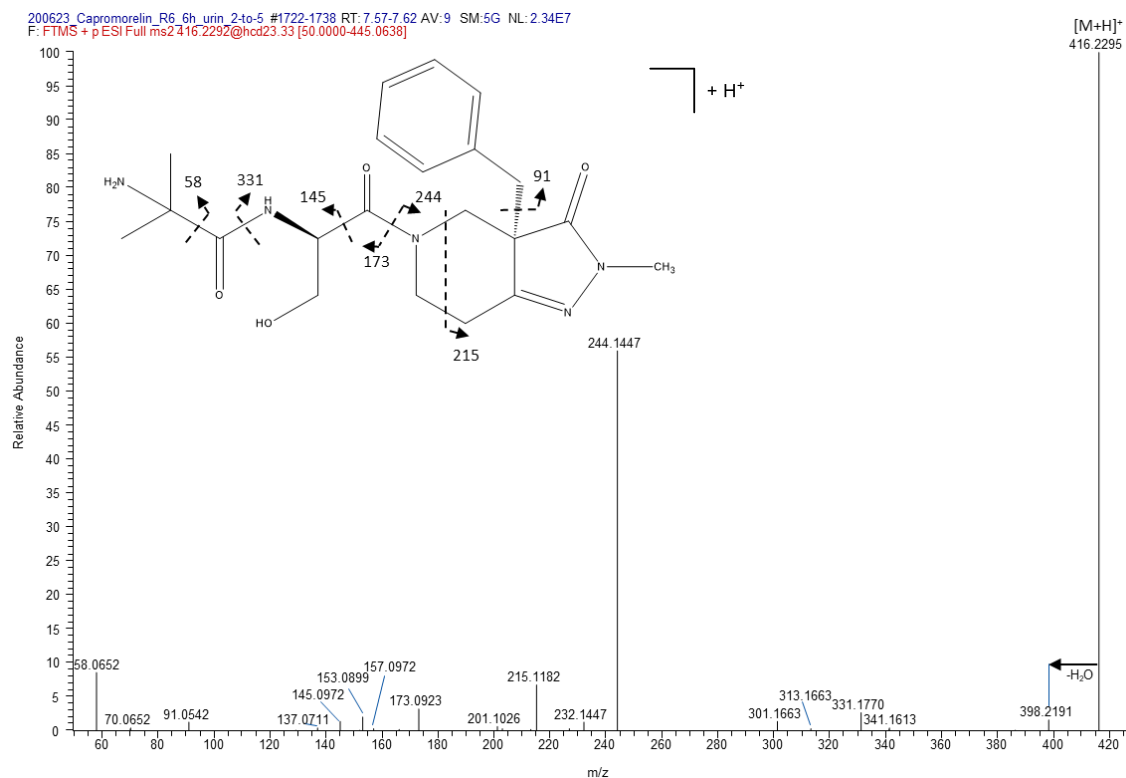


Figure 4.S11: MS² spectrum of the [M+H]⁺ ion of capromorelin M2-2 ($m/z = 416.2292$) from a rat urine sample collected 6 h post-administration, analyzed on an Orbitrap Exploris 480 mass spectrometer.

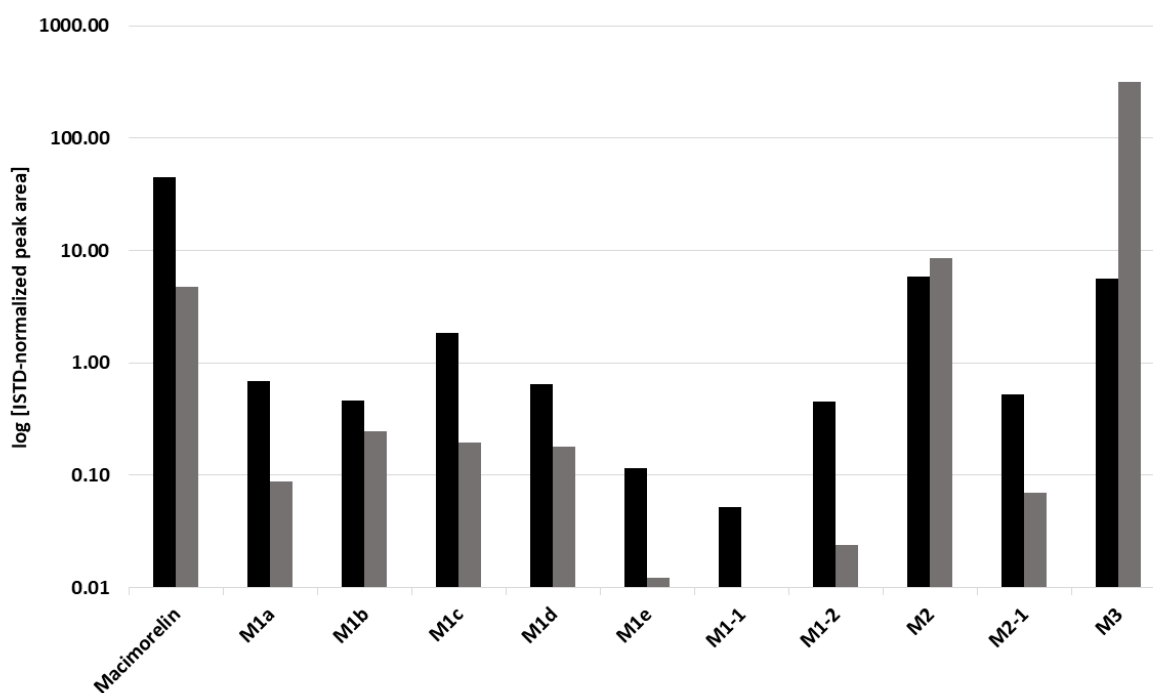


Figure 4.S12: Comparison of the absolute abundance of all metabolites of macimorelin detected in rat urine 6 h (black) and 12 h (grey) post-administration. The samples were analyzed on a Q Exactive HF-X mass spectrometer in full HRMS mode.

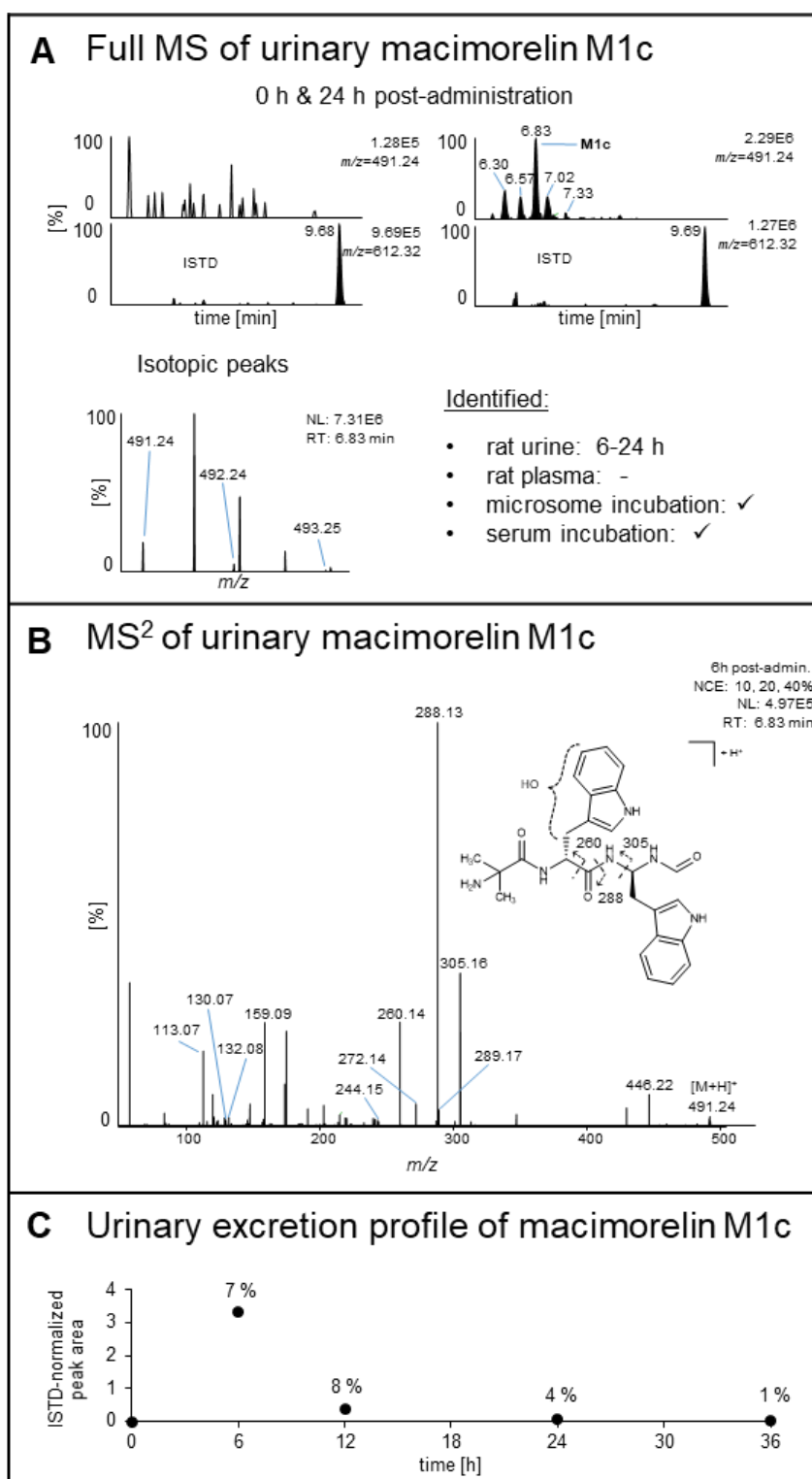


Figure 4.S13: A) The extracted ion chromatogram (mass tolerance ± 2 ppm) of the full HRMS of the urinary macimorelin mono-hydroxy M1c with the $[M+H]^+$ ion of $m/z = 491.2401$ at 0 h and 24 h post-administration. Below, there are the isotope signals of the mass spectrum at t_R 6.83 min from a sample collected 24 h post-administration, and the different matrices or *in vitro/in vivo* experiments in which this metabolite was detected with the corresponding detection windows for rat urine and rat EDTA-plasma. B) The MS² spectrum of the $[M+H]^+$ ion of the urinary macimorelin mono-hydroxy M1c of a sample collected 6 h post-administration. C) The urinary excretion profile of macimorelin mono-hydroxy M1c with the indicated percentages referring to the relative abundance of the ISTD-normalized peak area.

COMPREHENSIVE INSIGHTS INTO THE FORMATION OF METABOLITES OF THE GHRELIN MIMETICS CAPMORELIN, MACIMORELIN AND TABIMORELIN AS POTENTIAL MARKERS FOR DOPING CONTROL PURPOSES

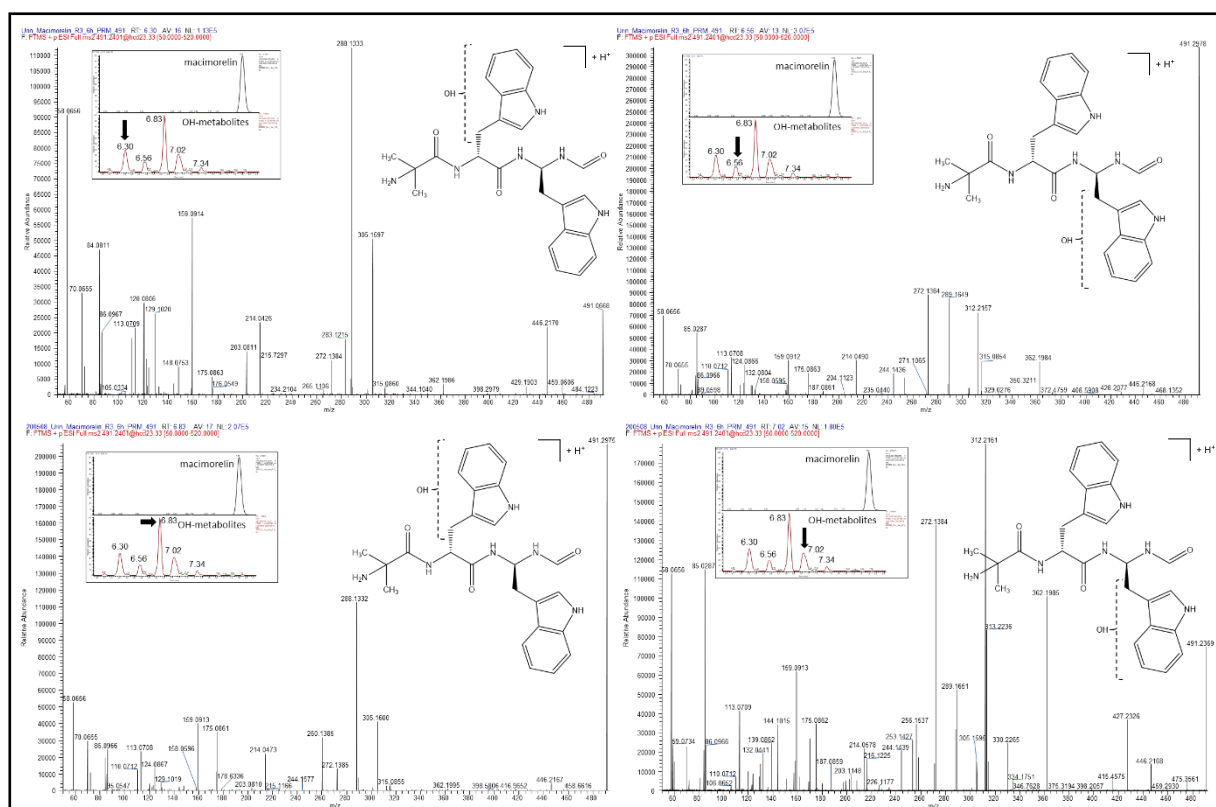


Figure 4.S14: MS² spectra of the [M+H]⁺ ion of the four macimorelin mono-hydroxy M1a, M1b, M1c, M1d (*m/z* = 491.2401) at *t_R* 6.30 min, 6.56 min, 6.83 min, and 7.02 min from a rat urine sample collected 6 h post-administration, analyzed on an Orbitrap Exploris 480 mass spectrometer. The small inset in each MS² spectrum on the upper left shows the extracted ion chromatogram and the black arrow indicates the respective *t_R* [min] of each metabolite. The dotted lines within the structural formula indicate the most likely site of modification.

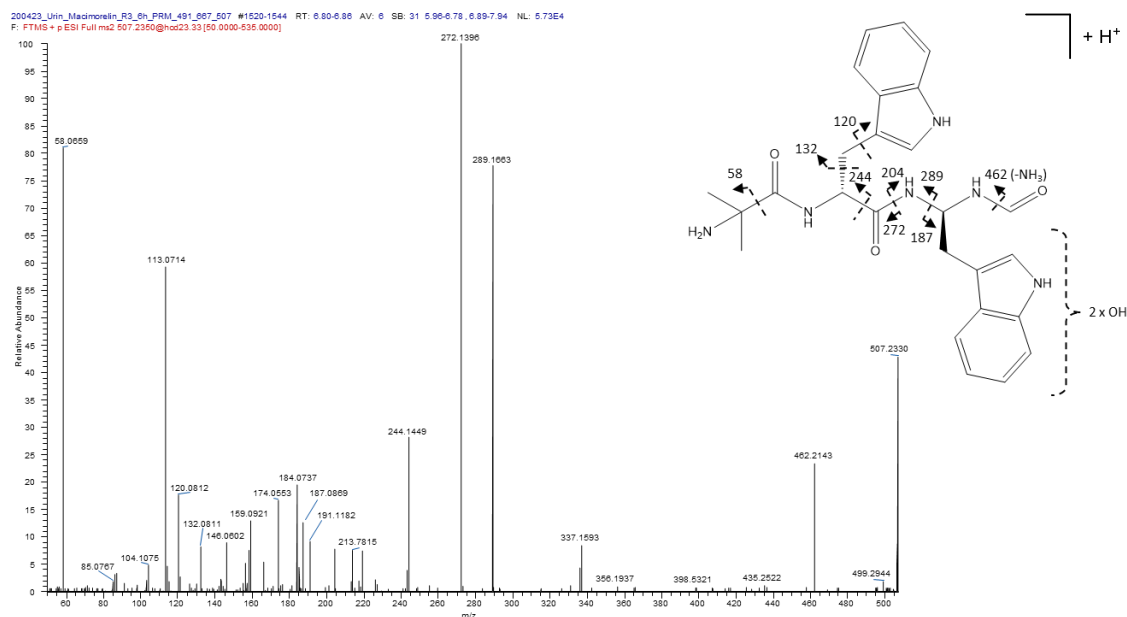


Figure 4.S15: MS² spectrum of the $[M+H]^+$ ion of macimorelin di-hydroxy M1-1b ($m/z = 507.2350$) from a rat urine sample collected 6 h post-administration, analyzed on an Orbitrap Exploris 480 mass spectrometer. The dotted lines within the structural formula indicate the most likely site of modification, however hydroxylation on the other tryptophan residue of this compound would also be possible.

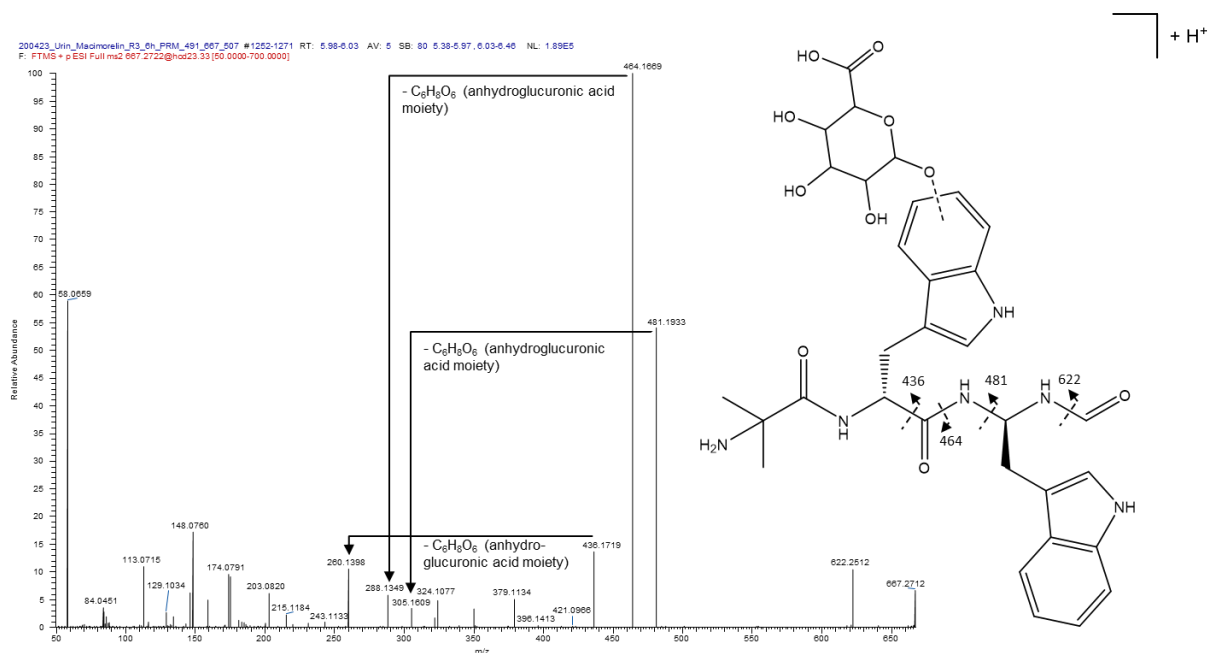


Figure 4.S16: MS² spectrum of the $[M+H]^+$ ion of macimorelin O-glucuronide M1-2 ($m/z = 667.2722$) from a rat urine sample collected 6 h post-administration, analyzed on an Orbitrap Exploris 480 mass spectrometer. The dotted line within the structural formula indicates the most likely site of modification.

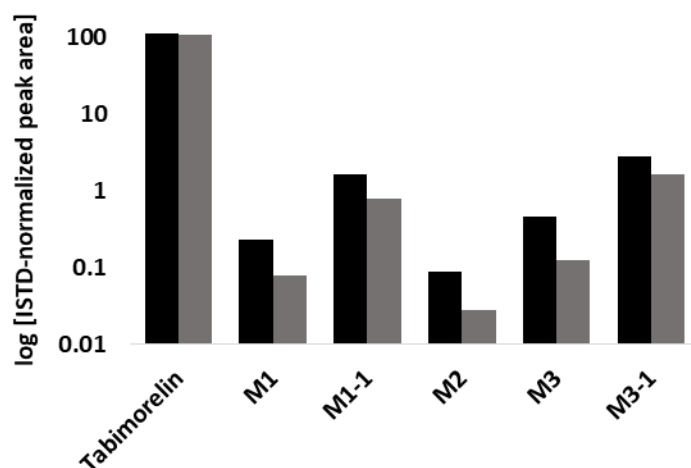


Figure 4.S17: Comparison of the absolute abundance of all metabolites of tabimorelin detected in rat urine 6 h (black) and 12 h (grey) post-administration. The samples were analyzed on a Q Exactive HF-X mass spectrometer in full HRMS mode.

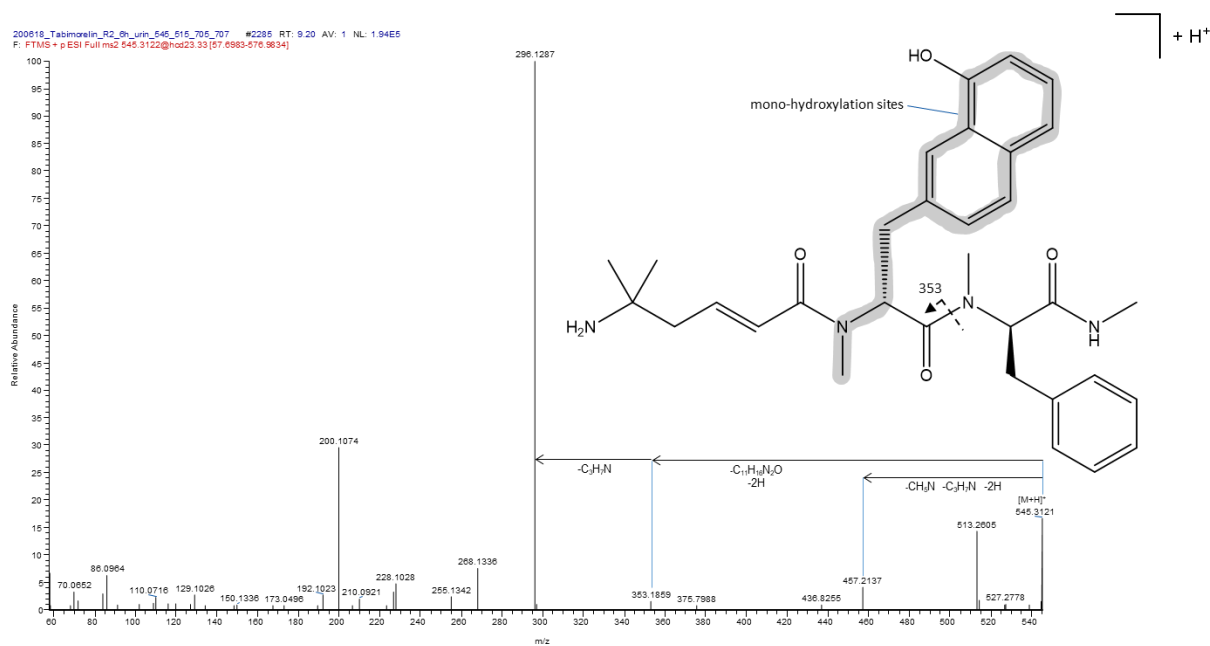


Figure 4.S18: MS² spectrum of the $[M+H]^+$ ion of tabimorelin mono-hydroxy M1 ($m/z = 545.3122$) from a rat urine sample collected 6 h post-administration, analyzed on an Orbitrap Exploris 480 mass spectrometer. The grey area within the structural formula indicates the most likely site of modification. An example of the possible structure is shown here.

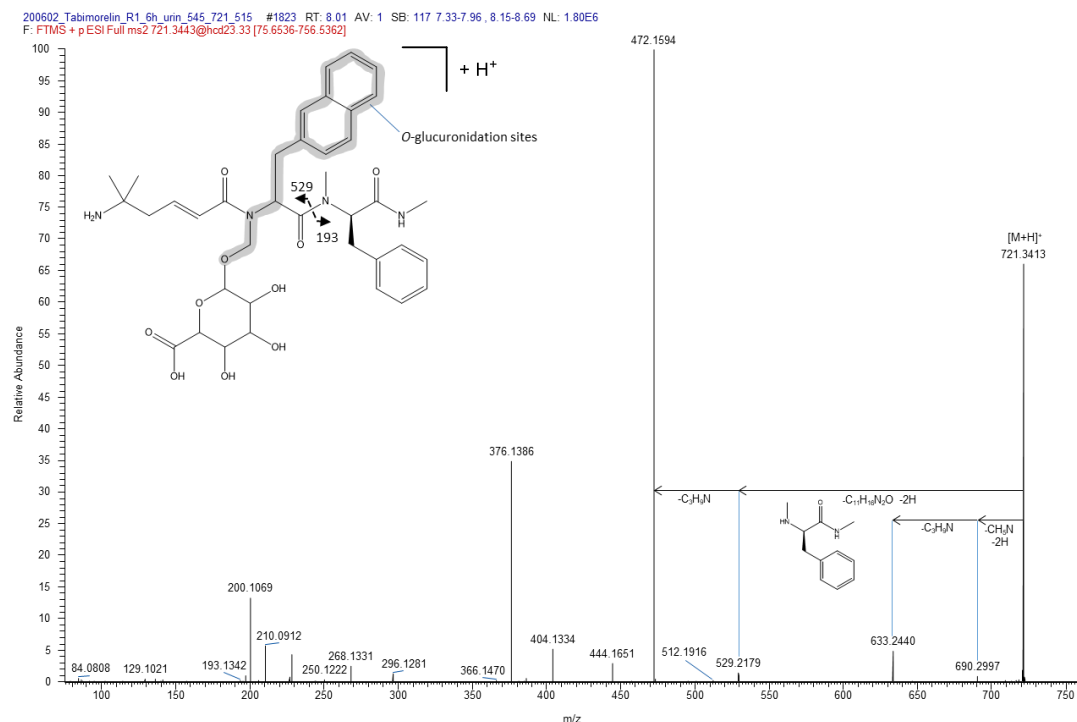


Figure 4.S19: MS² spectrum of the [M+H]⁺ ion of tabimorelin mono-O-glucuronide M1-1 ($m/z = 721.3443 (1+)$) from a rat urine sample collected 6 h post-administration, analyzed on an Orbitrap Exploris 480 mass spectrometer. The grey area within the structural formula indicates the most likely site of modification. An example of the possible structure is shown here.

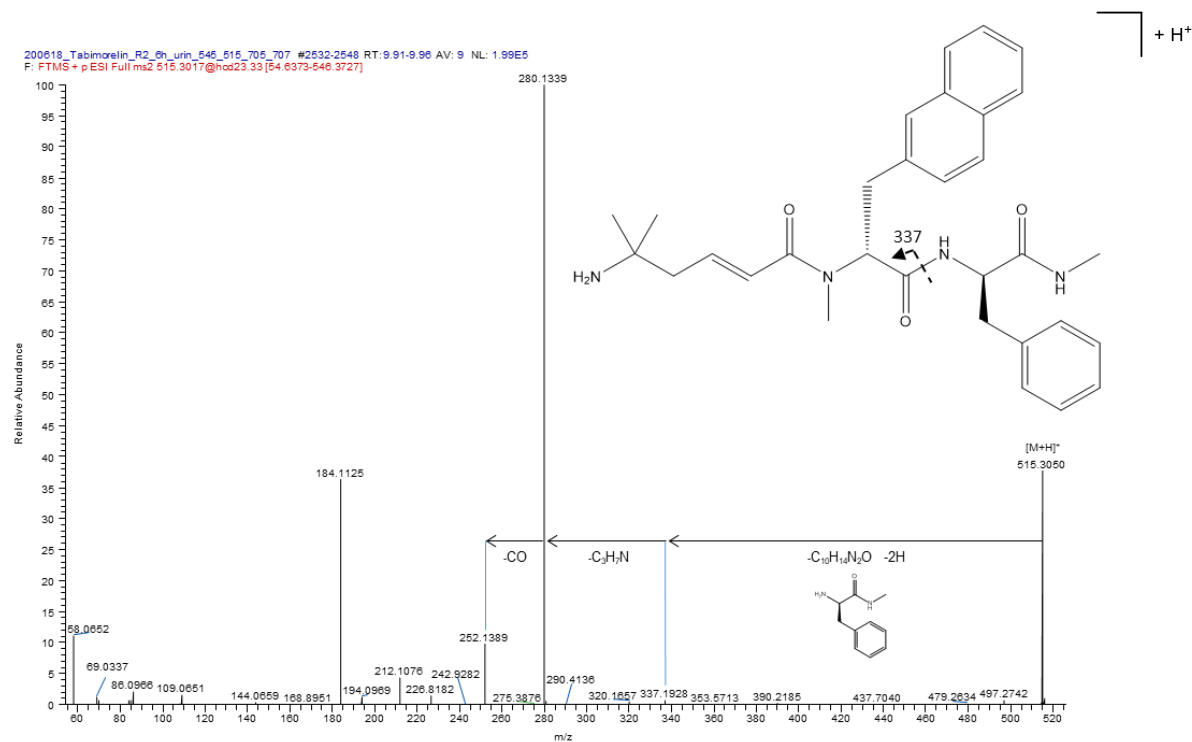


Figure 4.S20: MS² spectrum of the [M+H]⁺ ion of tabimorelin N-dealkylated M2 ($m/z = 515.3017$) from a rat urine sample collected 6 h post-administration, analyzed on an Orbitrap Exploris 480 mass spectrometer.

COMPREHENSIVE INSIGHTS INTO THE FORMATION OF METABOLITES OF THE GHRELIN MIMETICS CAPMORELIN, MACIMORELIN AND TABIMORELIN AS POTENTIAL MARKERS FOR DOPING CONTROL PURPOSES

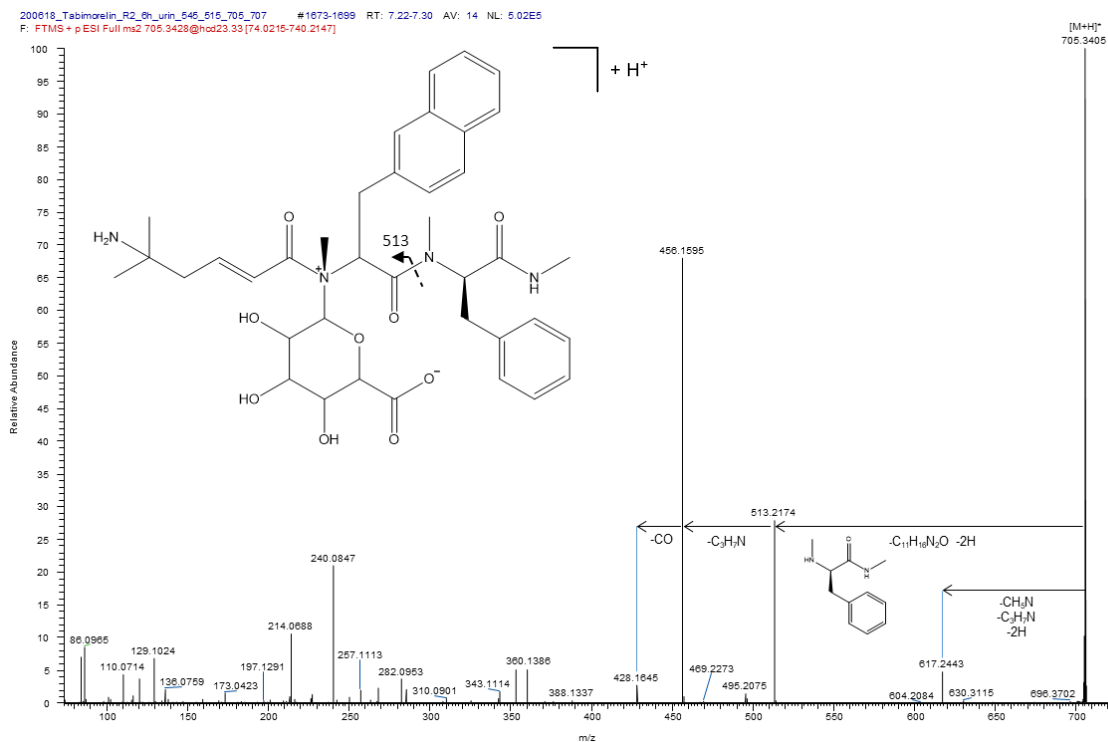


Figure 4.S21: MS² spectrum of the $[M+H]^+$ ion of tabimorelin N-glucuronide M3 ($m/z = 705.3428$) from a rat urine sample collected 6 h post-administration, analyzed on an Orbitrap Exploris 480 mass spectrometer.

4.5.4 Supplementary tables

Table 4.S1: Overview of all putative capromorelin metabolites detected from *in vitro* or *in vivo* experiments by full HRMS experiments on a Q Exactive HF-X mass spectrometer. The molecular formula, retention time (t_R), predominant charge state, three isotopic masses [m/z], reaction type, SMILES, and matrix in which the correspondent metabolite was detected were indicated.

Compound	Molecular formula	t_R [min]	Charge state	Isotope 1 Isotope 2 Isotope 3 [m/z]	Reaction type	SMILES	Compound detected in: 1) rat EDTA-plasma (<i>in vivo</i>) 2) rat urine (<i>in vivo</i>) 3) human microsomes (<i>in vitro</i>) 4) human serum (<i>in vitro</i>)
Capromorelin	C ₂₈ H ₃₅ N ₅ O ₄	9.05	1+	506.2762 507.2795 508.2829	-	CC(C)(C(=O)N[C@H](COCC1=CC=CC=C1)O)C(=O)N2CCC3=NN(C(=O)[C@@]3(C2)CC4=CC=C(C=C4)C)N	1) 3-36 h post-administration 2) 6-36 h post-administration 3) S, E+S 4) S, E+S
M1a, M1b, M1c, M1d, M1e, M1f, M1g, M1h, M1i, M1j or M5-1	C ₂₈ H ₃₅ N ₅ O ₅	6.67 7.53 7.82 7.96 8.14 8.39 8.92 9.02 10.03 11.00	1+	522.2711 523.2745 524.2778	(Mono)-hydroxylation, epoxidation (M1a-h, M1j or M5-1), or <i>N</i> -hydroxylation (M1i)	e.g. M1a (hydroxylation): CC(C)(C(=O)N[C@H](COCC1=CC=CC=C1)O)C(=O)N2CCC3=NN(C(=O)[C@@]3(C2)CC4=CC=C(C=C4)C)N or M5-1a (hydroxylation): C=CC1=NN(C)C(=O)C1(CNC(=O)C(COCC2=CC=CC=C2)NC(=O)C(C)N)CC3=C(C=CC=C3)O	1) M1a, M1b, M1c, M1j (3-12 h), M1i (3 h post-administration) 2) M1a, M1b, M1c, M1d, M1e, M1f, M1g, M1h, M1i (6-36 h post-administration) 3) M1b (E+S), M1c, M1d, M1e, M1f, M1g (S); M1c, M1d, M1e, M1f, M1g, M1h, M1i (S, E+S) 4) none or weak signal
M1-1a, M1-1b, M1-1c, M1-1d, M1-1e, M1-1f, M1-1g, M1-1h	C ₂₈ H ₃₅ N ₅ O ₆	6.21 6.79 7.09 7.27 7.42 8.26 8.49 8.65	1+	538.2660 539.2691 540.2717	(Di)-hydroxylation(s), and/or epoxidation(s)	e.g. M1a-1a: CC(C)(C(=O)N[C@H](COCC1=CC=CC=C1)O)C(=O)N2CCC3=NN(C(=O)[C@@]3(C2)C(C4=CC=C(C=C4)O)C)N	1) none 2) M1-1a, M1-1b, M1-1f, M1-1g, M1-1h (6-24 h post-administration), M1-1c, M1-1e (6-36 h post-administration) 3) M1-1b, M1-1d (E+S) 4) none or weak signal
M1b-2a, M1b-2b, M1b-2c, M1b-2d, M1b-2e	C ₃₄ H ₄₃ N ₅ O ₁₁	6.39 6.82 6.93 7.33 7.84	1+	698.3032 699.3063 700.3089	Aromatic <i>O</i> -glucuronidation	e.g. M1b-2a: CC(C)(C(=O)N[C@H](COCC1=CC=C(C=C1)OC2OC(C(O)C(O)C2O)C(=O)N3CCC4=N(C(=O)[C@@]4(C3)CC5=CC=CC=C5)C)N	1) none 2) M1b-2a, M1b-2b, M1b-2d, M1b-2e (6-24 h post-administration), M1b-2c (6-36 h post-administration) 3) none or weak signal 4) none or weak signal
M1-4a, M1-4b, M1-4c	C ₂₈ H ₃₃ N ₅ O ₅	8.29 9.00 11.92	1+	520.2554 521.2588 522.2622	Oxidation of nitrogen or oxidation of OH-group	e.g. M1-4a: CN4N=C2CCN(C(=O)[C@@]3(COCC1=CC=CC=C1)NC(=O)C(C)C)N(=O)C[C@@]2(Cc3ccccc3)C4=O	1) none or weak signals 2) M1-4a, M1-4b (6-12 h post-administration), M1-4c (6 h post-administration) 3) M1-4b (S, E+S) 4) M1-4b (S)
M1-5	C ₂₈ H ₃₃ N ₅ O ₆	11.88	1+	536.2504 537.2537 538.2571	Oxidation of nitrogen or oxidation of OH-group	CN4N=C2CCN(C(=O)[C@@]3(COCC1=CC=CC=C1)NC(=O)C(C)N(=O)O)C[C@@]2(Cc3ccccc3)C4=O	1) 3-6 h post-administration 2) 6-36 h post-administration 3) E+S 4) none or weak signals
M1-6a, M1-6b, M1-6c, M1-6d, M1-6e, M1-6f	C ₃₀ H ₃₇ N ₅ O ₅	8.75 9.58 9.79 10.05 10.25 10.70	1+	548.2867 549.2901 550.2935	<i>N</i> -acetylation	CC(=O)NC(C)C(=O)N[C@H](COCC1=CC=CC=C1)C(=O)N4CCC2=N(N(C)C(=O)[C@@]2(Cc3ccccc3)C4	1) none or weak signals 2) M1-6a (6-36 h post-administration), M1-6e, M1-6f (6-24 h post-administration) M1-6b, M1-6d (6-12 h post-administration) 3) none or weak signals 4) Metabolite 1-6c, e, f (E+S)
M1-1-1	C ₂₈ H ₃₅ N ₅ O ₇	7.65	1+	554.2609 555.2640 556.2666	(Triple)-hydroxylation(s) and / or epoxidation(s)	e.g. M1a-1a-1a: CC(C)(C(=O)N[C@H](COCC1=CC=C(C=C1)O)O)C(=O)N2CCC3=NN(C(=O)[C@@]3(C2)C(C4=CC=CC=C4)O)C)N	1) 3-36h post-administration 2) none or weak signals 3) none or weak signals 4) none or weak signals
M2 or M5-2	C ₂₁ H ₂₇ N ₅ O ₄	5.67 7.04 7.81	1+	414.2136 415.2169 416.2203	<i>O</i> -dealkylation of dialkylether (M2) or <i>N</i> -dealkylation followed by <i>O</i> -dealkylation of dialkylether (M5-2)	M2: CC(C)(C(=O)N[C@H](C(=O)C(=O)N1CCC2=NN(C(=O)[C@@]2(C1)CC3=CC=CC=C3)C)N Metabolite 5-2: C=CC1=NN(C)C(=O)C1(CNC(=O)C(C(=O)NC(=O)C(C)N)CC2=CC=CC=C2	1) none or weak signals 2) 3 signals for M2 and/or M5-2 (6-24 h post-administration) 3) none or weak signals 4) none or weak signals
M2-2	C ₂₁ H ₂₉ N ₅ O ₄	7.63	1+	416.2292 417.2326 418.2359	Reduction of aldehyde	CC(C)(C(=O)N[C@H](CO)C(=O)N1CCC2=NN(C(=O)[C@@]2(C1)CC3=CC=CC=C3)C)N	1) 3-12 h post-administration 2) 6-36 h post-administration 3) S, E+S 4) none or weak signals
M3	C ₂₄ H ₂₉ N ₄ O ₃	8.77	1+	421.2234 422.2265 423.2293	Hydrolysis	CN1N=C2C=CN(C(=O)C(=NH))COC=C3C=CC=CC3)CC2(C=C2CCCC2)C1=O	1) 3-36 h post-administration 2) 6-36 h post-administration 3) S, E+S 4) S, E+S
M3-1a, M3-1b, M3-1c	C ₂₄ H ₂₉ N ₄ O ₄	7.19 7.62 8.10	1+	437.2183 438.2217 439.2250	(Mono)-hydroxylation and/or epoxidation	e.g. M3-1b: CN1N=C2CCN(C(=O)C(N)COC3=CC=CC=C3)CC2(C(C4=C(C=CC=C4)O)C1=O	1) 3-12 h post-administration 2) one signal for 6-24 h post-administration and two signals for 6-36 h post-administration 3) none or weak signals 4) none or weak signals
M3-2	C ₁₇ H ₂₀ N ₄ O ₃	6.02	1+	329.1608 330.1642 331.1675	<i>O</i> -dealkylation of dialkylether	CN1N=C2CCN(C(=O)C(N)C(=O)CC2(C(C3=CC=CC=C3)C1=O	1) none or weak signals 2) 6-24 h post-administration 3) none or weak signals 4) none or weak signals

COMPREHENSIVE INSIGHTS INTO THE FORMATION OF METABOLITES OF THE GHRELIN MIMETICS CAPMORELIN, MACIMORELIN AND TABIMORELIN AS POTENTIAL MARKERS FOR DOPING CONTROL PURPOSES

M4	C ₂₇ H ₃₃ N ₅ O ₄	8.37	1+	492.2605 493.2639 494.2672	<i>N</i> -dealkylation	CC(C)(N)C(=O)NC(COCc1ccccc1)C(=O)N4CCC2=NNC(=O)C2(Cc3ccccc3)C4	1) 3-12 h post-administration 2) 3-36 h post-administration 3) S, E+S 4) S, E+S
M4-1a, M4-1b	C ₂₇ H ₃₃ N ₅ O ₅	6.66 7.10	1+	508.2554 509.2588 510.2622	(Mono)-hydroxylation and / or epoxidation	CC(C)(N)C(=O)NC(COC(C1=CC=CC=C1)O)C(=O)N2CCC3=NNC(=O)C3(CC4=CC=CC=C4)C2	1) none or weak signals 2) 6-36 h post-administration 3) none or weak signals 4) none or weak signals
M5	C ₂₈ H ₃₅ N ₅ O ₄	9.70	1+	506.2762 507.2795 508.2829	<i>N</i> -dealkylation	C=CC1=NN(C)C(=O)C1(CNC(=O)C(COCc2ccccc2)NC(=O)C(C)(C)N)Cc3ccccc3	1) none or weak signals 2) 6-36 h post-administration 3) S, E+S 4) S, E+S
M6	C ₂₈ H ₃₂ N ₄ O ₄	11.79	1+	489.2496 490.2530 491.2563	<i>N</i> -dealkylation	C=C(C)C(=O)NC(COCc1ccccc1)C(=O)N4CCC2=NN(C)C(=O)C2(Cc3ccccc3)C4	1) none or weak signals 2) 6-12 h post-administration 3) none or weak signals 4) none or weak signals
M7	C ₂₇ H ₃₁ N ₅ O ₄	11.92	1+	490.2585 491.2620 492.2650	<i>N</i> -dealkylation	CC(=N)C(=O)NC(COCc1ccccc1)C(=O)N4CCC2=NN(C)C(=O)C2(Cc3ccccc3)C4	1) none or weak signals 2) 6-36 h post-administration 3) E+S 4) none or weak signals

Table 4.S2: Overview of all putative macimorelin metabolites detected from *in vitro* or *in vivo* experiments by full HRMS experiments on a Q Exactive HF-X. The molecular formula, retention time (t_R), predominant charge state, three isotopic masses [m/z], reaction type, SMILES, and matrix in which the correspondent metabolite was detected were indicated.

Compound	Molecular formula	t_R [min]	Charge state	Isotope 1 Isotope 2 Isotope 3 [m/z]	Reaction type	SMILES	Compound detected in: 1) rat EDTA-plasma (<i>in vivo</i>) 2) rat urine (<i>in vivo</i>) 3) human microsomes (<i>in vitro</i>) 4) human serum (<i>in vitro</i>)
Macimorelin	C ₂₆ H ₃₀ N ₆ O ₃	7.92	1+	475.2452 476.2486 477.2519	-	CC(C)(C(=O)N[C@H](CC1=CC=C2=CC=CC=C2)C(=O)N[C@H](CC3=CNC4=CC=CC=C43)NC=O)N	1) 3 h post-administration (weak signal) 2) 6-36 h post-administration 3) S, E+S 4) S, E+S
M1a, M1b, M1c, M1d, M1e	C ₂₆ H ₃₀ N ₆ O ₄	6.30 6.57 6.83 7.02 7.33	1+	491.2401 492.2435 493.2468	(Mono)-hydroxylation or epoxidation	e.g. M1a: CC(N)(CO)C(=O)NC(Cc1c[nH]c2ccccc12)C(=O)NC(Cc3c[nH]c4ccccc34)NC=O	1) no signal 2) M1b (6-24 h post-administration), M1a, M1c, M1d, M1e (6-12 h post-administration) 3) M1b, M1c, M1d, M1e (S, E+S) 4) M1b, M1c, M1d, M1e (S, E+S)
M1-1a, M1-1b, M1-1c	C ₂₆ H ₃₀ N ₆ O ₅	6.29 6.96 7.26	1+	507.2350 508.2380 509.2406	(Di)-hydroxylation and/or epoxidation	e.g. M1a-1a: CC(C)(C(=O)N[C@H](CC1=CC=C2=CC=CC=C2)C(=O)N[C@H](C(C3=CNC4=CC=CC=C43)O)NC=O)N	1) no signal 2) M1-1b (6 h post-administration) 3) M1-1b, M1-1c (S, E+S) 4) M1-1a (E+S), M1-1b (S, E+S)
M1-2	C ₃₂ H ₃₈ N ₆ O ₁₀	6.12	1+	667.2722 668.2752 669.2778	O-glucuronidation	CC(C)(C(=O)N[C@H](CC1=CC=C2=CC=CC=C2)C(=O)N[C@H](C(C3=CNC4=CC=CC=C43)OC5OC(C(=O)O)C(C(C5O)O)NC=O)N	1) no signal 2) 6 h post-administration 3) no signal 4) no signal
M2	C ₁₅ H ₂₀ N ₄ O ₂	4.62	1+	289.1659 290.1693 291.1726	<i>N</i> -dealkylation	CC(C)(N)C(=O)NC(Cc1c[nH]c2ccccc12)C(N)=O	1) no signal 2) 6-36 h post-administration 3) S, E+S 4) S, E+S
M2-1	C ₁₅ H ₂₀ N ₄ O ₃	6.83	1+	305.1608 306.1642 307.1675	(Mono)-hydroxylation and/or epoxidation	e.g.: CC(C)(N)C(=O)NC(C(C1=CNC2=CC=CC=C12)O)C(N)=O	1) no signal 2) 6-12 h post-administration 3) no signal 4) no signal
M3	C ₁₁ H ₁₀ N ₂ O	4.17	1+	187.0866 188.0899 189.0933	<i>N</i> -dealkylation	OC/N=C=C=C1\1C=NC2C=CC=CC12	1) no signal 2) 6-36 h post-administration 3) S+E 4) no signal

Table 4.S3: Overview of all putative tabimorelin metabolites detected from *in vitro* or *in vivo* experiments by full HRMS experiments on a Q Exactive HF-X. The molecular formula, retention time (t_R), predominant charge state, three isotopic masses [m/z], reaction type, SMILES, and matrix in which the correspondent metabolite was detected were indicated.

Compound	Molecular formula	t_R [min]	Charge state	Isotope 1 Isotope 2 Isotope 3 [m/z]	Reaction type	SMILES	Compound detected in: 1) rat EDTA-plasma (<i>in vivo</i>) 2) rat urine (<i>in vivo</i>) 3) human microsomes (<i>in vitro</i>) 4) human serum (<i>in vitro</i>)
Tabimorelin	C ₃₂ H ₄₀ N ₄ O ₃	10.24	1+	529.3173 530.3207 531.3240	-	CC(C)(C/C=C/C(=O)N(C)[C@H](CC1=CC2=CC=CC=C2C=C1)C(=O)N(C)[C@H](CC3=CC=CC=C3)C(=O)N)N	1) 3-12 h post-administration (weak signal at 36 h post-administration) 2) 6-36 h post-administration 3) S, E+S 4) S, E+S
M1a, M1b, M1c	C ₃₂ H ₄₀ N ₄ O ₄	9.04 9.59 10.68	1+	545.3122 546.3156 547.3189	(Mono)-hydroxylation or epoxidation	e.g. M1a: CC(C)(C/C=C/C(=O)N(C)[C@H](CC1=CC2=CC=CC=C2C=C1)C(=O)N)N	1) no signal 2) M1a: 6-36 h post-administration

COMPREHENSIVE INSIGHTS INTO THE FORMATION OF METABOLITES OF THE GHRELIN MIMETICS
CAPROMORELIN, MACIMORELIN AND TABIMORELIN AS POTENTIAL MARKERS FOR DOPING CONTROL PURPOSES

						=O)N(C)[C@H](CC3=C(C=CC=C3)O)C(=O)NC)N	3) M1a, M1b, M1c: E+S 4) no signal
M1-1	C ₃₈ H ₄₈ N ₄ O ₁₀	7.91	1+	721.3443 722.3477 723.3503	O-glucuronidation	CC(C)(C/C=C/C(=O)N(C)[C@H](CC1=CC2=CC=CC=C2C=C1)C(=O)N(C)[C@H](CC3=C(C=CC=C3)OC4OC(C(O)C(O)C4O)C(O)=O)C(=O)NC)N	1) no signal 2) 6-36 h post-administration 3) no signal 4) no signal
M2a, M2b	C ₃₁ H ₃₈ N ₄ O ₃	9.77 10.48	1+	515.3017 516.3050 517.3084	N-dealkylation	CC(C)(C/C=C/C(=O)N(C)[C@H](CC1=CC2=CC=CC=C2C=C1)C(=O)N(C)[C@H](CC3=CC=CC=C3)C(=O)NC)N	1) no signal 2) M2a: 6-12 h post-administration (24-36 h post-administration, weak signal) 3) M2a (E+S), M2b (S, E+S) 4) M2b (S, E+S)
M3	C ₃₈ H ₄₈ N ₄ O ₉	7.11	2+	705.3428 706.3462 707.3490	N-glucuronidation	CNC(=O)C(Cc1cccc1)N(C)C(=O)C(Cc3ccc2ccccc2c3)N(C)C(=O)/C=C/CC(C)(C)NC4OC(O)C(O)C(O)C4C(=O)O	1) no signal 2) 6-12 h post-administration (24 h post-administration, weak signal) 3) no signal 4) no signal
M3-1	C ₃₈ H ₅₀ N ₄ O ₉	8.61	1+	707.3579 708.3612 709.3647	N-glucuronidation + hydrogenation of C=C	CNC(=O)C(CC1=CC=CC=C1)N(C)C(=O)C(CC2=CC=C3C=CC=CC3=C2)N(C)C(=O)CCCC(C)(C)NC4OC(O)C(O)C4C(=O)O	1) no signal 2) 6-24 h post-administration 3) no signal 4) no signal

4.6 Acknowledgements

The study was carried out with support of the Manfred Donike Institute for Doping Analysis (Cologne, Germany), the World Anti-Doping Agency (Montreal, Canada, 18A03MT), and the Federal Ministry of the Interior, Building and Community of the Federal Republic of Germany (Bonn, Germany).

4.7 References

1. WADA. *The World Anti-Doping Code. International Standard. Prohibited List January 2020* [07/02/2020]; Available from: https://www.wada-ama.org/sites/default/files/wada_2020_english_prohibited_list_0.pdf.
2. Moulin, A., et al., *Recent developments in ghrelin receptor ligands*. ChemMedChem, 2007. 2(9): p. 1242-59.
3. Cordido, F., et al., *Ghrelin and growth hormone secretagogues, physiological and pharmacological aspect*. Curr Drug Discov Technol, 2009. 6(1): p. 34-42.
4. WADA. *Anti-Doping Testing Figures*. 2019 [12/30/2020]; Available from: <https://www.wada-ama.org/en/resources/laboratories/anti-doping-testing-figures-report>.
5. Svensson, J., et al., *Oral administration of the growth hormone secretagogue NN703 in adult patients with growth hormone deficiency*. Clin Endocrinol (Oxf), 2003. 58(5): p. 572-80.
6. Zdravkovic, M., et al., *A clinical study investigating the pharmacokinetic interaction between NN703 (tabimorelin), a potential inhibitor of CYP3A4 activity, and midazolam, a CYP3A4 substrate*. Eur J Clin Pharmacol, 2003. 58(10): p. 683-8.
7. White, H.K., et al., *Effects of an oral growth hormone secretagogue in older adults*. J Clin Endocrinol Metab, 2009. 94(4): p. 1198-206.
8. Rhodes, L., et al., *Capromorelin: a ghrelin receptor agonist and novel therapy for stimulation of appetite in dogs*. Vet Med Sci, 2018. 4(1): p. 3-16.
9. Hansen, B.S., et al., *Pharmacological characterisation of a new oral GH secretagogue, NN703*. Eur J Endocrinol, 1999. 141(2): p. 180-9.
10. Ellis, A.G., et al., *Pharmacokinetics of the ghrelin agonist capromorelin in a single ascending dose Phase-I safety trial in spinal cord-injured and able-bodied volunteers*. Spinal Cord, 2015. 53(2): p. 103-8.
11. Piccoli, F., et al., *Pharmacokinetics and pharmacodynamic effects of an oral ghrelin agonist in healthy subjects*. J Clin Endocrinol Metab, 2007. 92(5): p. 1814-20.
12. Goergens, C., et al., *Recent improvements in sports drug testing concerning the initial testing for peptidic drugs (< 2 kDa) - sample preparation, mass spectrometric detection, and data review*. Drug Test Anal, 2018.
13. Judak, P., et al., *DMSO Assisted Electrospray Ionization for the Detection of Small Peptide Hormones in Urine by Dilute-and-Shoot-Liquid-Chromatography-High Resolution Mass Spectrometry*. J Am Soc Mass Spectrom, 2017. 28(8): p. 1657-1665.

14. Thomas, A., et al., *Simplifying and expanding the screening for peptides <2 kDa by direct urine injection, liquid chromatography, and ion mobility mass spectrometry*. J Sep Sci, 2016. 39(2): p. 333-41.
15. Kwok, K.Y., et al., *Detection of bioactive peptides including gonadotrophin-releasing factors (GnRHs) in horse urine using ultra-high performance liquid chromatography-high resolution mass spectrometry (UHPLC/HRMS)*. Drug Test Anal, 2020.
16. Pugliese, J., et al., *Dispersive SPE, an alternative to traditional SPE for extraction of 43 doping peptides from equine urine prior to LC-MS screening*. Forensic Toxicology, 2019. 38(2): p. 12.
17. Guan, F., et al., *A comprehensive approach to detecting multitudinous bioactive peptides in equine plasma and urine using HILIC coupled to high resolution mass spectrometry*. Drug Test Anal, 2019.
18. Kim, Y., et al., *Development of a multi-functional concurrent assay using weak cation-exchange solid-phase extraction (WCX-SPE) and reconstitution with a diluted sample aliquot for anti-doping analysis*. Rapid Commun Mass Spectrom, 2018. 32(11): p. 897-905.
19. Lange, T., et al., *Fully automated dried blood spot sample preparation enables the detection of lower molecular mass peptide and non-peptide doping agents by means of LC-HRMS*. Anal Bioanal Chem, 2020.
20. Esposito, S., et al., *In vitro models for metabolic studies of small peptide hormones in sport drug testing*. J Pept Sci, 2015. 21(1): p. 1-9.
21. Thomas, A., et al., *Metabolism of growth hormone releasing peptides*. Anal Chem, 2012. 84(23): p. 10252-9.
22. Thomas, A., et al., *Characterization of in vitro generated metabolites of selected peptides <2 kDa prohibited in sports*. Drug Test Anal, 2017. 9(11-12): p. 1799-1803.
23. Okano, M., et al., *Determination of growth hormone secretagogue pralmorelin (GHRP-2) and its metabolite in human urine by liquid chromatography/electrospray ionization tandem mass spectrometry*. Rapid Commun Mass Spectrom, 2010. 24(14): p. 2046-56.
24. Thomas, A., et al., *Determination of growth hormone releasing peptides (GHRP) and their major metabolites in human urine for doping controls by means of liquid chromatography mass spectrometry*. Anal Bioanal Chem, 2011. 401(2): p. 507-16.
25. Timms, M., et al., *A high-throughput LC-MS/MS screen for GHRP in equine and human urine, featuring peptide derivatization for improved chromatography*. Drug Test Anal, 2014. 6(10): p. 985-95.
26. Thomas, A., et al., *Metabolism of growth hormone releasing peptides*. Anal Chem, 2012. 84(23): p. 10252-9.

27. Semenistaya, E., et al., *Determination of growth hormone releasing peptides metabolites in human urine after nasal administration of GHRP-1, GHRP-2, GHRP-6, Hexarelin, and Ipamorelin*. Drug Test Anal, 2015. 7(10): p. 919-25.
28. Zvereva, I., et al., *Comparison of various in vitro model systems of the metabolism of synthetic doping peptides: Proteolytic enzymes, human blood serum, liver and kidney microsomes and liver S9 fraction*. J Proteomics, 2016. 149: p. 85-97.
29. Sobolevsky, T. and B. Ahrens, *High-throughput liquid chromatography tandem mass spectrometry assay as initial testing procedure for analysis of total urinary fraction*. Drug Test Anal, 2020.
30. Zaretzki, J., M. Matlock, and S.J. Swamidass, *XenoSite: accurately predicting CYP-mediated sites of metabolism with neural networks*. J Chem Inf Model, 2013. 53(12): p. 3373-83.
31. Djoumbou-Feunang, Y., et al., *BioTransformer: a comprehensive computational tool for small molecule metabolism prediction and metabolite identification*. J Cheminform, 2019. 11(1): p. 2.
32. Djoumbou-Feunang, Y., et al., *CFM-ID 3.0: Significantly Improved ESI-MS/MS Prediction and Compound Identification*. Metabolites, 2019. 9(4).
33. Knights, K.M., et al., *In Vitro Drug Metabolism Using Liver Microsomes*. Curr Protoc Pharmacol, 2016. 74: p. 7 8 1-7 8 24.
34. WADA. *The World Anti-Doping Code. International Standard for Laboratories January. 2019 25/03/2020*]; Available from: https://www.wada-ama.org/sites/default/files/resources/files/isl_nov2019.pdf.
35. WADA. *Minimum criteria for chromatographic-mass spectrometric confirmation of the identity of analytes for doping control purposes. 2015 21/03/2019*]; Available from: <https://www.wada-ama.org/en/resources/science-medicine/td2015idcr>.
36. Qi, X., et al., *Simultaneous characterization of pyrrolizidine alkaloids and N-oxides in Gynura segetum by liquid chromatography/ion trap mass spectrometry*. Rapid Commun Mass Spectrom, 2009. 23(2): p. 291-302.
37. Miller, R.R., G.A. Doss, and R.A. Stearns, *Identification of a hydroxylamine glucuronide metabolite of an oral hypoglycemic agent*. Drug Metab Dispos, 2004. 32(2): p. 178-85.
38. Fitch, W.L., et al., *Application of polarity switching in the identification of the metabolites of RO9237*. Rapid Commun Mass Spectrom, 2007. 21(10): p. 1661-8.
39. Ramanathan, R., et al., *Liquid chromatography/mass spectrometry methods for distinguishing N-oxides from hydroxylated compounds*. Anal Chem, 2000. 72(6): p. 1352-9.

40. Cribb, A.E. and S.P. Spielberg, *Sulfamethoxazole is metabolized to the hydroxylamine in humans*. Clin Pharmacol Ther, 1992. 51(5): p. 522-6.
41. Duncan, J.D. and A.K. Cho, *N-oxidation of phentermine to N-hydroxyphentermine by a reconstituted cytochrome P-450 oxidase system from rabbit liver*. Mol Pharmacol, 1982. 22(2): p. 235-8.
42. Hlavica, P. and L.A. Damani, *N-Oxidation of drugs: Biochemistry, pharmacology, toxicology*. 1991, Midsomer Norton, Bath, Avon: Springer Science+Business Media Dordrecht (p. 207-215).
43. Naisbitt, D.J., et al., *Covalent binding of the nitroso metabolite of sulfamethoxazole leads to toxicity and major histocompatibility complex-restricted antigen presentation*. Mol Pharmacol, 2002. 62(3): p. 628-37.
44. Iley, J. and R. Tolando, *The oxidative dealkylation of tertiary amides: mechanistic aspects*. Journal of the Chemical Society, Perkin Transactions 2, 2000(11): p. 2328-2336.
45. Kaji, H. and T. Kume, *Characterization of afloqualone N-glucuronidation: species differences and identification of human UDP-glucuronosyltransferase isoform(s)*. Drug Metab Dispos, 2005. 33(1): p. 60-7.
46. Miles, K.K., et al., *An investigation of human and rat liver microsomal mycophenolic acid glucuronidation: evidence for a principal role of UGT1A enzymes and species differences in UGT1A specificity*. Drug Metab Dispos, 2005. 33(10): p. 1513-20.
47. Beaumont, K., *Why Do We Need In Vivo Models in Drug Metabolism?*, in *Encyclopedia of Drug Metabolism and Interactions*, A.V. Lyubimov, Editor. 2012, John Wiley & Sons, Inc. p. 1-23.

5 Zusammenfassung

Im Rahmen dieser Doktorarbeit wurden Nachweismethoden von dopingrelevanten Substanzen peptidischer und pseudopeptidischer Natur aus Urin, Blut und *Dried Blood Spots* (DBS) entwickelt. Zusätzlich wurden zur Untersuchung der Biotransformation von drei neuen Ghrelin Mimetika umfassende Metabolismusstudien durchgeführt.

Die Ergebnisse wurden in drei wissenschaftlichen Artikeln in internationalen Fachzeitschriften nach Peer-Review-Verfahren veröffentlicht. Diese beschreiben die Entwicklung Flüssigkeitschromatographie-Massenspektrometrie-basierter Nachweisverfahren sowie die Ergebnisse von *in vitro/in vivo* Metabolismusstudien. Bei den Zielanalyten dieser Nachweisverfahren, welche aufgrund ihrer potentiellen leistungssteigernden Wirkungen missbräuchlich von Athleten eingesetzt werden könnten und daher auf der Verbotliste der Welt-Anti-Dopingagentur (WADA) vorzufinden sind, handelte es sich um Proteine oder Peptide bzw. Pseudopeptide. Im Einzelnen waren dies erstens Sotatercept und Luspatercept, zwei Fc-Fusionsproteine, und Bimagrumab, ein therapeutischer Antikörper, zweitens eine umfassende Auswahl von 46 Peptiden und Pseudopeptiden mit einem Molekulargewicht <2 kDa, darunter Wachstumshormon-freisetzenden Faktoren, luteinisierende Hormon-freisetzende Hormone, antidiuretische Hormone und andere verbotene Substanzen einschließlich repräsentativer Metaboliten, und drittens drei Ghrelin Mimetika, namentlich Capromorelin, Macimorelin und Tabimorelin. Für die Entwicklung dieser Methoden wurden sowohl die herkömmlichen biologischen Matrices Urin und Blut als auch die neuartige, alternative Matrix DBS berücksichtigt. Der Nachweis pharmakologisch relevanter Wirkstoffkonzentrationen aus geringen Volumina getrockneter Blutstopfen konnte durch die Verwendung effizienter Probenvorbereitungsstrategien und dem Einsatz modernster analytischer Instrumente erreicht werden. In den vorgestellten Studien kamen sowohl manuelle als auch automatisierte Probenvorbereitungen zum Einsatz. Die Extraktion und Reinigung der Analyten aus DBS erfolgte in wässrigem Puffer mittels Ultraschallbad und anschließender Immunoaffinitätsreinigung oder mittels robotergestützter, wässriger Durchflusdesorption mit anschließender Festphasenextraktion. Für die Ghrelin Mimetika wurde zur Vorbereitung der Urinproben eine manuelle Festphasenextraktion oder ein Ansatz über Direktinjektion („*dilute-and-inject*“) durchgeführt. Die Aufreinigung der Analyten aus Blutplasma erfolgte durch Proteinfällung mit Methanol. Die analytischen

Nachweise wurden als Screeningverfahren und/oder als Bestätigungsmethoden konzipiert, optimiert und nach den derzeit gültigen Richtlinien der WADA vollständig validiert. Abschließend konnten Machbarkeitsnachweise für authentische humane Proben erbracht werden, sofern die Anwendungen der Substanzen ethisch vertretbar waren.

Diese Doktorarbeit liefert einen wichtigen Beitrag zur Realisierung der Nachweisbarkeit dopingrelevanter (Pseudo-)Peptide und Proteine aus DBS, damit sich diese alternative Matrix komplementär zu den herkömmlichen Matrices Blut und Urin in den zukünftigen Doping-Kontroll-Verfahren etablieren kann. Mit Hinblick auf die Olympischen und Paralympischen Winterspiele in Beijing, China (2022), bei welchen DBS erstmals als offizielle Matrix zum Einsatz kommen sollen, konnte das analytische Spektrum der DBS-Analytik um diese Substanzen erfolgreich erweitert werden. Dabei erwiesen sich DBS als geeignete Matrix für Multikomponenten-Methoden, wodurch auch eine retrospektive Datenanalyse ermöglicht wird. Die neuen Methoden für den Nachweis der Ghrelin Mimetika aus humanem Blut und Urin erweitern fortan die multianalytischen Routine-Screenings der Wachstumshormon-freisetzenden Faktoren. Zusätzlich wurden wichtige Erkenntnisse über die Metaboliten dieser pseudopeptidischen kurzlebigen Substanzen gewonnen, welche in Zukunft die Spezifität und Sensitivität von analytischen Nachweisverfahren zur Dopingkontrolle humaner Proben weiter verbessern könnten.

6 Abstract

In the context of this thesis, detection methods for banned substances of peptidic and pseudo-peptidic nature were developed from urine, blood and dried blood spots (DBS). In addition, metabolism studies were conducted to study the biotransformation of three new ghrelin mimetics.

The results were published as three research articles in different international peer-reviewed scientific journals. These articles report on the development of liquid chromatography-mass spectrometry-based detection methods and *in vitro/in vivo* metabolism studies. The target analytes of these methods which were proteins or peptides and pseudo-peptides were expected to be misused by athletes due to their potential performance-enhancing effects. Therefore, they are part of the World Anti-Doping Agency's (WADA) Prohibited List. In detail, these were first, sotatercept and luspatercept, two Fc-fusion proteins, and bimagrumab, a therapeutic antibody; second, a total of 46 lower molecular mass peptides and pseudo-peptides (< 2 kDa), including growth hormone-releasing factors, luteinizing hormone releasing hormones, antidiuretic hormones, and other banned substances including representative metabolites, and third, three ghrelin mimetics, namely capromorelin, macimorelin and tabimorelin. Furthermore, both, the conventional biological matrices urine and blood and the upcoming alternative matrix DBS, were considered for method development. The detection of pharmacologically relevant drug levels from a small volume of DBS was successfully achieved by using efficient sample preparation protocols and state-of-the-art analytical instrumentation. Both, manual and automated sample preparation strategies were applied within the presented studies. The analytes were extracted and purified from DBS in aqueous buffer using ultrasonication and subsequent immunoaffinity purification or by robot-assisted aqueous flow-through desorption followed by solid phase extraction (SPE). For the ghrelin mimetics, manual SPE or a "dilute-and-inject" approach was applied for urine sample preparation. Purification of analytes from blood plasma was achieved by protein precipitation with methanol. The analytical methods were designed as initial testing procedures and/or confirmation procedures, and were optimized and fully validated according to the current version of the WADA guidelines. Finally, as a proof-of-concept, authentic human samples were analyzed, provided that the application of the drugs were ethically justifiable.

This thesis presents an important contribution to the detection of doping-relevant (pseudo-)peptides and proteins from DBS. The results could conduce to the establishment of DBS as an alternative matrix complementary to the conventional matrices blood and urine in future doping control scenarios. With regard to the upcoming Olympic and Paralympic Winter Games in Beijing, China (2022), where DBS will be used as official matrix for the first time, the analytical spectrum for DBS analysis was successfully extended by these substances. In this context, DBS proved to be a suitable matrix for multi-target screening approaches, also enabling retrospective data analysis. The new methods for the detection of ghrelin mimetics will henceforth extend the multiplexed analytical routine screenings of growth hormone releasing factors from human blood and urine. Moreover, important information about the metabolites of these pseudopeptidic substances (with suspected short plasma half-life) were obtained, which could further improve the specificity and sensitivity of analytical detection methods for future human doping controls.

7 Anhang

7.1 Abbildungsverzeichnis

Abbildung 1.1: Anzahl der durchgeführten jährlichen Dopingtests (Urin) für Wachstumshormon-freisetzende Faktoren (blaue Balken) und die Anzahl der jährlich auffälligen analytischen Befunde (engl. *adverse analytical findings*, grüne Linie). Die Daten sind aus den *Anti-Doping Testing Figures 2019* der Welt-Anti-Doping-Agentur entnommen [70]. Für das Jahr 2014 sind keine Zahlen für die durchgeführten Tests angegeben. 7

Figure 2.1: Method overview of the initial testing procedure (ITP) & confirmation procedure (CP). Detection of sotatercept from DBS with Protein G-based affinity purification (ITP) (**A & C**) and activin A-based affinity purification (CP) (**B & C**). 47

Figure 2.2: Assay development and optimization of the initial testing procedure. Four parameters that are crucial for the efficiency of the method were optimized. Extraction/binding buffer volume (**A**), blood-to-beads ratio (**B**), protein-to-enzyme ratio (**C**) and digestion time (**D**). In each experiment, one parameter was changed, while the others were kept close to the expected optimum. LC-MS results were evaluated with respect to the peak areas of the tryptic signature peptides. Optimal conditions were found with 300 μL of the buffer volume (**A**), with 160 μL of Protein G beads (blood : beads slurry volume of 1:8) (**B**), with a trypsin-to-protein ratio of 1:50 and an overnight digestion at 37 °C for 16 hours. Tosyl phenylalanyl chloromethyl ketone-treated trypsin T1426 (Sigma Aldrich) was used to cleave the proteins. 48

Figure 2.3: Extracted ion chromatograms (mass tolerance: ± 5 ppm) of a dried blood spot blank sample and a dried blood spot sample fortified with 0.25 $\mu\text{g}/\text{mL}$ (=limit of detection) of sotatercept. Samples were either purified via Protein G strategy (initial testing procedure) or via activin A strategy (confirmation procedure), and LC-HRMS analysis was performed on a Q Exactive HF-X (initial testing procedure) and on a Q Exactive HF mass spectrometer (confirmation procedure), respectively. 49

Figure 2.4: Extracted ion chromatograms (mass tolerance: ± 10 ppm) of a dried blood spot blank sample (A) and a dried blood spot sample fortified with 5.0 $\mu\text{g}/\text{mL}$ of sotatercept, luspatercept, and bimagrumab (B). The ^{13}C -

bimagrumab serves as a stable isotope-labeled (^{13}C -Lys, ^{13}C -Arg) ISTD. Samples were purified via Protein G strategy (ITP) and measured on a Q Exactive HF-X Hybrid Quadrupole-Orbitrap mass spectrometer.53

Figure 2.5: Extracted ion chromatograms (mass tolerance: ± 10 ppm) of pre-administration samples (blank subcutaneously and blank intravenously) and post-administration samples (subcutaneously and intravenously) of a bimagrumab clinical study by Novartis. The ^{13}C -bimagrumab serves as a stable isotope-labeled (^{13}C -Lys, ^{13}C -Arg) ISTD. Samples were purified via Protein G strategy (ITP) and measured on a Q Exactive HF-X Hybrid Quadrupole-Orbitrap mass spectrometer.54

Figure 2.S1: Schematic overview. Purification of a DBS extract using Hemoglobind (A) or HemoVoid (B). The Hemoglobind reagent was given to the dried blood spot extract, thus binding hemoglobin. After removing the obtained pellet, a hemoglobin-free sample extract was resulted. This sample could be further purified by for example Protein G and/or reduced, alkylated and digested before LC-HRMS analysis (A). The HemoVoid was placed in a filter tube and a dried blood spot extract was added. After binding, the extract, free of red cell lysates, was eluted and the obtained sample was further processed and analyzed (B).....60

Figure 2.S2: Comparison of two different dried blood spot cards, the Whatman FTA DMPK-C and the Q2 Solution DPS prototype. Colorimetric determination of IgG content was carried out using the Pierce 660 nm Protein assay (A). The LC-HRMS analyses was visualized as peak areas of the tryptic signature peptides of sotatercept originating from the Fc-tag and the AcR1IA domain, respectively (B).60

Figure 2.S3: Assay development and optimization; visualization of colorimetric quantitation experiments of human IgG using the Pierce 660 nm protein assay. Within the method, human IgG yields after the first and an additional, second acidic elution from the Protein G-coupled magnetic beads were investigated (A). Further, the extraction/binding buffers PBS and ABC were compared and human IgG yields were quantified (B).....61

Figure 2.S4: An IgG capture experiment by using a blood-to-beads slurry (v/v) ratio of 1:8 provided a total protein depletion of 97%, thus reduce sample complexity without losing IgG-based drug candidates. Colorimetric

quantitation was carried out using the Pierce 660 nm protein assay. The amount of protein was estimated by using a BSA standard calibration for total protein, and an adaption factor of 0.57 for human IgG..... 62

Figure 2.S5: Pre-purification using different strategies (no removal, ammonium sulfate precipitation, Hemoglobind, HemoVoid) within the sample work-up of the initial testing procedure for detecting sotatercept. Colorimetric determination of IgG concentration of the eluate was carried out using the Pierce 660 nm Protein assay (**A**). The LC-HRMS analyses revealed different responses visualized as peak areas of the tryptic signature peptides of sotatercept originating from the Fc-tag and the ActRIIA domain, respectively (**B**). 64

Figure 2.S6: Addition of DMSO to the eluent. Adding 1% DMSO to the organic eluent, acetonitrile, resulted in a 1.9-fold increase of signal peak area of the Fc-tag peptide of sotatercept, and a minor decrease of 0.8 of the signal peak area of the ActRIIA domain peptide using a 1:8 blood-to-beads slurry (v/v) ratio. Tosyl phenylalanyl chloromethyl ketone-treated trypsin T1426 (Sigma Aldrich) was used to cleave the proteins. 66

Figure 2.S7: NHS magnetic beads were coupled to activin A from two different suppliers, PeptideTech and ThermoFisher. The average peak areas from 12 (PeptideTech) respective 10 (ThermoFisher) LC-HRMS experiments are shown here. As no significant difference in performance was observed, PeptideTech's activin A was chosen due to cost issues. 66

Figure 3.1: Extracted ion chromatograms (mass tolerance \pm 5 ppm) of a sample from a female volunteer obtained by a finger prick. The sample was either analyzed as blank (dashed line) or with 20 ng/mL of a peptide mix containing all 46 target compounds. The rows of the 3 ISTDs are also shown at their respective retention time. 95

Figure 3.2: Extracted ion chromatograms (mass tolerance \pm 10 ppm) of a blank sample and a s.c. post-administration sample showing signals of GHRP-2 and GHRP-6. 96

Figure 3.3: The influence of storage time and temperature on the capillary DBS Hct measurements by NIR spectroscopy was studied. Several DBS cards were stored over a period of 3 weeks at RT, 4°C and -20°C and samples were measured in triplicate (spot 1-3). The error bars result from the standard deviations of the respective experiments. 98

- Figure 3.S1: Extracted ion chromatograms (mass tolerance ± 5 ppm) of a blank sample from a female volunteer obtained by a finger prick.** The rows of the 3 ISTDs are also shown at their respective retention time. Normalization levels (NL) are adapted from Figure 3.1. 103
- Figure 3.S2: The distribution of LODs.** Different LODs of the analytes in the range between 0.5-20 ng/mL were obtained after analysis of a DBS sample. 104
- Figure 4.1: In the upper panel, the extracted ion chromatogram (mass tolerance ± 5 ppm) of a full HRMS experiment of capromorelin (A), macimorelin (B), and tabimorelin (C) at 0 h and 6 h post-administration is shown.** The corresponding isotope signals are shown in the mass spectrum below. The middle panel contains a MS² spectrum of the reference compound ($c = 100$ ng/mL). The lower panel shows the drug's urinary excretion profile in rat. 123
- Figure 4.2: A set diagram showing the number of metabolites of capromorelin (A), macimorelin (B), and tabimorelin (C), detected by full HRMS experiments.** The overlapping sets represent the shared metabolites from two or all four different matrices and/or different *in vitro/vivo* approaches. 124
- Figure 4.3: Overview of all metabolites (M) found in the drug-administered rat urine 6 h post-administration of A) capromorelin, B) macimorelin, and C) tabimorelin.** The assumed chemical or enzymatic reactions that formed a metabolite are indicated on the right. 125
- Figure 4.4:** A) The extracted ion chromatogram (mass tolerance ± 5 ppm) of the full HRMS of the urinary capromorelin hydroxylamine M1i with the [M+H]⁺ ion of $m/z = 522.2711$ at 0 h and 36 h post-administration and, below, the isotope signals of the mass spectrum at retention time, t_R , 10.03 min (36 h post-administration). B) The MS² spectrum of the [M+H]⁺ ion of a sample collected 6 h post-administration. C) The urinary excretion profile with the indicated percentages referring to the relative abundance of the ISTD-normalized peak area. 128
- Figure 4.5:** A) The extracted ion chromatogram (mass tolerance ± 5 ppm) of the full HRMS of the urinary capromorelin hydrolyzed M3 with the [M+H]⁺ ion of $m/z = 421.2234$ at 0 h and 36 h post-administration and, below, the isotope signals of the mass spectrum at t_R 8.77 min (36 h post-administration). B) The MS² spectrum of the [M+H]⁺ ion of a sample collected 6 h post-administration. C) The urinary excretion profile with the indicated percentages referring to the relative abundance of the ISTD-normalized peak area. 130

Figure 4.6: A) The extracted ion chromatogram (mass tolerance ± 5 ppm) of the full HRMS of the urinary macimorelin *N*-dealkylated M2 with the $[M+H]^+$ ion of $m/z = 289.1659$ at 0 h and 36 h post-administration and, below, the isotope signals of the mass spectrum at t_R 4.62 min (36 h post-administration). B) The MS^2 spectrum of the $[M+H]^+$ ion of a sample collected 12 h post-administration. C) The urinary excretion profile with the indicated percentages referring to the relative abundance of the ISTD-normalized peak area. 132

Figure 4.7: A) The extracted ion chromatogram (mass tolerance ± 5 ppm) of the full HRMS of the urinary macimorelin M3 with the $[M+H]^+$ ion of $m/z = 187.0866$ at 0 h and 36 h post-administration and, below, the isotope signals of the mass spectrum at t_R 4.16 min (36 h post-administration). B) The MS^2 spectrum of the $[M+H]^+$ ion of a sample collected 12 h post-administration. C) The urinary excretion profile with the indicated percentages referring to the relative abundance of the ISTD-normalized peak area. 133

Figure 4.8: A) The extracted ion chromatograms (mass tolerance ± 5 ppm) of the full HRMS of the urinary tabimorelin *N*-glucuronidated M3-1 with the $[M+H]^+$ ion of $m/z = 707.3579$ at 0 h and 24 h post-administration, and below, the isotope signals of the mass spectrum at t_R 8.65 min from a sample collected 24 h post-administration. B) The MS_2 spectrum of the $[M+H]^+$ ion of a sample collected 6 h post-administration. C) The urinary excretion profile with the indicated percentages referring to the relative abundance of the ISTD-normalized peak area. 134

Figure 4.S1: Comparison of the absolute abundance of all metabolites of capromorelin detected in rat urine 6 h (black) and 12 h (grey) post-administration. The samples were analyzed on a Q Exactive HF-X mass spectrometer in full HRMS mode. 143

Figure 4.S2 A) The extracted ion chromatogram (mass tolerance ± 5 ppm) of the full HRMS of the urinary capromorelin *N*-dealkylated M4 with the $[M+H]^+$ ion of $m/z = 492.2605$ at 0 h and 36 h post-administration. Below, there are the isotope signals of the mass spectrum at t_R 8.37 min from a sample collected 36 h post-administration, and the different matrices and *in vitro/in vivo* experiments in which this metabolite was detected with the corresponding detection windows for rat urine and rat EDTA-plasma. B) The MS^2 spectrum of the $[M+H]^+$ ion of the urinary capromorelin *N*-dealkylated M4 of a sample collected 6 h post-administration. C) The urinary excretion profile of capromorelin *N*-dealkylated M4 with the indicated

- percentages referring to the relative abundance of the ISTD-normalized peak area.
.....144
- Figure 4.S3:** Pseudo-MS³ spectrum (SID + MS²) of the [M+H]⁺ ion of $m/z = 421.2233$ which is a MS² fragment of capromorelin hydroxylamine M1i. The sample (rat urine, 6 h post-administration) was analyzed on an Orbitrap Exploris 480 mass spectrometer.145
- Figure 4.S4:** Pseudo-MS³ spectrum (SID + MS²) of the [M+H]⁺ ion of $m/z = 279.1339$ which is a MS² fragment of capromorelin hydroxylamine M1i. In theory, both structures shown here would be plausible. The sample (rat urine, 6 h post-administration) was analyzed on an Orbitrap Exploris 480 mass spectrometer.
.....145
- Figure 4.S5:** Pseudo-MS³ spectrum (SID + MS²) of the [M+H]⁺ ion of $m/z = 251.1390$ which is a MS² fragment of capromorelin hydroxylamine M1i. In theory, both structures shown here would be plausible. The sample (rat urine, 6 h post-administration) was analyzed on an Orbitrap Exploris 480 mass spectrometer.
.....146
- Figure 4.S6:** A possible mechanism of capromorelin oxidation: First, capromorelin hydroxylamine M1i was generated by CYP2C9. Second, this compound was autoxidized to the nitroso M1-4 intermediate. Third, further oxidation resulted the capromorelin nitro M1-5.146
- Figure 4.S7:** MS² spectrum of the [M+H]⁺ ion of capromorelin nitro M1-5 ($m/z = 536.2504$) from a rat urine sample collected 6 h post-administration of capromorelin, analyzed on an Orbitrap Exploris 480 mass spectrometer.147
- Figure 4.S8:** To verify the identity of capromorelin nitro M1-5 ($m/z = 536.2 (1+)$), both a neutral loss experiment (left) and a precursor ion scan experiment (right) were conducted. The upper panel shows the extracted ion chromatogram of the [M+H]⁺ ion of a blank rat urine sample collected at 0 h and the lower panel shows the a sample collected 6 h post-administration. The samples were analyzed on a Xevo TQ-XS mass spectrometer.147
- Figure 4.S9:** Two rat urine samples (rat #5 and rat #6) containing capromorelin and its metabolites after 6 h post-administration were analyzed on four different days (full HRMS scan) within a period of almost 50 days and three freeze-thaw cycles of the samples. The ratios of the peak areas of capromorelin hydroxylamine M1i

- ($m/z = 522.27$ (1+)) and capromorelin nitro M1-5 ($m/z = 536.25$ (1+)) are shown. The samples were analyzed on a Q Exactive HF-X mass spectrometer..... 148
- Figure 4.S10:** MS² spectrum of the [M+H]⁺ ion of capromorelin *N*-acetylated M1-6 ($m/z = 548.2867$) from a rat urine sample collected 6 h post-administration, analyzed on an Orbitrap Exploris 480 mass spectrometer. 149
- Figure 4.S11:** MS² spectrum of the [M+H]⁺ ion of capromorelin M2-2 ($m/z = 416.2292$) from a rat urine sample collected 6 h post-administration, analyzed on an Orbitrap Exploris 480 mass spectrometer. 149
- Figure 4.S12:** Comparison of the absolute abundance of all metabolites of macimorelin detected in rat urine 6 h (black) and 12 h (grey) post-administration. The samples were analyzed on a Q Exactive HF-X mass spectrometer in full HRMS mode..... 150
- Figure 4.S13:** A) The extracted ion chromatogram (mass tolerance ± 2 ppm) of the full HRMS of the urinary macimorelin mono-hydroxy M1c with the [M+H]⁺ ion of $m/z = 491.2401$ at 0 h and 24 h post-administration. Below, there are the isotope signals of the mass spectrum at t_R 6.83 min from a sample collected 24 h post-administration, and the different matrices or *in vitro/in vivo* experiments in which this metabolite was detected with the corresponding detection windows for rat urine and rat EDTA-plasma. B) The MS² spectrum of the [M+H]⁺ ion of the urinary macimorelin mono-hydroxy M1c of a sample collected 6 h post-administration. C) The urinary excretion profile of macimorelin mono-hydroxy M1c with the indicated percentages referring to the relative abundance of the ISTD-normalized peak area. 151
- Figure 4.S14:** MS² spectra of the [M+H]⁺ ion of the four macimorelin mono-hydroxy M1a, M1b, M1c, M1d ($m/z = 491.2401$) at t_R 6.30 min, 6.56 min, 6.83 min, and 7.02 min from a rat urine sample collected 6 h post-administration, analyzed on an Orbitrap Exploris 480 mass spectrometer. The small inset in each MS² spectrum on the upper left shows the extracted ion chromatogram and the black arrow indicates the respective t_R [min] of each metabolite. The dotted lines within the structural formula indicate the most likely site of modification. 152
- Figure 4.S15:** MS² spectrum of the [M+H]⁺ ion of macimorelin di-hydroxy M1-1b ($m/z = 507.2350$) from a rat urine sample collected 6 h post-administration, analyzed on an Orbitrap Exploris 480 mass spectrometer. The dotted lines within the structural formula indicate the most likely site of modification, however

hydroxylation on the other tryptophan residue of this compound would also be possible.....153

Figure 4.S16: MS² spectrum of the [M+H]⁺ ion of macimorelin O-glucuronide M1-2 ($m/z = 667.2722$) from a rat urine sample collected 6 h post-administration, analyzed on an Orbitrap Exploris 480 mass spectrometer. The dotted line within the structural formula indicates the most likely site of modification.153

Figure 4.S17: Comparison of the absolute abundance of all metabolites of tabimorelin detected in rat urine 6 h (black) and 12 h (grey) post-administration. The samples were analyzed on a Q Exactive HF-X mass spectrometer in full HRMS mode. 154

Figure 4.S18: MS² spectrum of the [M+H]⁺ ion of tabimorelin mono-hydroxy M1 ($m/z = 545.3122$) from a rat urine sample collected 6 h post-administration, analyzed on an Orbitrap Exploris 480 mass spectrometer. The grey area within the structural formula indicates the most likely site of modification. An example of the possible structure is shown here.....154

Figure 4.S19: MS² spectrum of the [M+H]⁺ ion of tabimorelin mono-O-glucuronide M1-1 ($m/z = 721.3443$ (1+)) from a rat urine sample collected 6 h post-administration, analyzed on an Orbitrap Exploris 480 mass spectrometer. The grey area within the structural formula indicates the most likely site of modification. An example of the possible structure is shown here.....155

Figure 4.S20: MS² spectrum of the [M+H]⁺ ion of tabimorelin N-dealkylated M2 ($m/z = 515.3017$) from a rat urine sample collected 6 h post-administration, analyzed on an Orbitrap Exploris 480 mass spectrometer.....155

Figure 4.S21: MS² spectrum of the [M+H]⁺ ion of tabimorelin N-glucuronide M3 ($m/z = 705.3428$) from a rat urine sample collected 6 h post-administration, analyzed on an Orbitrap Exploris 480 mass spectrometer.....156

7.2 Tabellenverzeichnis

Table 2.1: Signature peptides of the target proteins for mass spectrometric detection.	45
Table 2.2: LC-HRMS dried blood spots validation results of sotatercept for the initial testing procedure and the confirmation procedure.	51
Table 2.S1: Overview of the most promising sample preparation strategies (ITP) under consideration of recovery, effectiveness of purification, time, costs and sensitivity. The parameters were roughly estimated or evaluated from LC-MS data. Light grey means a good value/ property, grey a medium and dark grey a rather poor one.....	65
Table 3.1: LC-HRMS related characteristics and categories of the target compounds.	89
Table 3.2: Main results of validation.	93
Table 3.S1: Supplier, location, specified peptide purity and peptide content of the standard substances.	104
Table 3.S2: In order to estimate the linearity of the analytes between LOD–100 ng/mL, a linear (1st order) regression was assumed. LOD, coefficient of correlation (r), intercept, and slope are indicated.	105
Table 4.1: Overview of the most abundant metabolites of capromorelin, macimorelin, and tabimorelin detected after <i>in vivo</i> or <i>in vitro</i> experiments.	127
Table 4.2: Results of the qualitative initial testing procedure (ITP) and confirmation procedure (CP) validation for human urine and human EDTA-plasma matrix	135
Table 4.S1: Overview of all putative capromorelin metabolites detected from <i>in vitro</i> or <i>in vivo</i> experiments by full HRMS experiments on a Q Exactive HF-X mass spectrometer. The molecular formula, retention time (t_R), predominant charge state, three isotopic masses [m/z], reaction type, SMILES, and matrix in which the correspondent metabolite was detected were indicated.....	157
Table 4.S2: Overview of all putative macimorelin metabolites detected from <i>in vitro</i> or <i>in vivo</i> experiments by full HRMS experiments on a Q Exactive HF-X. The molecular formula, retention time (t_R), predominant charge state, three	

isotopic masses [m/z], reaction type, SMILES, and matrix in which the correspondent metabolite was detected were indicated.158

Table 4.S3: Overview of all putative tabimorelin metabolites detected from *in vitro* or *in vivo* experiments by full HRMS experiments on a Q Exactive HF-X. The molecular formula, retention time (t_R), predominant charge state, three isotopic masses [m/z], reaction type, SMILES, and matrix in which the correspondent metabolite was detected were indicate158

7.3 Vollständige Publikationsliste

Artikel als Erstautor:

- T. Lange, A. Thomas, C. Görgens, M. Bidlingmaier, K. Schilbach, E. Fichant, P. Delahaut & Mario Thevis, Comprehensive insights into the formation of metabolites of the ghrelin mimetics capromorelin, macimorelin and tabimorelin as potential markers for doping control purposes, *Biomed. Chromatogr.*, 2021, 35(6): e5075.
- T. Lange, A. Thomas, K. Walpurgis & M. Thevis, Fully automated dried blood spot sample preparation enables the detection of lower molecular mass peptide and non-peptide doping agents by means of LC-HRMS, *Anal Bioanal Chem*, 2020, 412(15): 3765-3777.
- T. Lange, K. Walpurgis, A. Thomas, H. Geyer & M. Thevis, Development of two complementary LC–HRMS methods for analyzing sotatercept in dried blood spots for doping controls, *Bioanalysis*, 2019, 11(10): 923-940.

Artikel als Ko-Autor:

- K. Walpurgis, A. Thomas, T. Lange, C. Reichel, H. Geyer & M. Thevis, Combined detection of the ActRII-Fc fusion proteins sotatercept (ActRIIA-Fc) and luspatercept (modified ActRIIB-Fc) in serum by means of immunoaffinity purification, tryptic digestion, and LC-MS/MS, *Drug Test Anal*, 2018, 10(11-12): 1714-1721.

Vorträge:

- T. Lange, A. Thomas, C. Görgens, M. Bidlingmaier, K. Schilbach, E. Fichant, P. Delahaut & M. Thevis, *In vivo/in vitro*-Metabolismusstudien von Ghrelin Mimetika als potenzielle Marker für Dopingkontrollen, 31. *Doktorandenseminar des Arbeitskreis Separation Science der GDCh-Fachgruppe Analytische Chemie*, Hohenroda (online), Deutschland, 11. - 12. Januar 2021
- T. Lange, A. Thomas, K. Walpurgis & M. Thevis, Fully automated DBS sample preparation enables the detection of lower molecular mass peptide and non-peptide doping agents, *Manfred Donike Workshop, 38th Cologne Workshop on Dope Analysis*, Köln, Deutschland, 09. - 14. Februar, 2020
- T. Lange, K. Walpurgis, A. Thomas, H. Geyer & M. Thevis, Development of two complementary LC-HRMS methods for analyzing Sotatercept in dried blood spots for doping controls, *Manfred Donike Workshop, 37th Cologne Workshop on Dope Analysis*, Köln, Deutschland, 17. - 22. Februar, 2019

Poster-Präsentationen

- T. Lange, A. Thomas, K. Walpurgis & M. Thevis, Fully automated dried blood spot sample preparation enables the detection of lower molecular mass peptide and non-peptide doping agents by means of LC-HRMS, *53rd annual meeting of the German Society for Mass Spectrometry (DGMS) including 27th ICP-MS User's Meeting*, Münster, Deutschland, 1. - 4. März, 2020
- T. Lange, K. Walpurgis, A. Thomas & M. Thevis, Determination of Sotatercept (ACE-011) in dried blood spots for doping control analysis by means of LC-HRMS, *Manfred Donike Workshop, 36th Cologne Workshop on Dope Analysis*, Köln, Deutschland, 22. - 27. April, 2018
- T. Lange, K. Walpurgis, A. Thomas & M. Thevis, Determination of Sotatercept (ACE-011) in dried blood spots for doping control analysis by means of LC-HRMS, *European Mass Spectrometry Conference (EMSC) including the 51st annual meeting of the German Society for Mass Spectrometry (DGMS) and the 35th Journées Françaises de Spectrométrie de Masse (JFSM) of the French Mass Spectrometry Society*, Saarbrücken, Deutschland, 11. - 15. März, 2018

